Universität Bremen

marum

Spatial and temporal development of the Namibian cold-water coral mounds

Dissertation

zur Erlangung des

Doktorgrades der Naturwissenschaften

Doctor rerum naturalium (Dr. rer. nat.)

am Fachbereich Geowissenschaften

der Universität Bremen

vorgelegt von

Leonardo Tamborrino

Gutachter / Supervisor

Prof. Dr. Dierk Hebbeln, MARUM – Zentrum für Marine Umweltwissenschaften, Universität Bremen Leobenerstraße, 8, 28359 Bremen, Deutschland.

Gutachter / External reviewer

PD Dr. Jacek Raddatz, Goethe-Universität, Institut für Geowissenschaften, Altenhöferallee 1, 60438 Frankfurt am Main, Deutschland

Date of defence / Promotionskolloquium

02.09.2022

This dissertation is dedicated to Maria Galante, my mother

La semplicità è l'ultima sofisticazione

(Leonardo da Vinci)

List of abbreviations

CWC	Cold-Water Corals		SLM	Satellite lander module
CMP	Coral Mound Province		AR	Aggradation rate
SQM	Squid Mounds		RV	Research Vessel
CBM	Coral Belt Mounds		ROV	Remote Operated Vehicle
BUS	Benguela Upwelling System		AUV	Autonomous Underwater Vehicle
PUC	Poleward Undercurrent		MBES	Multibeam Echosounders
AC	Angola Current		GS	Grab sampler
ABF	Angola-Benguela Front		GBC	Giant box corer
SACW	South Atlantic Central Water		GC	Gravity corer
ESACW	Eastern South Atlantic Central Water		GIS	Geographic Information System
AAIW	Antarctic Intermediate Water		DEM	Digital Elevation Model
SASSW	South Atlantic Subtropical Surface Water		SLF	Secondary low frequency (Parasound)
OMZ	Oxygen minimum zone		PAR	Principal axes ratio
SHW	Southern Hemisphere Westerlies		PAX	Principal axis
INL	Intermediate Nepheloid Layer		OPAX	Axis orthogonal to PAX
DOC or DO	Dissolved Oxygen Concentrations		mbsl	meters below sea level
SPOM	Suspended Particulate Organic Matter		mbsf	meters below seafloor
TOC	Total Organic Carbon		cps	counts per second
CTD	Conductivity-Temperature-Depth		PSU	Practical Salinity Unit
PPS	McLane phytoplankton sampler			

General note: most abbreviations will be introduced again in the introduction of the thesis and in the chapter related to the manuscripts because they are aimed for a standalone format.

Abstract

Over the last 25 years, extensive geological investigations on coral mounds, seafloor structures in the deep-sea built by ecosystem-engineering cold-water corals (CWC), have revealed that the spatial and temporal occurrences of CWC depend on environmental and climate conditions. Coral mounds in the NE Atlantic were the first and have been the most studied coral mound provinces (CMPs), providing the fundamental evidence of the environmental forcing supporting CWC and on the development of coral mounds over glacial-interglacial cycles. However, the continuous discovery of coral mounds under the extremely variable oceanographic conditions along the Atlantic margins have brought new evidence to re-discuss our previous knowledge on CWC and coral mounds.

This study was designed for one of the latest CMP discovered: the Namibian coral mounds. More than 2000 mounds are sitting on the Namibian inner shelf (~20°S) between 160-270 m water depths. The Namibian CMP occurs under an oceanographic setting controlled by the Benguela Upwelling System (BUS). The BUS is one of the large eastern-boundary upwelling systems with the highest primary production in the world ocean. Due to these highly productive conditions, shelf-bottom waters become severely oxygen-depleted resulting from the consumption of oxygen through the decomposition of organic matter. The Namibian coral mounds occur exactly at the core of the local oxygen minimum zone (OMZ, 160–270 m water depth), where dissolved oxygen concentrations (DO) are 0-0.5 mL L^{-1} and accompanied by relatively high potential temperatures of 12.4 to 13.4 °C which can already be critical for CWC physiology. These present-day conditions prevent any CWC proliferation, and indeed no living colonies have been observed during the dives of a remotely operated vehicle.

After the analysis and discussion of the present-day environmental condition (Manuscript I), this thesis aimed to identify how oceanographic conditions controlled the spatial-morphological variability (Manuscript II) and temporal development (Manuscript III) of the Namibian coral mounds. The results show that spatial distribution and morphometric appearance of the coral mounds is highly controlled by the interplay between the underlying topography (erosional features) and the hydrodynamic regime (internal tides). Moreover, U-series dating on CWC skeletons combined with local paleoceanographic reconstructions link the temporal development (4.5-9.5 kyr BP) of the Namibian coral mounds to a decrease of the BUS activity, with a consequent relative relaxation of the local OMZ. This likely brought DO values comparable to the present-day hypoxic conditions on the Angola CMP, where living CWC colonies have been observed.

The findings of this thesis show how a comprehensive geological investigation on coral mounds can reveal important insights on the life and demise of CWC. The methods applied and the results obtained might serve as framework for investigating new CMPs, as well stimulating re-analyses of older datasets acquired from well-known CMPs. Moreover, improving our knowledge on CWC, to which this study on the Namibian coral mounds contributed, will provide insights on the fate of CWC under the changing ocean and climate conditions in the future.

Zusammenfassung

In den letzten 25 Jahren haben umfangreiche geologische Untersuchungen von Korallenhügeln, Strukturen am Meeresboden in der Tiefsee, die von ökosystembildenden Kaltwasserkorallen (KWK) gebildet werden, gezeigt, dass das räumliche und zeitliche Auftreten von CWC von den Umwelt- und Klimabedingungen abhängt. Korallenhügel im Nordostatlantik waren die ersten und am besten untersuchten Korallenhügelprovinzen (KHPs) und sie lieferten die grundlegenden Beweise dafür, dass Umweltfaktoren die KWK begünstigen und dass die Entwicklung von Korallenhügeln durch Glazial-Interglazial-Zyklen gesteuert wird. Die kontinuierliche Entdeckung von Korallenhügeln unter den extrem variablen ozeanographischen Bedingungen entlang der atlantischen Kontinentalränder brachte neue Beweise auf deren Basis unser bisheriges Wissen über KWK und Korallenhügel neu diskutiert werden kann.

Diese Studie wurde für eine der zuletzt entdeckten KHP konzipiert: die namibischen Korallenhügel. Mehr als 2000 Hügel befinden sich auf dem inneren Schelf von Namibia (~20°S) zwischen 160-270 m Wassertiefe. Die namibische KHP befindet sich in einem ozeanographischen Umfeld, das durch das Benguela Upwelling System (BUS) kontrolliert wird. Das BUS ist eines der großen östlichen Auftriebssysteme mit der höchsten Primärproduktion in den Weltmeeren. Aufgrund dieser hochproduktiven Bedingungen ist das Wasser am Schelfboden extrem sauerstoffarm, was auf den Verbrauch von Sauerstoff durch die Zersetzung organischer Substanz zurückzuführen ist. Die namibischen Korallenhügel befinden sich genau im Kern der lokalen Sauerstoffminimumzone (SMZ, 160-270 m Wassertiefe), in der die Konzentration an gelöstem Sauerstoff (GS) 0-0,5 mL L^{-1} beträgt, begleitet von relativ hohen Temperaturen von 12,4 und 13,4 °C, die für die Physiologie der Korallen bereits kritisch sein können. Unter diesen Bedingungen können KWK nicht überleben, und tatsächlich wurde bei den Tauchgängen eines ferngesteuerten Tauchroboters keine lebenden Kolonien beobachtet. Nach der Analyse und Diskussion der heutigen Umweltbedingungen (Manuskript I) wurde in dieser Arbeit untersucht, wie die ozeanographischen Bedingungen die räumlich-morphologische Variabilität (Manuskript II) und die zeitliche Entwicklung (Manuskript III) der namibischen Korallenhügel steuern. Die Ergebnisse zeigen, dass die räumliche Verteilung und das morphometrische Erscheinungsbild der Korallenhügel in hohem Maße durch das Zusammenspiel zwischen der zugrunde liegenden Topographie (Erosionsmerkmale) und dem hydrodynamischen Regime (interne Tiden) gesteuert wird. Darüber hinaus bringen U-Serien-Datierungen von KWK-Skeletten in Verbindung mit lokalen paläozeanographischen Rekonstruktionen die zeitliche Entwicklung (4,5-9,5 kyr BP) der namibischen Korallenhügel mit einer Abnahme der BUS-Aktivität in Verbindung, die zu einer relativen Schwächung der lokalen SMZ führte. Dies führte wahrscheinlich zu GS-Werten, die mit den heutigen hypoxischen Bedingungen in der Angola KHP vergleichbar sind, wo lebende KWK-Kolonien beobachtet wurden.

Die Ergebnisse dieser Arbeit zeigen, dass eine umfassende geologische Untersuchung von Korallenhügeln wichtige Erkenntnisse über das Leben und den Untergang von KWK liefern kann. Die angewandten Methoden und die erzielten Ergebnisse könnten als Beispiel für die Untersuchung neuer KHPs dienen,

aber auch eine Neuanalyse älterer Datensätze stimulieren, die von bekannten KHPs gewonnen wurden. Darüber hinaus wird die Verbreiterung unseres Wissens über KWK, wie es sich aus der Untersuchung der namibischen Korallenhügel ergeben hat, Einblicke in das Schicksal der KWK unter den sich verändernden Ozean- und dem Klimabedingungen in der Zukunft geben.

Contents

1. Introduction

1.1. Overview

Corals play a key role in the development of benthic (and benthic-pelagic) ecosystems in the Earth's oceans. In shallow tropical seas, coral polyps can develop calcareous skeletons thanks to the symbiotic relationship with azooxanthellate algae, which contribute to the formation of limestone bio-constructions well known as coral reefs. Coral reefs support the development of the most diverse species assemblages in the oceans, but not only in the shallow tropical seas. Besides these shallow-water corals, there are also corals living in the deep, dark, and cold waters. These "deep-sea" corals have been known and studied for centuries; however they have only been the focus of a few coral taxonomists, whose studies were mostly based on the material obtained from pioneering deep-sea expeditions (Burke *et al.*, 2010; Cairns, 2001a; Gagnon *et al.*, 2007; Roberts *et al.*, 2009).

The development of marine technologies (such as ROV, AUV, high-resolution MBES*, benthic landers) brought new eyes to explore the deep-sea environments, and therefore, the cold-water coral (CWC) ecosystems. In the last 30 years, continuous unexpected discoveries and scientific results have revealed the relevance of CWC ecosystems, although there are large gaps in our knowledge on this topic. Since the first findings, it has been clear that some framework-forming CWC are habitat-forming species with the ability to create deep-sea biodiversity hotspots, hosting thousands of other species (sponges, polychaetes, crustaceans, molluscs, bryozoans and fishes), comparable to the shallow tropical reefs (Costello *et al.*, 2005; Roberts *et al.*, 2006).

Unfortunately, CWC ecosystems share a similar vulnerability with their tropical counterparts in regards to climate change and human impact. The ecological needs of CWC make them sensitive to environmental conditions, and therefore, natural oceanographic/climate changes control(ed) their spatial distribution and temporal occurrences. Bottom trawling fisheries, hydrocarbon and mineral exploration and production, and recently, marine microplastics represent the major anthropogenic threats to CWC ecosystems (Chapron *et al.*, 2018; Ragnarsson *et al.*, 2017 and references therein). Ocean acidification derived from the ocean uptake of the human-produced atmospheric CO_2 was primarily hypothesized as a danger for CWC (Turley *et al.*, 2007). More and more studies are confirming the ability of CWC to cope with lower pH conditions (e.g. Büscher *et al.*, 2017; Carreiro-Silva *et al.*, 2014; Hennige *et al.*, 2014; Maier *et al.*, 2009). However, the ongoing global climate change will also contribute to ocean deoxygenation (Breitburg *et al.*, 2018; Burke *et al.*, 2010; Keeling *et al.*, 2010; Stramma *et al.*, 2008), which will impact benthic communities like CWC ecosystems (e.g., Fink *et al.*, 2012; Wienberg *et al.*, 2018).

The fate of CWC ecosystems under a changing climate is already written in the geological records. Today, we can understand how CWC ecosystems will respond to the ongoing climate change by knowing how environmental changes have affected CWC ecosystems in the past, following Lyell's principle. The sustained growth of framework-forming CWC, over millennial timescales, is responsible

*Abbreviations: ROV, remotely operated vehicle; AUV, autonomous unmanned vehicle; MBES, multibeam echosounders.

for the formation of 3D seafloor structures known as cold-water coral mounds (but also reefs or ridges). Spatial and temporal development of coral mounds reflect the conditions that have supported (or not) the proliferation of CWC (e.g., Bahr *et al.*, 2020; Cyr *et al.*, 2016; De Clippele *et al.*, 2017b; De Haas *et al.*, 2009; Douarin *et al.*, 2013; Eisele *et al.*, 2011; Fink *et al.*, 2013; Frank *et al.*, 2011; Hebbeln *et al.*, 2019; Kano *et al.*, 2010; Matos *et al.*, 2017; Wienberg *et al.*, 2010).

As food supply is the most relevant condition for thriving CWC colonies, the development of coral mounds is controlled by the variability of primary productivity (e.g., Eisele *et al.*, 2011; Fink *et al.*, 2013; Wang *et al.*, 2017; Wilson *et al.*, 2014), and the hydrodynamic regime (e.g., Dorschel *et al.*, 2005; Matos *et al.*, 2017). These two parameters have a binding relationship to another control on CWC physiology: dissolved oxygen concentration (DO). Most present-day occurrences of framework-forming CWC are linked to DO of around 4-6 mL L^{-1} (Wienberg and Titschack, 2017). The impact of low DO on CWC growth was observed clearly for the first time in the hiatus in a Mediterranean coral mound record coinciding with sapropel S1 event (Fink *et al.*, 2012). The giant coral mound province off Mauritania (Colman *et al.*, 2005) has been discovered within oxygen-depleted intermediate waters in which DO range between 0-1.3 mL L^{-1} (Ramos *et al.*, 2017). These low DO have been considered as the main stressor determining the scarce present-day occurrence of living CWC off Mauritania, but also one of the environmental factors responsible for the aggradational hiatuses in the regional coral mound records (Wienberg *et al.*, 2018).

The M122 ANNA cruise provided material to investigate the CWC/coral mounds provinces in the SE Atlantic (Hebbeln *et al.*, 2017). The extensive field investigations confirmed the occurrence of a large coral mound province on the Namibian shelf at ~260 m water depth. More than 2000 mounds have been detected where DO values drop to 0 mL L^{-1}. These low DO values are related to the oxygen minimum zone associated with the Benguela Upwelling System, the most world productive eastern boundary upwelling system (Carr, 2001). Under such extreme conditions, the Namibian mounds offered the opportunity to highlight new perspectives on how spatial and temporal development of coral mounds could be affected by the variability of the main environmental controls identified (primary productivity, hydrodynamic regime, DO).

1.2. From corals to mounds

The *Metamophoseon Libri XV*, the epic-narrative poem written by Ovid (43 BC-18 DC), collects most of the chronicles belonging to the Greek and Latin classic culture, including the myth of the origin of the corals. After slaying Medusa (Gorgon monster whose gaze upon would turn an onlooker to stone), Perseus used her head to petrify Cetus, the sea monster threatening Andromeda. Once Perseus saved Andromeda, he left the Medusa's head on the shore and he saw that the blood leaking from Medusa's head turned seaweeds into the red corals. The red coral (*Corallium rubrum*) is an octocoral CWC species typical of the Mediterranean Sea, well-known and largely used throughout the human history of this region. Indeed, the word "coral" is derived from the ancient Greek *korallion,* introduced by

Theophrastus (Aristotle's successor) to describe red corals. *Korallion* likely refers to the hard skeleton or derived from the ancient Hebrew word *goral*, a word for the little stones used by the oracles in the ancient Middle East. Red corals, as well as all octocorals, are not "hard" or "stony" corals, albeit some species have calcium carbonate portions (sclerites or internal branch axes). The capacity to build a robust aragonitic skeleton belongs to the corals of the Scleractinia taxon (Fig. 1.1a), hard or stony corals *in sensu strictu*. This unique characteristic made some scleractinian corals the most prevalent habitat-forming species around the world's oceans and in Earth history. This success regards also the scleractinian framework-forming CWC that are in the focus of this thesis. The ecological permutations and the evolutionary history of the scleractinian corals (Fig. 1.1b, c) will help to reconstruct the nature of the scleractinian CWC.

The first classification step is subdividing the scleractinian corals into zooxanthellate and azooxanthellate. Zooxanthellae are endosymbiontic dinoflagellates, which provide oxygen and glucose to the scleractinian corals, facilitating their calcification, and therefore, reef*-formation (Davy *et al.*, 2012; Tambutté *et al.*, 2011). The lack of zooxanthellae allows azooxanthellate corals (scleractinian and non), to live and thrive in darker, deeper and cooler waters, which identify them as cold-water corals (CWC) in contrast to the shallow warm/tropical-waters corals. The symbiotic relationship with zooxanthellae plays a key role for the modern corals and it is thought to be the main driver of the Triassic expansion (Fig. 1.1c) and diversification of shallow-water scleractinian corals (Frankowiak *et al.*, 2016; Stanley and Swart, 1995). Before the middle Triassic, the uncertain origin of scleractinian corals seems to be related to a Palaeozoic azooxanthellate soft-bodied ancestor, despite the occurrence of Palaeozoic stony corals like Tabulata-Rugosa fossils (Stolarski *et al.*, 2011). Scleractinian CWC occur in the fossil record much later than their shallow-water counterparts. The first record of azooxanthellate scleractinian CWC is a solitary dendrophyllidae in the Early Cretaceous (Fig. 1c, Cairns, 2001b). Most of the azooxanthellate scleractinian species are solitary corals (~74 %, Cairns, 2007), and they have no mound-forming capacity. The formation of CWC mounds is related to framework-forming scleractinian CWC, which are colonial rather than solitary. *Thickets* (a former term used for CWC frameworks) of colonial scleractinian CWC are known since the Aptian-Albian stages (Coates and Kauffman, 1973; Thomas, 1947).

Shortly after the K-T boundary (66 Ma), the first coral mounds constructed by dendrophylliids and oculinids (stony CWC families hosting also modern framework-forming species like *Enallopsammia profunda* and *Oculina varicosa*) appeared in the Danish Basin during the Danian (Bernecker and Weidlich, 1990; 2005). The most predominant mound-builder species occurring in the modern oceans is *Lophelia pertusa*. The first reliable appearance of coral mounds made by *Lophelia*-genus species occurs in the Upper Miocene in the Wairarapa district, New Zealand (Squires, 1964). The Cenozoic records of *Lophelia*, as well as other scleractinian CWC, present a worldwide paucity in the geological record until the Late Pliocene. The Late Pliocene onset of the formation of Challenger Mound off Ireland marked the beginning of a new era for scleractinian CWC, in which CWC started spreading out along

*here, the word "reef" refers to 3D seabed structures formed by colonies of scleractinian corals mostly in shallow waters, either azooxanthellate or azooxanthellate (e.g. Norwegian CWC reef, Fossa et al. 2005) due to the etymology of the word, which derived from Old Norse *rif* as submerged structure shallow enough to endanger ships.

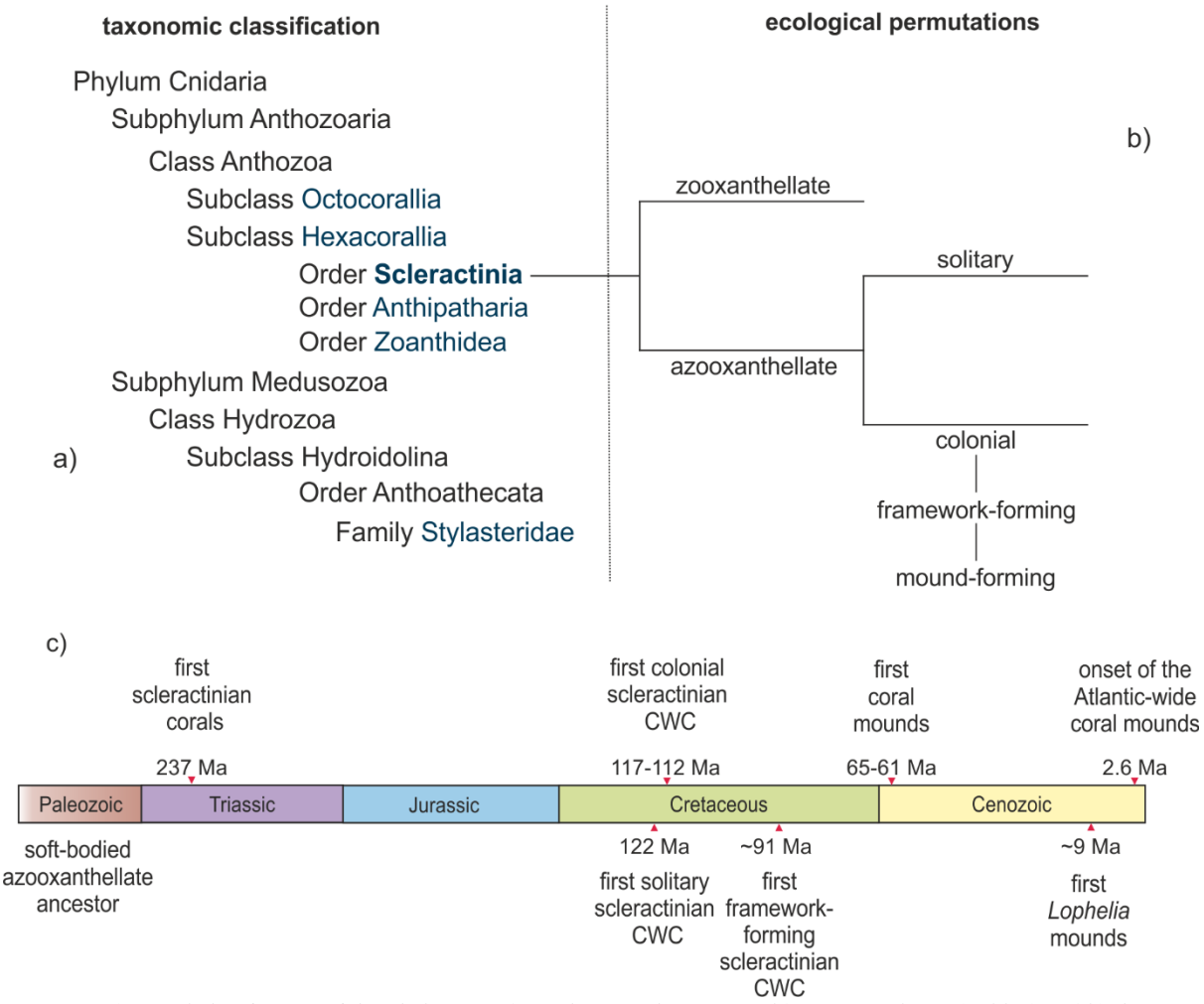

Figure 1.1 a) Partial classification of the phylum Cnidaria, showing the major cold-water coral taxa (in blue) and b) the main ecological permutations of the Scleractinian corals. c) Major steps in the evolutionary history of cold-water corals. The references for the evolutionary steps are the following ones: Palaeozoic ancestor (Stolarski *et al.*, 2011), Triassic azooxanthellate scleractinian (Stanley and Fautin, 2001), *Palaeopsammia* as the first record of solitary scleractinian CWC (Cairns, 2001b), Upper Aptian *Oculina hobley* as first colonial scleractinian CWC (Thomas, 1947), Middle-Turonian *Archohelia dartoni* thicket considered as first framework-forming CWC (Coates and Kauffman, 1973), first coral mounds formed in the Danian (Bernecker and Weidlich, 1990; 2005), first appeared in the Upper Miocene of coral mounds made by *Lophelia* species (Squires, 1964), Challenger Mound (off Ireland) record as the onset of the modern coral mounds along Atlantic margins (Kano *et al.*, 2007). Further details on the evolutional history of CWC are presented in Roberts *et al.* (2009). *Own illustration.*

the continental margins and out into the Atlantic Ocean through today.

Solitary corals are composed of a single corallite (skeleton of a single coral polyp), but some species can be gregarious, like *Desmophyllum dianthus* (Fig. 1.2a) that often occurs on coral mounds. Coral polyps of colonial scleractinian combine their corallites into branches composing the colony (a group of coral polyps with the same genome, Fig. 1.2b). Different branches of the same colony or different colonies can form frameworks (Fig, 1.2c), which include or are fully composed by dead portions of colonies (Fig. 1.2 d, e).

The presence of hard substrate and accelerated currents supplying food particles (see following chapter) are conditions defining the habitat of framework-forming CWC, which can also be habitat-forming for

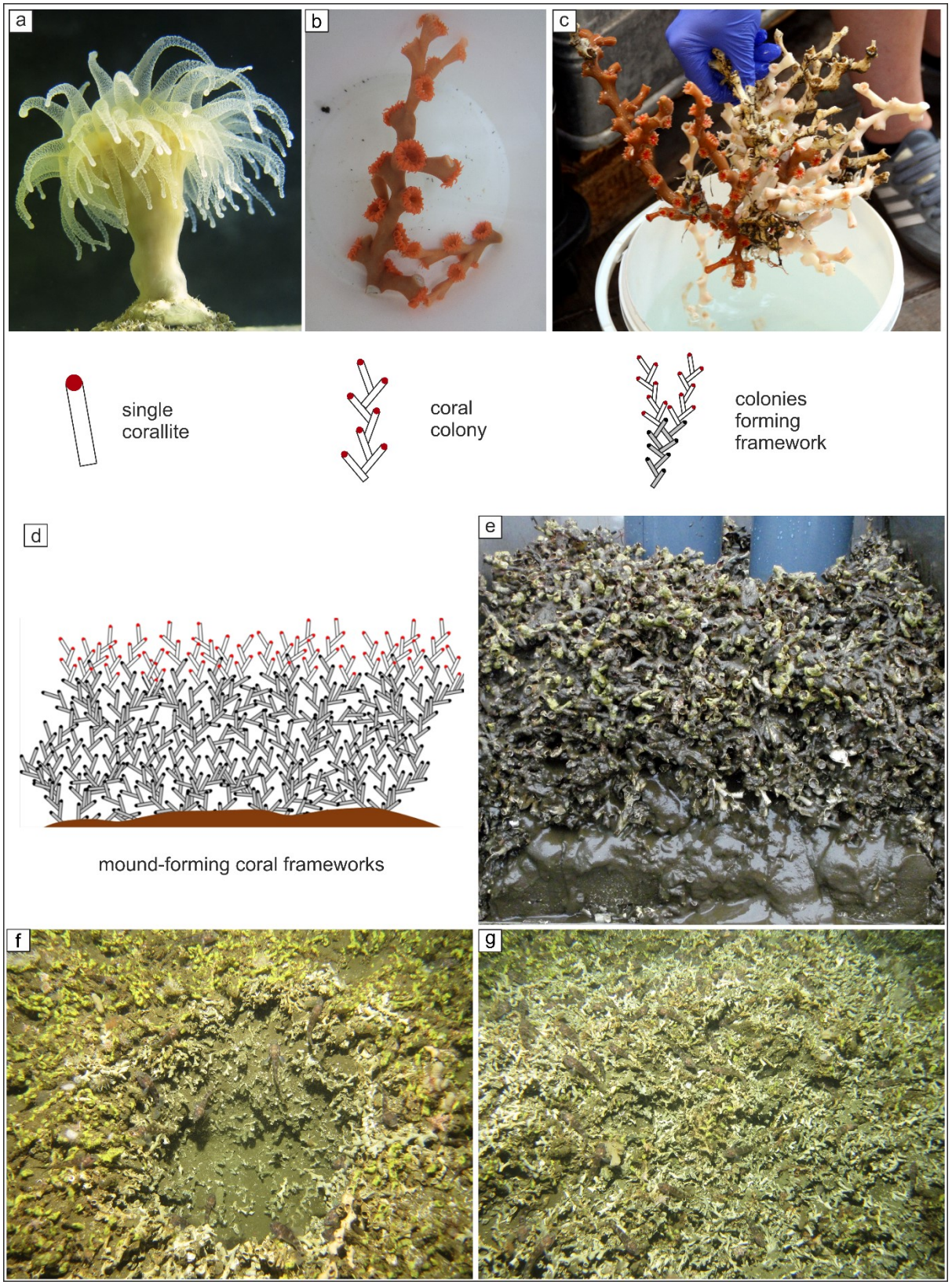

Figure 1.2. From corallites to mounds. a) Solitary coral *D. dianthus*. b) Branch of red *L. pertusa* colony. c) Framework built by different *L. pertusa* colonies (red and white colours indicative of different genomes). d) Sketch illustrating the mound-forming coral elements (based on Hebbeln *et al.*, 2016). e) Lateral view of a giant box core (GeoB20571-1) collected on top of a fossil *Lophelia* mound off Namibia (size of the giant box core: 50x50x55 cm). f) Coral mound surface sampled with a gravity corer, showing the sub-surface composition of the coral mound. g) Dense framework outcropping on the surface of a coral mound. f) and g) are ROV pictures collected off Namibia. Credits: a) A. Gori, University of Salento, Italy; b) M. Lavaleye, NIOZ, The

Netherlands; c) S. Col, GEOMAR, Germany; e) Hebbeln *et al.* (2017), f-g) MARUM ROV Squid Team, University of Bremen, Germany. *Own illustration.*

themselves. The proliferation of framework-forming CWC tends to be favoured where there are already fossil coral frameworks or coral rubble, instead of colonizing new spaces on the seafloor. This can support a continuous or cyclic aggradation of the frameworks and/or the merging of near-by frameworks, including frameworks of different species (De Mol *et al.*, 2005; Wilson, 1979). Coral frameworks can entrap suspended sediments, delivered from the accelerated currents that also contribute to the food supply necessary for the CWC. Over millennial and/or geological timescales, framework-forming CWC and sediments trapped within these frameworks (Fig. 1.2) can build up 3D seafloor structures known as coral mounds (but also described as CWC reefs or ridges). The resulting coral mounds are composed of coral frameworks, subordinate bioclasts (e.g., molluscs associated with the CWC ecosystems), and hemipelagic sediments (Dorschel *et al.*, 2007b; Titschack *et al.*, 2015; Titschack *et al.*, 2009).

CWC frameworks, colonies and reefs might turn into coral mounds only over millennial-geological timescales. As geological structures, coral mounds can be seen as stratigraphic units, which have a distinct origin, a relative age range, and lithological and palaeontological features that differentiate them from their surroundings. Coral mounds should be mappable/identifiable, like stratigraphic units, at the scale of observation. Unlike individual colonies and frameworks, coral mounds are seafloor structures identifiable at the scale of many high-resolution MBES-bathymetric maps.

So far, the most significant framework-forming species are *Lophelia pertusa**, *Madrepora oculata*, *Oculina varicosa*, *Goniocorella dumosa*, *Enallopsammia profunda* and *Solenosmilia variabilis* (Freiwald *et al.*, 2017). These six species have a worldwide distribution, although most of their records are concentrated in the Atlantic Ocean (Fig. 1.3). The coral frameworks of all these species can contribute

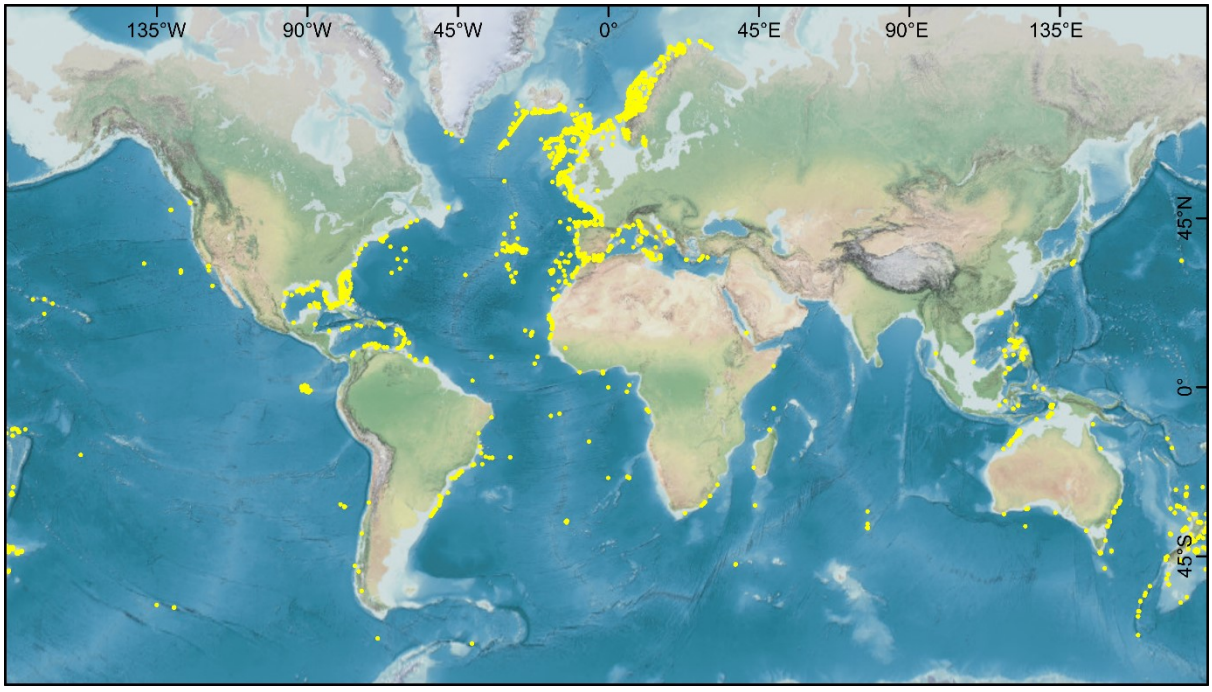

Figure 1.3. Geographical distribution of the six major framework-forming CWC species (*L. pertusa, M. oculata, S. variabilis, O. varicosa, E. profunda*). Based on Freiwald *et al.* (2017). *Own illustration.*

to mound formation (e.g., Cairns, 1996; Hebbeln *et al.*, 2014; Mangini *et al.*, 2010; Reed, 2002; Remia and Taviani, 2005), albeit the most predominant mound-forming species is *L. pertusa*, followed by *M. oculata.*

Azooxanthellate, scleractinian, colonial, framework- and mound-forming: these are the distinctive features of the CWC focus of this thesis. For this reason, the abbreviation "CWC" will be used to simplify the reference to the species with the above-mentioned characteristics.

1.3 Controls on the formation of coral mounds

The development of coral mounds is primarily controlled by the proliferation of the CWC, which in turn is controlled by an interplay and/or sum of different environmental conditions. One prerequisite is the presence of a hard substrate on the seafloor for the initial coral planulae settlement. Independent of the size, any hard element (shells, gravel, hardgrounds, etc.) on the seafloor will be suitable for coral larvae settlement (Wheeler *et al.*, 2007). The hard substrate is a prerequisite only for coral planulae settlement; after the initial stages, the fossil coral frameworks or fragments will be the settling ground for the new coral colonies, as suggested by Wilson (1979). The a hard substrate explains also why CWC colonies occur often in cold-seep sites, where hardgrounds are common (e. g., Hovland and Thomsen, 1997; Le Guilloux *et al.*, 2009).

The most evident ecological need for CWC is already in their name: cold temperature. Active coral mounds have been found in bottom-water temperatures ranging between 5.6 and 12.1°C (Wienberg and Titschack, 2017), a range that covers the optimal thermal range for *L. pertusa* and *M. oculata,* although these two species have been observed in a broader temperature range (1-14°C) (Dorey *et al.*, 2020; Hanz *et al.*, 2019; Mienis *et al.*, 2014).

CWC are sessile and opportunistic suspension-feeders living mostly at intermediate water depths (~200-900 mbsl). Their nutrition is based on variable food sources, including phytoplankton, mesozooplankton, phytodetritus, dissolved organic matter and bacteria (e.g., Dodds *et al.*, 2009; Duineveld *et al.*, 2007; Kiriakoulakis *et al.*, 2005; Mueller *et al.*, 2014; Murray *et al.*, 2019; Purser *et al.*, 2010). Despite this highly-variable diet, the nutrition of the CWC mostly relies on a steady or high-frequency (e.g. semi-diurnal or tidal) periodic supply of food particles (Duineveld *et al.*, 2007; Purser *et al.*, 2010). The proliferation of CWC supported only by a quasi-vertical transfer of food particles produced in ocean surface waters would be possible only under highly productive conditions, due to the low possibility of the passive sinking food particles to encounter the polyps sitting on the vertically-standing frameworks (Hebbeln *et al.*, 2016). A higher probability for the CWC to catch their food particles is offered by a dynamic lateral hydrodynamic regime, which might be represented by geostrophic currents, internal waves/tides, mixing processes resulting from interactions with topography (e.g. Taylor columns),

⋆ the taxon *Lophelia pertusa* has been recently synonymized as *Desmophyllum pertusum*, based on molecular evidence (Addamo *et al.*, 2016; Pratt *et al.*, 2019). This thesis will refer to the largely-used nomenclature (*L. pertusa*), since the question is under debate and more evidences would be necessary for a change of nomenclature of such a well-studied cosmopolitan species like *Lophelia pertusa.*

downwelling, and cascading density currents (e.g., Davies *et al.*, 2009; Frederiksen *et al.*, 1992; Mienis *et al.*, 2009; Mienis *et al.*, 2012b; Taviani *et al.*, 2016; Thiem *et al.*, 2006; White *et al.*, 2005).

Respiration is another essential metabolic process that environmental conditions should guarantee for thriving CWC. However, the consumption of dissolved oxygen in the water column, due to remineralization of organic matter produced in the surface waters, leads CWC to thrive also under relatively low (and sometimes scarce) DO. The lowest DO range for *L. pertusa* was assumed to be 2–3.7 mL L^{-1}, based on field observations (Brooke and Ross, 2014; Dullo *et al.*, 2008; Freiwald *et al.*, 2009; Georgian *et al.*, 2016). However, the recent discovery of coral mound provinces (CMPs) under tropical upwelling zones and associated oxygen minimum zones revealed living (but sporadic) *Lophelia* colonies 1.1–1.4 mL L^{-1} off Mauritania (Ramos *et al.*, 2017; Wienberg *et al.*, 2018) and thriving reefs (with associated large *M. oculata* colonies) even under DO values < 1 mL L^{-1} (Hanz *et al.*, 2019; Hebbeln *et al.*, 2020; Orejas *et al.*, 2021).

Habitat-suitability models (Davies and Guinotte, 2011; Davies *et al.*, 2008; Sundahl *et al.*, 2020; Tittensor *et al.*, 2009) collect several physico-chemical and biological parameters controlling the distribution of the CWC, in addition to the above-mentioned main factors related to the physiological activity of the CWC. Among these additional parameters, a major focus of the recent CWC research was dedicated to pH and aragonite saturation (e.g., Farfan *et al.*, 2018; Hennige *et al.*, 2015; McCulloch *et al.*, 2012), based on ocean acidification as a potential threat for the CWC communities. Field observation and aquaria experiments are showing contrasting results, likely suggesting the potential adaptability of scleractinian CWC towards acidifying conditions (e.g., Büscher *et al.*, 2017; Gómez *et al.*, 2018; Lunden *et al.*, 2014; Maier *et al.*, 2009).

Coral mounds are not only the result of the proliferation of CWC, but they also need additional fitting boundary conditions (e.g., sufficient sediment supply) (Wienberg and Titschack, 2017). However, optimal conditions for the proliferation of CWC are not the requisite *sine qua non* for mound formation. Coral mounds consist of a large portion of hemipelagic sediments (> 50%, Dorschel *et al.*, 2007b; Titschack *et al.*, 2015; Wang *et al.*, 2021). Like food particles, suspended sediments transported by a dynamic lateral bottom regime might be entrapped (or baffled) within the coral frameworks, due to the deceleration/mixing derived from the current-framework interaction (Hebbeln *et al.*, 2016). The deposition of hemipelagic sediments through sediment baffling likely provides a fundamental stabilizing effect on the structure of coral mounds (e.g., Eisele *et al.*, 2014; Huvenne *et al.*, 2009b; Mienis *et al.*, 2009).

The role of the sediment supply highlights that the development of the coral mounds is not only a function of the proliferation of CWC. Indeed, the dataset compiled by Wienberg and Titschack (2017) shows that mound development is likely constrained to more optimal environmental conditions than just bearable conditions for CWC. The mound development as a result of the better conditions in the proliferation of the CWC might be reasonable, considering also potential benefits from the relationship between CWC and the complex ecosystems that might be associated with the coral mounds.

The relevance of the factors controlling mound formation is highlighted by the geographical distribution of coral mounds and their temporal development (see sub-chapter 1.4.6). Furthermore, the development of deep-sea technologies boosting CWC research also has broadened the perspectives as well as the uncertainties regarding mound formation. The dataset on environmental conditions collected from several CMPs show how modern and paleo conditions affect(ed) the formation of coral mounds. However, regional-local factors do not allow a uniform and organized comparison among different CMPs. Also, the information on the "activity" of coral mounds needs to be classified (e.g. active mounds, quiescent mounds with sporadic colonies, inactive or buried mounds). Most of the knowledge on the development of mounds is based on sediment cores, which represent a punctual (not well-georeferenced) and often limited (the mound base is reached only in few exceptional cases) information on the aggradation of coral mounds. The temporal development reconstructed from dating coral skeletons taken at different core depths mostly provides an information on the vertical aggradation of the coral mounds, but they develop laterally more than they do vertically, as shown by many coral mounds where the ratio of mound height/length < 1/5 (e.g., Colman *et al.*, 2005; De Haas *et al.*, 2009; Hebbeln *et al.*, 2019; Huvenne *et al.*, 2003; Lo Iacono *et al.*, 2014; Wienberg and Titschack, 2017). Additionally, there is no other information on the internal structure of the coral mounds that can provide an accurate picture of their spatial and temporal development.

1.4. CWC and coral mounds research following the development of deep-sea technologies

CWC research has been continuously benefited from the development of technologies and methods in surveying, sampling and monitoring deep-sea environments. Indeed, the history of research on CWC and coral mounds followed the milestones of deep-sea technology developmnent. The following paragraphs describe the major scientific and technological achievements in CWC research.

1.4.1. First steps of deep-sea exploration and methodologies behind the CWC research

Until 1990s, the scientific interest and activity regarding CWC was limited to a few studies, with valuable results and observations. However, parallel to these findings, deep-sea exploration brought tools and methods that are currently in use for CWC research. This chapter presents a selection of major discoveries and advancements in deep-sea exploration, also relevant for CWC research. This selection focuses on: spatial analyses and GIS, development of seafloor and subseafloor mapping/imaging tools, underwater observations, sediment coring, water column measurements, navigation and informatics. These milestones in deep-sea exploration are presented in chronological order (and not thematically) to be temporarily correlated with the development of CWC research (see following chapter "Investigation on CWC until the research boost in the 1990s") and likely explaining the timing of the boost in CWC research, as well as the state-of-the-art scientific activity.

After the compilation of soundings for deploying Transatlantic telegraph cable (1958), M. F. Maury published the first deep-sea bathymetric map (based on plumb line measurement) covering most of the North Atlantic and "predicting" the occurrence of the Mid-Atlantic Ridge (Micallef *et al.*, 2018). During the first oceanographic expedition of the 19th century, the Challenger Expedition (1872-1876), ~500 soundings were collected, revealing the Mariana Trench. The General Bathymetric Chart of the Oceans (GEBCO, still actively operating for the production of reference world bathymetric maps) was launched by Prince Albert I of Monaco in 1903 (Carpine-Lancre *et al.*, 2003). In 1894, F. Nansen developed an ocean-water sampler to collect samples at specific depth, known as the Nansen bottle (further developed in 1966, into the Niskin bottle). During late 19th-early 20th centuries, underwater photography started to make its first steps with the first underwater picture of L. Boutan (1893) and the first colour underwater picture taken from the coral reefs of Florida Keys (C. Martin, 1923). Also first underwater video-recordings were taken with the motion pictures and films of J. E. Williamson (*Third leagues under the sea*, 1914).

In 1913, A. Behm was granted German patent No. 282009 for the invention of echo sounding "*Device for measuring depths of the sea and distances and headings of ships or obstacles by means of reflected sound waves"* (Reinking, 2010). The following pioneering echo-sounding systems and seismic imaging, developed before and during WWII, started to collect bathymetric data, confirming the non-flatness of the deep seafloors (Keppner, 1991; Spiess, 1985; Telford *et al.*, 1990; Wille, 2005). In this period, an early gravity corer was deployed in 1938 off California (Emery and Dietz, 1941), although similar sediment coring tools were deployed before that, e.g., during the legacy cruise of the German (first) *R V Meteor* (Bradley *et al.*, 1940; Piggot, 1936; Pratje, 1934). Additionally, the line soundings from *R V Meteor I* documented the existence of the Mid-Atlantic Ridge in the South Atlantic. Advances in piston coring in the 1940s allowed for the recovery of long sediment sections during the deep-sea expedition of the Swedish *R V Albatross* (Pettersson, 1948).

After WWII, radiocarbon and uranium series dating started to progress, especially after the knowledge-gain acquired from the Project Manhattan (Arnold and Libby, 1949; Barnes *et al.*, 1956; Urey, 1947). This was followed by the first application of stable isotopes for paleotemperature reconstruction of biogenic carbonates (Emiliani, 1955; Epstein *et al.*, 1953; McCrea, 1950; Urey *et al.*, 1951). In the 1950s, the first ocean-basin bathymetric map of the North Atlantic was compiled with echo-sounding profiles (Heezen-Tharp physiographic map, Heezen *et al.*, 1959). This map provided for the first time the evidence of the large-scale rift on the top of the Mid-Atlantic Ridge, supporting the upcoming theory of plate tectonics (Barton, 2002). In this period, the first underwater documentaries of F. Quilici (*Sesto continente*, 1954) and J. Costeau (*Le monde du silence*, 1956) brought the poorly-known biological variability of marine ecosystems into the public eye for the first time. The first remotely operated vehicle (ROV), POODLE, was deployed by D. Rebikoff, 1953. Few years later (1957), the Special Purpose Underwater Research Vehicle (SPURV) was the first autonomous underwater vehicle (AUV) deployed.

In early 1960s, the first true operational geographic information system (Canada GIS) was developed thanks to the emerging computer technology (Foresman, 1997). In the mid-1960s, the first uranium-series method was used to date shallow-water corals from Eniwetok Atoll (Pacific O.) and from Bahamas-Florida Keys (Broecker and Thurber, 1965; Thurber *et al.*, 1965). In 1968, the drillship *Glomar Challenger* sailed for the first time, starting the Deep Sea Drilling Project (DSDP), the first international scientific ocean drilling program. It lasted until 1985, and continued as Ocean Drilling Program (ODP, 1985-2003) and International Ocean Discovery Program (IODP, 2003-present) with the *DV JOIDES Resolution*. The DSDP-ODP-IODP expeditions have made cutting-edge discoveries in a wide range of Earth science topics, including past climate and ocean conditions, monsoon systems, seismogenic zones, the formation of continental crust and ocean basins, major extinction events, the role of serpentinization in driving hydrothermal systems, and the temperature limits of life in the deep biosphere (Koopers and Coggon, 2020).

Advancements in engineering sensors for measuring seawater temperature and salinity culminated in 1969 with the invention of the microprofiler, or CTD, by N. Brown (Brown and Morrison, 1978). In the same period, uranium-series datings from Barbados (tropical) coral reefs provided a further evidence of astronomical forcing (Milankovitch cycles) on Quaternary climate processes (Broecker *et al.*, 1968; Mesolella *et al.*, 1969). In these years, first digital devices supported the passage from military to commercial use for single-beam echosounders and side-scan sonars, and the acquisition of 3D seismic surveys necessary for the oil companies (Farr, 1980; Sternlicht, 2017). In 1970s, ground-breaking scientific results in tectonics and marine geology were collected by the GLORIA side-scan sonar, which operated at low frequency to obtain long-range datasets (e.g., Kenyon *et al.*, 1975; Laughton *et al.*, 1972; Searle, 1983). In 1975-1977, the first multibeam echosounders for shallow (Burke and Robson, 1975) and deep waters (Renard and Allenou, 1979) were tested. In the 1980s, MBES were also installed on research vessels, like the deep-sea MBES Hydrosweep DS on board of *RV Meteor (1986)* and *RV Polarstern*. In 1986, the first GIS software was released for desktop computers with a DOS operating system (Zhu, 2016).

The decade from 1980-1990 saw many discoveries of seafloor features as every survey and expedition seemed to find new and sometimes surprising features. This boom in discoveries was due to the increasing ability to define better the shape of seamounts, underwater volcanoes, great fracture zones, great salt domes and canyon pathways (Theberge and Cherkis, 2013). The increased resolution of these surveying tools led to better targeting of both manned submersible and ROV explorations. As the decade went on, navigation systems experienced a quantum leap in absolute positioning capabilities with the Global Positioning System (GPS) becoming increasingly available, although not fully operational until the mid-1990s. This better navigation capability resulted in improved map quality. Besides having an accurate position, the development of the ultra-short baseline positioning system (USBL) and dynamic positioning systems (using directional thrusters) enabled underwater devices to locate and hold the position of the vessel more accurately, respectively (Mandt *et al.*, 2001; Opderbecke, 1997; Vickery, 1998). In these

years, development of MBES made it possible to generate also backscatter records, allowing the characterization of the physical attributes of the seabed (Kostylev *et al.*, 2001; Todd *et al.*, 1999). The MBES technology, as well as other acoustic instrumentation, was revolutionized by the possibility of recording digitally discrete files after the invention of the .mp3 file format (1995).

1.4.2.. Investigation on CWC until the research boost in the 1990s

The first records of CWC were provided by 18th century Scandinavian naturalists (Gunnerus, 1768; Linné, 1758; Pontoppidan, 1755). Afterwards, CWC were mostly in the focus of taxonomists, limited to the dredged samples collected during pioneering deep-sea expeditions (Cairns, 2001a). Among these samples, there are also some fossil frameworks of *L. pertusa* collected at 234–242 mbsl on Walvis Ridge (Marenzeller, 1904; Zibrowius and Gili, 1990). In the following decades, the remarkable information from these first oceanographic expeditions were collected, summarised and updated in several works (Dons, 1944; Joubin, 1922; Le Danois, 1948; Teichert, 1958).

In the late 1960s–1970s, the first direct observation of CWC on the seafloor came with manned research submersibles. The first CWC were directly observed during one of the first dives of the deep-sea submersible *Alvin* on the Blake Plateau, organized after the detection of "coral banks" (Milliman *et al.*, 1967), following earlier echo-sounding observations (Pratt *et al.*, 1962). Echo-sounding detected the first coral mound in the Pacific Ocean (defined as *coppice*) off New Zealand (Squires, 1965) and in the Gulf of Mexico (likely the first coral mound hydroacustically detected, Moore and Bullis Jr, 1960).

Submersible dives in the 1970s on the Little Bahama Banks (Strait of Florida) and the Rockall Bank (off Ireland) revealed large colonies of *L. pertusa*, described as "lithoherms" and "coral patches", respectively (Neumann *et al.*, 1977; Wilson, 1979), followed by the introduction of the term "coral mounds" for CWC-built seabed structures by Mullins *et al.* (1981). During the 1970s–1980s, first radiocarbon and stable isotopic studies were carried out on CWC skeletons (Emiliani *et al.*, 1978; Mikkelsen *et al.*, 1982; Mullins *et al.*, 1981; Swart, 1983; Weber, 1973). Although several discoveries were conducted in marine geosciences during 1980s, the "modern era" of CWC.

1.4.3. The boost of the CWC research and the drilling of Challenger Mound

Some relevant discoveries related to CWC were carried out during the 1990s, with the detection of coral mounds off Norway and Ireland by seismic reflection (Hovland, 1990; Hovland *et al.*, 1994a), as well as the first observation of thriving CWC thanks to internal waves activity (Frederiksen *et al.*, 1992). Although the occurrence of *L. pertusa* has been lengthily documented for Norwegian waters (Dons, 1944; Gunnerus, 1768; Nordgaard, 1912; Sars, 1865; Strömgren, 1971; Teichert, 1958), seismic (Hovland, 1990; Hovland *et al.*, 1994b; Hovland and Thomsen, 1997) and underwater (towed video-camera, ROV, manned submersible) observations (Fosså *et al.*, 2002; Freiwald *et al.*, 1997; Freiwald and Wilson, 1998; Lundalv and Jonsson, 2003; Mortensen *et al.*, 1995) brushed up the knowledge on the CWC colonies/small coral mounds distributed along the Norwegian shelf. The resulting first compilation

of the global distribution of CWC already highlighted the high concentrations of CWC and coral mounds/reefs off Norway (Freiwald, 1998; Rogers, 1999). On the Irish margin, seismic surveys in Porcupine Seabight detected large exposed and buried coral mounds (De Mol *et al.*, 2002; Henriet *et al.*, 1998; Hovland *et al.*, 1994a; Huvenne *et al.*, 2003; Van Rooij *et al.*, 2003) rather than widespread small-sized coral mounds of the Norwegian shelf. Among the results of these studies, the first basic morphometric and spatial information (mound orientation) were reported from a 3D seismic study on the Magellan Mounds (Huvenne *et al.*, 2003). First MBES mapping on the Irish mounds was carried out during an *R V Polarstern* cruise in 2000 (Beyer *et al.*, 2003). Besides, seismic and MBES, high-resolution side-scan sonars were also used to map the coral mounds and the surrounding seafloor (De Haas *et al.*, 2002; Huvenne *et al.*, 2002; Masson *et al.*, 2003; Wheeler *et al.*, 2000). Further relevant discoveries were carried out as part of the Training Through Research (TTR) program (1991-2010). Among the outcomes of the TTR cruises, there is the discovery of the world's tallest coral mounds on Rockall Though (TTR-7, Kenyon *et al.*, 1998) and the coral build-ups in the Gulf of Cadiz (TTR12-14-15 cruises, Foubert *et al.*, 2008) after the CWC colonies discovered on top of the mud volcanoes (Somoza *et al.*, 2003). The discoveries on the Irish margin led to the proposal for the IODP Exp. 307 to drill the Challenger Mound completely, from top to base (Belgica Mounds, Ferdelman *et al.*, 2006). Besides dating the Pliocene onset of the coral mounds off Ireland, the drilled core of the Exp. 307 revealed that the entire structure of the Challenger Mound is composed of a mixture of CWC frameworks and hemipelagic sediments (Kano *et al.*, 2007). The results obtained from the Exp. 307, combined with the continuous development of deep-sea technologies, represent the turning point in the scientific research on coral mounds, from which three major research themes have characterized the investigations on CWC and coral mounds: (i) detection of new CMPs and development of mapping and spatial acquisition and processing techniques, (ii) detection and modelling of environmental conditions for living CWC and development of coral mounds, (iii) reconstruction of the temporal development of coral mounds combined with paleoceanographic information, as well reconstruction of paleoceanographic conditions using fossil CWC.

1.4.4. Discovery and mapping of coral mounds

The drilling of the Challenger Mound also benefited from the resolution of the mapping tools available before the Exp. 307. Many coral mounds on the Irish margin were easily detected due to their large size. Indeed, no mounds have been found to be taller than the one in Rockall Though (Kenyon *et al.*, 1998). The widespread use and improvement of MBES and parametric sub-bottom profilers (e.g., TOPAS, PARASOUND, chirp) installed on research and industry vessels, as well as the combined forces of large international research projects (e.g., ECOMOUND, MOUNDFORCE, HERMES, HERMIONE), has led to discoveries of new coral mounds in the NE Atlantic, as well as of others in other regions. Many additional coral mounds were discovered on the Irish margin: Macnas (Wilson *et al.*, 2007), Enya (Van Rooij *et al.*, 2009), Franken (Wienberg *et al.*, 2008), Viking (Foubert *et al.*, 2011), Arc (Rengstorf

et al., 2012) and the mounds in Dangaerd-Explorer (Stewart *et al.*, 2014) and Porcupine Bank (Mazzini *et al.*, 2012) canyons. Further CMPs in the NE Atlantic were discovered on the Scottish (Roberts *et al.*, 2005a) and Norwegian shelves (Fosså *et al.*, 2005; Lindberg *et al.*, 2007; Mortensen *et al.*, 2001), as well as along the Iberian margin-Gulf of Biscay (Collart *et al.*, 2018; De Mol *et al.*, 2011; Somoza *et al.*, 2014). The availability of deep-sea technologies uncovered new CMPs, like Santa Maria di Leuca (Savini and Corselli, 2010; Taviani *et al.*, 2005) in the Mediterranean Sea, although the occurrence of CWC colonies here was known for decades (Zibrowius, 1980 and references therein). Further CMPs in the Mediterranean Sea were found in the Alboran Sea (East Melilla, Comas *et al.*, 2009; Cabliers, Corbera *et al.*, 2019; West Melilla, Lo Iacono *et al.*, 2014; Chella Bank, Lo Iacono *et al.*, 2019), Tyrrhenian Sea (Angeletti *et al.*, 2020; Remia and Taviani, 2005) and Strait of Sicily (Martorelli *et al.*, 2011).

The Gulf of Cadiz is a region hosting several mud volcanoes (e.g., Menapace *et al.*, 2021) and their investigation provided the first evidence of CWC colonies in this region (Pinheiro *et al.*, 2003; Somoza *et al.*, 2003). Profiting from exposure to an enhanced local hydrodynamic regime offered by the mud volcano reliefs and the hard substrate from authigenic seep-carbonates (Rincón-Tomás *et al.*, 2019), CWC might build >1m on the surface of mud volcanoes, as observed by a camera sledge (Wienberg *et al.*, 2009). After the discovery of coral mounds on Renard Ridge and Pen Duick Escarpment (Foubert *et al.*, 2008; Van Rooij *et al.*, 2011), further findings were made moving southward along the Atlantic Moroccan margin. Here, one of the largest CMP so far discovered, with more than 3400 coral mounds on the seafloor and 781 buried coral mounds, were detected by MBES (Hebbeln *et al.*, 2019) and seismic-PARASOUND sub-bottom profiles (Vandorpe *et al.*, 2017). Further south, side-scan sonar detected a CMP close to the Agadir canyon (Glogowski *et al.*, 2015).

The exploration of coral mounds along the western African margin started with the detection of the Mauritanian "wall", an almost continuous slope-parallel complex of coral mounds/ridges extending for ~400 km, firstly (partly) mapped with 3D seismic by Colman *et al.* (2005). So far, MBES mapping revealed few other coral mounds along the W African margins in low latitudes, like the Ghana mound (Buhl-Mortensen *et al.*, 2017a), the mound-like structures in the Congo canyon (Gay *et al.*, 2007) and a CMP on the northern Angolan margin (Le Guilloux *et al.*, 2009). The last CMPs discovered on the SW African margin were the coral mounds south of Cuanza river (Angolan margin) and off the Skeleton Coast (Namibian shelf, Hebbeln *et al.*, 2017), as well as a cluster of coral mounds south of the Kunene river (Rush *et al.*, 2019).

Several CMPs have been also detected along the western margins of the Atlantic Ocean. MBES mapping has revealed the morphology of Cape Lookout mounds (Mienis *et al.*, 2014), although coral banks north of the Blake Ridge were the first mounds acoustically-detected (Pratt *et al.*, 1962). After the detection of the coral mounds in Blake Ridge, most of the research activity on the coral mounds "shifted" south towards the Straits of Florida (Anselmetti *et al.*, 2000; Correa *et al.*, 2012a; Correa *et al.*, 2012b; Grasmueck *et al.*, 2006; Mullins *et al.*, 1981; Neumann *et al.*, 1977; Paull *et al.*, 2010; Reed, 2002). Occurrences of CWC colonies and build-ups were also known for long time in the Gulf of Mexico

(Cairns, 1979; de Pourtalès, 1871; Moore and Bullis Jr, 1960; Smith, 1954), but only recently have these sites were been extensively studied, especially for constraining the relationship between CWC and environmental conditions (e.g., Davies *et al.*, 2010; Hebbeln *et al.*, 2014; Lunden *et al.*, 2014; Mienis *et al.*, 2012b). A few discoveries of CMPs also came from the South American margin. After exploratory data collected by Viana *et al.* (1998), the coral mounds of the Campos and Santos Basins (off Brazil) were first MBES-mapped by Bahr *et al.* (2016). Farther south, other CMPs have been found along the Uruguayan (Carranza *et al.*, 2012) and Patagonian margins (Muñoz *et al.*, 2012). Only recently a large CMP has been detected (MBES and sub-bottom profiler) along the northern Argentinian margin (Steinmann *et al.*, 2020).

In 20 years, improved mapping technologies brought our knowledge of coral mounds from the few giant coral mounds on the Irish margin and reefs on the Norwegian shelf to several CMPs (and thousands of coral mounds) all around the Atlantic margins (Fig. 1.4). So far, no CMPs have been discovered outside the Atlantic Ocean, but several CWC ecosystems have been detected, mapped and observed by using the abovementioned deep-sea technologies in the Indian (e.g., Reolid *et al.*, 2017) and Pacific (e.g., Mackay *et al.*, 2014) Oceans.

Compared to the distribution of the six mound-forming species (Fig. 1.3), the global distribution of coral mounds (Fig. 1.4) follows a distinct control: closeness to the continents. Many CWC colonies have been observed far from continental margins (e.g., Baco *et al.*, 2017; Mortensen *et al.*, 2008; Robinson *et al.*, 2007), where the lack of sediment supply does not allow the formation of coral mounds, suggesting the closeness to continents of the CMPs reflecting the sediment supply as an important control on the distribution of coral mounds. Contrarily, fast or abundant sediment load might cause even the burial of (inactive/quiescent) coral mounds as observed in the seismic profiles in several CMPs (e.g., Huvenne *et al.*, 2003; Vandorpe *et al.*, 2017). Coral mounds do not only share a common closeness to the continent but they are often associated with contouritic/drift deposits (Hebbeln *et al.*, 2016). The closeness to sediment sources (continents) and sediment bodies related to vigorous current regimes suggest that a balanced sediment supply is not only fundamental for mound formation but also strongly controls their basin-scale distribution.

Most of the locations of coral mounds shown in Fig. 1.4 have been mapped by hull-mounted MBES, making it the most cost-efficient acoustic tool for the detection and collection of first exploratory data on coral mounds. However, MBES is a depth-dependent tool (resolution and accuracy decreasing with water depth), limiting the detection of small structures (e.g., Douarin *et al.*, 2013; MAREANO, 2020; Tamborrino *et al.*, 2019) and the collection of high-quality data for (geo)morphometric-based ecological investigations (Sundahl *et al.*, 2020; Tamborrino *et al.*, submitted) mostly on continental shelves. Therefore, towed equipment has played a key role in the discovery and investigation of small coral mounds in deeper waters, like the Moira Mounds first detected with a deep-towed side-scan sonar (Wheeler *et al.*, 2000). In addition, this approach offered relatively detailed imagery of the surface of the

first coral mounds investigated (De Mol *et al.*, 2002; Freiwald *et al.*, 2002; Huvenne *et al.*, 2002; Kenyon *et al.*, 2003; Masson *et al.*, 2003; O'Reilly *et al.*, 2003).

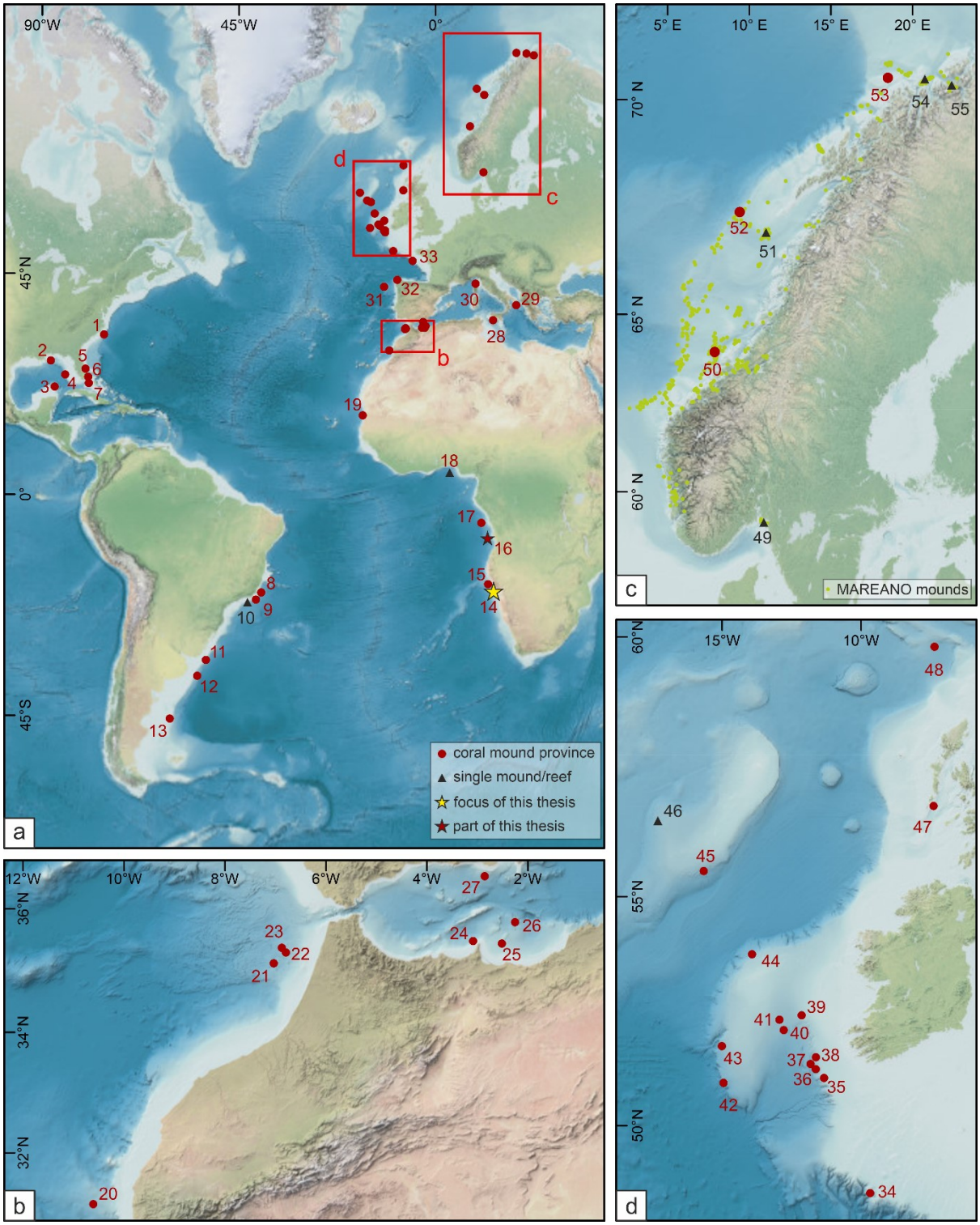

Figure 1.4. A. Distribution of coral mounds and reefs along the Atlantic margins and Mediterranean Sea, with close view on the Moroccan-Alboran margins (B), Norwegian margin (yellow dots, MAREANO data) (C) and Irish-Scottish margin (D). 1, Cape Lookout (Mienis *et al.*, 2014; Pratt *et al.*, 1962). 2, Vioska Knoll (Brooke and Schroeder, 2007; Davies *et al.*, 2010). 3, Campeche (Hebbeln *et al.*, 2014; Hübscher *et al.*, 2010). 4, West Florida (Neumann *et al.*, 1977). 5, *Oculina* reefs (Reed, 2002). 6, Bimini mounds (Hebbeln *et al.*, 2012). 7, Santaren Channel (Correa *et al.*, 2012b; Grasmueck *et al.*, 2006). 8, Campos Basin (Lopes and Hajdu, 2014; Viana *et al.*, 1998). 9, Santos Basin (Mazzini *et al.*, 2012). 10, Bowie *Solenosmilia*-mound (Raddatz *et al.*, 2020). 11, Uruguay (Carranza *et al.*, 2012). 12, Ewing Terrace mounds (Steinmann *et al.*, 2020). 13, Nagera –

Perito Moreno Terraces (Muñoz *et al.*, 2012). 14, Namibian mounds (Tamborrino *et al.*, 2019). 15, "Kunene" mounds (Rush *et al.*, 2019). 16, "Cuanza" mounds (Hebbeln *et al.*, 2020; Orejas *et al.*, 2021). 17, Angolan mini mounds (Le Guilloux *et al.*, 2009). 18, Ghana (Buhl-Mortensen *et al.*, 2017a). 19, Mauretania (Colman *et al.*, 2005). 20, Eugen Seibolds (Glogowski *et al.*, 2015). 21, Atlantic Morocco (Hebbeln *et al.*, 2019; Vandorpe *et al.*, 2017). 22, Pen Duick Escarpment (Foubert *et al.*, 2008; Van Rooij *et al.*, 2011). 23, Renard Ridge (Foubert *et al.*, 2008; Wienberg *et al.*, 2010). 24, West Melilla (Lo Iacono *et al.*, 2014). 25, East Melilla (Colman *et al.*, 2005; Fink *et al.*, 2013). 26, Cabliers (Corbera *et al.*, 2019). 27 Chella Bank (Lo Iacono *et al.*, 2019). 28, Strait of Sicily (Martorelli *et al.*, 2011). 29, Santa Maria di Leuca (Bargain *et al.*, 2017; Savini and Corselli, 2010; Taviani *et al.*, 2005). 30, Tuscan Archipelago (Angeletti *et al.*, 2020; Remia and Taviani, 2005). 31, Galicia Bank mini-mounds (Somoza *et al.*, 2014). 32, Ferrol canyon (Collart *et al.*, 2018). 33, Penmarc'h & Guilvinec Canyons (De Mol *et al.*, 2011). 34, Explorer-Dangeard canyon (Stewart *et al.*, 2014). 35 Enya (Van Rooij *et al.*, 2009). 36 Belgica (Beyer *et al.*, 2003; De Mol *et al.*, 2002; Foubert *et al.*, 2005; Wienberg *et al.*, 2020). 37, Moira (Foubert *et al.*, 2011; Lim *et al.*, 2018; Wheeler *et al.*, 2011). 38, Macnas (Wilson *et al.*, 2007). 39, Viking (Foubert *et al.*, 2011). 40, Hovland-Propeller (Dorschel *et al.*, 2007b; Heindel *et al.*, 2010; Hovland *et al.*, 1994a; Rüggeberg *et al.*, 2007). 41, Magellan (Hovland *et al.*, 1994a; Huvenne *et al.*, 2003). 42, Arc (Mohn *et al.*, 2014). 43, Porcupine Bank canyon (Mazzini *et al.*, 2012). 44, Pelagia (De Haas *et al.*, 2009; Kenyon *et al.*, 2003). 45, Logachev (De Haas *et al.*, 2009; Kenyon *et al.*, 2003; Mienis *et al.*, 2006). 46, Francken (Wienberg *et al.*, 2008). 47, Mingulay (De Clippele *et al.*, 2017a; Douarin *et al.*, 2013). 48, Darwin (Huvenne *et al.*, 2009a; Masson *et al.*, 2003; Wheeler *et al.*, 2008). 49, Tisler reef (De Clippele *et al.*, 2017b; Lavaleye *et al.*, 2009). 50, Sula reef (Freiwald *et al.*, 2002). 51, Traena (Cathalot *et al.*, 2015; Fosså *et al.*, 2005; Lindberg, 2004). 52, Røst Reef (Fosså *et al.*, 2002; Purser *et al.*, 2013). 53, Stjernsund (Freiwald *et al.*, 1997; Rüggeberg *et al.*, 2011). 54, Fugloy reef (Lindberg *et al.*, 2007). 55. Lopphavet reef (Stalder *et al.*, 2014).

The availability of AUV- and ROV-MBES improved resolution in mapping coral mounds, highlighting mound morphological variability (Correa *et al.*, 2012b; Lim *et al.*, 2018) and providing detailed information of mound sedimentary context (Foubert *et al.*, 2011). Advances in mapping even enabled the mapping of CWC colonies on vertical submarine cliffs (Huvenne *et al.*, 2011). The collection of video and images has opened great opportunities to investigate in detail the sedimentology and ecology on the surface of a coral mound, with studies on sedimentary facies distribution (Dorschel *et al.*, 2007a; Heindel *et al.*, 2010; Wienberg *et al.*, 2013) and habitat mapping (De Clippele *et al.*, 2017a; Lim *et al.*, 2017; Purser *et al.*, 2009). The increasing resolution of MBES and the availability of imagery data has followed also the improvement of processing the datasets acquired, passing from manual, to automated and then to machine-learning-based approaches through time (Lim *et al.*, 2021). However, the focus of these spatial-mapping investigations has initially been on the ecological aspects of CWC colonies and their associated fauna (e.g., Boolukos *et al.*, 2019; Corbera *et al.*, 2019; De Clippele *et al.*, 2021a; Dolan *et al.*, 2008; Georgian *et al.*, 2014; Guinan *et al.*, 2009; Vertino *et al.*, 2010) rather than on coral mounds as morphological features.

1.4.5. Defining environmental conditions allowing CWC to thrive

The occurrences of *L. pertusa* connected to enhanced current regimes has been known since the beginning of the 20th century (Murray and Hjort, 1912), followed by other studies suggesting that topographic features could have positively affected current velocities and food supply for CWC (Broch, 1922; Dons, 1944; Strömgren, 1971; Tambs-Lyche, 1958). The interplay of hydrodynamic regime with topography as a measn to generate potentially favourable conditions for CWC (non-scleractinian) was first confirmed by Genin *et al.* (1986). Frederiksen *et al.* (1992) first identified the occurrence of *L. pertusa* to be related to the action of internal tides, which represents a constant hydrodynamic regime

ideal for supporting the food supply to CWC. The focus on the process of the formation of coral mounds shifted from the "hydrodynamic" to the "hydraulic theory" during the 1990s, with the discoveries of hydrocarbon seepage in the proximity of Norwegian CWC reefs (Hovland, 1990; Hovland and Thomsen, 1997) as well as the detection of the giant coral mounds off Ireland (Hovland *et al.*, 1994a) interpreted as knolls linked to hydrocarbon seepage, and even gas hydrates (Henriet *et al.*, 1998). This led to the "hydraulic theory" (Hovland and Mortensen, 1999), which suggest that CWC are partly fed by a food chain based on chemosynthetic methanotrophic bacteria, as well as other macrofaunal species associated with cold seeps (Sahling *et al.*, 2002; Sibuet and Olu, 1998). However, no evidence has been provided to support the direct relationship between CWC and hydrocarbon seepage. The "hydraulic theory" was in part disproved by the first submersible and aquaria observations of CWC actively capturing live prey and dead food particles (Freiwald, 2002; Mortensen *et al.*, 2001). Further evidence was provided by the lack of C^{13}-depleted skeletons and organic tissues of *L. pertusa* (Duineveld *et al.*, 2004; Spiro *et al.*, 2000), excluding the assimilation of hydrocarbon-derived carbon with its extremely low δ^{13} values (Whiticar, 1999). The drilling of Challenger Mound was also proposed to obtain evidence supporting the "hydraulic evidence" (Henriet *et al.*, 2002). However, the material collected during Exp. 307 showed that the coral mound is entirely composed of a mixture of coral frameworks and hemipelagic sediment, with no signals (sedimentological, geochemical or microbiological) of hydrocarbon seepage (Ferdelman *et al.*, 2006; William *et al.*, 2006). The only potential (indirect) support for CWC that can be provided by hydrocarbon seepage is the precipitation of authigenic seep carbonates (e.g., Aloisi *et al.*, 2000; Peckmann and Thiel, 2004) derived from the anaerobic oxidation of methane (Boetius *et al.*, 2000; Orphan *et al.*, 2001). Indeed, seep-carbonates might provide a suitable hard substrate for CWC colonies, as observed in the Gulf of Mexico and Gulf of Cadiz (Cordes *et al.*, 2008; Rincón-Tomás *et al.*, 2019; Schroeder, 2002).

Consequently with the lack of supporting evidence for the "hydraulic theory", studies on coral mounds after Exp. 307 started to collect more data (relatively scarce until the 2000s) to confirm that the development of coral mounds relies mostly on specific environmental conditions. First evidences for an important role of a dynamic hydrodynamic regime were provided by the observation of contourite channels, sand sheets, sediment waves and ripples in the mound provinces, as well as scoured out moats and tails associated with many mounds (De Mol *et al.*, 2005; De Mol *et al.*, 2002; Dorschel *et al.*, 2005; Huvenne *et al.*, 2003; Masson *et al.*, 2003; Mienis *et al.*, 2006; Rüggeberg *et al.*, 2005; Van Rooij *et al.*, 2003; Wheeler *et al.*, 2005). However, these geomorphological-sedimentary results could not prove the direct relationship between the development of coral mounds and hydrodynamic-hydrographic conditions. The environmental control on CWC has been mostly demonstrated (until nowadays) by only three major research approaches: (i) definition of the boundary conditions, (ii) identification of the most-favourable supporting conditions, and (iii) modelling of oceanographic datasets.

The first overview of the oceanographic boundary conditions for CWC (temperature, salinity, dissolved oxygen) was presented by Freiwald (2002), based on the first compilation of the global distribution of

CWC (Rogers, 1999) and continued as the UNEP global distribution of CWC (first issue, Freiwald *et al.*, 2004; last update, Freiwald *et al.*, 2021). These studies were the first to constrain favourable conditions for CWC and also represented the starting point for habitat-suitability models based on global oceanograpahic datasets (Davies and Guinotte, 2011; Davies *et al.*, 2008; Tittensor *et al.*, 2009). The probability that *L. pertusa* and other CWC colonies flourish in specific habitats is also supported by several environmental conditions (e.g., aragonite saturation, dissolved inorganic carbon, nitrate, phosphate, silicate, pH, particulate organic carbon, primary and export production, Flögel *et al.*, 2014). Among all these parameters, food supply seems to play the most relevant condition for thriving CWC colonies (Buhl-Mortensen *et al.*, 2017b; Portilho-Ramos *et al.*, 2022). Turning the CWC colonies into coral mounds require that favourable conditions for CWC are maintained over millennial timescales, combined with sufficient sediment supply, as suggested by the compilation of Wienberg and Titschack (2017). The discoveries of new CMPs (e.g., CMPs under low dissolved oxygen concentrations; Colman *et al.*, 2005; Hanz *et al.*, 2019; Hebbeln *et al.*, 2020; Ramos *et al.*, 2017; Wienberg *et al.*, 2018), as well as by several biological studies based on aquaria experiments (Baussant *et al.*, 2017; e.g., Brooke and Young, 2009; Büscher *et al.*, 2017; Dorey *et al.*, 2020; Hennige *et al.*, 2014; Larsson *et al.*, 2013; Lunden *et al.*, 2014; Maier *et al.*, 2009; Naumann *et al.*, 2014; Orejas *et al.*, 2016; Weinnig *et al.*, 2020) constantly improve the definition of the boundary conditions for CWC. The wide range of boundary conditions detected so far likely suggests a potential capacity of CWC to cope with quite different environmental conditions (phenotypic plasticity) apparently without evident genetic variations (Flot *et al.*, 2013).

The definition of the boundary conditions relies upon measurement of environmental conditions, which are mostly recorded by CTD (conductivity-temperature-depth) casts/rosette since the firsts CWC-focused research cruises (Duineveld *et al.*, 2004; Freiwald and Dullo, 2000; Hebbeln *et al.*, 2006; Roberts *et al.*, 2003; Taviani *et al.*, 2005). By chasing the salinity-oxygen-temperature thresholds of the environmental envelope of CWC, water column measurements by CTD has offered another perspective on how hydrography controls the proliferation of CWC and coral mound formation. In this context, a few studies have focused on salinity as a potential major environmental control on coral mound formation (e.g., the role of Mediterranean Outflow Waters for the Belgica Mounds, De Mol *et al.*, 2002; Freiwald, 2002; Wheeler *et al.*, 2005). White (2007) first identified how the geometry of water masses can control the benthic hydrodynamic regime (internal waves/tides) and therefore the delivery of food particles to CWC colonies. Dullo *et al.* (2008) highlighted that salinity had an indirect control on CWC, and therefore on coral mounds, by identifying the (potential) density of water masses and density gradients as a key factor for the support and distribution of CWC. The link between the distribution of coral mounds and thermo/pycnocline was confirmed by the hydrographic-hydrodynamic data of White and Dorschel (2010). After these findings, the collection of water mass information become relevant for the research on CWC, as highlighted on CTD data collected in several research cruises (e.g., Bahr *et al.*, 2016; De Mol *et al.*, 2011; Hebbeln *et al.*, 2020; Hebbeln *et al.*, 2014; Mienis and de Haas, 2004; Rüggeberg *et al.*, 2011) or by reconstructing water column with previously collected data (De Clippele

et al., 2021b; Kazanidis *et al.*, 2021; Steinmann *et al.*, 2020). Recently, environmental conditions can be measured also by CTD profiler mounted on ROV during their dives/transects across coral mounds, offering the chance to collect more detailed information on environmental conditions in the proximity of CWC colonies (e.g., Boolukos *et al.*, 2019; Orejas *et al.*, 2021).

The measuring of benthic environmental conditions has likely provided the most relevant evidence for the role of the hydrodynamic regime as a supporting factor for CWC proliferation and coral mound formation. A compilation of hydro-biogeochemical and physical parameters of bottom seawaters of different CWC sites in the NE Atlantic updated the environmental envelope for CWC (Flögel *et al.*, 2014), but it did not offer any information about the hydrodynamics acting at the mound surface. Duineveld *et al.* (1997, 2000) deployed the first free-falling benthic lander (BOLAS) in the Porcupine Seabight, although not for CWC research. The development of multi-sensor benthic lander (BOBO, van Weering *et al.*, 2000) enabled the acquisition of long-term records of physical (temperature, salinity, turbidity) and hydrodynamic (near-bottom current velocity, particulate flux) parameters at the surface of several coral mounds located in Rockall Though (Mienis *et al.*, 2007). These datasets (collected from 1999 - 2006), coupled with CTD measurements, detected the action of internal tides/waves where living corals have been found (on top of the mounds). Vigorous current regimes were also recorded by photolander deployments at the Sula Ridge and in the Belgica CMP (Roberts *et al.*, 2005b). The data from benthic lander (BOBO, Logachev mounds, Fig. 1.4d) of Duineveld *et al.* (2007) showed stronger current regimes off mounds, but the analyses on the organic particles collected demonstrated that the smoother hydrodynamic regime of the internal tides delivered fresh particles laterally to the CWC. These results likely predicted/suggested that the current regime should be strong enough to support CWC, but without being too strong to compromise the efficiency of prey/food particle capture of the CWC polyps (Gori *et al.*, 2015; Orejas *et al.*, 2016; Purser *et al.*, 2010). With current meter (cluster of acoustic doppler current profilers, ADCP) data, Dorschel *et al.* (2007a) discerned which current regime (geostrophic poleward current or internal tides) likely controlled facies distribution and the mound development for Galway Mound (Belgica mound province). In addition to the data from the Irish margins, new evidence from benthic measurements came from other CMPs, confirming the primary role of internal waves/tides in supporting CWC (Hanz *et al.*, 2019; Mienis *et al.*, 2012a; Mienis *et al.*, 2012b), as well as conditions that might negatively affect CWC colonies (Hanz *et al.*, 2019; Mienis *et al.*, 2014). Latest benthic landers, developed with new sensors (e.g., ADCP, De Clippele *et al.*, 2017b) and with high-precision ROV-guided deployment, improved the efficient acquisition of environmental data (Lim *et al.*, 2020; Wheeler *et al.*, 2021)

The data collected with benthic landers are often coupled with CTD data combined with other sources (ADCP, satellite, world ocean database), and combined offer valuable datasets for modeling oceanographic conditions favouring CWC proliferation. Coupling surface ocean productivity data with current regime models at regional scale brought White *et al.* (2005) to conceptualize a valid food source-supply mechanism for the proliferation of CWC over the topographic feature of Rockall Trough (Irish

margin, NE Atlantic). A similar model has been generated by Thiem *et al.* (2006) with information collected on the Norwegian margin. The combination of the global tides model and current meter data highlighted the "tidal" nature of the benthic regime at coral mounds (White *et al.*, 2007). Through high-resolution modeling of oceanographic conditions at the scale of three CMPs (Logachev, Arc and Belgica, Fig. 1.4d), Mohn *et al.* (2014) showed that a constantly intensified hydrodynamic regime corresponds to coral occurrences and that only ephemeral currents appeared in non-coral sites. CTD data and models have been also used to highlight potential climate-induced threats for CWC (Findlay *et al.*, 2013).
Modeling also helped to understand the influence of a coral mound itself on the hydrodynamic regime. Scouring at the mound footprint was observed for many coral mounds with different mapping tools and interpreted as erosional feature derived from the interaction between the bottom current regime and coral mounds (Correa *et al.*, 2012b; Huvenne *et al.*, 2003; Masson *et al.*, 2003; Mienis *et al.*, 2006; Wheeler *et al.*, 2007). However, only the numerical simulations of Cyr *et al.* (2016) showed how the coral mounds themselves influence the hydrodynamic regime and how in turn this influcence is dependent on the size of the coral mounds. The latest frontier in modeling environmental conditions for CWC is represented by the "self-assembly" approach. These models consider mound development as summary of positive or negative feedbacks, which corresponds to processes or environmental conditions that positively or negatively control mound formation (van der Kaaden *et al.*, 2020).

1.4.6. Coring the coral mounds: reconstructing the history of CWC, reconstructing their environment

Like any carbonate-secreting organisms, the aragonitic skeletons of CWC precipitated in equilibrium with the environmental physico-chemical conditions under which the CWC lived. By analysing the geochemical composition of CWC skeletons it is then possible to determine their age (dating) and the environmental conditions in which they lived (paleoceanographic proxy).
The determination of the age of CWC provides valuable insights into their temporal occurrence* and the temporal development of coral mounds. Radiocarbon and uranium-series dating are the most common techniques to reconstruct the development of coral mounds, which can provide ages mostly for recent material (radiocarbon: 40-50 kyr; U-series: ~500 kyr; Wienberg and Titschack, 2017). For this purpose, datings can be carried out on coral fragments taken from surface sediment samples (grab sampler, box corer) and from sediment cores (gravity, piston and drilling cores) collected from coral mounds, providing information on the latest CWC temporal occurrence (surface sample) or on a portion of (and in few cases, the entire) aggradational history of a coral mound (core samples).

The first dating results to investigate the development of coral mounds through core material were conducted by Dorschel *et al.* (2005) and Frank *et al.* (2005), followed by the datings of CWC skeletons from Challenger Mound, drilled during the IODP Exp. 307. Uniquely, Challenger Mound samples were dated with strontium isotopes (Kano *et al.*, 2007), considering the potential age (Miocene–Pliocene boundary) of the erosional discontinuity identified at the base of the mound by seismic reflection (De Mol *et al.*, 2002; Van Rooij *et al.*, 2003) and the shipboard nannofossil biostratigraphic reconstruction (Ferdelman *et al.*, 2006). Besides the absence of any signs for the hydraulic support for CWC, the findings of the IODP Exp. 307 represent a stepping stone for understanding the temporal development of coral mounds for several reasons:

(i) coral mounds are completely built by CWC. During the Exp. 307, *DV JOIDES Resolution* drilled the whole Challenger Mound and the underlying sediments (Ferdelman *et al.*, 2006). At that time, there was no evidence that the entire structure of coral mounds could be made up by a mix of coral frameworks and the baffled hemipelagic sediments. Indeed, these structures were named as "carbonate mud mound", "lithoherm", "coral-topped mounds", etc. (see De Mol *et al.*, 2002; Roberts *et al.*, 2006);

(ii) the onset of modern coral mounds in the Atlantic Ocean dated at the beginning of the Pliocene (Fig. 1.1), coinciding with the intensification of the northern hemisphere glaciations (Kano *et al.*, 2007);

(iii) the development of coral mounds is not stratigraphically and/or temporally continuous, and it might contain stratigraphic hiatuses that are also very long compared to the whole aggradational history (in the case of the Challenger Mound., hiatus between 1.7–1.0 Ma; Kano *et al.*, 2007).

Combined with the datings from the gravity cores from Propeller Mound (Dorschel *et al.*, 2005) and surface material from several mound locations (Schröder-Ritzrau *et al.*, 2005), the results from IODP Exp. 307 showed that the temporal development of coral mounds is likely controlled by glacial-interglacial cycles, as highlighted by Roberts *et al.* (2006). The glacial-interglacial influence was observed also by the first paleoceanographic reconstructions of productivity (De Haas *et al.*, 2009; Dorschel *et al.*, 2005; Eisele *et al.*, 2008; Foubert *et al.*, 2007; Rüggeberg *et al.*, 2007).

Until today, many paleo-reconstructions of coral mound development mostly confirm that glacial-interglacial cycle impact on CWC ecosystems over millennial timescales. The first datings from the NE Atlantic highlighted a north-south trend (Frank *et al.*, 2011), with northern CMPs (off Ireland, Norway) mostly developed during interglacial periods (Dorschel *et al.*, 2007b; Eisele *et al.*, 2008; Frank *et al.*, 2009; López Correa *et al.*, 2012; Raddatz *et al.*, 2014; van der Land *et al.*, 2014), while southern CMPs (Morocco, Mauritania) formed predominantly during ice ages (Eisele *et al.*, 2011; Frank *et al.*, 2011;

*NB, In this thesis, the term „CWC" refer to mound-forming colonial scleractinian CWC. There are many studies focused on temporal development, as well as reconstructions of paleocenographic conditions, based on solitary scleractinian, soft CWC, hydrozoans, and using dating (U-series, radiometric carbon), sclerochronology, stable isotopes and element ratios (e.g., Adkins *et al.*, 1998; Anagnostou *et al.*, 2011; Andrews *et al.*, 2005; Cheng *et al.*, 2000; Delibrias and Taviani, 1984; Druffel *et al.*, 1990; Gagnon *et al.*, 2007; Hemsing *et al.*, 2018; Hill *et al.*, 2011; King *et al.*, 2018; Little *et al.*, 2021; Mangini *et al.*, 1998; Montagna *et al.*, 2006; Pratt *et al.*, 2019; Roark *et al.*, 2005; Robinson *et al.*, 2006; Robinson *et al.*, 2014; Samperiz *et al.*, 2020; Sherwood and Risk, 2007; Smith *et al.*, 1997; Smith *et al.*, 2000; Studer *et al.*, 2018; Thresher *et al.*, 2011; van de Flierdt *et al.*, 2010; Wang *et al.*, 2017; Wilson *et al.*, 2014).

Wienberg *et al.*, 2010; Wienberg *et al.*, 2009). Several local conditions might be variably affected by glacial–interglacial cycles, providing a unique aggradational history for any CMP, or even single mounds. As food availability as the main supportive control for CWC, palaeoceanographic reconstructions showed that increased primary productivity and export production can be considered a key parameter for coral mound development (Eisele *et al.*, 2011; Fink *et al.*, 2013; Stalder *et al.*, 2015; Wienberg *et al.*, 2010). On millennial timescales, primary productivity is strongly influenced by orbitally-forced variations of wind stress and hydrological processes. Indeed, mound aggradational histories might follow insolation-controlled processes like the monsoonal cycle (Bahr *et al.*, 2020), as well as being interrupted or ceased by the depletion in benthic dissolved oxygen linked to sapropel formation (Corbera *et al.*, 2021; Fink *et al.*, 2012) or upwelling/oxygen minimum zone intensification in the eastern boundary upwelling systems (Tamborrino *et al.*, 2019; Wienberg *et al.*, 2018).

Considering the key role of productivity, a direct effect of the glacial–interglacial cycle on the development of coral mounds might be considered most relevant through eustatic sea-level variations. So far, actual CMPs on continental shelves developed only during the Holocene (Douarin *et al.*, 2013; López Correa *et al.*, 2012; Tamborrino *et al.*, 2019), likely as a result of the post-Younger Dryas sea level rise. The location of these shallow-water CMPs in high latitudes and upwelling regions suggest that their formation relied on the interglacial generation of aggradation space for coral mounds and a decrease in benthic seawater temperature, combined with fundamental pre-requisites like high productivity and food supply. Along the continental slopes, changes in sea level might correspond also to vertical relocations of water mass boundaries. Consequently, these changes in water mass geometry might be detected by the development of coral mounds linked to the intensification of intermediate water masses (Matos *et al.*, 2015; Matos *et al.*, 2017; Raddatz *et al.*, 2020) and to the changes in the activity of internal waves (Wang *et al.*, 2019), as well as by spatial shifts in mound development with shoaling/sinking of the pycno/thermocline (Steinmann *et al.*, 2020; Wienberg *et al.*, 2020).

The glacial–interglacial eustatic sea level changes, as well as insolation-induced productivity variations, might have a combined complex control on the temporal development of coral mounds, as it has been observed for the CMPs in the Gulf of Cadiz–Alboran Sea, identified as the "Gibraltar seesaw pattern" (Hebbeln *et al.*, 2015). The compilation of Krengel (2020) of several CWC datings from Gulf of Cadiz (Dubois-Dauphin *et al.*, 2016; Frank *et al.*, 2011; Hemsing, 2017; Wienberg *et al.*, 2010; Wienberg *et al.*, 2009) and the Alboran Sea (Feenstra *et al.*, 2020; Fink *et al.*, 2015; Fink *et al.*, 2013; Wang *et al.*, 2019) highlight how the aggradational histories of coral mounds east and west of the Gibraltar Strait are chronologically opposing (mostly glacial development in the Gulf of Cadiz, interglacial for the Alboran Sea). Besides eustatic sea level variations, the glacial–interglacial cycle might have strong atmospheric-hydrological variations impacting the water surface–intermediate water circulation of a small basin like the Mediterranean Sea. This impacted several environmental conditions influencing CWC (temperature, salinity, benthic hydrodynamic regime), as well as the productivity-driven development of the coral mounds in this region. However, insolation-induced climate changes on N Africa (e.g., African Humid

period, but also small changes in the African monsoon) might not only directly influence the primary productivity and therefore the flourishing of CWC colonies in this region but might also be partially involved in the dissolved oxygen depletion (sapropel formation) in the central-eastern Mediterranean Sea. This did not only impact the development of CMP there (Fink *et al.*, 2012), but also in the Alboran Sea (Corbera *et al.*, 2021).

Besides dating, the aragonitic skeleton of mound-forming CWC represents a paleoarchive for physical oceanographic conditions that can be reconstructed with geochemical proxies, although several limitations (e.g., "vital effect", species-specific calibrations) should be considered. CWC can be analysed to reconstruct:

- benthic seawater temperature by Sr/Ca ratios (Cohen *et al.*, 2006; Raddatz *et al.*, 2013), and Li/Mg ratios (Case *et al.*, 2010; Montagna *et al.*, 2014; Montero-Serrano *et al.*, 2013; Raddatz *et al.*, 2013; Raddatz *et al.*, 2014)
- seawater density by stable isotopes (Rüggeberg *et al.*, 2016)
- carbonate system (pH, CO_3^{2-} concentration and saturation) with B isotopes and U/Ca ratio (McCulloch *et al.*, 2012; Raddatz *et al.*, 2016; Raddatz *et al.*, 2014)
- nutrients by Ba/Ca ratio (Raddatz *et al.*, 2016; Raddatz *et al.*, 2014)
- water masses with Nd isotopes (εNd) (Copard *et al.*, 2012; Montero-Serrano *et al.*, 2013)
- seasonal environmental changes from the micro-layers thickness and Sr concentrations (Mouchi *et al.*, 2014)

Further calibration of these proxies, as well extending the application of promising geochemical proxies, already carried out on solitary CWC, benthic/planktonic foraminifera and other marine carbonates, to mound-forming CWC, will highlight to what extent coral mounds represent interesting paleoceanographic archives (Raddatz and Rüggeberg, 2021).

Besides datings and proxy analyses, the CWC-skeletons within sediment cores can be investigated with non-destructive analyses providing useful information on coral mound development, as well as CWC ecosystems, namely by X-ray computed tomography (CT). The contrast in density between CWC skeletons and the baffled sediment matrix detected by CT scans offers the chance to investigate the internal 3D structure of CWC-bearing cores (as well as other sediment cores), before splitting the cores. This might allow CWC recognition and quantification, as well as identification of hiatuses, facies, bioturbation and other sedimentary structures (Angeletti *et al.*, 2019; Douarin *et al.*, 2013; Eisele *et al.*, 2014; Rüggeberg *et al.*, 2005; Titschack *et al.*, 2015; Titschack *et al.*, 2016; Titschack *et al.*, 2009; van der Land *et al.*, 2011; Van der Land *et al.*, 2010; Victorero *et al.*, 2016; Wang *et al.*, 2019). CT scans also allow to identify skeletal parts of other organisms living in the CWC ecosystem (solitary corals, molluscs, bryozoans, etc.) as well as the signature of diagenetic processes (Eisele *et al.*, 2014; Titschack *et al.*, 2016; van der Land *et al.*, 2011), which can be further investigated with micro-CT scans (Pirlet *et al.*, 2010; Pirlet *et al.*, 2012). CT scans allow the evaluation of the volume of the CWC frameworks and other bioclasts, which when combined with datings, offer the opportunity to calculate carbonate

accumulation rates during coral mound development (Titschack *et al.*, 2015; Titschack *et al.*, 2016; Wang *et al.*, 2021).

Volume measurement of the coral mounds (Hebbeln *et al.*, 2019; Tamborrino *et al.*, submitted) combined with CT scans might point to coral mounds as a relevant carbonate factory, especially for the aphotic zone.

1.5. Thesis objectives and outline

The aim of this thesis is to constrain all the factors that have controlled spatially and temporally the development of the Namibian coral mounds. The hypotheses of this thesis mostly reflect the fact that this CMP was (mostly) unknown before the M122 ANNA cruise. During the M122 cruise, extensive multidisciplinary site investigations were carried out, providing the exploratory material on which this thesis and its hypotheses rely. The three hypotheses of this thesis address the three major research themes on coral mounds (characterization of the environmental conditions, examination of the spatial variables, and reconstruction of the temporal development):

> *Hypothesis I. Coral mounds can be found under unfavourable conditions for CWC if the main supportive control (food supply) is guaranteed.*

The oceanographic setting off Namibia is characterized by the Benguela Upwelling System (BUS). To understand how BUS-related environmental factors controlled the formation of the Namibian mounds, a compilation of environmental data (CTD and benthic lander) collected during the M122 cruise were analysed to understand spatial and temporal variations of the local oceanographic conditions off Namibia. From these measurements, three parameters have been identified as key controls on the development of the Namibian coral mounds: quality and quantity of food supply available for the CWC, hydrodynamic regime, and bottom water dissolved oxygen concentrations. The analyses of the environmental conditions of the Namibian site are extensively documented in Manuscript I (chapter 3). These results are also partially re-presented in Manuscript II & III, highlighting how the characterization of environmental conditions is relevant to understanding the spatial and temporal development of a CMP.

> *Hypothesis II. The spatial distribution and morphology of the coral mounds is indicative of the processes influencing their formation. Therefore, quantitative measurement of spatial-morphometric variables can be correlated to the measurements of CWC-supporting environmental conditions.*

The Namibian coral mounds represent a suitable dataset for several aspects (number, sizes, distribution, and ages) that allow testing this hypothesis through quantitative spatial-morphometric analyses. Manuscript II discusses on patterns of the spatial distribution and morphometry of the Namibian mounds together with the measured environmental conditions (chapter 4).

Hypothesis III. In many CMPs, coral mound development is negatively affected by a drop in surface productivity and limited food supply. However, the consumption of DO by extremely high primary and export productivity can also be lethal for CWC, interrupting coral mound formation.

The development of coral mounds is mostly linked to primary productivity, as observed in several CMPs. The BUS is responsible for making the Namibian coastal and shelf waters one of the most productive regions on Earth. However, the re-mineralization of an extremely large amount of organic matter drops the dissolved oxygen concentration to 0 mL L^{-1} at the depths of the Namibian coral mounds. Indeed, no living CWC have been observed on these mounds by the ROV dives during the M122 cruise. How did BUS-related conditions foster and cease the development of the Namibian coral mounds? U-series dating on CWC frameworks combined with literature paleoceanographic results allowed to reconstruct the development of coral mounds accordingly to the variability of the BUS. These results are presented in Manuscript III (chapter 5)

This is as a cumulative thesis consisting of three individual manuscripts addressing the three working hypotheses outlined above. Two manuscripts are already published: Manuscript I is published in the journal *Biogeosciences,* while Manuscript III is published in *Geology*. Manuscript II is submitted and under revision in the journal *Frontiers in Marine Sciences*. Here, the author contributions for the three manuscripts are listed:

Manuscript I: Environmental factors influencing benthic communities in the oxygen minimum zones on the Angolan and Namibian margins

Author name	Statement of contribution
Ulrike Hanz	Principal author of this manuscript and of all figures; conception and design of the study; data analyses and interpretations
Claudia Wienberg	Co-chief scientist (M122 cruise), planning seabed investigations and sampling; critical revision of the manuscript
Dierk Hebbeln	Chief scientist (M122 cruise), critical revision of the manuscript
Gerard Duineveld	Design of benthic lander research
Marc Lavaleye	Designed lander research. Lander data acquisition during M122 cruise
Katriina Juva	Tidal analysis and SML Lander data
Wolf-Christian Dullo	Water column measurements with the CTD
André Freiwald	Habitat characteristics and species identification
Leonardo Tamborrino	MBES data processing. Intellectual contribution on the Namibian site
Gert-Jan Reichart	Support for the interpretation the results
Sascha Flögel	SML Lander data
Furu Mienis	Design of benthic lander research. Lander data acquisition during M122 cruise. critical revision of the manuscript

Manuscript II: Spatial distribution and morphometry of the Namibian coral mounds controlled by hydrodynamic regime and outer-shelf topography

Author name	Statement of contribution
Leonardo Tamborrino	Principal author of this manuscript and of all figures; conception and design of the study; data analyses and interpretation; hydroacustic data processing; morphometric analyses,
Jürgen Titschack	Acquisition and preliminary processing of bathymetry data; conception and design of the study, critical revision of the manuscript
Claudia Wienberg	Co-chief scientist (M122 cruise), planning seabed investigations and sampling; critical revision of the manuscript
Sam Purkis	Extraction of morphometric data
Gregor Eberli	Support for morphometric analyses
Dierk Hebbeln	Chief Scientist M122 cruise; conception and design of the study, critical revision of manuscript

Manuscript III: Mid-Holocene extinction of cold-water corals on the Namibian shelf steered by the Benguela oxygen minimum zone

Author name	Statement of contribution
Leonardo Tamborrino	Principal author of this manuscript and of all figures; conception and design of the study; data analyses and interpretation; bathymetry processing.
Claudia Wienberg	Co-chief scientist (M122 cruise), planning seabed investigations and sampling; critical revision of the manuscript
Jürgen Titschack	Acquisition and preliminary processing of hydroacoustic data; critical revision of the manuscript
Paul Wintersteller	Planning and acquisition of hydroacoustic data
Furu Mienis	Benthic lander data acquisition and processing; critical revision of the manuscript
Andrea Schröder-Ritzau	U/Th dating analyses
André Freiwald	ROV planning; seabed investigations
Covadonga Orejas	ROV seabed investigations; contributions to the manuscript (biology)
Wolf-Christian Dullo	Water column data analyses; contributions to the manuscript (oceanography)
Julia Haberkern	Geophysical data acquisition during M122 cruise
Dierk Hebbeln	Chief Scientist M122 cruise; conception and design of the study, critical revision of manuscript

2. Methods

The advancement in deep-sea technologies and methodologies played a key role for the advances in CWC and coral mounds investigations over the last decades, as shown by the results achieved in the highlighted three main CWC research themes. The research activity of this thesis relies on tools and methods that corresponds to these themes, and therefore, to the hypotheses formulated.

2.1. Characterization of the modern environmental conditions

2.1.1. CTD and water sampler

The main objective of the Conductivity-Temperature-Depth (CTD) measurements combined with a water sampler was (i) to determine the physical parameters and (ii) to collect water samples for geochemical analyses of the water masses in the area of the Namibian coral mounds. During RV *Meteor* cruise M122, 12 CTD casts were performed around and among the Namibian mounds, arranged parallel and perpendicular to the shelf (water depth range: 150-250 m), while 4 casts were performed in the western deeper areas (water depth range: 286-391 m). The CTD measurements were conducted using a SEABIRD "SBE 9 plus" underwater unit and a SEABIRD "SBE 11 plus V2" deck unit. Vertical profiles over the water column provided standard data for conductivity, potential temperature, pressure, and dissolved oxygen concentrations.

2.1.2. Benthic lander

During M122, two NIOZ ALBEX landers (Fig. 2.1) were deployed for short durations (~8 days) close to the Sylvester and Coral Belt Mounds (Hebbeln et al. 2017). The landers were equipped with an Aquadopp (Nortek™) profiling current meter, a combined OBS and Fluorometer (Wetlabs™) connected to a datalogger, and a combined temperature and dissolved oxygen sensor (RINCO). The landers were furthermore equipped with a sediment trap (Technicap PPS4/3) with 12 bottles, programmed to sample at a daily interval. One of the ALBEX landers was additionally equipped with a McLane particle pump (24 filter units for each 7.5L of seawater, 2 h intervals) to sample particulate organic matter. Suspended particulate organic matter samples were stored and analysed for stable nitrogen and carbon isotopes.

Figure 2.1 The two ALBEX landers (NIOZ) on the main deck of the RV *Meteor* during the M122 cruise (Credits. D. Hebbeln).

2.2. Investigating spatial variables: seafloor observation and mapping

2.2.1. Multibeam echosounders

Most of the hydroacoustic data presented in this study were collected during RV *Meteor* expedition M122 ANNA in December 2015-January 2016 (Hebbeln et al., 2017). The hydroacoustic dataset has been completed with data previously collected during R/V *Maria S. Merian* expedition MSM 20-1 (Geissler et al., 2013).

Seafloor mapping was performed utilizing two different hull-mounted multibeam echosounders (MBES): KONGSBERG MBES EM1002 (95 kHz) during expedition MSM20/1 and EM710 (70-100 kHz) during expedition M122. The EM1002 emitted 111 beams per ping, covering a depth range of 2-1000 m. Achievable swath width on a flat bottom was up to 5 times the water depth. The EM710 acquires 200 beams per ping and 400 soundings ("soft-beams") in the used high-density mode, with a maximum coverage of 6 times water depth down to 800 mbsl covering a depth range of several meters up to ~800 m. Both MBES surveyed with a swath angle 120°.

Sound velocity profiles (SVPs) through the water column, which are essential for the correction of the hydroacoustic measurements, were repeatedly recorded using either CTD casts or sound velocity probes. Spatial integrity of the mapping data was achieved by combining the ship's SEAPATH 200 inertial navigation systems including differential global positioning system information with motion data (roll, pitch, heave) provided by the motion reference units. The open-source software package MB-System v. 5.3 (Caress and Chayes, 1995) was used for bathymetric data post-processing. The post-processing includes the application of tide and the SVPs corrections, besides the calibration of roll-pitch-yaw error. After manual editing, the amplitude (backscatter) and sidescan (time series) values are corrected based on a function of grazing angle with respect to the seafloor (slope). Once changes are applied to the raw files, the bathymetric maps were gridded using the netCDF (GMT) file format. ESRI ArcGIS v.10 was used to create maps from the grid files (grid cell size: 10 m) for spatial data management and for the quantification of coral mounds on the Namibian shelf.

2.2.2. Morphometric analyses

Morphometric analyses can be carried out only if coral mounds are objectively defined. Because some mounds are coalesced and/or have relevant underlying topographic features associated with them, mound perimeters are complex and difficult to define consistently by eye. Furthermore, many mounds are distributed on a variable seafloor slope; thus, up-slope and down-slope mound flanks can initiate at different depths. To account for this variability, a reproducible, automated method for extracting mound features from the DEM was applied using Petrel™ (Schlumberger). This method, fully described in Correa et al., (2012), relies on the change of slope angle between the mound and surrounding area. Thus, dip angle maps were generated from the DEM, and closed polygons were generated following the contour line where the slope angle exceeds 3° (Fig. 2.2a, b). This 3°-cutoff was determined based on an attempt to delineate mound perimeters manually.

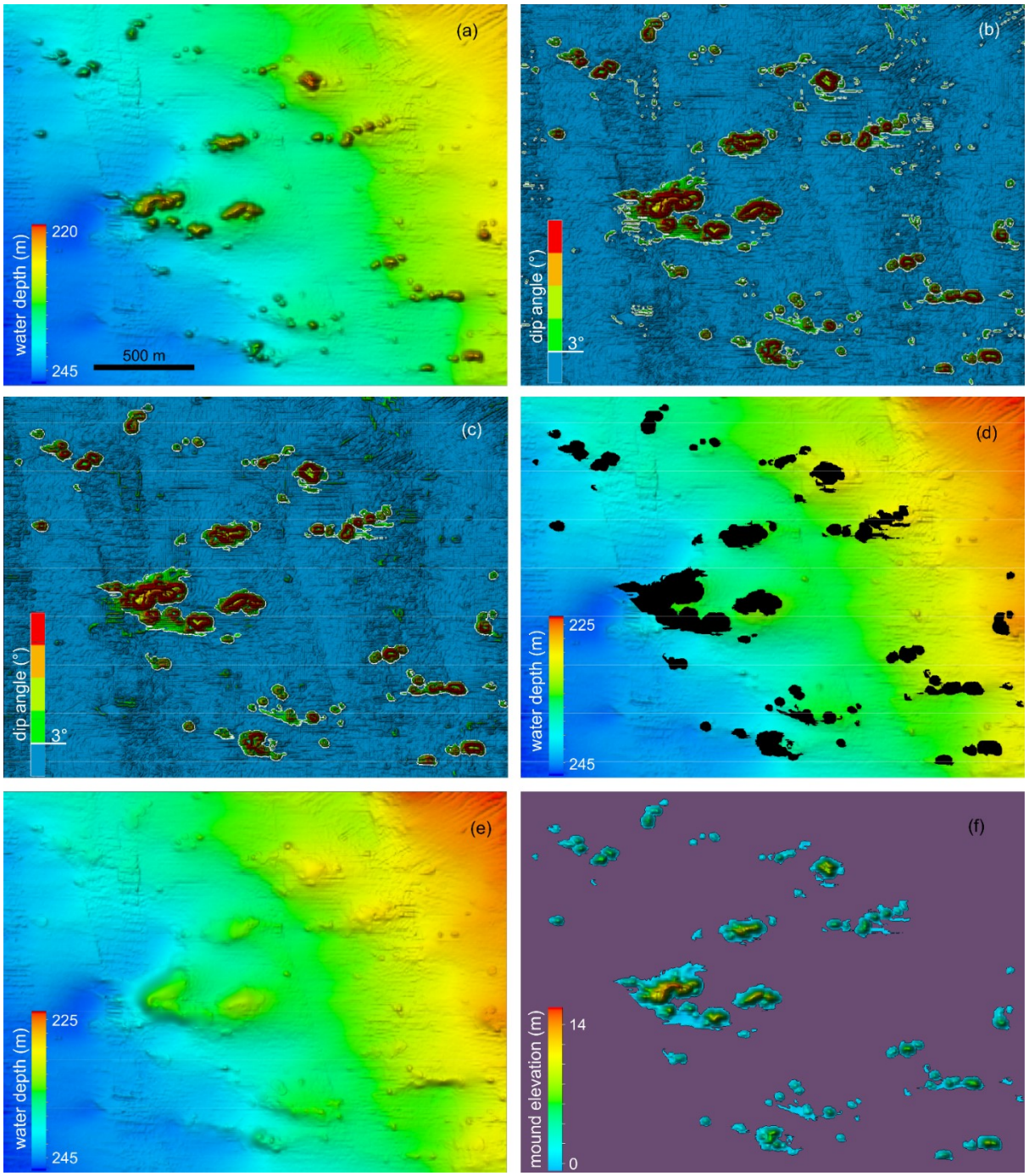

Figure. 2.2. Workflow to automatically extract and delineate mound perimeters. This workflow is applied to the entire survey at once but, for clarity, only a subset of the data is shown here. (a) High-resolution DEM showing mound structures. (b) Dip angle map based on the DEM. Closed polygons are generated along the contour line where the slope angle exceeds 3°. (c) All polygons that are within another polygon are filtered out. Polygons related to the MBES artifacts have been removed. Polygons that remain represent mound perimeters. (d) Original DEM with areas enclosed by mound perimeters being removed. (e) DEM, with mound data removed, re-interpolated to calculate the vertical relief of the mound base. (f) The newly gridded surface is subtracted from the original DEM to produce an isopach map in which the vertical relief within mound perimeters is displayed in meters (mound thickness = 'map a' – 'map e'). *Own illustration.*

This manual delineation indicated that the majority of the mounds rise out of the surrounding seafloor with a cutoff plane of ca 3°. The selected cutoff value has been qualitatively validated with a comparison between DEM and dip angle (see Manuscript II). Because features with >3° slope angle also have been identified inside the mound perimeter, these have been filtered out under the assumption that these

represent mound internal sloping features (Fig. 2.2c). The DEM was subsequently re-gridded to generate hypothetical bathymetric maps without mounds (Fig. 2.2d) in which the slope architecture was preserved. The vertical relief within each removed mound was interpolated from the mound perimeters (Fig. 2.2e). The newly interpolated surfaces were then subtracted from the original DEMs to evaluate the volume and heights of the coral mounds above the seafloor (Fig. 2.2f). Only features with a footprint area > 900 m^2 (corresponding to a two-dimensional array of 3^x3^x grid cells size) and with height above 2 m (2x vertical precision between MSM20-1 and M122 MBES datasets) were considered coral mounds and quantitatively analysed.

2.2.3. Parasound sub-bottom profiler

The Parasound Sediment Echosounder P70, which is installed on RV *Meteor,* utilizes the parametric effect to create a high intensity signal suitable for sediment profiling in a narrow cone providing high-resolution data on the structure of sub-surface sediments. Therefore, two waves of similar frequencies are emitted simultaneously; one of these primary frequencies is fixed to 18 kHz the second primary frequency can be varied between 18.5 and 24 kHz. The parametric effect leads to the development of so-called secondary frequencies, which are equal to the sum and the difference of the two primary frequencies.

Usually the second primary frequency is chosen to create a secondary low frequency (SLF) around 4 kHz, which then travels in the narrow cone (4.5°) of the high primary frequencies. This significantly reduces and, thus, improves the footprint compared to the wide opening angles (30°) of conventional sediment echosounders. Combined with a sub-meter scale vertical resolution, the SLF is able to image sedimentary structures in a high resolution with penetration depths of 20 - 200 mbsf depending on the sediments encountered. The data acquisition was performed with the real-time values of surface sound velocity measured close to the Tx/Rx-array (System C-Keel) and a static sound velocity profile of 1500 m/s (C-Mean). The program ATLAS PARASTORE is used for storing and displaying echograms, while the program ATLAS Hydromap Control is used to set proper hydroacoustic settings during acquisition. ReflexW (v. 8.5.4) is used for processing (muting, 2D-filtering and automatic gain control) the PARASOUND profiles.

2.2.4. ROV observations

During RV *Meteor* cruise M122, the remotely operated vehicle (ROV) MARUM-SQUID (manufactured by SAAB Seaeye, UK; Fig. 2.3) was applied to explore directly the seafloor appearance of and around the Namibian coral mounds (Hebbeln et al. 2017). Seven ROV dives crossing six coral mound locations allowed for the collection of ground-truthing information about the geological origin and faunal composition of the coral mound surfaces. The ROV was equipped with five video and still cameras. Main working video camera was the *Insite Pacific MiniZEUS MKII* full HD camera with a resolution of 2.38 megapixels. It has a hemispherical dome port and a fully corrected optical lens with a

10x optical zoom. Two *DSPL MultiseaCams* served as forward looking and rear cameras to monitor the orientation of the ROV umbilical, while a *DSPL Wide-i SeaCam* was used as a downward looking camera providing a full overview of the area in front of the vehicle. An *Imenco Tigershark* still camera acquired images at a resolution of 12 megapixels. The external flashgun of the still camera was installed at a 45° angle on the upper porch of the ROV. Two *Imenco Dusky Shark* line lasers projected two parallel laser beams (lines) at a distance of 30 cm and were used to calculate density of specimens as well as to perform size measurements of organisms on the seafloor. The ROV SQUID used the POSIDONIA USBL positioning system installed on RV *Meteor*, but it is also equipped with its own positioning system (MiniPOS). Further information about the ROV observations carried out during M122 cruise is presented in Hebbeln et al. (2017).

Figure 2.3. Deployment of the MARUM ROV SQUID during the M122 cruise (Credits: S. Flöter).

2.3 Determination of coral ages

2.3.1. Coral sampling

Sediment and corals were collected using three devices (Fig. 2.4): a grab sampler (GS), a giant box corer (GBC), and a gravity corer (GC). For dating the the skeleton of CWC off Namibia, we collected in total 19 samples of fossil *L. pertusa* from surface sediments (9 GS, 7 GBC, 1 GC top). A further 17 samples were collected from the mound-base-penetrating sediment core GeoB20531-1 to reconstruct mound development from its initiation to the end of its aggradation. Metadata information of the samples used for this thesis are provided in the Manuscript III (chap. 5). Complete descriptions of GS and GBC collected off Namibia are presented in the Appendix C of the M122 cruise report (Hebbeln et al. 2017).

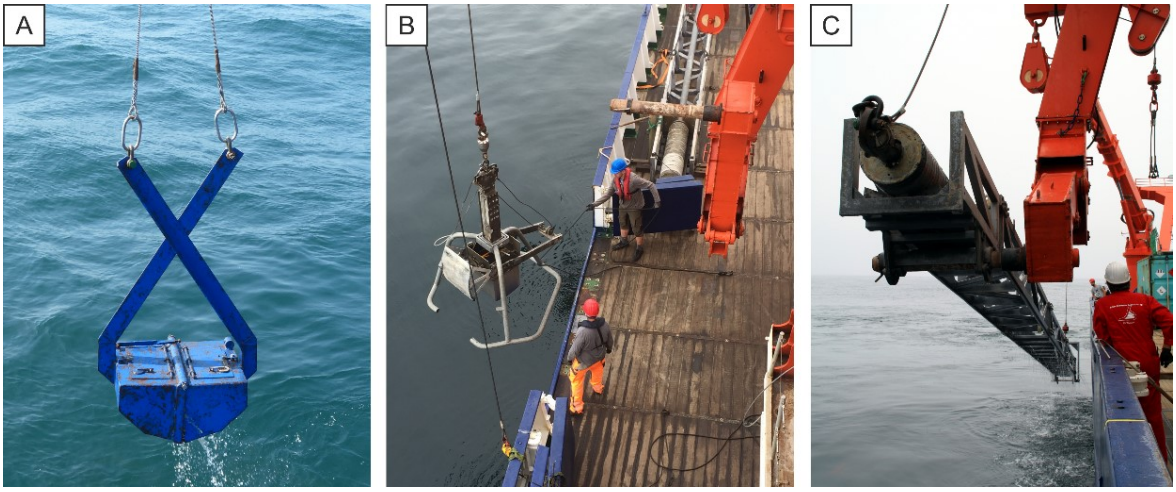

Figure 2.4. Sediment sampling devices used during the M122 cruise: (a) recovery of a grab sampler, (b) and (c) deployment of the giant box corer and the gravity corer, respectively. Credits: D. Hebbeln (a), A. Freiwald (b) and S. Flöter (c).

2.3.2. Age determination by the U/Th method

The CWC aragonitic skeleton is suitable for various dating methods to determine the age of a coral specimen or more precisely to determine the years since the coral died. Prior to the analyses, all the coral fragments were cleaned mechanically to remove contaminants from the external surface of the fossil skeletons (e.g., borings by organisms, iron–manganese crusts, coatings) and prepared chemically using weak acid leaching and water rinsing procedures as described by Frank *et al.* (2004). The U/Th analyses were carried out with a multi-collector inductively coupled plasma mass spectrometer (Institute of Environmental Physics, University of Heidelberg, Germany; Wefing et al., 2017). The reproducibility of mass spectrometric measurements was assessed using the international Uranium standard material HU1 (Cheng *et al.*, 2000; Frank *et al.*, 2004; Wefing *et al.*, 2017). All CWC fragments showed only minor physico-chemical alteration or dissolution not affecting the interpretation of the resulting U/Th ages. Measured ^{232}Th concentrations are small with <2.5 ppb for 94 % of all samples. Initial $\delta^{234}U_i$ values are variable and range between 146.6 ± 0.7 ‰ and 150.7 ± 0.6 ‰. All samples rely on $\delta^{234}U_i$ values within the narrow band of ±10 ‰ compared to the value of modern seawater (146.8 ‰; Andersen et al., 2010) and can therefore be treated as being reliable. Metadata and ages are reported in the Manuscript III (chap. 5).

3. Manuscript I

Environmental factors influencing benthic communities in the oxygen minimum zones on the Angolan and Namibian margins

Ulrike Hanz[1], Claudia Wienberg[2], Dierk Hebbeln[2], Gerard Duineveld[1], Marc Lavaleye[1], Katriina Juva[3], Wolf-Christian Dullo[3], André Freiwald[4], Leonardo Tamborrino[2], Gert-Jan Reichart[1, 5], Sascha Flögel[3], and Furu Mienis[1]

[1]Department of Ocean Systems, NIOZ Royal Netherlands Institute for Sea Research and Utrecht University, Texel, 1797SH, the Netherlands

[2]MARUM–Center for Marine Environmental Sciences, University of Bremen, 28359 Bremen, Germany

[3]GEOMAR Helmholtz Centre for Ocean Research, 24148 Kiel, Germany

[4]Department for Marine Research, Senckenberg Institute, 26382 Wilhelmshaven, Germany

[5]Faculty of Geosciences, Earth Sciences Department, Utrecht University, Utrecht, 3512JE, the Netherlands

Manuscript submitted in *Biogeosciences* (07.02.2019), accepted (10.10.2019) and published (15.11.2019)

Abstract

Thriving benthic communities were observed in the oxygen minimum zones along the southwestern African margin. On the Namibian margin, fossil cold-water coral mounds were overgrown by sponges and bryozoans, while the Angolan margin was characterized by cold-water coral mounds covered by a living coral reef. To explore why benthic communities differ in both areas, present-day environmental conditions were assessed, using conductivity–temperature–depth (CTD) transects and bottom landers to investigate spatial and temporal variations of environmental properties. Near-bottom measurements recorded low dissolved oxygen concentrations on the Namibian margin of 0–0.15 mL L^{-1} (≙0 %–9% saturation) and on the Angolan margin of 0.5–1.5 mL L^{-1} (≙7 %–18% saturation), which were associated with relatively high temperatures (11.8–13.2 °C and 6.4–12.6 °C, respectively). Semidiurnal barotropic tides were found to interact with the margin topography producing internal waves. These tidal movements deliver water with more suitable characteristics to the benthic communities from below and above the zone of low oxygen. Concurrently, the delivery of a high quantity and quality of organic matter was observed, being an important food source for the benthic fauna. On the Namibian margin, organic matter originated directly from the surface productive zone, whereas on the Angolan margin the geochemical signature of organic matter suggested an additional mechanism of food supply. A nepheloid layer observed above the cold-water corals may constitute a reservoir of organic matter, facilitating a constant supply of food particles by tidal mixing. Our data suggest that the benthic fauna on the Namibian margin, as well as the cold-water coral communities on the Angolan margin, may compensate for unfavorable conditions of low oxygen levels and high temperatures with enhanced availability of food, while anoxic conditions on the Namibian margin are at present a limiting factor for cold-water coral growth. This study provides an example of how benthic ecosystems cope with such extreme environmental conditions since it is expected that oxygen minimum zones will expand in the future due to anthropogenic activities.

3.1. Introduction

Cold-water corals (CWCs) form 3-D structures in the deep sea, providing important habitats for dense aggregations of sessile and mobile organisms ranging from mega- to macrofauna (Henry and Roberts, 2007; van Soest *et al.*, 2007) and fish (Costello *et al.*, 2005). Consequently, CWC areas are considered as deep-sea hotspots of biomass and biodiversity (Buhl-Mortensen *et al.*, 2010; Henry and Roberts, 2017). Moreover, they form hotspots for carbon cycling by transferring carbon from the water column towards associated benthic organisms (van Oevelen *et al.*, 2009; White *et al.*, 2012). Some framework-forming scleractinian species, with *Lophelia pertusa* and *Madrepora oculata* being the most common species in the Atlantic Ocean (Cairns, 2007; Freiwald *et al.*, 2004; Roberts *et al.*, 2006; White *et al.*, 2005) are capable of forming large elevated seabed structures, so-called coral mounds (De Haas *et al.*, 2009; Titschack *et al.*, 2015; Wienberg and Titschack, 2017; Wilson, 1979). These coral mounds, consisting of coral debris and hemipelagic sediments, commonly reach heights between 20 and 100 m

and can be several kilometers in diameter. They are widely distributed along the North Atlantic margins, being mainly restricted to water depths between 200 and 1000 m, while records of single colonies of *L. pertusa* are reported from a broader depth range of 50–4000 m depth (Davies *et al.*, 2008; Freiwald, 2002; Freiwald *et al.*, 2004; Grasmueck *et al.*, 2006; Hebbeln *et al.*, 2014; Mortensen *et al.*, 2001; Roberts *et al.*, 2006; Wheeler *et al.*, 2007).

A global ecological-niche factor analysis by Davies *et al.* (2008) and Davies and Guinotte (2011), predicting suitable habitats for *L. pertusa*, showed that this species generally thrives in areas which are nutrient rich, well oxygenated and affected by relatively strong bottom water currents. Other factors potentially important for proliferation of *L. pertusa* include chemical and physical properties of the ambient water masses, for example aragonite saturation state, salinity and temperature (Davies and Guinotte, 2011; Davies *et al.*, 2008; Dullo *et al.*, 2008; Flögel *et al.*, 2014). *L. pertusa* is most commonly found at temperatures between 4 and 12 °C and a very wide salinity range between 32 and 38.8 (Freiwald *et al.*, 2004). The link of *L. pertusa* to particular salinity and temperature within the NE Atlantic led Dullo *et al.* (2008) to suggest that they are restricted to a specific density envelope of sigma-theta ($\sigma\theta$) = 27.35– 27.65 kg m^{-3}. In addition, the majority of occurrences of live *L. pertusa* comes from sites with dissolved oxygen (DO) concentrations between 6 and 6.5 mL L^{-1}(Davies *et al.*, 2008), with lowest recorded oxygen values being 2.1–3.2 mL L^{-1} at CWC sites in the Gulf of Mexico (Brooke and Ross, 2014; Davies *et al.*, 2010; Schroeder, 2002) or even as low as 1–1.5 mL L^{-1} off Mauritania, where CWC mounds are in a dormant stage presently showing only scarce living coral occurrences (Ramos *et al.*, 2017; Wienberg *et al.*, 2018). Dissolved oxygen levels hence seem to affect the formation of CWC structures as was also shown by Holocene records obtained from the Mediterranean Sea, which revealed periods of reef demise and growth in conjunction with hypoxia (with 2 mL L-1 seemingly forming a threshold value for active coral growth; Fink *et al.*, 2012).

Another essential constraint for CWC growth and therefore mound development in the deep sea is food supply. *L. pertusa* is an opportunistic feeder, exploiting a wide variety of different food sources, including phytodetritus, phytoplankton, mesozooplankton, bacteria and dissolved organic matter (Dodds *et al.*, 2009; Duineveld *et al.*, 2007; Gori *et al.*, 2014; Kiriakoulakis *et al.*, 2005; Mueller *et al.*, 2014). Not only quantity but also quality of food particles are of crucial importance for the uptake efficiency as well as ecosystem functioning of CWCs (Mueller *et al.*, 2014; Ruhl, 2008). Transport of surface organic matter towards CWC sites at intermediate water depths has been found to involve either active swimming (zooplankton), passive sinking, advection, local downwelling, and internal waves and associated mixing processes resulting from interactions with topography (Davies *et al.*, 2009; Frederiksen *et al.*, 1992; Mienis *et al.*, 2009; Thiem *et al.*, 2006; van Haren *et al.*, 2014; White *et al.*, 2005). With worldwide efforts to map CWC communities, *L. pertusa* was also found under conditions which are environmentally stressful or extreme in the sense of the global limits defined by Davies *et al.* (2008) and by Davies and Guinotte (2011). Examples are the warm and salty waters of the Mediterranean and the high bottom water temperatures along the US coast (Cape Lookout; Freiwald *et al.*, 2009; Mienis *et al.*,

2014; Taviani *et al.*, 2005). Environmental stress generally increases energy needs for organisms to recover and maintain optimal functioning, which accordingly increases their food demand (Sokolova *et al.*, 2012).

For the SW African margin one of the few records of living CWC comes from the Angolan margin (Le Guilloux *et al.*, 2009), which raises the questions whether environmental factors limit CWC growth due to the presence of an oxygen minimum zone (OMZ; see Karstensen *et al.*, 2008), or whether this is related to a lack of data. Hydroacoustic campaigns revealed extended areas off Angola and Namibia with structures that morphologically resemble coral mound structures known from the NE Atlantic (M76-3, MSM20-1; Geissler *et al.*, 2013; Zabel *et al.*, 2012). Therefore two of such mound areas on the margins off Namibia and Angola were visited during the RV Meteor cruise M122 "ANNA" (ANgola and NAmibia) in January 2016 (Hebbeln *et al.*, 2017). During this cruise, fossil CWC mound structures were found near Namibia, while flourishing CWC reef-covered mound structures were observed on the Angolan margin. The aim of the present study was to assess present-day environmental conditions at the southwestern African margin to explore why CWCs thrive on the Angolan margin and are absent on the Namibian margin. Key parameters influencing CWCs, hydrographic parameters as well as chemical properties of the water column were measured to characterize the difference in environmental conditions and food supply. These data are used to improve understanding of the potential fate of CWC mounds in a changing ocean.

3.2. Material and methods

3.2.1. Setting

3.2.1.1. Oceanographic setting

The SW African margin is one of the four major eastern boundary regions in the world and is characterized by upwelling of nutrient-rich cold waters (Shannon and Nelson, 1996a). The availability of nutrients triggers a high primary production, making it one of the most productive marine areas worldwide with an estimated production of 0.37 GtC yr^{-1} (Carr and Kearns, 2003). Remineralization of high fluxes of organic particles settling through the water column results in severe mid-depth oxygen depletion and an intense OMZ over large areas along the SW African margin (Chapman and Shannon, 1987). The extension of the OMZ is highly dynamic, being controlled by upwelling intensity, which depends on the prevailing winds and two current systems along the SW African margin, i.e., the Benguela and the Angola currents (Chapman and Shannon, 1987; Kostianoy and Lutjeharms, 1999; Fig. 3.1). The Benguela Current originates from the South Atlantic Current, which mixes with water from the Indian Ocean at the southern tip of Africa (Mohrholz *et al.*, 2008; Poole and Tomczak, 1999; Rae, 2005) and introduces relatively cold and oxygen-rich Eastern South Atlantic Central Water (ESACW; Poole and Tomczak, 1999) to the SW African margin (Mohrholz *et al.*, 2008). The Angola Current originates from the South Equatorial Counter Current and introduces warmer, nutrient-poor and less oxygenated South Atlantic Central Water (SACW; Poole and Tomczak, 1999) to the continental margin (Fig. 3.1a). SACW

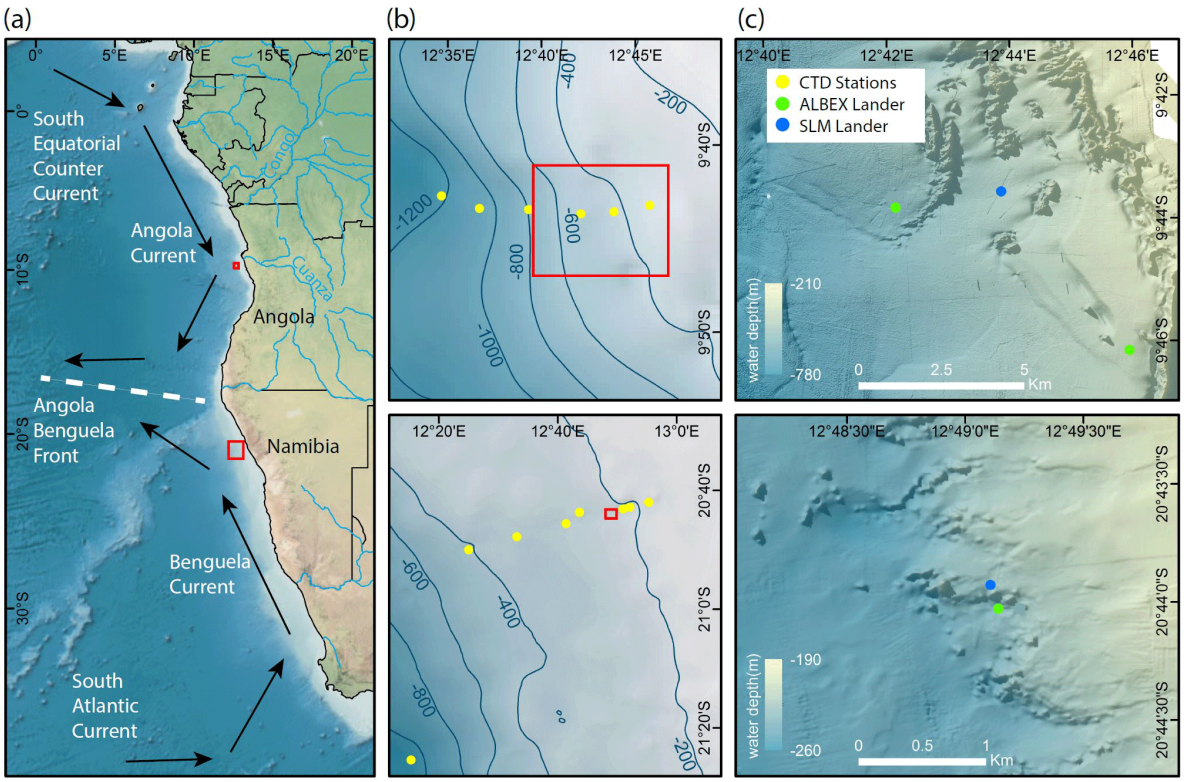

Figure 3.1. (a) Overview map showing the research areas off Angola and Namibia (red squares) and main features of the surface water circulation (arrows) and frontal zone (dashed line) as well as the two main rivers discharging at the Angolan margin. Detailed bathymetry maps of the Angolan (upper maps) and Namibian margins (lower maps) showing the position of (b) CTD transects (note the deep CTD cast down to 1000 m water depth conducted off Namibia) and (c) bottom lander deployments (red squares shown in b indicate the cutouts displayed in c).

is defined by a linear relationship between temperature and salinity in a T –S plot (Shannon *et al.*, 1987). While the SACW flows along the continental margin the oxygen concentration is decreasing continuously due to remineralization processes of organic matter on the SW African shelf (Mohrholz *et al.*, 2008). Both currents converge at around 14–16° S, resulting in the Angola–Benguela front (Lutjeharms and Stockton, 1987). In austral summer, the Angola–Benguela front can move southward to 23° S (Shannon *et al.*, 1986), thus increasing the influence of the SACW along the Namibian coast (Chapman and Shannon, 1987; Junker *et al.*, 2017), contributing to the pronounced OMZ due to its low initial oxygen concentration (Poole and Tomczak, 1999). ESACW is the dominant water mass at the Namibian margin during the main upwelling season in austral winter, expanding from the oceanic zone about 350 km towards the coast (Mohrholz *et al.*, 2014). The surface water mass at the Namibian margin is a mixture of sun-warmed upwelled water and water of the Agulhas Current, which mixes in complex eddies and filaments and is called South Atlantic Subtropical Surface Water (SASSW) (Hutchings *et al.*, 2009). At the Angolan margin the surface water is additionally influenced by water from the Cuanza and Congo rivers (Kopte *et al.*, 2017; Fig. 3.1). Antarctic Intermediate Water (AAIW) is situated in deeper areas at the African continental margin and can be identified as the freshest water mass around 700–800 m depth (Shannon and Nelson, 1996a).

3.2.1.2. Coral mounds along the Angolan and Namibian margins

During *RV Meteor* cruise M122 in 2016, over 2000 coral mounds were observed between 160 and 260 m water depth on the Namibian shelf (Hebbeln *et al.*, 2017). All mounds were densely covered with coral rubble and dead coral framework, while no living corals were observed in the study area (Hebbeln *et al.*, 2017; Fig. 3.2a, b). Few species were locally very abundant, viz. a yellow cheilostome bryozoan, which was the most common species, and five sponge species. The bryozoans were encrusting the coral rubble, whereas some sponge species reached heights of up to 30 cm (Fig. 3.2a, b). The remaining community consisted of an impoverished fauna overgrowing *L. pertusa* debris. Commonly found sessile organism were actiniarians, zoanthids, hydroids, some thin encrusting sponges, serpulids and sabellid polychaetes. The mobile fauna comprised asteroids, ophiuroids, two shrimp species, amphipods, cumaceans and holothurians. Locally high abundances of *Suffogobius bibarbatus*, a fish that is known to be adapted to hypoxic conditions, were observed in cavities in the coral framework (Hebbeln *et al.*, 2017). Dead corals collected from the surface of various Namibian mounds date back

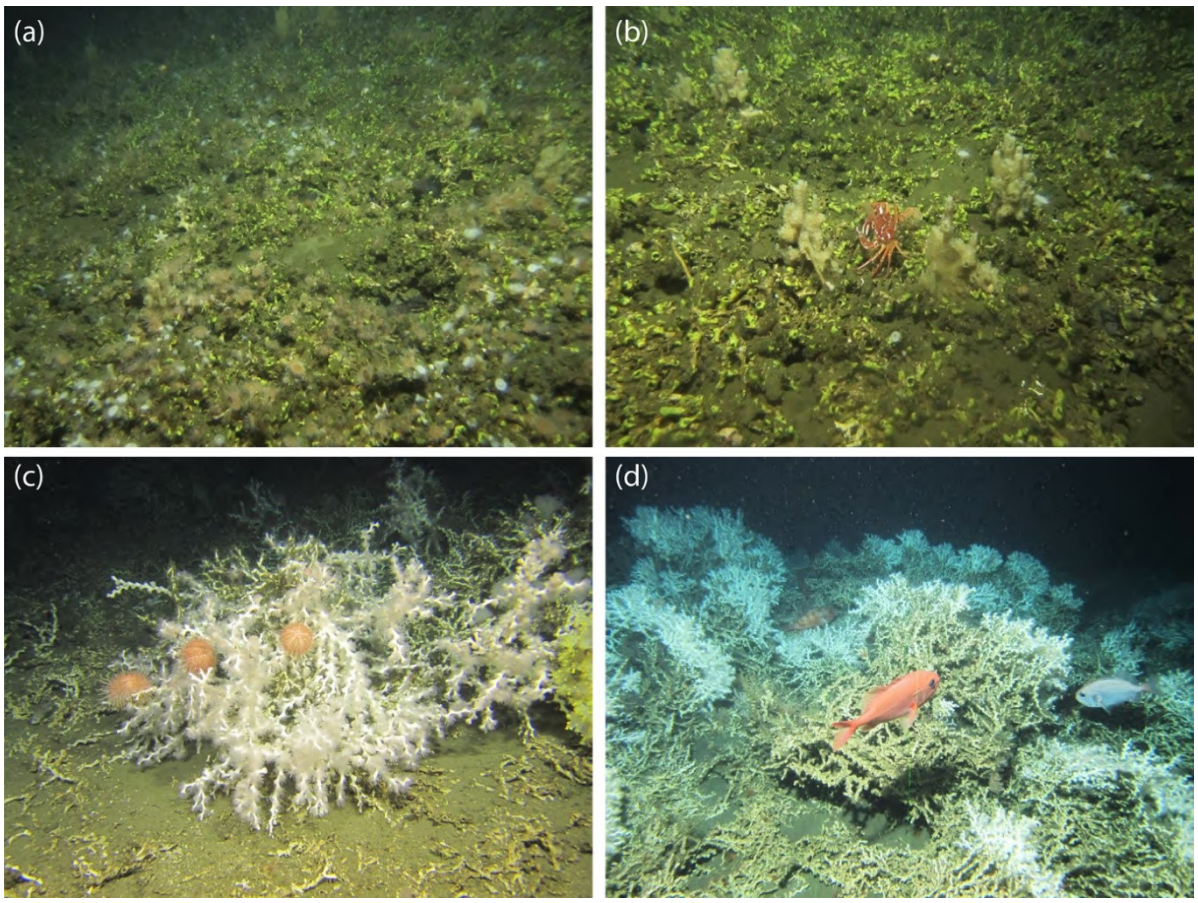

Figure 3.2. ROV images (copyright MARUM ROV SQUID, Bremen, Germany) showing the surface coverage of cold-water coral mounds discovered off Namibia (a, b) and Angola (c, d). Images were recorded and briefly described for their faunal composition during RV *Meteor* cruise M122 "ANNA" (see Hebbeln et al., 2017). (a) Sylvester mound, 225 m water depth. Dead coral framework entirely consisting of *L. pertusa*. The framework is intensely colonized by the yellow bryozoan *Metropriella* sp., zoanthids, actiniarians and sponges. Vagile fauna consists of asteroids and gobiid fishes (*Sufflogobius bibarbatus*) that hide in hollows in the coral framework. (b) Sylvester mound, 238m water depth. Dense coral rubble (*L. pertusa*) heavily overgrown by Metropriella sp. and sponges. Note the decapod crab *Macropipus australis* (center of the image). (c) Valentine mound, 238 m water depth. Live *L. pertusa* colony being grazed by echinoids. Note the sponge *Aphrocallistes* sp. with its actiniarian symbionts (right side of the image). (d) Buffalo mound, 345 m water depth. Living CWC reef observed on top of an Angolan coral mound. Many fishes are present around the reef (*Helicolenus dactylopterus*, *Gephyroberyx darwinii*).

to about 5 ka pointing to a simultaneous demise of these mounds during the mid-Holocene (Tamborrino *et al.*, 2019).

On the Angolan margin, CWC structures varied from individual mounds to long ridges. Some mounds reached heights of more than 100 m above the seafloor. At shallow depths (~ 250 m) some isolated smaller mounds were also present (Hebbeln *et al.*, 2017). All mounds showed a thriving CWC cover, which was dominated by *L. pertusa* (estimated 99 % relative abundance), along with some *M. oculata* and solitary corals. Mounds with a flourishing coral cover were mainly situated at water depths between 330 and 470 m, whereas single colonies were found over a broader depth range between 250 and 500 m (Fig. 3.2c, d; Hebbeln *et al.*, 2017). Additionally, large aggregations of hexactinellid sponges (*Aphrocallistes*, *Sympagella*) were observed. First estimates for coral ages obtained from a gravity core collected at one of the Angolan coral mounds revealed continuous coral mound formation during the last 34 kyr until today (Wefing *et al.*, 2017).

3.2.2. Methodology

During *RV Meteor* expedition M122 in January 2016, two conductivity–temperature–depth (CTD) transects and three short-term bottom lander deployments (Table 3.1, Fig. 3.1) were carried out to measure environmental conditions influencing benthic habitats. In addition, weather data were continuously recorded by the *RV Meteor* weather station, providing real-time information on local wind speed and wind direction.

3.2.2.1. Lander deployments

Sites for deployment of the NIOZ-designed lander (ALBEX) were selected based on multibeam bathymetric data. On the Namibian margin, the bottom lander was deployed on top of a mound structure (water depth 220 m). Off Angola, the lander was deployed in the relatively shallow part of the mound zone at 340 m water depth and in the deeper part at 530 m (Fig. 3.1, Table 3.1). Additionally, a GEOMAR satellite lander module (SLM) was deployed off-mound at 230 m depth at the Namibian margin and at 430 m depth at the Angolan margin (Fig. 3.1, Table 3.1). The lander was equipped with an AROUSB oxygen sensor (JFE Advantech™), a combined OBS-fluorometer (Wet Labs™) and an Aquadopp (Nortek™) profiling current meter. The lander was furthermore equipped with a Technicap PPS4/3 sediment trap with 12 bottles (allowing daily samples) and a McLane particle pump (24 filter units for each 7.5 L of seawater, 2 h interval) to sample particulate organic matter in the near-bottom water (40 cm above bottom).

The SLM was equipped with a 600 kHz ADCP Workhorse Sentinel 600 from RDI, a CTD (SBE SBE16V2™), a combined fluorescence and turbidity sensor (WET Labs ECOAFL/ FL), a dissolved oxygen sensor (SBE™) and a pH sensor (SBE™) (Hebbeln *et al.*, 2017). From the SLM only pH measurements are used here, complementing the data from the NIOZ lander.

Table 3.1. Metadata of lander deployment conducted during RV Meteor cruise M122 (ANNA) in January 2016. The deployment sites are shown in Fig. 3.1.

	Station no. (GeoB ID)	Area	Lander	Date (dd.mm.yy)	Latitude (S)	Longitude (E)	Depth (m)	Duration (d)	Devices
Namibia	20507-1	on-mound	ALBEX	01-09.01.16	20°44.03'	12° 49.23'	210	7.8	+ particle pump
	20506-1	off-mound	SLM	01-16.01.16	20°43.93'	12°49.11'	230	12.5	
Angola	20921-1	off-mound	ALBEX	20-23.01.16	9°46.16'	12°45.96'	340	2.5	+ particle pump
	20940-1	off-mound	ALBEX	23-26.01.16	9°43.84'	12°42.15'	530	2.6	+ particle pump
	20915-2	off-mound	SLM	19-26.01.16	9°43.87'	12°43.87'	430	6.8	

3.2.2.2. CTD transects

Vertical profiles of hydrographic parameters in the water column, viz. temperature, conductivity, oxygen and turbidity, were obtained using a Sea-Bird CTD–Rosette system (Sea- Bird SBE 9 plus). The additional sensors on the CTD were a dissolved oxygen sensor (SBE 43 membrane-type DO Sensor) and a combined fluorescence and turbidity sensor (WET Labs ECO-AFL/FL). The CTD was combined with a rosette water sampler consisting of 24 Niskin® water sampling bottles (10 L). CTD casts were carried out along two downslope CTD transects (Fig. 3.1). Owing to technical problems, turbidity data were only collected on the Angolan slope.

3.2.2.3. Hydrographic data processing

The CTD data were processed using the processing software Sea-Bird data SBE 11plus v. 5.2 and were visualized using the program Ocean Data View (Schlitzer, 2011; Version 4.7.8). Hydrographic data recorded by the landers were analyzed and plotted using the program R (R Core Team, 2010). Data from the different instruments (temperature, turbidity, current speed, oxygen concentration, fluorescence were averaged over a period of 1.5 h to remove shorter-term trends and occasional spikes. Correlations between variables were assessed by Spearman's rank correlation tests.

3.2.2.4. Suspended particulate matter

Near-bottom suspended particulate organic matter (SPOM) was sampled by means of a phytoplankton sampler (McLane PPS) mounted on the ALBEX lander. The PPS was fitted with 24 GF/F filters (47 mm Whatman™ GF/F filters precombusted at 450 °C). A maximum of 7.5 L was pumped over each filter during a 2 h period, yielding a time series of near-bottom SPOM supply and its variability over a period of 48 h.

3.2.2.5. C/N analysis and isotope measurements

Filters from the phytoplankton sampler were freeze-dried before further analysis. Half of each filter was used for phytopigment analysis and a 1/4 section of each filter was used for analyzing organic carbon, nitrogen and their stable isotope ratios. The filters used for carbon analysis were decarbonized by vapor of concentrated hydrochloric acid (2M HCl supra) prior to analyses. Filters were transferred into pressed tin capsules (12 mm x 5 mm, Elemental Microanalysis), and $\delta^{15}N$, $\delta^{13}C$ and total weight percent of organic carbon and nitrogen were analyzed by a Delta V Advantage isotope ratio MS coupled online to an Elemental Analyzer (Flash 2000 EA-IRMS) by a ConFlo IV (Thermo Fisher Scientific Inc.). The reference gas was purified atmospheric N_2. As standards for $\delta^{13}C$ benzoic acid and acetanilide were used, for $\delta^{15}N$ acetanilide, urea and casein were used. For $\delta^{13}C$ analysis a high-signal method was used including a 70 % dilution. Values are reported relative to v-pdb and the atmosphere respectively. Precision and accuracy based on replicate analyses and comparison with international standards for $\delta^{13}C$ and $\delta^{15}N$ was $\pm$0.15 ‰. The C/N ratio is based on the weight ratios between total organic carbon (TOC) and N.

3.2.2.6. Phytopigments

Phytopigments were measured by reverse-phase high-performance liquid chromatography (RP-HPLC, Waters Acquity UPLC) with a gradient based on the method published by Kraay *et al.* (1992). For each sample half of a GF/F filter was used and freeze-dried before extraction. Pigments were extracted using 95 % methanol and sonification. All steps were performed in a dark and cooled environment. Pigments were identified by means of their absorption spectrum, fluorescence and the elution time. Identification and quantification took place as described by Tahey *et al.* (1994). The absorbance peak areas of chlorophyll α were converted into concentrations using conversion factors determined with a certified standard. The Σphaeopigment/chlorophyll α ratio gives an indication of the degradation status of the organic material, since phaeopigments form as a result of bacterial or autolytic cell lysis and grazing activity (Welschmeyer and Lorenzen, 1985).

3.2.2.7. Tidal analysis

The barotropic (due to the sea level and pressure change) and baroclinic (internal "free waves" propagating along the pycnoclines) tidal signals obtained by the Aquadopp (Nortek™) profiling current meter were analyzed from the bottom pressure and from the horizontal flow components recorded 6 m above the sea floor, using the T_Tide Harmonic Analysis Toolbox (Pawlowicz *et al.*, 2002). The data mean and trends were subtracted from the data before analysis.

3.3. Results

3.3.1. Water column properties

3.3.1.1. Namibian margin

The hydrographic data obtained by CTD measurements along a downslope transect from the surface to 1000 m water depth revealed distinct changes in temperature and salinity throughout the water column. These are ascribed to the different water masses in the study area (Fig. 3.3a). In the upper 85 m of the water column, temperatures were above 14 °C and salinities > 35.2, which correspond to South Atlantic Subtropical Surface Water (SASSW). SACW was situated underneath the SASSW and reaches down to about 700 m, characterized by a temperature from 14 to 7 °C and a salinity from 35.4 to 34.5 (Fig. 3.3a). A deep CTD cast about 130 km from the coastline recorded a water mass with the signature of ESACW, having a lower temperature (Δ1.3 °C) and lower salinity (Δ0.2) than SACW (in 200 m depth, not included in CTD transects of Fig. 3.4). Underneath these two central water masses Antarctic Intermediate Water (AAIW) was found with a temperature < 7 °C.

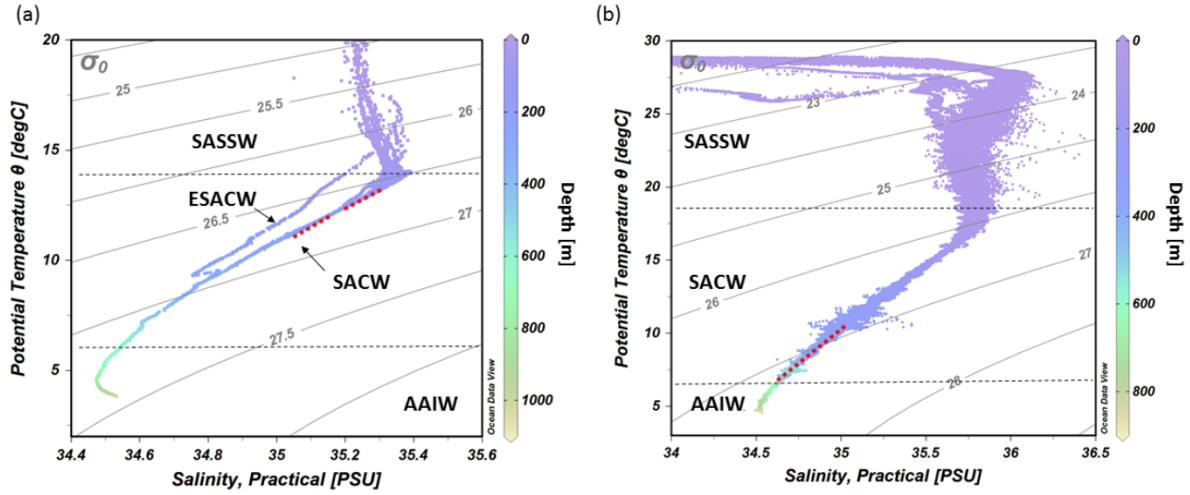

Figure 3.3. T –S diagrams showing the different water masses being present at the (a) Namibian and (b) Angolan margins: South Atlantic Subtropical Surface Water (SASSW), South Atlantic Central Water (SACW) and Eastern South Atlantic Central water (ESACW), Antarctic Intermediate Water (AAIW) (data plotted using Ocean Data View v.4.7.8; http://odv.awi.de, last access: 12 February 2016; Schlitzer, 2011). Red dotted line indicates the depth range of cold-water coral mound occurrence

The CTD transect showed decreasing DO (dissolved oxygen) concentration from the surface (6 mL L^{-1}) towards a minimum in 150 to 200 m depth (0 mL L^{-1}). Lowest values for DO concentrations were found on the continental margin between 100 and 335 m water depth. The DO concentrations in this pronounced OMZ ranged from < 1 mL L^{-1} down to 0 mL L^{-1} (≙9 % to 0 % saturation). The zone of low DO concentrations (< 1 mL L^{-1}) stretched horizontally over the complete transect from about 50 km to at least 100 km offshore (Fig. 3.4c). The upper boundary of the OMZ was relatively sharp compared to its lower limits and corresponded with the border between SASSW at the surface and SACW below.

Within the OMZ, a small increase in fluorescence (0.2 mg m^{-3}) was recorded, whereas fluorescence was otherwise not traceable below the surface layer (Fig. 3.4d). Within the surface layer, highest surface

fluorescence (> 2 mg m^{-3}) was found ~40 km offshore. Above the center of the OMZ fluorescence reached only 0.4 mg m^{-3}.

3.3.1.2. Angolan margin

The hydrographic data obtained by CTD measurements along a downslope transect from the surface to 800 m water depth revealed distinct changes in temperature and salinity throughout the water column, related to four different water masses. At the surface a distinct shallow layer (> 20 m) with a distinctly lower salinity (27.3–35.5) and higher temperature (29.5–27 °C, Fig. 3.3b) was observed. Below the surface layer, SASSW was found down to a depth of 70 m, characterized by a higher salinity (35.8). SACW was observed between 70 and 600 m, showing the expected linear relationship between temperature and salinity. Temperature and salinity decreased from 17.5 °C and 35.8 to 7 °C and 34.6. At 700 m depth AAIW was recorded, characterized by a low salinity (< 34.4) and temperature (< 7 °C, Fig. 3.3b).

The CTD transect showed a sharp decrease in the DO concentrations underneath the SASSW from 5 to < 2 mL L^{-1} (Fig. 3.5). DO concentrations decreased further to a minimum of 0.6 mL L^{-1} at 350 m and then increased to > 3 mL L^{-1} at 800m depth. Lowest DO concentrations were not found at the slope but 70 km offshore in the center of the zone of reduced DO concentrations between 200 and 450 m water depth (< 1 mL L^{-1}). Compared to the Namibian margin (see Fig. 3.4), the hypoxic layer was situated further offshore, slightly deeper, and overall DO concentrations were higher (compare Fig. 3.4c). Also, the boundaries of the hypoxic zone were not as sharp. Fluorescence near the sea surface was generally low (around 0.2 with small maxima of 0.78 mg m^{-3}) and not detectable deeper than 150 m

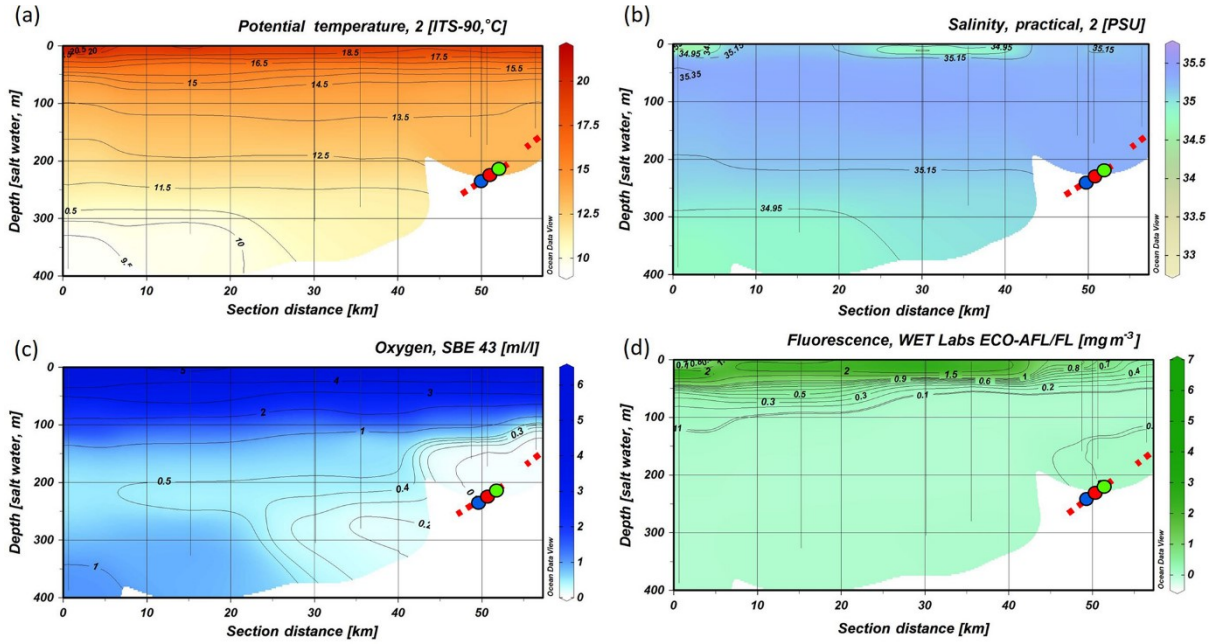

Figure 3.4. CTD transect across the Namibian margin (see Fig. 3.1b for location). Data are presented for (a) potential temperature (°C), (b) salinity (PSU), (c) dissolved oxygen concentrations (mL L^{-1}), note the pronounced oxygen minimum zone (OMZ) between 100 and 335 m water depth, and (d) fluorescence (mg m^{-3}) (data plotted using Ocean Data View v.4.7.8; http://odv.awi.de, last access: 12 February 2016; Schlitzer, 2011). The occurrence of fossil CWC mounds is indicated by a red dashed line, colored dots indicate bottom lander deployments.

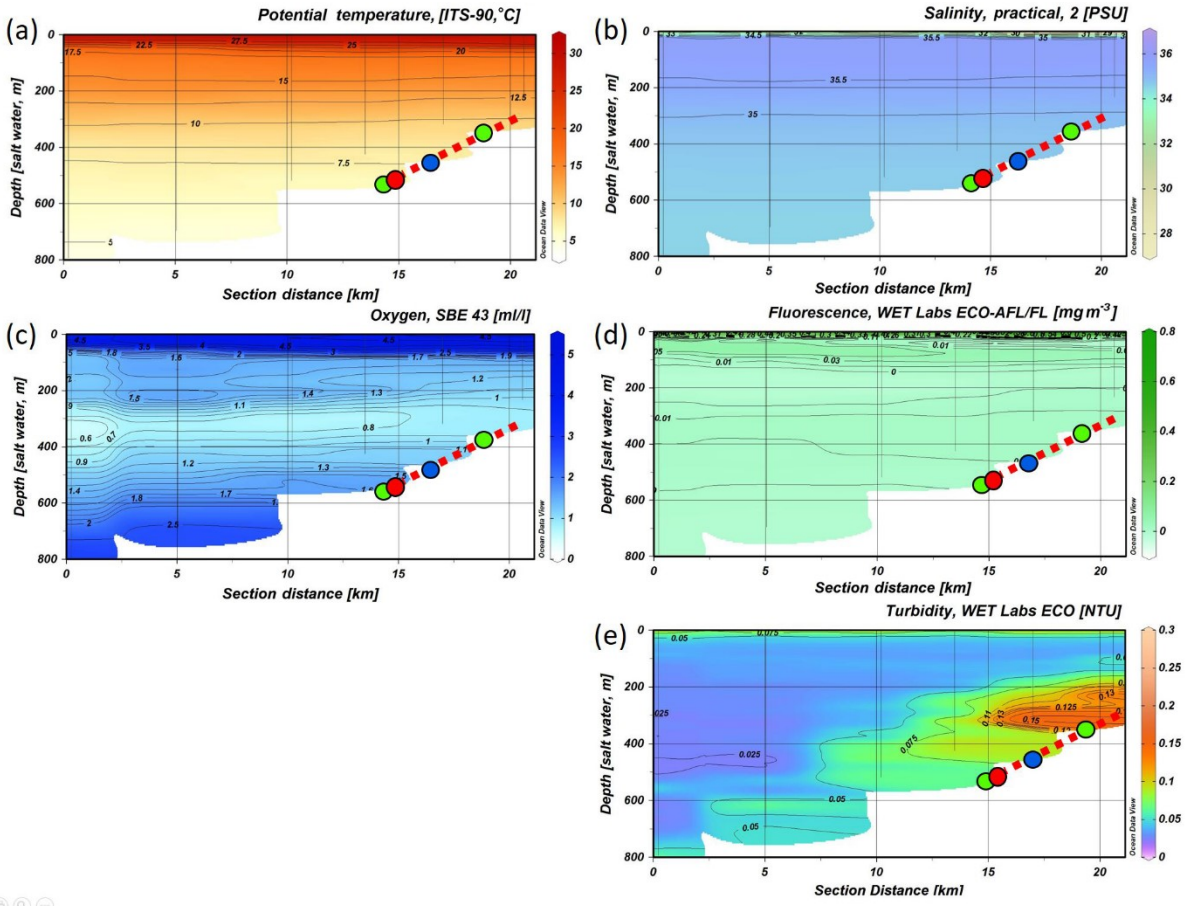

Figure 3.5. CTD transect across the Angolan margin. Shown are data for (a) potential temperature (°C), (b) salinity (PSU), (c) dissolved oxygen concentration (mL L^{-1}), (d) fluorescence (mg m^{-3}), (e) turbidity (NTU) (data plotted using Ocean Data View v.4.7.8; http://odv.awi.de, last access: 12 February 2016; Schlitzer, 2011). The depth occurrence of CWC mounds is marked by a red, dashed line, and the lander deployments are indicated by colored dots.

depth. A distinct zone of enhanced turbidity was observed on the continental margin between 200 and 350 m water depth.

3.3.2. Near-bottom environmental data

3.3.2.1.Namibian margin

Bottom temperature ranged from 11.8 to 13.2 °C during the deployment of the ALBEX lander (Table 3.2, Fig. 3.6), showing oscillating fluctuations with a maximum semidiurnal (ΔT ~ 6 h) change of ~ Δ1 °C (on 9 January 2016). The DO concentrations fluctuated between 0 and 0.15 mL L^{-1} and were negatively correlated with temperature (r = -0.39, p<0.01). Fluorescence ranged from 42 to 45 NTU during the deployment and was positively correlated with temperature (r = 0.38, p<0.01). Hence, both temperature and fluorescence were negatively correlated with DO concentrations (r = -0.39, p<0.01) and turbidity (optical backscatter, r = -0.35, p<0.01). Turbidity was low until it increased markedly during the second half of the deployment. During this period on the 6 January, wind speed increased from 10 m s^{-1} to a maximum of 17 m s^{-1} and remained high for the next 6 days. The wind direction changed from counterclockwise cyclonic rotation towards alongshore winds. During the strong wind

period, colder water (correlation between wind speed and water temperature, r = -0.55, p<0.01) with a higher turbidity (correlation of wind speed and turbidity, r = 0.42, p<0.01) and on average higher DO concentrations was present. The SLM lander recorded an average pH of 8.01.

Maximum current speeds measured during the deployment period were 0.21 m s^{-1}, with average current speeds of 0.09 m s^{-1} (Table 3.2). The tidal cycle explained > 80% of the pressure fluctuations (Table 3.3), with a semidiurnal signal, M2 (principal lunar semidiurnal), generating an amplitude of > 0.35 dbar and thus being the most important constituent. Before the 6 January, the current direction oscillated between SW and SE after which it changed to a dominant northerly current direction (Fig. 3.6).

The observed fluctuations in bottom water temperature at the deployment site imply a vertical tidal movement of around 70 m. This was estimated by comparing the temperature change recorded by the lander to the respective temperature–depth gradient based on water column measurements (CTD site GeoB20553, 12.58 °C at 245 m, 12.93 °C at 179 m). Due to these vertical tidal movements, the oxygen-depleted water from the core of the OMZ is regularly being replaced with somewhat colder and slightly more oxygenated water (1 up to 0.2 mL L^{-1}).

Table 3.2. Environmental properties at the Namibian and Angolan margins.

	Namibia	Angola
Temperature (°C)	11.8–13.2	6.73–12.9
DO concentrations (mL L^{-1})	0–0.15	0.5–1.5
Fluorescence (NTU)	42–45	38.5–41.5
Current speed max. (m s^{-1})	0.21	0.3
Current speed average (m s^{-1})	0.09	0.1
Tidal cycle	Semidiurnal (0.37 dbar, 3 cm s^{-1})	Semidiurnal (0.6 dbar, 8.2 cm s^{-1})
Average pH	8.01	8.12

3.3.2.2. Angolan margin

Mean bottom water temperatures were 6.73 °C at the deeper site (530 m) and 10.06 °C at the shallower site (340 m, Fig. 3.7, Table 3.2). The maximum semidiurnal (ΔT ~ 6 h) temperature change was Δ1.60 °C at the deepest site and Δ2.4 °C at the shallow site (Fig. 3.7). DO concentrations at the deep site were a factor of 2 higher than those at the shallow site, i.e., 0.9–1.5 vs. 0.5–0.8 mL L^{-1} respectively (≙range between 4 % and 14 % saturation of both sites), whereas the range of diurnal fluctuations was much smaller compared to the shallow site. DO concentrations were negatively correlated with temperature at the deep site (r = -0.99, p<0.01), while positively correlated at the shallow site (r = 0.91, p<0.01). Fluorescence was low during both deployments and showed only small fluctuations, being slightly higher at the shallow site (between 38.5 and 41.5 NTU at both sites). Current speeds were relatively high (between 0 and 0.3 m s^{-1}, average 0.1 m s^{-1}) and positively correlated with temperature at the shallow site (r = 0.31, p<0.01) and negatively correlated at the deep site (r = -0.22, p<0.01). Analysis of the tidal cycle showed that it explained 29.8 %–54.9 % of the horizontal current fluctuations. The M2 amplitude was 0.06–0.09 s^{-1} and was the most important signal (Table 3.3). A decrease in turbidity was

observed during the deployment at the shallow station. This station was located directly below the turbidity maximum between 200 and 350 m depth as observed in the CTD transect (Fig. 5). In contrast, a relative constant and low turbidity was observed for the deep deployment. Turbidity during both deployments was positively correlated to DO concentrations (r = 0.47, p<0.01, shallow deployment and r = 0.50, p<0.01, deep deployment). The SLM lander recorded an average pH of 8.12. The short-term temperature fluctuations imply a vertical tidal movement of around 130m (12.9–9.1 °C measured by lander, ≙218–349 m depth in CTD above lander at station GeoB20966).

Table 3.3. Tidal analysis of the ALBEX lander from 6 m above the sea floor. Depth, mean current speed, mean current direction, tidal predictions of pressure fluctuations, two most important harmonics with amplitude, tidal prediction of horizontal current field, two most important harmonics with semi-major' amplitudes.

	Station no. (GeoB ID)	Depth (m)	Mean current speed (cm s^{-1})	Current direction (°)	Tides (%) (p)	Const. (dbar)	Tides (%) (u)	Const. (cm s^{-1})
Namibia	20507-1	430	9.34	221.6	81.8	M2 0.37	10.5	M2: 3.1 M3: 0.8
Angola	20921-1	340	9.96	247.9	91.6	M2: 0.59	36	M2: 7.8 M3: 0.7
	20940-1	530	8.82	275.6	86.8	M3: 0.04	50.9	M2: 8.6 M3: 3.7

3.3.3. Suspended particulate matter

3.3.3.1.Namibian margin

The nitrogen (N) concentration of the SPOM measured on the filters of the McLane pump fluctuated between 0.25 and 0.45 mg L^{-1}(Fig. 3.8). The highest N concentration corresponded with a peak in turbidity (r = 0.42, p<0.01). The $\delta^{15}N$ values of the lander time series fluctuated between 5.1 and 6.9 with an average value of 5.7 ‰. Total organic carbon (TOC) showed a similar pattern as nitrogen, with relative concentrations ranging between 1.8 and 3.5 mg L^{-1}. The $\delta^{13}C$ value of the TOC increased during the surveyed time period from -22.39 ‰ to -21.24 ‰ with an average of -21.7 ‰ (Fig. 3.8a). The C=N ratio ranged from 8.5–6.8 and was on average 7.4 (Fig. 3.8b). During periods of low temperature and more turbid conditions TOC and N as well as the $\delta^{13}C$ values of the SPOM were higher.

Chlorophyll α concentrations of SPOM were on average 0.042 µg L^{-1} and correlated with the record of the fluorescence (r = 0.43, p = 0.04). A 6 times higher amount of chlorophyll α degradation products was found during the lander deployment (0.248 µg L^{-1}) compared to the amount of chlorophyll α, giving a Σphaeopigment/chlorophyll α ratio of 6.5 (not shown). Additionally, carotenoids (0.08–0.12 µg L^{-1}) and fucoxanthin (0.22 µg L^{-1}), which are common in diatoms, were major components of the pigment fraction. Zeaxanthin, indicating the presence of prokaryotic cyanobacteria, was only observed in small quantities (0.066 µg L^{-1}).

3.3.3.2. Angolan margin

In general TOC and N concentrations of SPOM were higher at the shallow site compared to the deep site. Nitrogen concentrations varied around 0.14 mg L^{-1} at 340 m and around 0.1 mg L^{-1} at 530 m depth (Fig. 3.8b). The $\delta^{15}N$ values at the shallow site ranged from 1.6 ‰ to 6.2 ‰ (3.7 ‰ average) and were even lower deeper in the water column, viz. Range 0.3–3.7 ‰ with an average of 1.4 ‰. The TOC concentrations were on average 1.43 mg L^{-1} at 340m and 0.9 mg L^{-1} at 530 m, with corresponding $\delta^{13}C$ values ranging between -23.0 and -24.2 (average of -23.6 ‰) at the shallow, and between -22.9 and -23.9 (average -23.4 ‰) at the deep site.

The chlorophyll α concentrations of the SPOM collected by the McLane pump varied between 0.1 and 0.02 µg L^{-1}, with average Σphaeopigment/chlorophyll α ratios of 2.6 and 0.5 at the shallow and deep sites, respectively. Phytopigments recorded by the shallow deployment included 0.3 µg L^{-1} of fucoxanthin, while at the deep site only a concentration of 0.1 µg L^{-1} was found. No zeaxanthin was recorded in the pigment fraction.

3.4. Discussion

Even though the ecological-niche factor analyses of Davies *et al.* (2008) and Davies and Guinotte (2011) predict *L. pertusa* to be absent along the oxygen-limited southwestern African margin, CWC mounds with two distinct benthic ecosystems were found. The coral mounds on the Namibian shelf host no living CWCs; instead the dead coral framework covering the mounds was overgrown with fauna dominated by bryozoans and sponges. Along the slope of the Angolan margin an extended coral mound area with thriving CWC communities was encountered. It is probably that differences in present-day environmental conditions between the areas influence the faunal assemblages inhabiting them. The potential impact of the key environmental factors will be discussed below.

3.4.1. Short-term vs. long-term variations in environmental properties

On the Namibian margin, seasonality has a major impact on local mid-depth oxygen concentration due to the periodically varying influence of the Angola current and its associated low DO concentrations (Chapman and Shannon, 1987). The lowest DO concentration is expected from high wind conditions on the Namibian margin (Fig. 3.6), leading to an intrusion of ESACW with higher DO concentrations (Δ 0.007 mL L^{-1} on average) and lower temperatures (Δ 0.23 °C on average, Fig. 3.5) than the SACW. This led to a temporal increase in the DO concentrations. This shows that variations in the local flow field have the capability to change water properties on relatively short time scales, which might provide an analogue to the water mass variability related to the different seasons (Mohrholz *et al.*, 2008). Such relaxations are possibly important for the survival of the abundant benthic fauna present on the relict coral mounds (Gibson and Atkinson, 2003). Other seasonal changes, like riverine outflow, do not have decisive impacts on the ecosystem since only relatively small rivers discharge February to May when

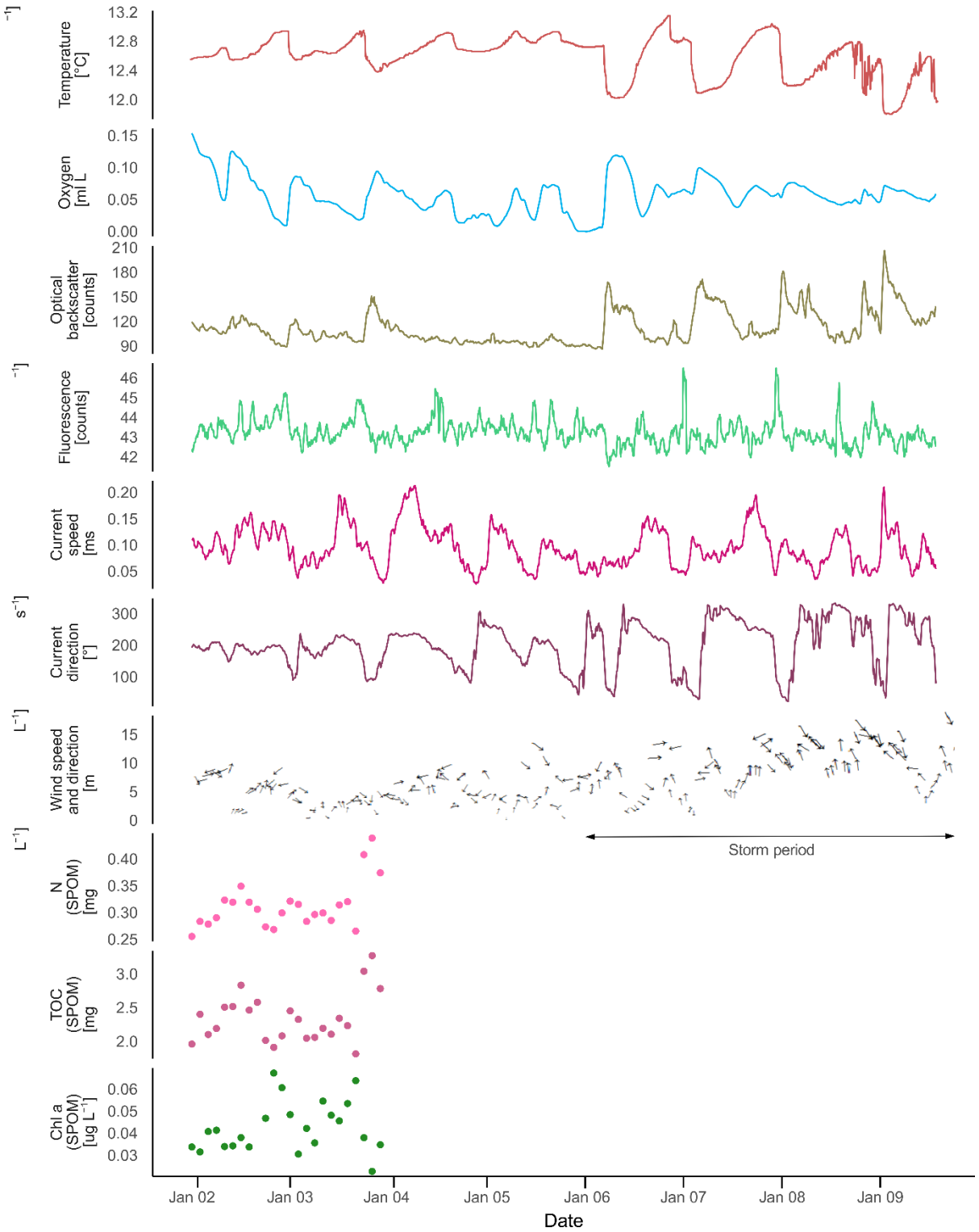

Figure 3.6. Data recorded by the ALBEX lander (210 m) at the Namibian margin in January 2016. Shown are data for temperature (°C; red), dissolved oxygen concentrations (mL L^{-1}; blue), optical backscatter (turbidity; moss green), fluorescence (counts per second; green), current speed (m s^{-1}; pink), current direction (°: 0–360°; dark red) as well as nitrogen (mg L^{-1}; pink dots), carbon (mg L^{-1}; purple dots), and chlorophyll α concentration (µg L^{-1}; green dots) of SPOM collected during the first 48 h by the McLane pump. These data are supplemented by wind speed and direction (small black arrows) recorded concurrently to the lander deployment by ship bound devices. Note that current directions changed from a generally south-poleward to an equatorward direction when wind speed exceeded 10 m s^{-1} (stormy period indicated by black arrow).

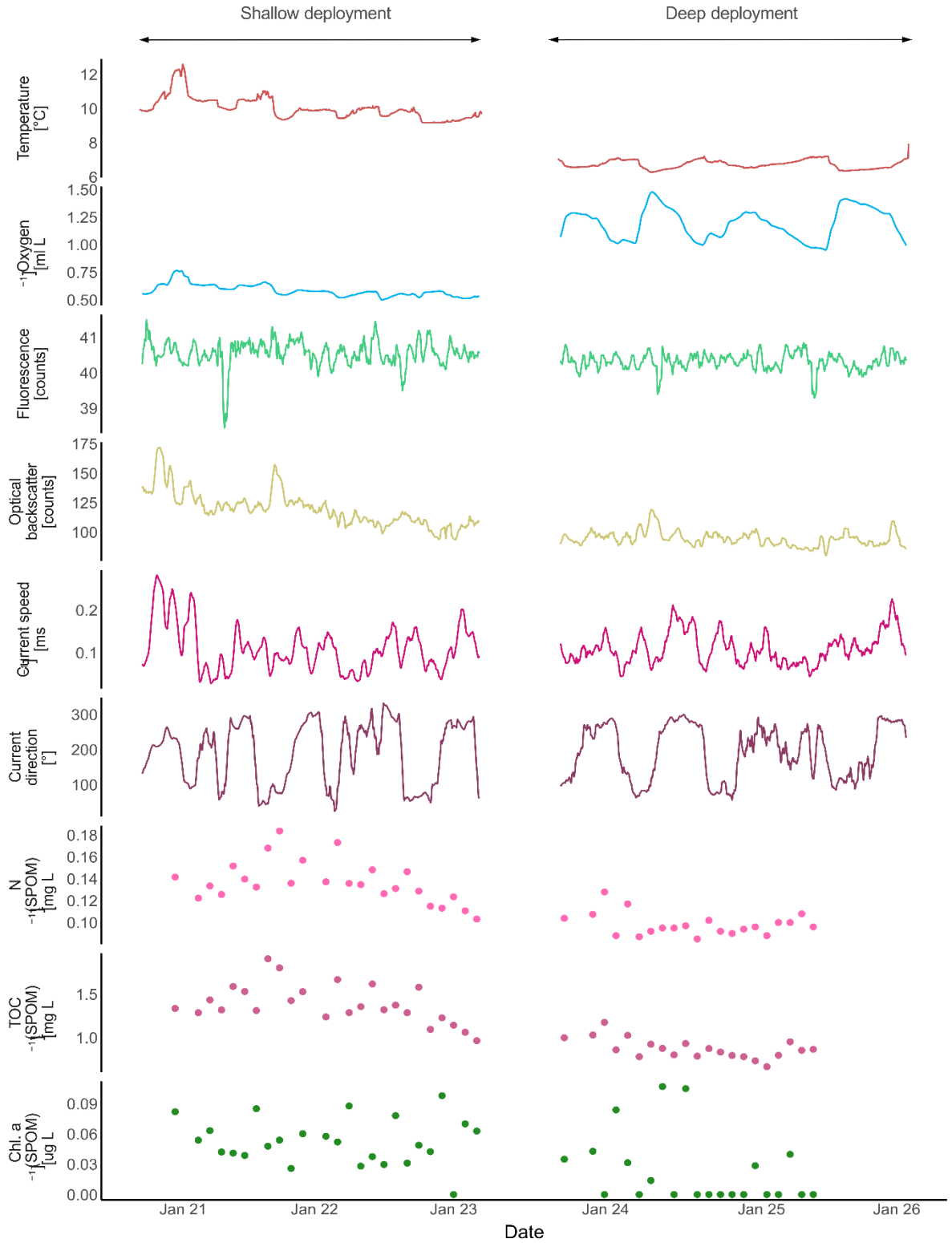

Figure 3.7. Lander data (ALBEX) recorded during at the shallow (~ 340m water depth) and deep sites (~ 530m water depth) off Angola (January 2016). Shown are temperature (°C; red), dissolved oxygen concentration (mL L^{-1}; blue), fluorescence (counts per second; green), optical backscatter (turbidity; yellow), current speed (m s^{-1}; pink) and current direction (°: 0–360°; purple) as well as nitrogen (mg L^{-1}; pink dots), carbon (mg L^{-1}; purple dots), and chlorophyll α concentration (µg L^{-1}, green dots) of SPOM collected during the both deployments by the McLane pump.

SACW is the dominating water mass on the Namibian margin and the contribution of ESACW is smaller (Mohrholz *et al.*, 2008). Due to this seasonal pattern, the DO concentrations measured in this

study (January; Fig. 3.4) probably do not represent minimum concentrations, which are expected tooccur in the following months, but nevertheless give a valuable impression about the extent of the OMZ (February to May; Mohrholz *et al.*, 2014). Interestingly, we captured a flow reversal after 6 January from a southward to an equatorward current direction during from the Namibian margin. This is also reflected by the dominant marine isotopic signature of the isotopic ratios of $\delta^{15}N$ and $\delta^{13}C$ of the SPOM at the mound areas (Fig. 3.8, cf. Tyrrell and Lucas, 2002).

Flow reversals were not observed during the lander deployments on the Angolan margin, where winds are reported to be weak throughout the year providing more stable conditions (Shannon, 2001). Instead river outflow seems to exert a strong influence on the DO concentrations on the Angolan margin. The runoff of the Cuanza and Congo river reach their seasonal maximum in December and January (Kopte *et al.*, 2017), intensifying upper water column stratification. This stratification is restricting vertical mixing and thereby limits ventilation of the oxygen-depleted subsurface water masses. In addition rivers transport terrestrial organic matter to the margin, which is reflected by the isotopic signals of the SPOM (-1 ‰ to 3 ‰; Montoya, 2007) which is well below the average isotopic ratio of the marine waters of 5.5 ‰ (Meisel et al., 2011). Also $\delta^{13}C$ values are in line with the $\delta^{13}C$ values of terrestrial matter which is on average -27 ‰ in this area (Boutton, 1991; Mariotti *et al.*, 1991). The C=N ratio of SPOM is higher compared to material from the Namibian margin, also confirming admixing of terrestrial matter (Perdue and Koprivnjak, 2007). This terrestrial matter contains suitable food sources as well as less suitable food sources, like carbon-rich polymeric material (cellulose, hemicellulose and lignin), which cannot easily be taken up by marine organisms (Hedges and Oades, 1997). The combined effects of decreased vertical mixing and additional input of organic matter potentially result in the lowest DO

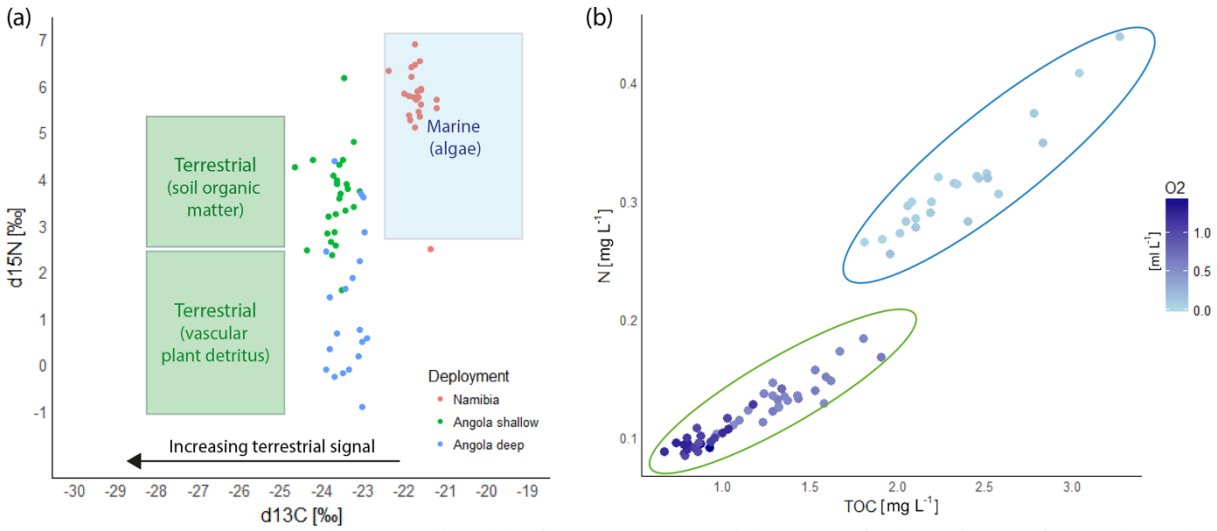

Figure 3.8. Composite records of SPOM collected by the McLane pump of the ALBEX lander at the Namibian and Angolan margins during all three deployments. (a) $\delta^{15}N$ and $\delta^{13}C$ isotopic values at the Namibian (red dots) and Angolan (blue and green dots) margins. Indicated by the square boxes are common isotopic values of terrestrial and marine organic matter (Boutton, 1991; Holmes *et al.*, 1997; Sigman *et al.*, 2009). The relative contribution of terrestrial material (green boxes) is increasing with a more negative $\delta^{13}C$ value. (b) Total organic carbon (TOC) and nitrogen (N) concentration of the SPOM. Values of the Namibian margin are marked by a blue circle (C/N ratio = 7.8), values of the Angolan margin are marked by a green circle (C/N ratio = 9.6). Dissolved oxygen concentrations are included to show the higher nutrient concentrations in less oxygenated water.

concentrations of the year during the investigated time period (January), since the highest river outflow and therefore strongest stratification is expected during this period.

3.4.2. Main stressors – oxygen and temperature

Environmental conditions marked by severe hypoxia and temporal anoxia (< 0.17 mL L^{-1}) likely explain the present day absence of living CWCs along the Namibian margin. During the measurement period the DO concentrations off Namibia were considerably lower than the thus far recorded minimum concentrations near living CWCs (1–1.3 mL L^{-1}), which were found off Mauritania where only isolated living CWCs are found (Ramos *et al.*, 2017). Age dating of the Namibian fossil coral framework showed that CWCs disappeared about 5 ka which coincides with an intensification in upwelling and therefore most likely a decline of DO concentrations (Tamborrino *et al.*, 2019), supporting the assumption that the low DO concentrations are responsible for the demise of CWCs on the Namibian margin. Although no living corals were observed on the Namibian coral mounds, we observed a dense living community dominated by sponges and bryozoans (Hebbeln *et al.*, 2017). Several sponge species have been reported to survive at extremely low DO concentrations within OMZs. For instance, along the lower boundary of the Peruvian OMZ, sponges were found at DO concentrations as low as 0.06–0.18 mL L^{-1} (Mosch *et al.*, 2012). Mills *et al.* (2018) recently found a sponge (*Tethya wilhelma*) to be physiologically almost insensitive to oxygen stress and respires aerobically under low DO concentrations (0.02 mL L^{-1}). Sponges can potentially stop their metabolic activity during unfavorable conditions and restart their metabolism when some oxygen becomes available, for instance during diurnal irrigation of water with somewhat higher DO concentrations. The existence of a living sponge community off Namibia might therefore be explained by the diurnal tides occasionally flushing the sponges with more oxic water, enabling them to metabolize, when food availability is highest (Fig. 3.6). Increased biomass and abundances in these temporary hypoxic–anoxic transition zones were already observed for macro- and megafauna in other OMZs and is referred to as the "edge effect" (Levin *et al.*, 1991; Mullins *et al.*, 1985; Sanders, 1969). It is very likely that this mechanism plays a role for the benthic communities on the Namibian as well as the Angolan margin.

Along the Angolan margin, low oxygen concentrations apparently do not restrict the proliferation of thriving CWC reefs even though DO concentrations are considered hypoxic (0.5–1.5 mL L^{-1}). The DO concentrations measured off Angola are well below the lower DO concentration limits for *L. pertusa* based on laboratory experiments and earlier field observations (Brooke and Ross, 2014; Schroeder, 2002). The DO concentrations encountered at the shallow mound sites (< 0.8 mL L^{-1}) are even below the so far lowest limits known for single CWC colonies from the Mauritanian margin (Ramos *et al.*, 2017). Since in the present study measured DO concentrations were even lower than the earlier established lower limits, this could suggest a much higher tolerance of *L. pertusa* to oxygen levels as low as 0.5 mL L^{-1} at least in a limited time period (4 % O_2 saturation).

In addition to oxygen stress, heat stress is expected to put additional pressure on CWCs. Temperatures at the CWC mounds off Angola ranged from 6.4 to 12.6 °C, with the upper limit being close to reported maximum temperatures (~ 12–14.9 °C; Davies and Guinotte, 2011) and are hence expected to impair the ability of CWCs to form mounds (see Wienberg and Titschack, 2017). The CWCs were also occurring outside of the expected density envelope of 27.35–27.65 kg m^{-3}in densities well below 27 kg m^{-3} (Fig. 3.3, Dullo *et al.*, 2008). In most aquatic invertebrates, respiration rates roughly double with every 10 °C increase (Q_{10} temperature coefficient = 2–3, e.g., Coma, 2002), which at the same time doubles energy demand. Dodds *et al.* (2007) found a doubling of the respiration rate of *L. pertusa* with an increase at ambient temperature of only 2 °C (viz. Q_{10} D 7–8). This would limit the survival of *L. pertusa* at high temperatures to areas where the increased demand in energy (due to increased respiration) can be compensated by high food availability. Higher respiration rates also imply that enough oxygen needs to be available for the increased respiration. However this creates a negative feedback, since with increased food availability and higher temperatures the oxygen concentration will decrease due to bacterial decomposition of organic substances.

Survival of *L. pertusa* under hypoxic conditions along the shallow Angolan CWC areas is probably positively influenced by the fact that periods of highest temperatures coincide with highest DO concentrations during the tidal cycle. Probably here the increase of one stressor is compensated by a reduction of another stressor. On the Namibian margin and the deeper Angolan mound sites the opposite pattern was found, with highest temperatures during lowest DO concentrations. However, at the deeper Angolan mound sites DO concentrations are higher and temperatures more within a suitable range compared to the shallow sites (0.9– 1.5 mL L^{-1}, 6.4–8 °C, Fig. 3.7). Additionally it was shown by ex situ experiments that *L. pertusa* is able to survive periods of hypoxic conditions similar to those found along the Angolan margin for several days, which could be crucial in periods of most adverse conditions (Dodds *et al.*, 2007).

3.4.3. Food supply

As mentioned above, environmental stresses like high temperature or low DO concentration result in a loss of energy (Odum, 1971; Sokolova *et al.*, 2012), which needs to be balanced by an increased energy (food) availability. Food availability therefore plays a significant role for faunal abundance under hypoxia or unfavorable temperatures (Diaz and Rosenberg, 1995). Above, we argued that survival of sponges and bryozoans on the relict mounds off Namibia and of CWCs, and their associated fauna at the Angolan margin, may be partly due to a high input of high-quality organic matter, compensating oxygen and thermal stresses. The importance of the food availability for CWCs was already suggested by Eisele *et al.* (2011), who mechanistically linked CWC mound growth periods with enhanced surface water productivity and hence organic matter supply. Here we found evidence for high quality and quantity of SPOM in both areas indicated by high TOC and N concentrations (Figs. 3.6 and 3.7) in combination with a low C/N ratio (Fig. 3.8), a low isotopic signature of $\delta^{15}N$ and only slightly degraded pigments.

The Namibian margin is known for its upwelling cells, where phytoplankton growth is fueled by nutrients from deeper water layers producing high amounts of phytodetritus (Chapman and Shannon, 1987), which subsequently sinks down to the relict mounds on the slope. Benthic communities on the mounds off Namibia occur at relatively shallow depths, hence downward transport of SPOM from the surface waters is rapid and time for decomposition of the sinking particles in the water column is limited. The higher turbidity during lower current speeds provides additional evidence that the material settling from the surface is not transported away with the strong currents (Fig. 3.6).

At the Angolan coral mounds, SPOM appeared to have a signature corresponding to higher quality organic matter compared to the SPOM off Namibia. The phytopigments were less degraded and the $\delta^{15}N$, TOC and N concentrations of the SPOM were lower. However, here lower $\delta^{15}N$ and a higher Σphaeopigment = chlorophyll α ratio are likely connected to a mixture with terrestrial OM input, which might constitute a less suitable food source for CWCs (Hedges and Oades, 1997). On the other hand, the riverine input delivers dissolved nutrients, which can support the growth of phytoplankton, indirectly influencing food supply (Kiriakoulakis *et al.*, 2007; Mienis *et al.*, 2012b). Moreover, the variations in food quality at the shallow Angolan reefs, which were relatively small during this study, did not seem to be related to the presence of other environmental stressors. At the Angolan margin we see a rather constant availability of SPOM. The slightly higher turbidity during periods of highest DO concentrations (Fig. 3.7) suggests that the SPOM on the Angolan margin originates from the bottom nepheloid layer on the margin directly above the CWC mounds (Fig. 3.5e), which may represent a constant reservoir of fresh SPOM. This reservoir is probably fueled by directly sinking as well as advected organic matter from the surface ocean.

3.4.4. Tidal currents

The semidiurnal tidal currents observed probably play a major role in the survival of benthic fauna on the SW African margin. On the Namibian margin, internal waves deliver oxygen from the surface and deeper waters to the OMZ and thereby enable benthic fauna on the fossil coral framework to survive in hypoxic conditions (Fig. 3.9a). At the same time these currents are probably responsible for the delivery of fresh SPOM from the surface productive zone to the communities on the margin, since they promote mixing between the water masses as well as they vertically displace the different water layers.

On the Angolan margin, internal tides produce slightly faster currents and vertical excursions of up to 130m which are twice as high as those on the Namibian margin. Similar to the Namibian margin, these tidal excursions deliver oxygen from shallower and deeper waters to the mound zone and thereby deliver water with more suitable characteristics over the whole extent of the parts of the OMZ which otherwise may be unsuitable for CWCs (Fig. 3.9b). Internal tides are also responsible for the formation of a bottom nepheloid layer at 200–350 m depth (Fig. 3.5e). This layer is formed by trapping of organic matter as well as bottom erosion due to turbulence created by the interaction of internal waves with the margin topography, which intensifies near-bottom water movements. These internal waves are able to move

on the density gradient between water masses, which are located at 225 and 300 m depth (Fig. 3.3). Tidal waves will be amplified due to a critical match between the characteristic slope of the internal M2 tide and the bottom slope of the Angolan margin, as is known from other continental slope regions (Dickson and McCave, 1986; Mienis *et al.*, 2007). As argued above, this turbid layer is likely important for the nutrition of the slightly deeper situated CWC mounds, since vertical mixing is otherwise hindered by the strong stratification.

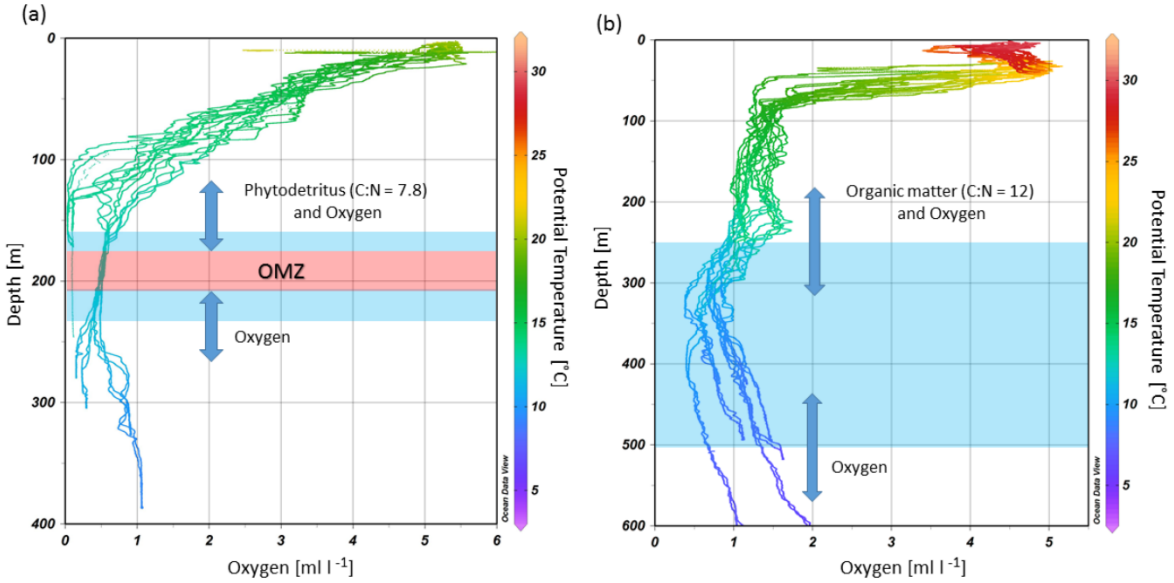

Figure 3.9. Depth range of cold-water coral mound occurrences (blue shaded areas) at the (a) Namibian and (b) Angolan margins in relation to the dissolved oxygen concentrations and potential temperature. Diurnal tides are delivering mainly phytodetritus (shown in a) and organic matter from the benthic nepheloid layer (shown in b) as well as oxygen from above and from below to the mound sites (indicated by blue arrows, the lengths of which indicate the tidal ranges).

3.5. Conclusions

Different environmental properties explain the present conditions of the benthic communities on the southwestern African margin including temperature, DO concentration, food supply and tidal movements. The DO concentrations probably define the limits of a suitable habitat for CWCs along the Namibian and the Angolan margin, whereas high temperatures constitute additional stress by increasing the respiration rate and therefore energy demand. On the Namibian margin, where DO concentrations dropped below 0.01 mL L^{-1}, only fossil CWC mounds covered by a community dominated by sponges and bryozoans were found. This benthic community survives as it receives periodically waters with slightly higher DO concentrations (>0.03 mL L^{-1}) due to regular tidal oscillations (semidiurnal) and erratic wind events (seasonal). At the same time, a high quality and quantity of SPOM sinking down from the surface water mass enables the epifaunal community to survive despite the oxygen stress and to sustain its metabolic energy demand at the Namibian OMZ, while CWCs are not capable to withstand such extreme conditions. In contrast, thriving CWCs on the Angolan coral mounds were encountered despite the overall hypoxic conditions. The DO concentrations were slightly higher than those on the Namibian margin but nevertheless below the lowest threshold that was so far reported for *L. pertusa* (Davies *et al.*, 2010; Davies *et al.*, 2008; Ramos *et al.*, 2017). In combination

with temperatures close to the upper limits for *L. pertusa*, metabolic energy demand probably reached a maximum. High energy requirements might have been compensated by the general high availability of fresh re-suspended SPOM. Fresh SPOM accumulates on the Angolan margin just above the CWC area and is regularly supplied due to mixing by semidiurnal tidal currents, despite the restricted sinking of SPOM from the surface due to the strong stratification.

CWC and sponge communities are known to play an important role as a refuge, feeding ground and nursery for commercial fishes (Miller *et al.*, 2012), and have a crucial role in the marine benthic pelagic coupling (Cathalot *et al.*, 2015). Their ecosystem services are threatened by the expected expansion of OMZs due to anthropogenic activities like rising nutrient loads and climate change (Breitburg *et al.*, 2018). This study showed that benthic fauna is able to cope with low oxygen levels as long as sufficient high-quality food is available. Further, reef-associated sponge grounds, as encountered on the Namibian margin could play a crucial role in taking over the function of CWCs in marine carbon cycling as well as in providing a habitat for associated fauna, when conditions become unsuitable for CWCs.

Acknowledgements

We thank the captain of the *R V Meteor* cruise M122, Rainer Hammacher, his officers and crew, who contributed to the success of this cruise. We also would like to thank the scientific and technical staff for their assistance during the cruise and their work in the laboratory. Greatly acknowledged are the efforts from the German Diplomatic Corps in the German embassies in Windhoek and Luanda and in the Foreign Office in Berlin. We thank the German Science Foundation (DFG) for providing ship time on *R V Meteor* and for funding the ROV Squid operations to investigate the cold-water coral ecosystems off Angola and Namibia.

Financial support

This research has been supported by the DFG Research Center/Cluster of Excellence "MARUM – The Ocean in the Earth System". Ulrike Hanz is funded by the SponGES project, which received funding from the European Union's Horizon 2020 research and innovation program (grant no. 679849). Furu Mienis is supported by the Innovational Research Incentives Scheme of the Netherlands Organisation for Scientific Research (NWO-VIDI grant no. 016.161.360). Gert-Jan Reichart is supported by the Netherlands Earth System Science Centre (NESSC), financially supported by the Ministry of Education, Culture and Science (OCW). Katriina Juva is funded through the FATE project (Fate of cold-water coral reefs – identifying drivers of ecosystem change), supported by the Norwegian Research Council (NRC).

4. Manuscript II

Spatial distribution and morphometry of the Namibian coral mounds controlled by the hydrodynamic regime and outer-shelf topography

Leonardo Tamborrino[1,2], Jürgen Titschack[1,3], Claudia Wienberg[1], Sam Purkis[4], Gregor Eberli[4] and Dierk Hebbeln[1]

[1] MARUM–Center for Marine Environmental Sciences, University of Bremen, Bremen, Germany

[2] Green Rebel, Crosshaven, Ireland

[3] Marine Research Department, Senckenberg am Meer, Wilhelmshaven, Germany

[3] Department of Geosciences, University of Bremen, Bremen, Germany

[4] Marine and Atmospheric Sciences, University of Miami, Miami, USA

Manuscript submitted (16.02.2022) in *Frontiers in Marine Sciences, after first review (09.06.2022).*

Abstract

Over millennial timescales, the proliferation of cold-water corals combined with sediment deposition within their frameworks are responsible of the formation of coral mounds. So far, these mounds have been mostly investigated as deep-sea biodiversity hotspots and geo-biological paleo-archives, whereas their morphological appearance has received much less attention. Here, we analysed the spatial distribution and the morphometry of the Namibian coral mounds to investigate the spatio-morphological development of early stage-coral mounds. As the Namibian mounds rarely exceed 20 m in height, key steps in the development of early-stage coral mounds (e.g. elongation, merging, limited gain in height compared to lateral extension) have been identified. With increasing size, coral mounds tend to be more elongated and downslope orientated. We interpret these data as result of the transition from an "inherited" to a "developed" morphology, thereby supporting an earlier hypothesis on the spatial development of coral mounds. This study reveals that the spatial-morphological appearance of coral mounds, often treated as a descriptive information, can provide valid information to understand their formation.

4.1. Introduction

Coral mounds are seafloor structures built by framework-forming scleractinian cold-water corals (CWC; Roberts et al., 2006). The development of the coral mounds firstly depends on CWC proliferation, controlled by a wide range of environmental parameters (dissolved oxygen concentrations, temperature, aragonite saturation state, pH, etc.; e.g., Davies et al., 2008). When their physic-chemical boundary conditions are met, the distribution of CWC is strongly controlled by food supply, since CWC are sessile opportunistic suspension feeders with a diet based on particulate and dissolved organic matter (Kiriakoulakis et al., 2005; Duineveld et al., 2007; Dodds et al., 2009; Mueller et al., 2014). The required food is mostly delivered by a moderate to strong hydrodynamic regime induced by geostrophic bottom currents and/or turbulent mixing triggered by internal waves, downwelling, cascading density currents, and Taylor columns (e.g., Frederiksen et al., 1992; Taviani et al., 2005; White et al., 2005; Thiem et al., 2006; Mienis et al., 2007; Davies et al., 2009; Mienis et al., 2009; Mienis et al., 2012; van Haren et al., 2014). The bottom currents do not only deliver food to the CWC, but also suspended sediments, which become trapped (baffling effect) by the coral frameworks (Mienis et al., 2019; Bartzke et al., 2021; Hennige et al., 2021). This baffled sediments within the coral frameworks usually contributes >50% to the coral mound deposits (e.g., Dorschel *et al.*, 2007b; Titschack *et al.*, 2015; Wang *et al.*, 2021).

Coral mounds are often clustered in coral mound provinces (CMPs) with 10s to 1000s of mounds (e.g., Wheeler et al., 2011; Lo Iacono et al., 2014; Glogowski et al., 2015; Hebbeln et al., 2019; MAREANO, 2020; Steinmann et al., 2020). Most of these CMPs occur around the continental margins of the Atlantic Ocean, on the upper to mid continental slopes (e.g., Kenyon et al., 2003; Colman et al., 2005; Grasmueck et al., 2006; Le Guilloux et al., 2009; Carranza et al., 2012; Hebbeln et al., 2014; Glogowski et al., 2015; Steinmann et al., 2020), but a large number of mounds appear also on continental shelves

(e.g., Reed, 2002; Fosså et al., 2005; Douarin et al., 2013; Tamborrino et al., 2019). Often the occurrence of the CMPs correspond to present or past boundaries of intermediate water masses (Dullo et al., 2008; White and Dorschel, 2010; Mohn et al., 2014; Matos et al., 2017; Wang et al., 2019). Density gradients (pycnocline) between water-mass boundaries allow for the accumulation of (re-)suspended organic particles and fine-grained sediments, resulting in the formation of intermediate and/or bottom nepheloid layers (Wang et al., 2001; Cacchione et al., 2002; Hosegood et al., 2004; Cheriton et al., 2014). Density gradients also play a key role for the formation of internal waves when intersecting relative steep slopes, which causes turbulent mixing (Garrett and Kunze, 2007; Klymak et al., 2011; Pomar et al., 2012; van Haren and GostIaux, 2012). Both processes support CWC proliferation and coral mound formation as they enhance the availability and supply of food and sediments (Frederiksen et al., 1992; Mienis et al., 2007; Davies et al., 2009; White and Dorschel, 2010; Hebbeln et al., 2014; Wang et al., 2019).

The presence of a suitable hard substrate of any size (from rocky outcrop to mm-sized bioclasts or gravel) represents an important prerequisite for the settlement of CWC planula (Wilson, 1979). Moderately enhanced hydrodynamics increasing the probability of food capture by the CWC is another advantageous prerequisite (Wheeler et al., 2007). This leads to a preferential CWC settlement on pre-existing seabed topography of variable scale, such as erosional features (De Mol et al., 2005), mud volcanoes (Wienberg et al., 2009; Margreth et al., 2011), underlying faults (Haberkern, 2017), iceberg plough marks (Freiwald et al., 1999; Fosså et al., 2005) and dropstones-boulders (Hübscher et al., 2010; Hebbeln et al., 2012; Savini et al., 2014; Buhl-Mortensen et al., 2017), which eventually reflect preferred sites for the initiation of coral mounds. However, some CMPs seem to have developed without any relevant underlying topographic features (Hebbeln et al., 2014; Bøe et al., 2016), thus, revealing a potential self-organizational pattern in the distribution of coral mounds.

To document the self-organization or other controls on mound distribution/formation in CMPs, a large-scale spatial and morphometric analyses are needed but are still largely lacking. First studies were predominantly based on qualitative observations on coral mound morphologies by multibeam echosounders (MBES), side-scan sonars and seismic reflection data (e.g., Hovland, 1990; De Mol et al., 2002; Beyer et al., 2003; Masson et al., 2003; Fosså et al., 2005; Foubert et al., 2005; Mienis et al., 2006). Based on these studies, Wheeler et al. (2007) outlined that coral mound morphology can be "inherited" and "developed". Inherited mounds owe their morphology to the underlying topographic features (e.g., De Mol et al., 2007; Savini et al., 2014). "Developed" mound morphologies are independent of the underlying topography, assuming a morphology more closely related to the prevailing hydrodynamic regime. Wheeler et al. (2008) suggested that coral mounds may transform from inherited to developed morphologies. Whether inherited or developed, coral mounds exhibit a wide qualitatively-described morphological variety: simple conical, conical with an oval footprint, elongated, arcuate, ridge-like, V-shaped and multi-peaked (e.g., Colman et al., 2005; Grasmueck et al., 2006; Wheeler et al., 2007; De Haas et al., 2009; Hebbeln, 2019) but discrete quantitative measurements are still rare (Mortensen et al., 2001; Huvenne et al., 2003; Correa et al., 2012b; Lim et al., 2018).

Coral mounds can rise from their surrounding seafloor from a few meters (e.g., Collart et al., 2018; Foubert et al., 2008; Lim et al., 2018; Somoza et al., 2014) up to >350 m (Kenyon et al., 1998) and have a lateral extension that can reach the km-size scale (e.g., Beyer et al., 2003; Colman et al., 2005; Mienis et al., 2007). Most of the morphometric information on coral mounds is based on manual measurements describing mostly the size ranges or the highest values (e.g., Colman et al., 2005; Wheeler et al., 2007; De Haas et al., 2009; Angeletti et al., 2020; Steinmann et al., 2020). Crucial for a morphometric analyses of the coral mounds are objective measurements based on solid definitions. Already basic terrain variables obtained from the digital elevation model (DEM), such as slope angle or bathymetric positioning index, allowed (semi)automated identification and extraction of the coral mounds by thresholding and the subsequent determination of morphometric parameters like footprint area and lateral extension (Correa et al., 2012b; Hebbeln et al., 2019). However, a relevant morphometric parameter such as mound height has often been measured only manually (Huvenne et al., 2003; Lo Iacono et al., 2014; Vandorpe et al., 2017; Hebbeln et al., 2019).

In recent years, a large variety of mapping classification methods for coral mounds based on manual, semi-automated, automated and machine-learning-based approaches have been developed (Lim et al., 2021). These methodologies benefited from high-resolution MBES datasets (e.g., De Clippele et al., 2017a; Lim et al., 2018), combined with imagery data (side-scan sonar, ROV photogrammetry; e.g., Savini et al., 2014; Price et al., 2019). Often the focus of these spatial-mapping investigations was rather on ecological aspects of CWC colonies and their associated fauna (e.g., Boolukos et al., 2019; Corbera et al., 2019; De Clippele et al., 2021) than on coral mounds as morphological features. The morphology of coral mounds represents a synthesis of complex biological and physical processes interacting on geological timescales, which likely can be assessed retrospectively by the extraction of morphometric parameters. Some morphometric parameters, such as mound height and length, are commonly mentioned for coral mounds (e.g., De Mol et al., 2002; Colman et al., 2005; Carranza et al., 2012; Hebbeln et al., 2014; Angeletti et al., 2020), but only few studies used these information to classify coral mounds (e.g., Mortensen et al., 2001; Lo Iacono et al., 2014; Vandorpe et al., 2017; Lim et al., 2018) and even less linked mound morphology with mound formation processes (Correa et al., 2012a; Hebbeln et al., 2019).

Our study presents a detailed analyses of the spatial distribution pattern and morphometric parameters of coral mounds, which were recently discovered on the outer Namibian shelf (Hebbeln et al., 2017). The large number of >2000 small mounds forming the Namibian CMP (Tamborrino et al., 2019) provides an excellent and extensive database to explore the potential of spatial-morphometric analyses to better understand the effect of regional oceanographic and local hydrodynamic processes and the underlying topography on mound formation. Due to extremely low ambient dissolved oxygen concentrations nowadays, no living corals occur on these mounds (Hanz et al. 2019). According to Tamborrino et al. (2019), the Namibian coral mounds show the typical mound composition of coral fragments embedded in a matrix of hemipelagic sediments and formed during a well-defined short period during the Early to

Mid-Holocene, which suggest well-constrained environmental conditions during their formation. Accordingly, this study analyses the spatial distribution and morphology of the Namibian coral mounds to unravel the partly competing influence of the regional oceanography, local hydrodynamics and underlying topographic features on the spatial distribution and mound shape development at different scales. Finally, our study outlines an approach to exploit spatial and morphometric analyses that could be easily applied to other CMPs, which would allow an observer-independent comparison of different CMPs and could contribute to the understanding of basic principles of coral mound development.

4.2. Material and methods

4.2.1. Study area

The Namibian CMP consists of ~2,000 coral mounds in ~160-270 m below sea level (mbsl) extending over a distance of (at least) 80 km along the northern outer Namibian shelf/upper slope (Fig. 4.1). The Namibian coral mounds are grouped in three clusters or sub-provinces, which occur on top (Escarpment mounds) and west (Squid Mounds, SQM; Coral Belt Mounds, CBM) of a large NNE-SSW-trending Escarpment (Tamborrino et al. 2019). The Namibian mounds developed during one short (~5 kyr) period corresponding to the Early to Mid-Holocene. Today, they are densely covered by fossil coral rubble clogged by hemipelagic sediments (Tamborrino *et al.*, 2019).

The water masses along the Namibian margin are surface waters (0-85 mbsl) and the central water masses (85-480 mbsl), South Atlantic Central Water (SACW) and Eastern South Atlantic Central Waters (ESACW). Southern-sourced surface waters and the ESACW are carried equatorward from the southern tip of Africa (37°S) by the Benguela Current, while the oxygen-depleted SACW and related surface waters are transported southward from the Angolan margin by the Angola Current (AC) and the Poleward Undercurrent (PUC; Fig. 4.1a). The two surface water masses converge at the Angola-Benguela Front (14-17°S, ABF), which is a pronounced frontal system (von Bodungen *et al.*, 2008). Within the underlying central water masses, no sharp boundary exists between the SACW and ESACW, but rather a broad transition zone (Mohrholz *et al.*, 2008). The southward migration of the SACW by the PUC contributes to the well-developed OMZ off Namibia (Schmidt and Eggert, 2016). Here, the OMZ is further influenced by the Benguela Upwelling System (BUS), which enhances surface productivity leading to an increased export of organic matter and enhanced oxygen consumption (Schmidt and Eggert, 2016). The Namibian coral mounds are today located within the core of the OMZ (160-270 mbsl), where dissolved oxygen concentrations are below 0.5 ml l^{-1} and even drop to 0.1 ml l^{-1} (Hanz *et al.*, 2019). An intensification of the BUS, and therefore, of the OMZ likely caused the Mid-Holocene demise of the CWC off Namibia (Tamborrino *et al.*, 2019).

At a regional scale, large portions of organic particles, derived from the BUS, are laterally transported and deposited on the Namibian outer shelf, contributing to the formation of intermediate nepheloid layers (INL, Giraudeau *et al.*, 2000; Inthorn *et al.*, 2006a). A semi-diurnal internal tide has been measured by a benthic lander also in the Namibian CMP, close to the CBM (Hanz *et al.*, 2019). Thus the formation

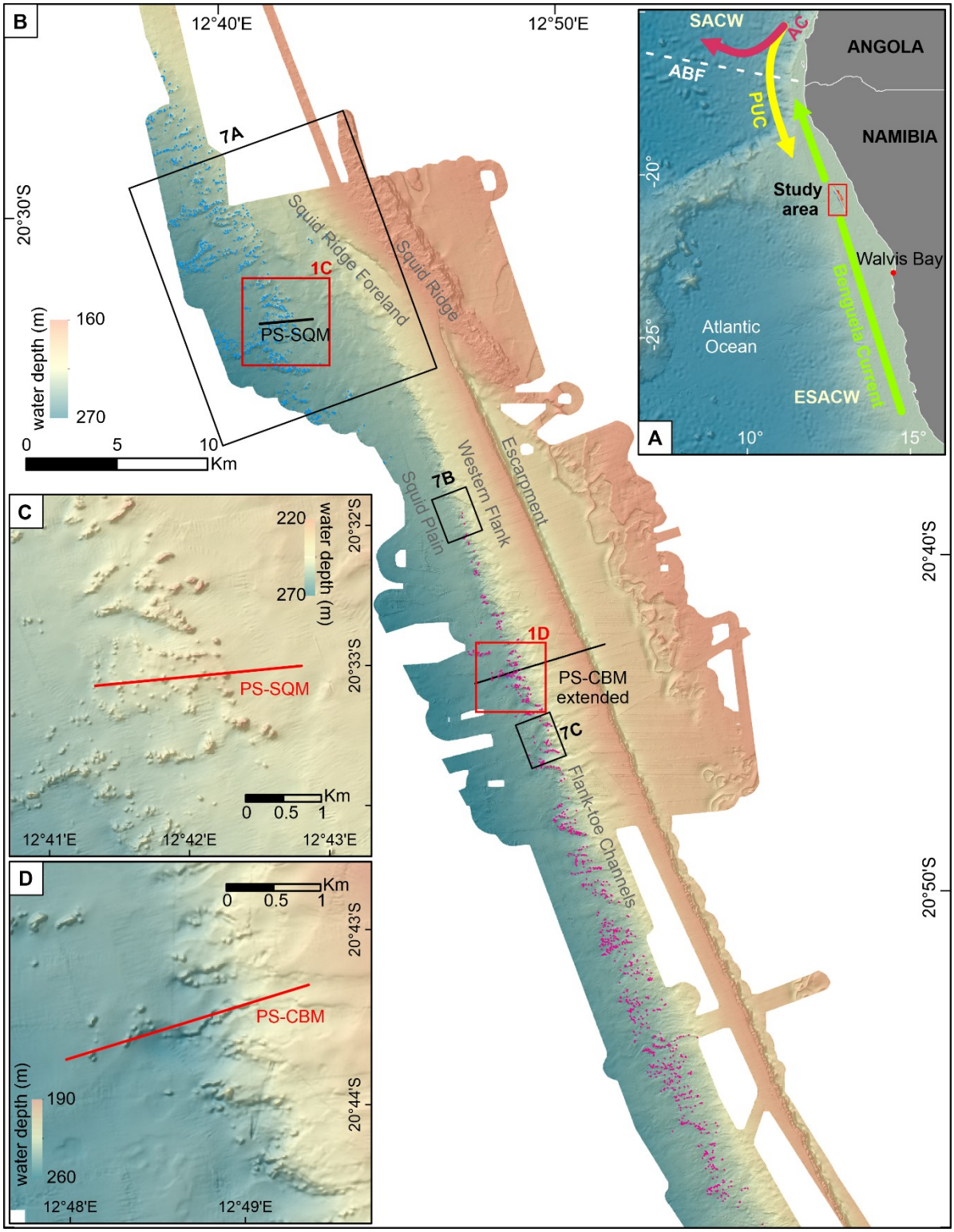

Figure 4.1. (A) Overview map showing the oceanographic circulation along the Namibian coast. Red square highlights the study area. Bathymetric map (B) showing the Namibian coral mound province. Dots are indicative of the mound peaks, light blue for Squid Mounds (SQM) and pink for Coral Belt Mounds (CBM). For the position of the Escarpment Mounds see Tamborrino et al. (2019). (C-D) Detailed view of some SQM and CBM, respectively. Position of the Parasound profiles (see Fig. 4.3) are shown by black (Fig. 4.1b) and red lines (Fig. 4.1c-d). Black boxes indicate the position of the 3D view maps in Fig. 4.7. Acronyms: ABF-Angola Benguela Front; AC-Angola Current; PUC-Poleward Undercurrent; SACW-South Atlantic Central Waters; ESACW-Eastern South Atlantic Central Waters

of this INL is likely derived from the interaction between topography of the outer Namibian shelf and the pycnocline, with the formation of the internal tide at the boundary between PUC-delivered SACW and the surface waters, that keep particles in suspension (Zabel *et al.*, 2019).

4.2.2. Hydroacoustics

The hydroacoustic data for this study were collected during *R/V Meteor* expedition M122 (Hebbeln et al., 2017) and during *R/V Maria S. Merian* expedition MSM 20-1 (Geissler et al., 2013). Seabed mapping was performed by two different hull-mounted Kongsberg multibeam echosounders (MBES): EM710 (70-100 kHz) and EM1002 (95 kHz) during expedition M122 and MSM20/1, respectively. The EM710 acquired 200 beams per ping and 400 soundings ("soft-beams") in the high-density mode covering a depth range of several meters up to ~800 m The EM1002 emitted 111 beams per ping, covering a depth range of 2-1000 m. During both cruises, the spatial integrity of the mapping data was achieved by combining the ship's inertial navigation systems including differential global positioning system information with motion data (roll, pitch, heave) provided by the motion reference units (Kongsberg Seapath 320 and 200, respectively for *R/V Meteor* and *R/V Maria S. Merian*). Based on comparing the two independent MBES bathymetric data sets, their vertical precision is ±50 cm. For the correction of the hydroacoustic measurements, sound velocity profiles through the water column were repeatedly recorded using either a CTD or sound velocity probes. The open-source software package MB-System v.5.3.1 (Caress and Chayes, 1995) was used for bathymetric data post-processing, editing and evaluation. MBES data were interpolated to make a digital elevation model (DEM) with 10 x 10 m grid cell size (using MB-system mbgrid tool). Maps were produced with ESRI ArcGIS v.10 and Global Mapper v.20. During the M122 expedition, seismoacoustic sub-seafloor information was acquired with ATLAS PARASOUND PS70, a deep-sea sub-bottom profiler that utilizes the parametric effect based on non-linear relation of pressure and density during sonar propagation. The sub-bottom profiling relies on the signal from the secondary low frequency at ~4 kHz. The opening angle of the transducer array is 4° by 5°, which corresponds to a footprint size of about 7 % of the water depth. The data acquisition was performed with the real-time values of surface sound velocity measured close to the Tx/Rx-array (System C-Keel) and a static sound velocity profile of 1500 m s^{-1} (C-Mean). The program Teledyne PARASTORE 3.0 was used for storing and displaying echograms. Within the Teledyne Hydromap Control program, the proper hydroacoustic settings were set before the acquisition. Kingdom IHS was used for reproducing the PARASOUND profiles with a bandpass filter (low-high cut 2000-4000 Hz, low-high pass 2500-4500 Hz).

4.2.3. Mound extraction and morphometric analyses

Analyses of morphometric data were carried out for each mound following the workflows presented by Purkis et al. (2007). Most of the processing was performed with the Petrel™ software package (Schlumberger, license: University of Miami, US). The coral mound base was defined following the

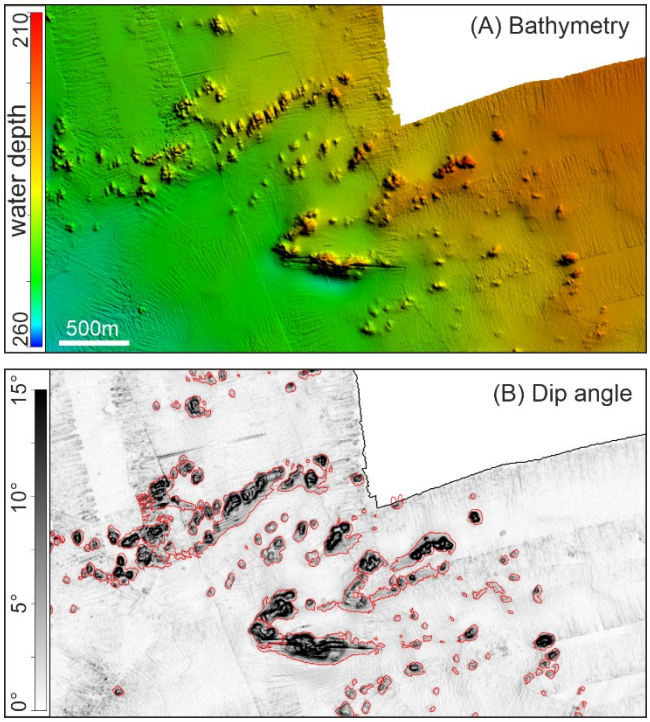

Figure 4.2. Comparison between (A) digital elevation model (DEM) and (B) dip angles exemplified for an area within Squid Mound cluster. The red line indicates the polygons obtained by applying the 3°-cutoff value, after editing. DEM and dip angles are gridded at 10 m. The scale (shown in the DEM frame) bar is equal for both frames. This highlights also the morphological appearance of merging coral mounds.

methodological approach of **Correa *et al.* (2012b)** using the dip angle map ("Petrel/Op./Surface operations/Dip Angle"), generated from the original DEM, to extract closed polygons describing the mound footprints that follow the 3°-contour line ("Petrel/Op./Convert points, polygons, surfaces/Create intersection with plane"). This 3°-cutoff has been qualitatively validated with a comparison between the DEM and the dip angle (Fig. **4.**2). Small-scaled polygons obtained by the automated 3° cut-off value (e.g. bathymetry artifacts or decrease in slope within mound perimeter) were removed. Unrealistic mound footprint polygons, more common by CBM due to steeper underlying slope, were corrected by removing single polygon nodes. Polygon nodes were also manually edited to split twin-peaks mounds on the base of higher cut-off dip angle values (5°). The DEM was subsequently re-gridded to generate hypothetical bathymetric maps without mounds ("Petrel/Calc./Eliminate inside" to remove the coral mounds, and "Utilities/Make-edit new surface" to create an interpolated map from the DEM with no mounds), for which the vertical relief beneath each removed mound was interpolated from the mound perimeters. The newly interpolated surfaces were then subtracted from the original DEMs to calculate the volume and heights of the coral mounds. Only features with a footprint area greater than 900 m^2 (corresponding to a two-dimensional array of 3 × 3 DEM grid cells) and with a height of >2 m above the surrounding seafloor (4 × 0.5 m of vertical precision) were considered as coral mounds. Because the small size (mostly <2 m height) and number (138) of the Escarpment mounds **(Tamborrino *et al.*, 2019)**, the analyses reported here focus on the CBM and SQM only (Fig. **4.**1).

A summary of the morphometric parameters used to quantify the spatial variability of the Namibian coral mounds is presented in Table 1. For all obtained morphometric parameters descriptive statistics, such as mean, standard deviation (SD) and median, were determined. To evaluate the spatial distribution and density of the coral mounds, heatmaps were calculated with the kernel density tool of ArcGIS 10.3 and an output raster cell neighborhood of 50 m and a search radius of 1 km, after projecting the DEM into UTM Zone 33S, following Lim *et al.* (2018). Slope and aspect maps are based on the interpolated DEM without coral mounds (grid size: 20 m) and were calculated with the ArcGIS tool Benthic Terrain Modeler, using the Horn method (Horn, 1981).

Table 4.1 Summary of parameters used to quantify the spatial-morphometric variability of Squid (SQM) and Coral Belt Mounds (CBM) off Namibia.

Parameter	Definition	Unit	Range	
			SQM	CBM
Mean depth	Average depth within the mound perimeter	mbsl	211 – 266	225 – 258
Mound footprint area	Area of mound perimeter based on 3° cutoff	m^2	900* – 115,639	900* – 47,040
Mound height	Maximum elevation within mound perimeter, after subtracting the interpolated surface without mounds	m	2* – 21	2* – 15
Mound volume	Volume of the mound above the interpolated surface without mounds	m^3	92 – 492,198	270 – 114,282
PAX (principal axis) length	Length of the principal axis crossing the centroid of the mound footprint (Peura and Iivarinen, 1997)	m	38 – 1,100	39 – 428
OPAX length	Length of the axis orthogonal to PAX	m	4 – 255	9 –205
PAX direction	Direction of the principal axis	°	1 – 180	0 – 180
PAR	OPAX/PAX ratio	0 to 1 ratio	0.03 – 0.97	0.06 – 0.98
Average slope	Average slope angle within the mound perimeter	°	2 – 14	2 – 24
Underlying-mound average slope	Average slope angle within the mound perimeter on the interpolated surface after mound removal	°	0 – 8	1 – 12

* defined lower threshold for mound detection

4.3. Results

4.3.1. Prominent morphological features of the Namibian coral mound province

The MBES bathymetric map of the Namibian CMP covers an area of 1179 km^2 along the northern Namibian shelf (Fig. 4.1). The most prominent morphological feature is represented by a straight ~63-km-long NNW-SSE trending Escarpment with heights of up to ~50 m (top of the escarpment: ~165 mbsl). Its eastern steep margin exhibits a slope angle of up to 40° and ends in a moat (maximal depth: ~215 mbsl) developed parallel to the Escarpment. Several irregular-shaped erosive features occur east of the Escarpment (~150-190 mbsl; Fig. 4.1b). The Western Flank of the Escarpment (~ 165-220 mbsl) is much more gently dipping (slope angle <5°) and shows no pronounced surface features. Close to its western limit just below 220 mbsl, slope-indenting channels and headwalls (referred to as Flank-toe Channels, 220-260 mbsl, Fig. 4.1b, d) incise the foot of the Western Flank. Most of these channels have a NE-SW orientation, hence are orientated perpendicular to the shelf. The area west of the Flank-toe

Channels changes towards the gently westward-dipping Squid Plain (240–310 mbsl; Fig. 4.1b). The northern termination of the Escarpment (at ~20°34'S) is bordered by the NW-SE-trending Squid Ridge (top: 140 mbsl). The western flank of the Squid Ridge is shaped by a 5-km-long headwall (up to 20 m high). West of this headwall, the Western Flank of the Escarpment fades into a slightly westward-dipping slope with a faintly-carved surface (referred to as Squid Ridge Foreland, 210–240 mbsl). West of the Squid Ridge Foreland, low relief furrows incise the flat morphology of the Squid Plain.

The PARASOUND profiles exhibit a relatively good penetration (>50 m) and reveal mainly seaward-dipping reflectors (Fig. 4.3). Only close to the Flank-toe Channels the sub-bottom reflectors are partly horizontal (Fig. 4.3b, c). Furthermore, some unconformities can be observed beneath the seabed, with the seabed itself also partly representing an erosive surface (Fig. 4.3a–c). PARASOUND profiles do not show any buried portions of the SQM and the CBM, which are sitting on topographic highs made up of exposed older strata (Fig. 4.3).

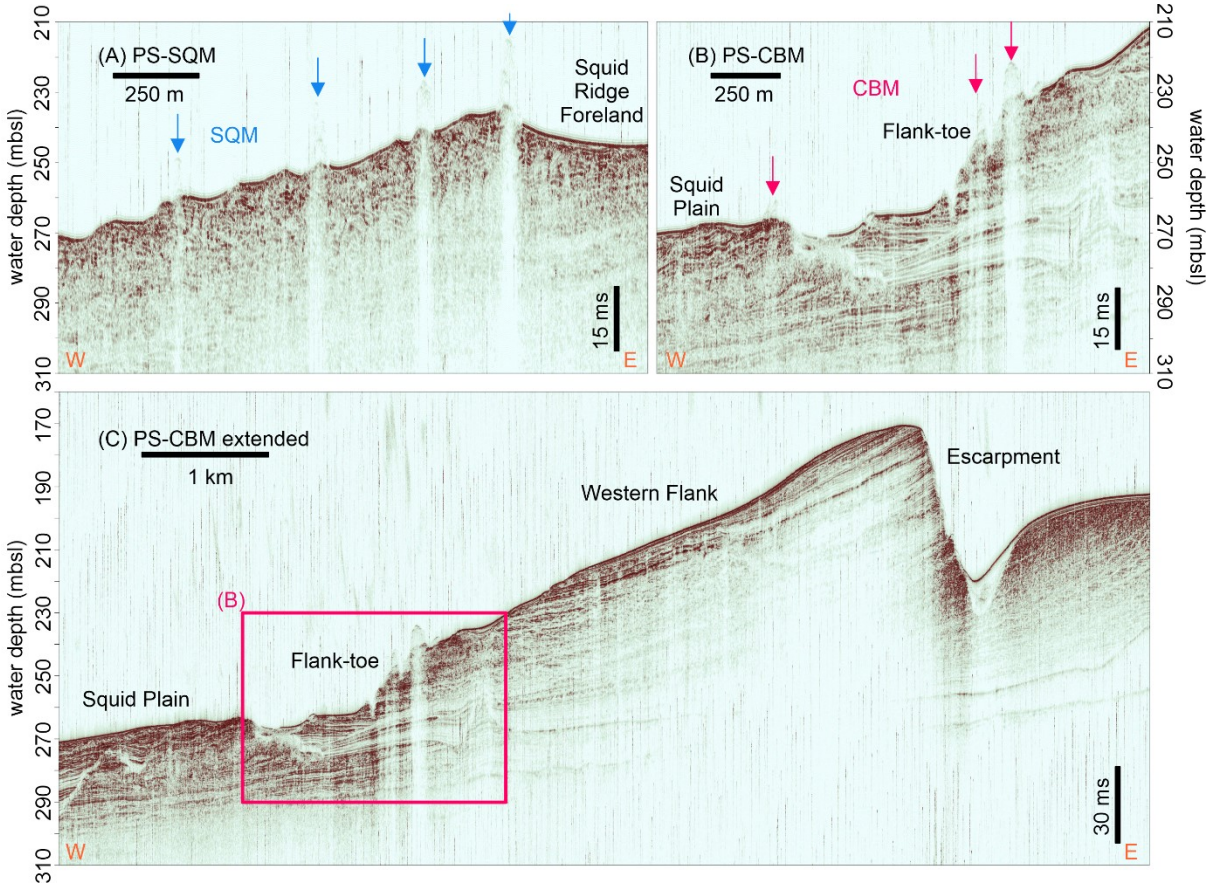

Figure 4.3. PARASOUND sub-bottom profiles crossing the major topographical features of the Namibian coral mound province: (A) the Squid Mounds (SQM), (B) and (C) the Coral Belt Mounds (CBM). Position of the PARASOUND profiles is shown in Fig. 4.1. Orientation (E–W) is indicated at the bottom of the profile (orange letters).

4.3.2. Spatial distribution and density pattern of the Namibian coral mounds

A total of 659 and 542 coral mounds were extracted from the SQM and CBM sub-provinces, respectively. These numbers are slightly lower as initially proposed by Tamborrino et al. (2019; SQM: 959; CBM: 896), who manually counted the total number of mound peaks. This difference is ascribed

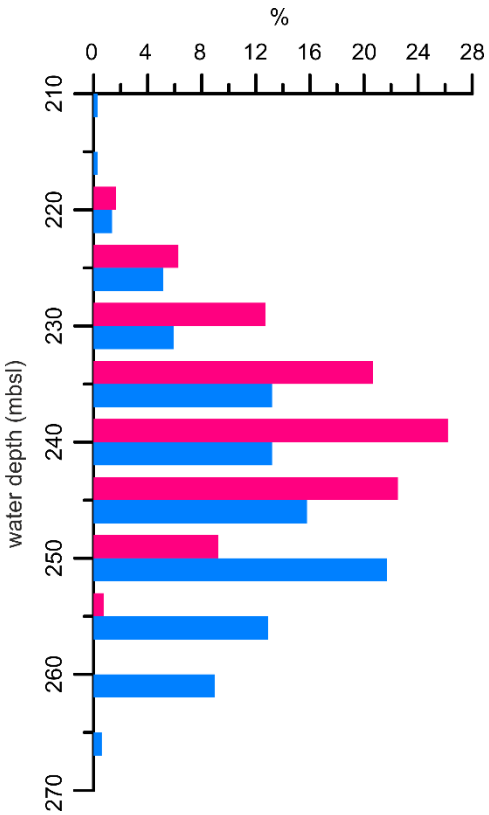

Figure 4.4. Histogram plot showing the relative depth distribution of the Squid Mounds (light blue) and Coral Belt Mounds (pink) based on the mean water depth of the mound footprint area. Interval of the bin: 5 m. Histogram bar plotted at upper limit (lowest water depth)

to the here applied cutoff-based method to discern multi-peak mounds and the exclusion of very small mounds (height: <2 m, footprint: <900 m^2).

The SQM extend for at least 5 km downslope and 20 km alongslope on the northern portion of Squid Plain (Fig. 4.1b), where they partly sit on the margin of low-relief furrows (Fig. 4.1c). Further to the south, the CBM are mostly associated with the Flank-toe Channels (Fig. 4.1b, d) and stretch in a narrow (mostly <3 km) belt for >40 km from SSE to NNW. Together the SQM and the CBM encompass ~1,200 mounds that are located between ~210 and 270 mbsl (Fig. 4.4). The 659 SQM cover a slightly broader depth interval (~210-270 m) with a slightly deeper mode of 250-255 mbsl compared to the 542 CBM occurring between ~220-260 mbsl with a mode of 240-245 mbsl (Fig. 4.4).

The extension of the mapped portion of the two sub-provinces is given by the heatmaps (based on outer limits of all 1 km radii around the individual mound peaks), which amount to ~95 km^2 for the SQM and ~100 km^2 for the CBM. Although in both areas mound densities vary between 1 and 40 mounds/km^2 (Fig. 4.5a, d), the average density is slightly higher for the SQM (10.1 mounds/km^2) compared to the CBM (8.9 mounds/km^2). The sum of the mound footprint areas covers 6.0 % and 2.9 % of the extension of the SQM and CBM sub-provinces, respectively. The heatmaps highlight a general alongslope distribution of the coral mounds in both sub-provinces. In detail, areas of high concentrations of SQM stretch in different directions such as NE-SW, E-W and NW-SE (Fig. 4.5a). The CBM are largely concentrated in a general belt-like NW-SE trend (Fig. 4.5d).

The seabed area occupied by the Namibian coral mounds is relatively flat with a mean slope of 0.7° (SD 0.7°) in the SQM area and a slightly steeper mean slope of 1.5° (SD 1.5°) in the CBM area (Fig. 4.5b, e). This slight difference is also expressed by more topographic features characterizing the CBM (channels indenting the flank-toe) than the SQM area. The Namibian CMP covers a seabed area with a general SW orientation, with the topography underlying the SQM sub-province trending more towards the S, while the aspect of the CBM sub-province is more directed to the west (Fig. 4.5c, f). Areas of slightly-dipping E-orientated values appear on the eastern shallow limit of the SQM (Fig. 4.5c), as also indicated by the slope change in the PARASOUND profile (Fig. 4.3a).

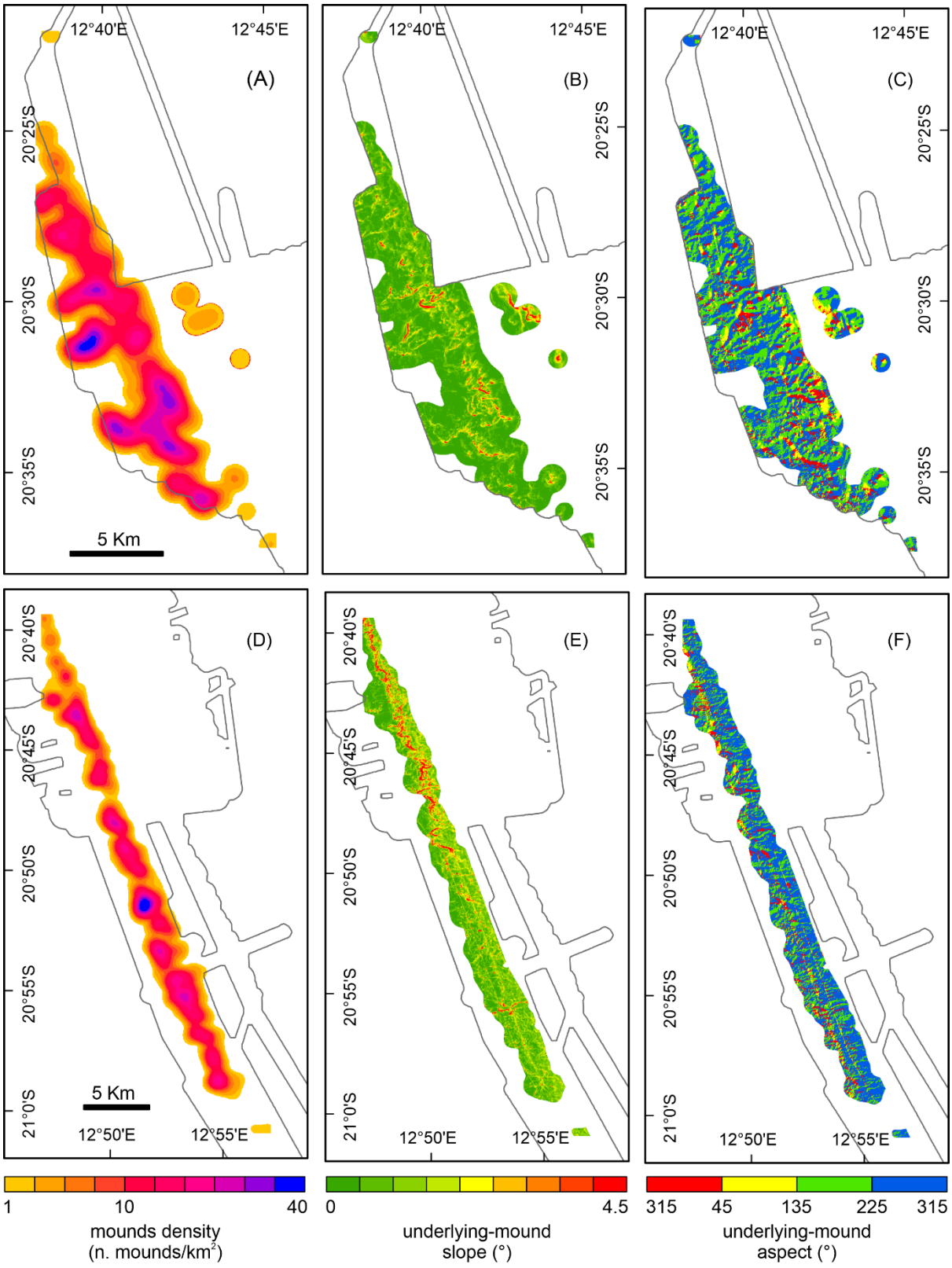

Figure 4.5. Density of coral mounds, slope and aspect maps of mound-underlying topography for Squid Mounds (A-C) and Coral Belt Mounds (D-F). Density is expressed as a number of mound peaks per km² over a neighborhood of 50 m retrieved from a search radius of 1 km. Zero values are excluded. Slope and aspect are computed by the ArcGIS Benthic Terrain Modeler using DEM after mound removal. In the background, the border of the bathymetric dataset is indicated by a thin black line (see Fig. 4.1 for orientation).

4.3.3. Morphometric parameters of the Namibian coral mounds

Size-related morphometric parameters, such as footprint area, volume, height and PAX (principal axis of the mound footprint polygon) length, show similar trends in both sub-provinces, the SQM and the CBM (Fig. 4.6a-d). The exponential decline of mound numbers with increasing size indicate the dominance of small mounds off Namibia: most of the SQM and CBM have a footprint area of <10,000 m^2 (SQM: 78%, CBM: 90%), a volume of <10,000 m^3 (SQM: 70%, CBM: 79 %), a height of <10 m (SQM: 88%, CBM: 98%), and a PAX length of <120 m (SQM: 67%, CBM: 78%). Despite similar sizes of most coral mounds, differences between the SQM and CBM are highlighted by comparing the maximum (Table 4.1) and mean values (Fig. 4.6). The mean values represent the overall similarity of the two sub-provinces with slightly higher average values for the SQM (Fig. 4.6), While the major differences are caused by the presence of a few relatively large mounds among the SQM (Table 4.1; Fig. 4.6).

The shape-related parameters reveal some more differences between the two regions. The principal axes ratio (PAR) shows mostly similar trends in the two sub-provinces (Fig. 4.6e). However, a larger number of the SQM (21%) show a PAR of <0.3, indicative of more elongated mounds on the Squid Plain compared to the CBM (16%). The PAX directions of the SQM have three maxima: 45°, 90-95° and 135°, while the PAX directions of CBM are generally concentrated between 55° and 100° (Fig. 4.6f). The average slopes of the mounds show a similar distribution for both the SQM and CBM (Fig. 4.6g). However, the SQM have a much steeper mean slope angle than the CBM, considering the number of mounds with slope angles of <6° (SQM: 25%, CBM: 40%) and >8° (SQM: 40%, CBM: 27%). The average slope of the underlying topography where the coral mounds sit on, have very small values of <3° for 79% of the SQM and for 58% of the CBM (Fig. 4.6h). However, values steeper than 8° occur only on CBM, although in rather low numbers (2%, Fig. 4.6h).

4.4. Discussion

4.4.1. Spatial distribution

The Namibian coral mounds occur on the outer shelf in relatively shallow water depths (210 – 270 mbsl, Fig. 4.4) compared to the majority of CMPs in the Atlantic Ocean that are found on the upper continental slope in much deeper depths of 500 and 1,000 m (e.g., Galvez, 2020; Hebbeln *et al.*, 2019; Raddatz *et al.*, 2020; Schroeder, 2002; Steinmann *et al.*, 2020; Wheeler *et al.*, 2007). *Lophelia*-dominated mounds developed in shallow shelf waters are mainly known from high latitudes in the NE Atlantic, such as off Norway (38 - 400 mbsl, e.g., Fosså *et al.*, 2005; Lavaleye *et al.*, 2009; Lindberg *et al.*, 2007; Mortensen *et al.*, 2001) and off Scotland (Mingulay Reef, 90-200 mbsl, Duineveld *et al.*, 2012), while the Namibian CMP is the first shelf site described from the SE Atlantic and positioned in low latitudes. All shelf coral mounds (Norway, Scotland, Namibia) have in common that they have relatively small elevation (<20 m; Bøe *et al.*, 2016; De Clippele *et al.*, 2017b), which reflects most likely their short (but often rapid) formation history that formation history that started only during the Early Holocene

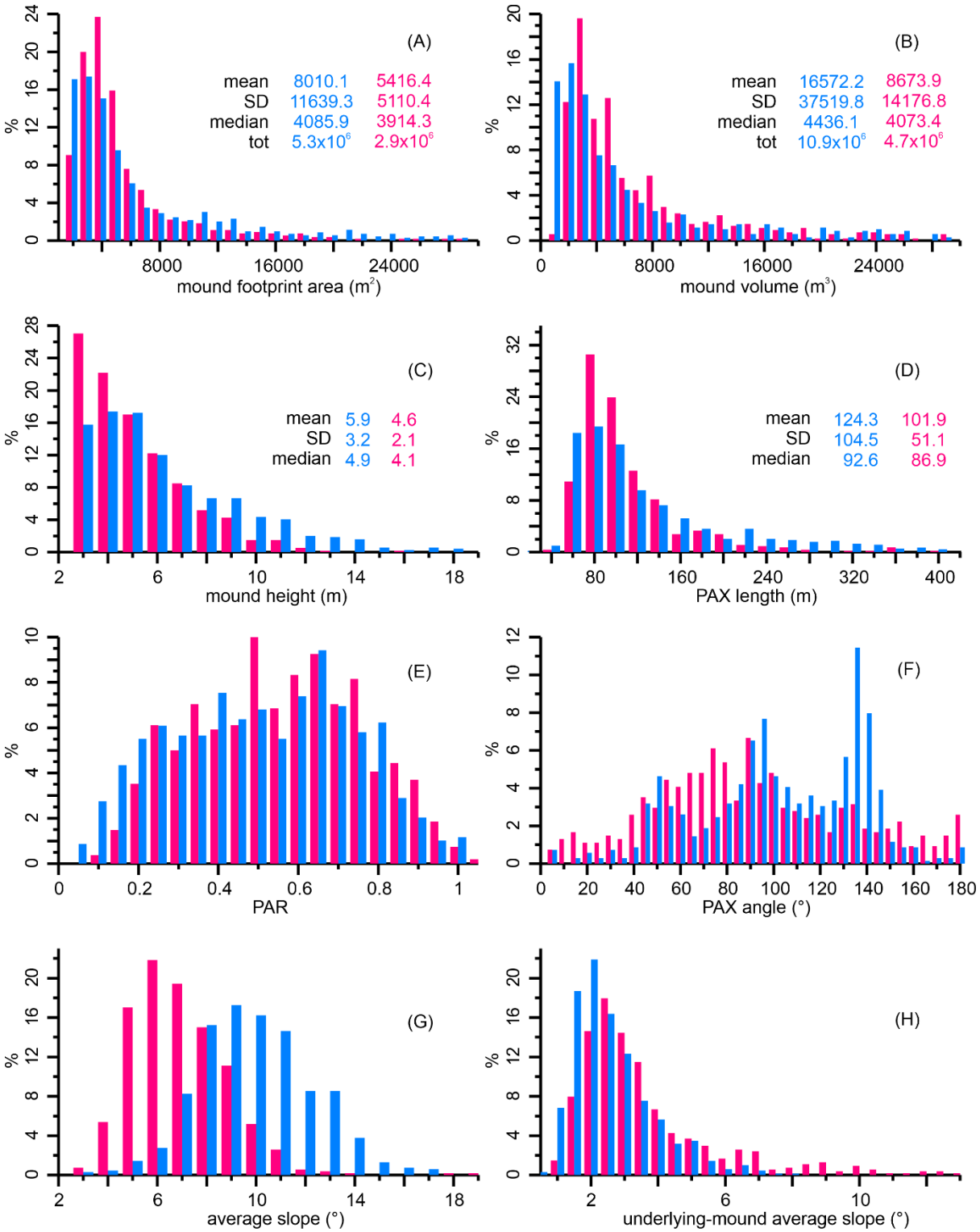

Figure 4,6. Histogram plots showing the relative distribution of selected morphometric parameters collected from the Squid Mounds (light blue) and Coral Belt Mounds (pink): (A) mound footprint area (bin size: 1000 m^2), (B) mound volume (bin size: 1000 m^3), (C) mound height (bin size: 1 m), (D) PAX length (bin size: 20 m), (E) PAR (bin size: 0.05), (F) PAX angle (bin size: 5°), (G) average slope of the mounds (bin size: 0.5°), (H) average slope of topography underlying the mounds (bin size: 0.5°). Descriptive statistics (mean, standard deviation (SD) and median) are provided for data interpretation of size-related parameters. Units of the descriptive statistics refer to the units of the parameter (see x-axis). Further details (description, unit and range) on morphometric parameters are presented in Table 4.1.

with the drowning of the shelves during the deglacial sea-level rise (Douarin *et al.*, 2013; López Correa *et al.*, 2012; Tamborrino *et al.*, 2019).

The Namibian coral mounds extend alongslope for >80 km in a narrow water depth interval (<60 m) in NNW-SSE direction (Fig. 4.1, 4.4, 4.5a). This regional-scale alongslope distribution (*first-order* pattern) is also observed in other Atlantic CMPs, e.g., on the Irish margin (De Haas *et al.*, 2009; White and Dorschel, 2010), the southern Gulf of Mexico (Hebbeln *et al.*, 2014), and the Argentine margin (Steinmann *et al.*, 2020). In some CMPs, coral mounds are distributed in two alongslope chains (Porcupine Seabight, Beyer *et al.*, 2003; Atlantic Morocco, Hebbeln *et al.*, 2019) or are merged to more or less continuous alongslope ridges (Mauritania, Colman *et al.*, 2005; Angola, Hebbeln *et al.*, 2020). Considering that the development of coral mounds relies primarily on the proliferation of the CWC, which depends on environmental conditions fitting their physiological needs (e.g., food, dissolved oxygen, temperature; Davies and Guinotte, 2011; Roberts *et al.*, 2009; Wienberg and Titschack, 2017), suggests that the regional-scale distribution of coral mounds is primarily controlled by the regional oceanography. Off Namibia, the occurrence of intermediate nepheloid layers (Inthorn *et al.*, 2006a) along the boundary between the SACW and the surface waters (Hanz et al., 2019) probably plays a key role for the food supply to the CWC and, thus, these present a potential mechanism that could have triggered the observed alongslope distribution of the Namibian coral mounds.

On a local scale the distribution density maps show a downslope component in the SQM distribution (Fig. 4.5a). A comparable distribution pattern is not observed (on the heatmaps) for the CBM (Fig. 4.5d), which might be explained by the steeper slope of the underlying topography causing most likely the narrower E-W extension of the CBM sub-province. However, a closer look at the MBES bathymetry reveals that the CBM have been formed along the rims of the Flank-toe Channels, comparably to the SQM that are aligned along the low-relief furrows in the Squid Plain (Fig. 4.7). These downslope-directed topographic features have an erosive origin and were most likely formed before corals colonized the area. Elevated topographic features at the seafloor are well known as preferential settling grounds for CWC (and subsequent formation of coral mounds) due to the related enhanced turbulence that supports food (and sediment) supply (e.g., Frederiksen *et al.*, 1992; Genin *et al.*, 1986; Mienis *et al.*, 2007; Mohn *et al.*, 2014; White, 2003; White *et al.*, 2005). Consequently, off Namibia pre-existing sea floor topography is suggested to play an important role on a local-scale and the downslope component in SQM and CBM distribution, mainly steered by this underlying topography, reflects a distinct *second-order* pattern for the spatial distribution of the coral mounds On the individual mound scale, many Namibian coral mounds have a downslope orientation (*third-order* pattern) as reflected by their PAX angles (Fig. 4.6f and 4.8). The PAX angles of the CBM show a broad range of preferred directions between 55° and 100° that overlaps with two PAX angle maxima of the SQM (at 45° and 90°), which have an additional maximum at ~130° (Fig. 4.8). The observed range of PAX angles follows the predominantly SW-dipping regional topography (Fig. 4.5c, f, 4.8) and aligns with the direction of the regional tidal currents (Hanz

et al., 2019). Coral mounds with specific orientations as a response to hydrodynamic forcing are often observed (e.g., Beyer *et al.*, 2003; Masson *et al.*, 2003; Mortensen *et al.*, 2001), however, depending on

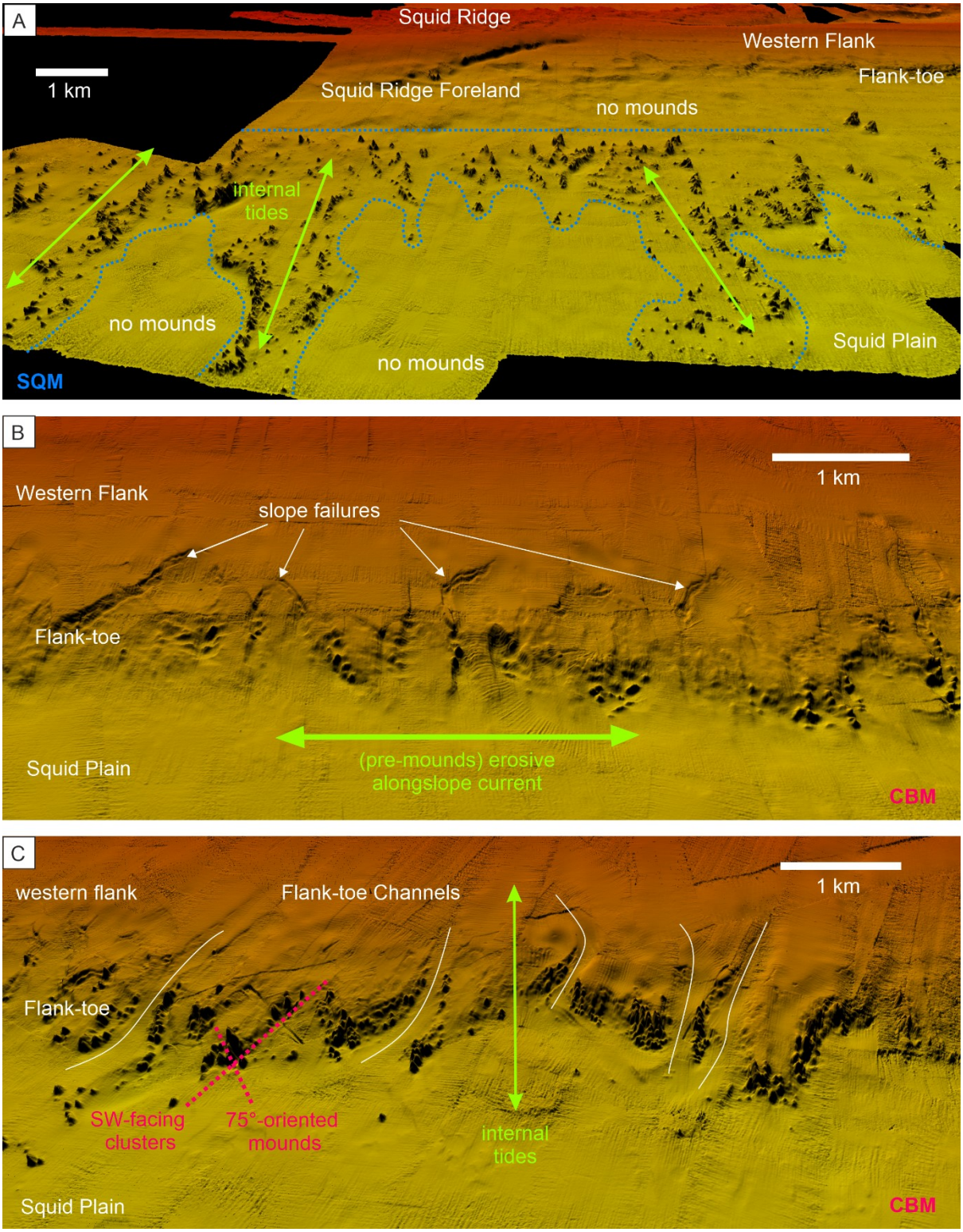

Figure 4,7. Detailed 3D-view of topographic features associated with the Namibian coral mounds. (A) 3D-view of the Squid Mounds (SQM). The blue dashed line marks the occurrence of SQM from the surrounding areas with no mounds (B) Slope failures appear to be associated with the underlying topography of the northernmost Coral Belt Mounds (CBM). (C) Channels (white lines) indenting the Flank-toe with coral mounds along their edges. Vertical exaggeration: 10x. The locations of these 1038 examples are shown in Fig. 4.1.

the overall setting, these are either aligned to the main current direction (i.e., *first-order* pattern; e.g., Wheeler et al., 2011; Mienis et al., 2014) or to internal tides (e.g., Hebbeln et al., 2019). As off Namibia orientations of the mounds are mostly parallel to the direction of the internal tides (and perpendicular to the main current direction), thus, tidal action appears to be the dominant forcing causing the elongation of the mounds and the *third-order* pattern.

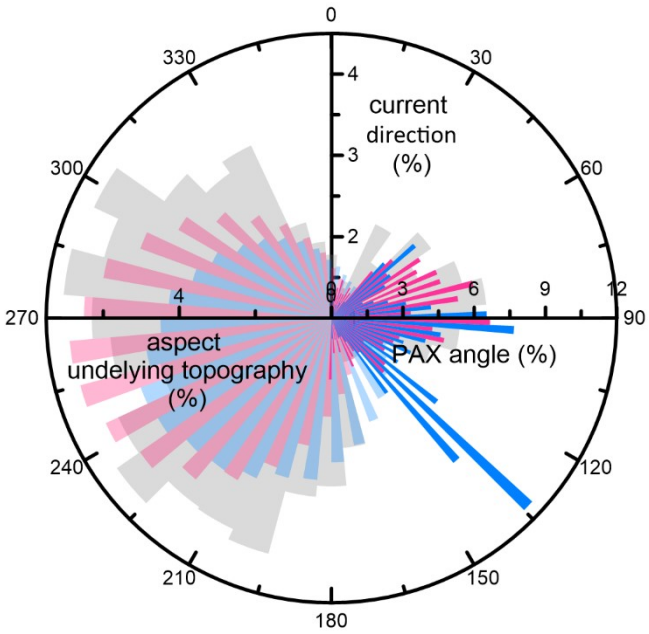

Figure 4.8. Rose diagram with percentages of PAX angle (full colors) and aspect of underlying topography (transparent colors) of Squid Mounds (light blue) and Coral Belt Mounds (pink). In addition, the local bottom current direction among the CBM (collected over 8 days, Hanz et al., 2019) are shown in light gray. Bin size: 10°.

In summary, the spatial distribution and the orientation of the Namibian coral mounds are interpreted to reflect a hierarchy of three different patterns (*first-* to *third-order*) controlled by the interplay of the regional oceanography, the seafloor topography, and the local hydrodynamic regime. While the *first-order* pattern addressing the large-scale coral mound distribution is steered by the overall slope topography and the water column structure and results in an alongslope organization of the coral mounds within the entire CMP, the *second-order* pattern addressing the small-scale mound distribution is controlled by the underlying topography. In addition, the impact of the local hydrodynamic regime and of internal tides creates the *third-order* pattern at the individual mound scale impacting on mound shape and orientation. As mentioned above, previous studies on other CMPs have partially identified similar patterns in the distribution of coral mounds (e.g., De Mol *et al.*, 2002; Fosså *et al.*, 2005; Hebbeln *et al.*, 2019; Lim *et al.*, 2018; White and Dorschel, 2010).

4.4.2. Morphometric variability

Coral mounds or ridges can reach heights of >350 m above the surrounding seafloor (Kenyon *et al.*, 2003) and stretch laterally of >10 km (Colman *et al.*, 2005; Hebbeln *et al.*, 2020). Whereas large coral mounds are comparably easy to detect (e.g., Beyer *et al.*, 2003; Colman *et al.*, 2005; De Mol *et al.*, 2002; Hovland *et al.*, 1994b; Kenyon *et al.*, 1998), only recent technological advances in deep-sea acoustic mapping allowed the detection and mapping of small coral mounds (even with heights of <5 m) (e.g., Correa *et al.*, 2012b; De Clippele *et al.*, 2017a; Diesing and Thorsnes, 2018; Lim *et al.*, 2018), also facilitating the detection of new CMPs (e.g., Glogowski *et al.*, 2015; Hebbeln *et al.*, 2019; Hebbeln *et al.*, 2014; Lo Iacono *et al.*, 2014; Somoza *et al.*, 2014; Steinmann *et al.*, 2020), including the Namibian coral mounds (Tamborrino *et al.*, 2019). With a maximum mound height of ca. 20 m and the majority of mounds (83%) having heights of <8 m, the Namibian coral mounds are clearly among the smallest

coral mounds discovered so far. Nevertheless, other large CMPs also comprising hundreds to even thousands of individual mounds have similar or only slightly larger mound heights (e.g., Florida Straits, Correa *et al.*, 2012b; Atlantic Morocco, Hebbeln *et al.*, 2019; Magellan mounds, Irish margin, Huvenne *et al.*, 2003). The exponential decrease of mound numbers with increasing mound sizes (Fig. 4.6) has been observed earlier for coral mounds (Correa *et al.*, 2012b) as well as for other carbonate geobodies ranging from shallow-water shoals, to reefs, to karst terrain (Harris *et al.*, 2018; Harris *et al.*, 2011; Purkis and Harris, 2017; Purkis *et al.*, 2016; Purkis *et al.*, 2010).

Initial settlement and widespread occurrence of CWC at several sites might correspond to the high number of small mounds, which likely decreased in the course of mound development as two or more mounds have merged into larger and more complex mound structures (De Mol *et al.*, 2005; Huvenne *et al.*, 2005). Indeed, the small size and the high number of the Namibian mounds clearly indicate multiple initiation sites. Their small sizes are probably related to the relative short mound formation interval (~5 kyr, Tamborrino et al. 2019), which in most cases was probably too short to allow for the merging of two or more mounds, as it also has been hypothesized for the small Moira Mounds on the Irish margin (Wheeler *et al.*, 2011).

Overall, the coral mounds in both sub-provinces off Namibia exhibit a high morphometric similarity (Fig. 4.6 a–d), though there are also a few but distinct differences between the SQM and CBM. The examination of size parameters shows that the total footprint area (5.7×10^6 m^2) and volume (10.9×10^6 m^3) of the SQM are ~2 times greater than those of the CBM (2.9×10^6 m^2; 5.3×10^6 m^3), despite the comparably minor difference in population size (SQM; 659 mounds, CBM: 542 mounds). Furthermore, the mean, the median and the variability (i.e., standard deviation) are higher in SQM compared to CBM not only for the footprint area and volume but also for the height and PAX length (Fig. 4.6 a–d). The height difference between the sub-provinces becomes especially conspicuous for mound heights >8 m, which are reached by 23% of the SQM but only by 8% of the CBM. These observations reveal the occurrence of some larger, higher, and more voluminous SQM that have hardly any counterparts among the CBM (Fig. 4.6).

Mound-shape parameters exhibit that there is a larger number of elongated mounds with PAR of <0.3 among the SQM (21%) compared to the CBM (16%; Fig. 4.6e). This pattern goes along with larger PAX lengths of SQM relative to CBM – 23 % of SQM exceed a PAX length of 150 m, which is only reached by12 % of the CBM (Fig. 6d). A cross-plot of PAX length versus mound height shows that PAX length increase progressively faster than height (Fig. 4.9a) and comparing PAX length versus PAR exhibits that PAR decrease with increasing length (Fig. 4.9c). These results clearly suggest that the Namibian mounds tend to form laterally without gaining substantial additional height, a pattern that is most obvious for the largest SQM (Fig. 4.9c). The mound elongation becomes most apparent when PAX lengths of ~150 m and heights of ~8 m are exceeded and likely reflects the preferential coral growth on mound flanks facing a favorable hydrodynamic regime (Cathalot *et al.*, 2015; Correa *et al.*, 2012b; De Clippele *et al.*, 2017b; Freiwald *et al.*, 1997; Lim *et al.*, 2017; e.g., Messing *et al.*, 1990; Mienis *et*

al., 2014). However, some of these elongated mounds might result from the merging of smaller mounds (see Fig. 4.2). This merging could be facilitated by the high-density of mounds (Fig. 4.5a) and the alignment of coral mounds along underlying topographic features that are also largely oriented downslope (*second-order* pattern, Figs. 4.5b, 4.7, 4.8). The lack of large elongated mounds in the CBM sub-province (Fig. 4.9c) suggests that the two sub-provinces were subject to (slightly) different forcing, which favored the merging of mounds in SQM. Possible forcing factors could be, e.g., slightly better living conditions for CWC on the SQM enabling faster formation or shorter distances between "early-stage" mounds facilitating earlier merging.

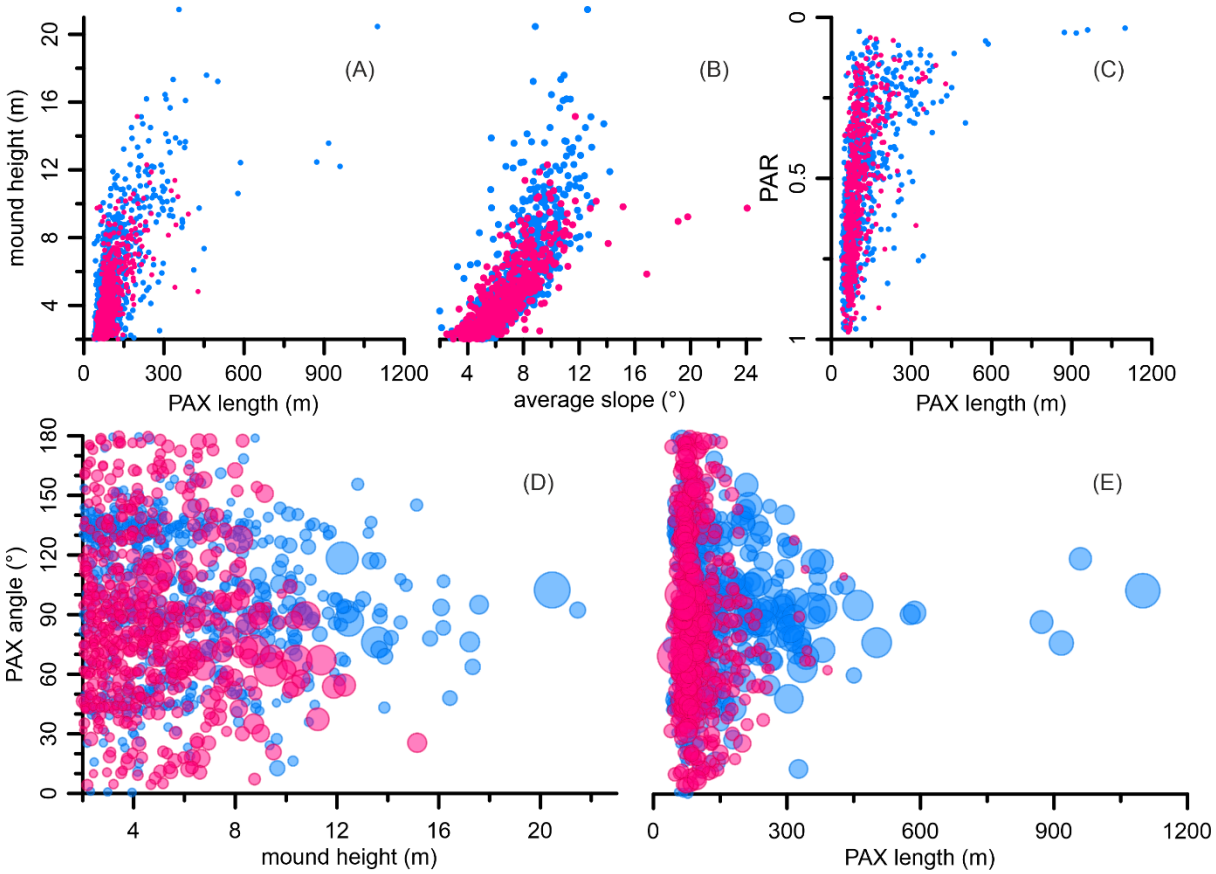

Figure 4.9. (A-B) Crossplots with mound height versus PAX length (A) and average slope (B). (C) Crossplot with PAR versus PAX length (descending order for the y-axis). (D-E) Crossplots with mound height and PAX length versus PAX angle. Size of the dots is proportional to the PAX length 1048 (D) and mound height (E). Color: light blue, Squid Mounds; pink, Coral Belt Mounds.

The evaluation of coral mound orientation shows variable PAX angles of smaller mounds (comprising the majority of the CBM and many SQM). This might be ascribed to their more circular mound footprint areas (PAR, Fig. 4.9c) and an additional influence of the underlying topography on their orientation (PAX angles, Fig. 4.6f), which could result in mound orientations completely unrelated to the hydrodynamic regime, as observed by the PAX angles of early-stage coral mounds developing on carbonate blocks/boulders in the Florida Straits (Correa *et al.*, 2012b; Hebbeln *et al.*, 2012). In contrast, larger coral mounds with heights >~8 m and PAX lengths >~150 m (mostly SQM) exhibit a preferential PAX orientation that narrows towards ~90° with increasing size (Figs. 4.9d, e). This preferred PAX

orientation of ~90°, is roughly parallel to the modern local tidal regime (Hanz *et al.*, 2019)), which suggests an increasingly hydrodynamic control on the shape of the mounds.

The average slope is a morphometric parameter strongly dependent on mound height, as it is, for example, shown by the consistent parallel increase of mound height and average slope (Fig. 4.9b). This is interpreted to reflect the gain of relief from the surrounding seafloor during the early mound formation stage. With increasing height, the local hydrodynamic regime strengthened around the mound summit resulting in an enhanced lateral food supply to the CWC there – as also implicated in the development of shallow-water reefs (Schlager and Purkis, 2013). This is supported by the common observation from various CMPs in which CWC predominantly thrive on mound tops (Heindel *et al.*, 2010; e.g., Huvenne *et al.*, 2005; Le Guilloux *et al.*, 2009; Westphal *et al.*, 2012; Wienberg *et al.*, 2008).

Whereas the elongation and direction of individual mounds are probably largely controlled by hydrodynamics, the interplay of the duration of the formation period and the mound formation rate might play a key role for the size parameters, as suggested by Mortensen *et al.* (2001). Excluding the large (most likely merged) SQM, the populations of SQM and CBM have very similar size-frequency distributions (Fig. 4.6). Considering the relative shallow occurrence and post-glacial development of the Namibian mounds combined with the synchronous demise of the CWC in both sub-provinces (Tamborrino et al., 2019), suggests that similar mound sizes in the sub-provinces likely correspond to a similar temporal development (quasi-synchronous initiation and akin formation rates). Thus, probably only small offsets, e.g., in the environmental factors supporting CWC or in the initial distance between mounds, controlled the small differences between SQM and CBM, most prominently expressed by the more frequent merging of mounds in the SQM sub-province.

The relationship between mound height and PAX length from the Namibian mounds follows a common trend in coral mound development, identifiable also in other CMPs, for which instead of PAX lengths partly comparable measures, such as mound length or max diameter of the mound footprint area have been used. The overall ratio of mound height to PAX length measured for the Namibian coral mounds is <0.2 (98% is even <0.1), comparable with the (mean) values of height and PAX-like parameters measured from other CMPs (e.g., Hebbeln *et al.*, 2019; Huvenne *et al.*, 2003; Lo Iacono *et al.*, 2014; Wheeler *et al.*, 2007; Wheeler *et al.*, 2008). These low ratios highlight the "shield-like" morphology of most coral mounds rather than the conical morphology often described in the literature (e.g., van Rooij et al., 2003; Wheeler et al., 2007). This latter term most likely results from the vertical exaggeration often applied to seabed maps and seismic sections, which can visually transfer a shield-like to a conical morphology.

Finally, the coral mound development off Namibia from small, rather round mounds with variable orientations and relative flat slopes towards larger elongated mounds with preferred orientations and steeper slopes supports the hypothesis of Wheeler et al. (2007) about "inherited" and "developed" mound morphologies. As pointed out above, this transition from the small "inherited" to the larger "developed" mounds probably reflects the increasing control of the local hydrodynamic regime on the

formation of mounds. Furthermore, based on the observed transition of the rather "inherited" to a predominantly "developed" mound morphology at a mound height of ~8 m and a PAX length of ~150 m, we postulate these values as size thresholds for the transition from "inherited" to "developed" coral mounds. If these thresholds are valid for this region only or reflect general thresholds must be tested in the future at other CMPs.

4.4.3. Carbonate deposition in the Namibian Mounds

The morphometric analyses also allow the calculation of mound volumes (Fig. 4.6b). Based on this calculation, the total volume of the Namibia coral mounds is estimated to be 16.2×10^6 m^3 (SQM: 10.9×10^6 m^3; CBM: 5.3×10^6 m^3). These values are a conservative estimate as mounds with a footprint area of <900 m^2 or height of <2 m are not considered, and the mapped area likely does not cover the entire extent of the Namibian CMP. Following the approach of Hebbeln *et al.* (2019a), the stored coral carbonate within the Namibian mounds is estimated by using the following assumptions: based on a volume ratio of 20 vol.% CWC to 80 vol.% matrix sediment (Titschack et al. 2015, 2016) and applying average density values for coral aragonite of ~2.66 g cm^{-3} and for matrix sediments of 1.52 g cm^{-3} (Dorschel *et al.*, 2007b; Hamilton, 1976), the average sediment density of the coral mounds is estimated to be ~1.75 g cm^{-3} with a 30 wt.% contribution of CWC. Based on these assumptions, the total mass of the Namibian mounds is calculated to 28.2×10^6 tons to which CWC contribute 8.5×10^6 tons of carbonate. Considering a mound development period lasting for ~5 kyr (Tamborrino *et al.*, 2019), the CWC-related carbonate production of the Namibian coral mounds had a rate of ~1,900 tons yr^{-1}, which is very close to the number of ~1,550 tons yr^{-1} obtained from a large CMP located on the Moroccan slope in the NE Atlantic (ca. 10x volume of the Namibian CMP, Hebbeln *et al.*, 2019). With an extension of ~200 km^2 as derived from the heatmaps (Fig. 4.5), the coral-derived carbonate productivity in the SQM and CBM sub-provinces was approximately 9.5 g m^{-2} yr^{-1} during their development (4.9–9.5 kyr, Tamborrino et al. 2019). These numbers confirm the capacity of the coral mounds to accumulate carbonate much faster (2.5 times) than the surrounding seafloor (Milliman, 1993; Titschack *et al.*, 2015; Titschack *et al.*, 2016; Titschack *et al.*, 2009).

4.5. Conclusions

The combined analysis of the spatial distribution of the Namibian coral mounds and their morphometric characteristics enables to outline a potential concept for understanding the initiation and the early development of these mounds. A *first-order* pattern derived from the depth interval, in which CWC could thrive due to the supporting environmental conditions created along a water-mass boundary that stretches along the margin. The *second-order* pattern likely corresponds to the sites colonized by the first pioneering coral planulae, which successfully developed in colonies/patches that are aligned along topographic features at the seafloor which off Namibia are erosive in nature and stretch downslope. Mound orientation represents the *third-order* pattern documenting the increasing hydrodynamic control

on mound morphology along their formation. These patterns reflect how environmental conditions, namely the interplay of topography with the regional oceanography and local hydrography, influenced mound development off Namibia at different scales (from colony to coral mound province).

The progressively faster increase in PAX length compared to mound height, especially beyond the thresholds of ~150 m in length and ~8 m in height, probably documents the initial from inherited to developed mounds as this trend aligns with the change from rather random PAX orientations to orientations parallel to the main direction of the tidal bottom current. This is most pronounced for the larger SQM. These numbers can be seen as the first size criteria for the transition from the inherited to the developed mound stage.

This analysis of an extensive morphometric database increases our understanding of the formation of the Namibian coral mounds (incl. e.g. carbonate production) and the involved processes. Similar approaches should be considered for future studies on other CMPs in the Atlantic Ocean (and beyond), which would allow to differentiate between locally unique features and regionally or basin-wide common features of coral mound formation. Such common features to be identified bear a large potential for the definition of a set of basic principles to describe the formation of coral mounds.

Aknowledgements

We thank the officers and the crew of the *R V Meteor*, the Shipboard Scientific Party and the German Diplomatic Corps for the substantial support for the cruise M112 ANNA. This research was supported by the German Academic Exchange Service (DAAD; LT), the German Science Foundation (DH, CW), and the Cluster of Excellence 'The Ocean Floor – Earth's Uncharted Interface' (EXC-2077–390741603; JT). We thank Schlumberger for providing the license of Petrel™ software to University of Miami, Furu Mienis and Ulrike Hanz (NIOZ) are thanked for providing the datasets collected by the benthic lander. Paul Wintersteller, Stefanie Gaide (MARUM), Manuel Jesus Roman Alpiste (CSIC, IACT, Granada) and Débora Duarte (Royal Holloway, University of London) are thanked for the support with the hydroacoustic data. The data reported in this paper are archived in Pangea (www.pangea.de).

5. Manuscript III

Mid-Holocene extinction of cold-water corals on the Namibian shelf steered by the Benguela oxygen minimum zone

Leonardo Tamborrino[1], Claudia Wienberg[1], Jürgen Titschack[1,2], Paul Wintersteller[1,3], Furu Mienis[4], Andrea Schröder-Ritzrau[5], André Freiwald[2], Covadonga Orejas[6], Wolf-Christian Dullo[7], Julia Haberkern[1,3] and Dierk Hebbeln[1]

[1] MARUM–Center for Marine Environmental Sciences, University of Bremen, Bremen, Germany

[2] Marine Research Department, Senckenberg am Meer, Wilhelmshaven, Germany

[3] Department of Geosciences, University of Bremen, Bremen, Germany

[4] NIOZ–Royal Netherlands Institute for Sea Research and Utrecht University, Den Burg, The Netherlands

[5] IUP–Institute of Environmental Physics, Heidelberg University, Heidelberg, Germany

[6] Centro Oceanográfico de Baleares, Instituto Español de Oceanografia, Palma, Spain

[7] GEOMAR–Helmholtz Centre for Ocean Research, 24148 Kiel, Germany

Manuscript submitted in *Geology* (21.06.2019), accepted (10.09.2019) and published online (15.10.2019)

Abstract

An exceptionally large cold-water coral mound province (CMP) was recently discovered extending over 80 km along the Namibian shelf (offshore southwestern Africa) in water depths of 160–270 m. This hitherto unknown CMP comprises >2000 mounds with heights of up to 20 m and constitutes the largest CMP known from the southeastern Atlantic Ocean. Uranium-series dating revealed a short but intense pulse in mound formation during the early to mid-Holocene. Coral proliferation during this period was potentially supported by slightly enhanced dissolved oxygen concentrations compared to the present Benguela oxygen minimum zone (OMZ). The subsequent mid-Holocene strengthening of the Benguela Upwelling System and a simultaneous northward migration of the Angola-Benguela Front resulted in an intensification of the OMZ that caused the sudden local extinction of the Namibian corals and prevented their reoccurrence until today.

5.1 Introduction

Cold-water corals (CWCs) play an important role as ecosystem engineers supporting biodiversity and biomass hotspots in the deep sea, comparable to tropical coral reefs (Henry and Roberts, 2017). Frameworks built by colonial scleractinian CWCs, like *Lophelia pertusa*, have the capacity to efficiently baffle bypassing sediments, supporting the formation of three-dimensional seabed structures, which develop over geological time scales (millennia and more) to large reef buildups known as "coral mounds" (Roberts et al., 2006). A remarkably widespread occurrence of coral mounds clustered into distinct coral mound provinces (CMPs) has been documented for the continental slopes of the North Atlantic Ocean (Wienberg and Titschack, 2017), while only few CMPs are reported from shallow shelf settings (e.g., Lindberg and Mienert, 2005).

Two recent expeditions to the southeastern Atlantic revealed the presence of numerous coral mounds extending over a large area along the Namibian shelf (Geissler et al., 2013; Hebbeln et al., 2017). The discovery of this hitherto unknown Namibian CMP (at ~20 °S) is exceptional because (1) it constitutes the largest CMP discovered so far in the entire southeastern Atlantic (Fig. 5.1); (2) besides the giant Mauritania CMP (Wienberg et al., 2018), it is the only other known CMP occurring under an eastern boundary upwelling system; and (3) it is impacted by one of the strongest oxygen minimum zones (OMZs) worldwide. Today, living CWCs are absent from the area (Hebbeln et al., 2017). With uranium-series coral dating, we aim to elucidate the timing of the mound formation as a response to millennial-scale palaeoceanographic changes in the southeastern Atlantic. Environmental parameters being identified as the main controls for the extinction of the Namibian CWCs and the subsequent cessation in mound formation will significantly contribute to the ongoing debate on the impact of climate-driven deoxygenation processes on large marine ecosystems.

5.2. Namibian coral mounds

Multibeam echosounder mapping performed during two expeditions (RV *Maria S. Merian* cruise MSM20-1: Geissler et al., 2013; *RV Meteor* cruise M122: Hebbeln et al., 2017) revealed a CMP consisting of >2000 coral mounds in ~160–270 m water depth that extends over a distance of (at least) 80 km along the Namibian shelf (Fig. 5.1S). The topography underlying the Namibian CMP is predominantly characterized by erosive features, dominated by a straight NNW-SSE–trending escarpment as much as 45 m high and 63 km long (Fig. 5.1b). The Namibian coral mounds are concentrated in three main areas (Fig. 5.1b). The northern Squid Mounds (maximum height 20 m) occur between 210 and 270 m water depth on a gently westward-dipping plain. The southern Coral Belt Mounds (height 5–12 m) are developed in 230–255 m water depth parallel to the escarpment, where they are mainly distributed along small ridges and furrows indenting the lower slope of the escarpment.

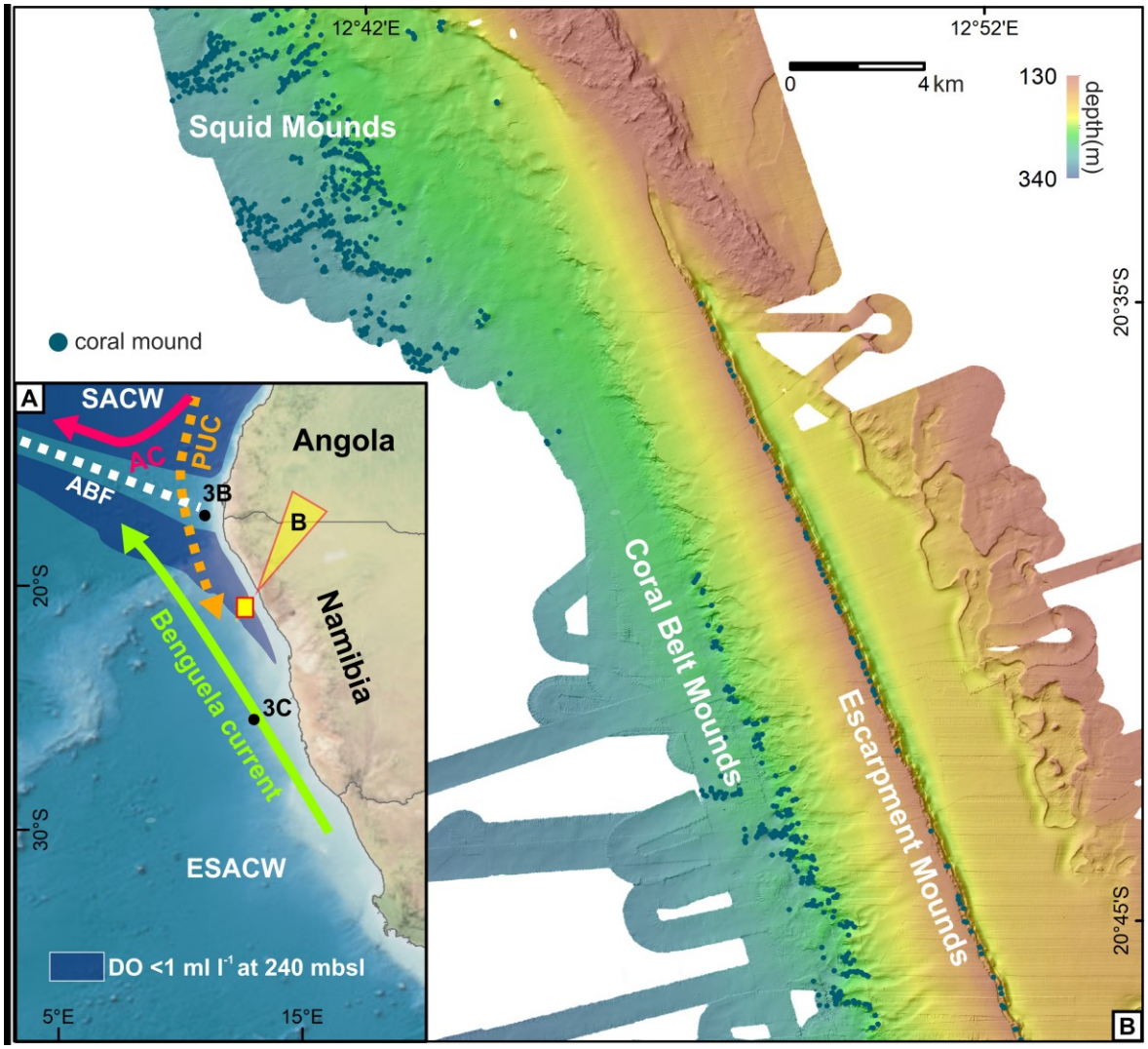

Figure 5.1. (A) Overview map showing oceanographic circulation patterns off southwestern Africa (ABF—Angola-Benguela Front; AC—Angola Current; PUC—poleward undercurrent; SACW—South Atlantic Central Water; ESACW—Eastern South Atlantic Central Water; mbsl—meters below sea level). Spatial extent of oxygen minimum zone (dissolved oxygen concentrations (DOCs) <1 mL L^{-1} in 240 m water depth; dark-blue shading) is based on Schmidt and Eggert (2016) and GENUS (2017). Corresponding DOCs at the ABF are <2 mL L^{-1}. Yellow square and arrow indicate the Namibian coral mound province shown in B. "3B" and "3C" refer to data sets presented in Figures 3B and 3C, respectively. (B) Bathymetric map showing amount and distribution of coral mounds (see the Suppl. Mat. for extended and detailed maps).

The small group of Escarpment Mounds (height 4–6 m) occurs on top of the escarpment along the ~160 m isobath.

Gravity cores were collected from different mounds within the Namibian CMP. All cores showed a typical mound facies comprising a mixture of CWC fragments embedded in hemipelagic sediments, and hence, proved their formation by CWCs (Hebbeln et al., 2017).

Remotely operated vehicle video observations revealed that all mounds are densely covered by exposed fossil *L. pertusa*, being sparsely covered by fine sediment and colonized by rare living megabenthic fauna (e.g., sponges, bryozoans; see Suppl. Material; Hebbeln et al., 2017). To assess the time of CWC extinction off Namibia, 17 coral mounds, widely distributed across the entire CMP, were sampled by box corer and grab sampler. Fossil *L. pertusa* specimens were selected for uranium-series dating from all available surface samples (n = 19; see Suppl. Material). The obtained ages revealed a rather narrow age range (Squid Mounds: 4.8–5.7 kyr B.P., n = 6; Coral Belt Mounds: 4.4–5.8 kyr B.P., n = 10; Escarpment Mounds: 5.0–7.1 kyr B.P., n = 3), suggesting a simultaneous regional extinction of *L. pertusa* at ca. 4.5 kyr B.P. In addition, a gravity core penetrating a Coral Belt Mound down to its base allowed dating of the onset of its formation at 9.5 kyr B.P. (age of the oldest coral at the mound base). Coral samples (n = 17) collected at various core depths reveal a continuous mound aggradation until ca. 5.0 kyr B.P. (age of the youngest coral at the core top), which is in agreement with the youngest coral ages obtained from the mound surfaces. Overall, these data suggest a short (~5 k.y.) but intense pulse of mound growth for the Namibian CMP, with a calculated average mound aggradation rate of 158 cm k.y^{-1} (see Suppl. Material).

5.3. Modern oceanographic setting

The Namibian CMP (at ~20°S) occurs under an oceanographic setting controlled by the Benguela Upwelling System (BUS). The BUS is one of the large eastern-boundary upwelling systems with the highest primary production in the world ocean (0.37 Gt carbon per year; Carr, 2001). Due to these highly productive conditions, shelf-bottom waters become severely oxygen depleted, resulting from the consumption of oxygen through the decomposition of organic matter. Dissolved oxygen concentrations (DOCs) in the Benguela OMZ are further controlled by the mixing of southern-sourced

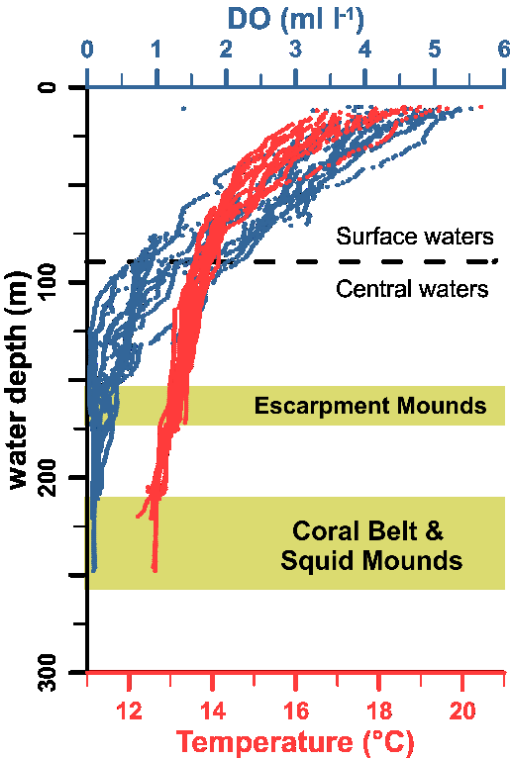

Figure 5.2. Dissolved oxygen concentrations (DOCs, blue) and potential temperatures (red) measured by 12 conductivity-temperature-depth (CTD) casts collected within the Namibian coral mound province. All data were obtained in January 2016 (austral summer) during the *R V Meteor* expedition M122. Bars indicate depth levels of coral mound occurrences.

surface waters and the underlying well-ventilated Eastern South Atlantic Central Water (ESACW), both carried equatorward by the Benguela Current, with northern-sourced surface waters and the oxygen-depleted South Atlantic Central Water (SACW) transported to the south by the Angola Current (Fig. 5.1; Mohrholz et al., 2008). The two surface water masses (<85 m water depth) converge at the Angola-Benguela Front (ABF) at 15°–18°S (Veitch *et al.*, 2006), which also forms the northern boundary of the BUS. Enhanced dynamics related to this frontal zone cause a vertical mixing of the upper waters (Koseki *et al.*, 2019), which result in slightly increased DOCs down to mid-depths (~240 m; Fig. 3.1; GENUS, 2017; Schmidt and Eggert, 2016). Between the SACW and ESACW, a rather broad transition zone is developed. This is related to the effect of the poleward undercurrent that flows as an extension of the AC (Fig. 5.1) below the surface waters along the Namibian shelf edge at least as far south as 27°S (Mohrholz et al., 2008) and transports oxygen-depleted SACW onto the Namibian shelf.

Conductivity-temperature-depth (CTD) data obtained during cruise M122 (January 2016) show that the Namibian coral mounds occur exactly at the depth level (160–270 m water depth) with lowest DOCs of <0.5 mL L^{-1} accompanied by relatively high potential temperatures, ranging between 12.4 and 13.4 °C (Fig. 5.2; Hebbeln et al., 2017). Time-series CTD data recorded by bottom landers deployed in the area of the Coral Belt mounds confirmed very low DOCs between 210 and 220 m water depth, fluctuating within tidal cycles between 0 and 0.15 mL L^{-1} (Hebbeln et al., 2017). Monthly resolved World Ocean Atlas (WOA, https://www.nodc.noaa.gov/OC5/woa18/; Boyer *et al.*, 2013) data suggest that the low DOCs measured during austral summer persist throughout the year (even though the WOA-derived DOCs are higher due to the more offshore position of the WOA reference point; see Suppl. Material).

5.4. Discussion and conclusion

The distribution of the >2000 coral mounds we studied on the Namibian shelf aligns well with distinct topographic features, such as the prominent escarpment and small ridges indenting its western lower slope (Fig. 5.1). This reflects the preference of CWCs to initially settle on topographic highs, where they benefit from more-turbulent hydrographic conditions that increase the food supply (Roberts et al., 2006). Compared to other CMPs in the Atlantic Ocean (e.g., Wheeler *et al.*, 2007; Wienberg *et al.*, 2018) the Namibian coral mounds are relatively small, as they do not exceed heights of 20 m, likely due to the short mound formation period lasting only for ~5 k.y. (Fig. 5.3; see Suppl. Material).

The present-day absence of CWCs on the Namibian shelf points to an environmental setting that hampers their survival for the past ~4.5 k.y. Overall, the proliferation of CWCs is controlled by distinct oceanographic boundary conditions, with food supply (being a function of productivity and hydrodynamics delivering food particles), temperature, and DOCs being the most critical parameters (e.g., Davies and Guinotte, 2011). For the Namibian shelf, food supply is sustained by the high primary productivity induced by the BUS, complemented by high vertical and lateral flux rates of particulate material (Inthorn *et al.*, 2006b; Vorrath *et al.*, 2018). The high quantity and quality of suspended

particulate organic matter recorded by the benthic landers deployed within the Namibian CMP indicate a sufficient food supply today (U. Hanz, 2019, personal commun.). Although the relatively high temperatures (12.4–13.4 °C; Fig. 5.2) depict a stressor for CWC growth, because they are only slightly below the upper thermal limit for *L. pertusa* (Dodds et al., 2007; Davies and Guinotte, 2011), the prevailing eutrophic conditions might allow the CWCs to maintain their metabolism rates (Büscher *et al.*, 2017). Consequently, the low DOCs of <0.5 mL L^{-1} are the most probable stressor that hampers coral proliferation today. These values are far below the lowest reported DOCs associated with living *L. pertusa* within the modern Atlantic (~1–2 mL L^{-1}) (Brooke and Ross, 2014; Georgian *et al.*, 2016; Wienberg *et al.*, 2018). The present-day low DOCs of the Benguela OMZ are controlled by three processes: (1) the strength of the BUS steering the regional primary production and the linked rate of oxygen consumption by organic-matter remineralization, (2) the southward advection of oxygen-depleted SACW by the poleward undercurrent, and (3) the vertical mixing associated with the ABF. Any changes of these processes should have had an impact on the past (millennial-scale) variability of the intensity and extension of the OMZ.

For the early to mid-Holocene, when CWCs were thriving, various regional proxy records have revealed a weakened BUS (Fig. 5.3c; Farmer *et al.*, 2005), triggered by a southward position of the Southern Westerlies (Lamy *et al.*, 2001). At the same time, an increased southward flow of warm tropical surface waters (Fig. 5,3b; Kim *et al.*, 2002; Shi *et al.*, 2000) points to a southward displacement of the ABF (Kirst *et al.*, 1999). At first glance, it may seem that this would have caused an enhanced delivery of oxygen-depleted SACW, but with the ABF moving toward the Namibian CMP (at ~20°S), enhanced mixing due to frontal processes would have provided slightly better-ventilated conditions down to >200 m water depth, as it is observed today (Fig. 5.1a). Thus, it is assumed that the decrease in upwelling combined with the mixing effect of the ABF triggered conditions of slightly higher DOCs compared to today, which allowed coral growth and mound formation on the Namibian shelf.

During the mid-Holocene, the oceanographic setting dramatically changed in response to the northward shift of the westerlies toward their present-day position (Lamy *et al.*, 2001). The resulting equatorward shift of the trade winds caused a strengthening of the BUS on the northern Namibian shelf (Emeis *et al.*, 2009) and allowed the Benguela Current to progress further north, thereby pushing the ABF to the north (Kirst *et al.*, 1999). Hence, the combination of the BUS-related increased oxygen consumption and the decline of the ABF ventilating effect at the Namibian CMP resulted in an intensification of the Benguela OMZ. As a consequence, the vivid CWC community supporting the rapid aggradation of the >2000 Namibian coral mounds suddenly faced its local extinction at ca. 4.5 kyr B.P., after ~5 k.y. of proliferation. Since then, extremely low DOCs on the Namibian shelf have precluded the presence of CWCs within this largest known southeastern Atlantic CMP. As CWCs in the nearby CMP off Angola survive today under DOCs of just above 0.5 mL L^{-1} (Hebbeln et al., 2017), this value might define a new lowermost threshold for DOC tolerable for *L. pertusa,* and in general for CWCs. It also shows that CWCs in the southeastern Atlantic are able to cope with lower DOCs compared to other Atlantic sites.

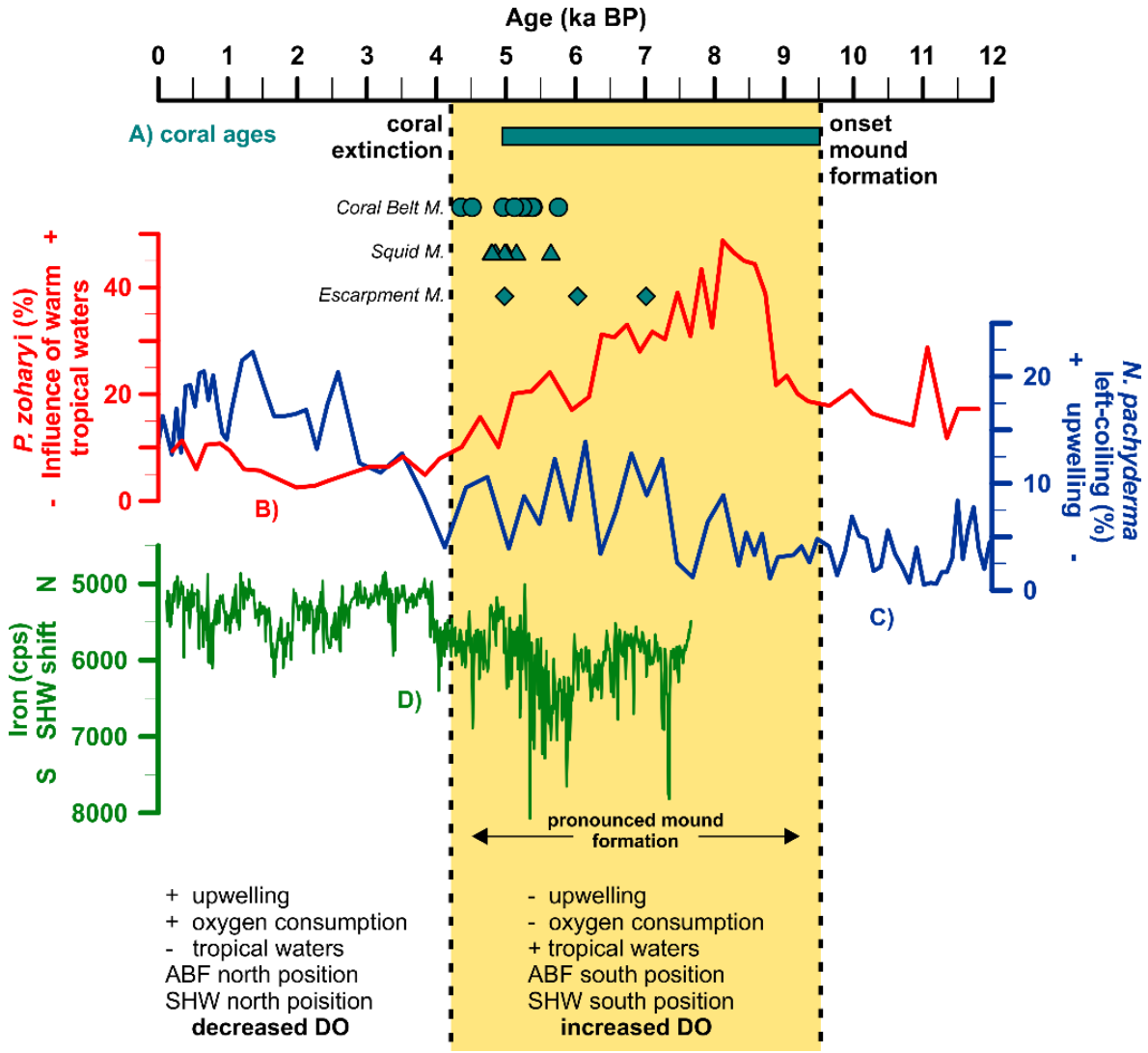

Figure 5.3. Uranium-series cold-water coral ages (A) obtained from 19 surface sediment samples (green symbols) collected from various Namibian shelf coral mounds differentiated into three mound settings, and the age range derived from one gravity core fully penetrating one Coral Belt Mound (green bar). Coral ages reveal a pronounced period in mound formation restricted to the early to mid-Holocene, which coincides with enhanced influence of warm tropical waters (indicated by high percentages of the tropical dinoflagellate *Polysphaeridium zoharyi*; Shi et al., 2000) (B), and weakened upwelling (indicated by low percentages of the planktonic foraminifera *Neogloboquadrina pachyderma* (left coiling); Farmer et al., 2005) (C), pointing to southward displacement of the Angola-Benguela Front (ABF) due to southward displacement of the Southern Hemisphere westerlies (SHW; indicated by enhanced iron contents in Chilean margin sediments; Lamy et al., 2001) (D). M.—Mounds; DOC—dissolved oxygen concentration; cps—counts per second. Locations for B and C are indicated in Figure 5.1a.

Our findings show that highly productive upwelling areas inhabited by CWCs such as off Namibia and off Mauritania (Wienberg et al., 2018) can exert decisive influences on marine benthic ecosystems. Increased upwelling results in enhanced food supply supporting these ecosystems (e.g., Wienberg et al., 2018). However, depleted oxygen conditions in the related OMZs can trigger the local extinction of benthic fauna. Due to the further increase in ocean deoxygenation expected over the coming decades as a consequence of ongoing global climate change (Keeling *et al.*, 2010; Stramma *et al.*, 2008; Sweetman *et al.*, 2017), our results from the Namibian CMP might serve as an example highlighting how marine benthic ecosystems suffer from such a development. For regions with CWCs that currently thrive under

comparably low DOCs (e.g., Angola, Mauritania, Gulf of Mexico; Georgian et al., 2016; Hebbeln et al., 2017; Wienberg et al., 2018), further decreasing DOCs might wipe out biodiversity hotspots engineered by CWCs within the coming decades to centuries.

Aknowledgements

We thank the nautical and scientific crews for on-board assistance during R/V *Meteor* cruise M122; and N. Frank, R. Eichstädter, and A. M. Wefing (Institute of Environmental Physics, Heidelberg University, Germany) for their support in uranium-series dating. We thank all the reviewers whose comments improved our original manuscript. This research was supported by the German Science Foundation and the Cluster of Excellence "The Ocean Floor—Earth's Uncharted Interface" (Hebbeln, Wienberg, Titschack), the German Academic Exchange Service (Tamborrino), and the Innovational Research Incentives Scheme of the Netherlands Organization for Scientific Research (Mienis).

Supplementary material

All data and material from the Namibian cold-water coral mound province (CMP) used for this study were obtained during R/V *Maria S. Merian* expedition MSM20/1 in January 2012 (mapping; Geissler et al., 2013) and during R/V *Meteor* expedition M122 ANNA in December 2015/January 2016 (mapping, CTD measurements, benthic lander deployment, ROV video surveys, sampling of surface sediments and core material; Hebbeln et al., 2017).

S.1. Multibeam echosounder mapping

Instrument specifications and applied settings for the mapping by multibeam echosounder systems (MBES) are described in detail in Geissler et al. (2013) and Hebbeln et al. (2017). For all the hydroacoustic measurements, sound velocity profiles were obtained from CTD casts. Seabed mapping was performed utilising two different hull-mounted KONGSBERG MBES: EM1002 (95 kHz) during expedition MSM20/1 and EM710 (70-100 kHz) during expedition M122. The EM1002 emitted 111 beams per ping, covering a depth range of 2-1000 m and achieving a depth resolution of 2-8 cm, depending on the pulse length (0.2-2 ms). Achievable swath width on a flat bottom was up to 5 times the water depth, depending on the depth and character of the seafloor. During mapping, the swath width was adjusted to 120° (~3.5 times water depth). The EM710 acquires 200 beams per ping and 400 soundings ("soft-beams") in the used high-density mode, while covering a depth range of several meters up to ~800 m and achieves a depth accuracy of 0.3% of the depth.

Spatial integrity of the mapping data was achieved by combining the ship's SEAPATH 200 inertial navigation systems (INS) including differential global positioning system (DGPS) information with motion data (roll, pitch, heave) provided by the motion reference units (MRU5+). The open-source software package MB-System v.5.3.1 (Caress and Chayes, 1995) was used for bathymetric data post-processing, editing and evaluation. ESRI ArcGIS v.10 was used to create maps (grid cell size: 10 m,

hillshade with 10 times vertical exaggeration), for spatial data management and for the quantification of coral mounds on the Namibian shelf. Bathymetric raw data and products will be available in PANGAEA (www.pangaea.de).

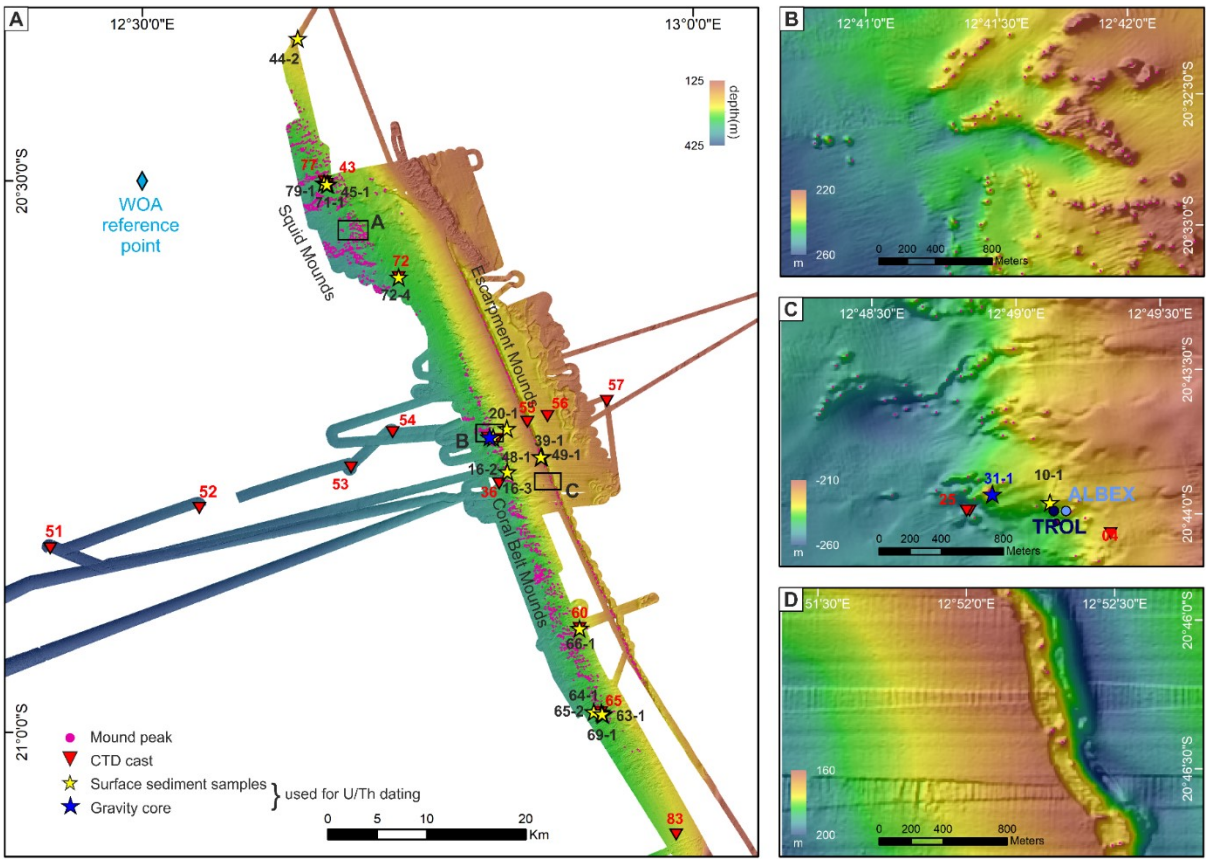

Figure 5.1S. A) Bathymetric map (based on MBES data obtained during expeditions M122 and MSM20/1) showing the distribution of >2,000 coral mounds (pink dots) on the Namibian shelf. Positions of CTD casts (red triangles), surface sediment samples (yellow stars) and the gravity core (blue star) used for this study are indicated. Labels next to the symbols refer to the last two and three digits of the GeoB-ID (GeoB 205xx-x) presented in Table S2 and Table S4, respectively. WOA reference point indicated in light blue. A-C. Detailed maps showing examples for mounds from the three sub-cluster present in the Namibian CMP: (B) *Squid Mounds*, (C) *Coral Belt Mounds* showing the deployment sites of the benthic landers (ALBEX and TROL; blue dots) and (D) *Escarpment Mounds*.

S.2. Quantification of coral mounds

The processed MBES map (grid cell size: 10 m) was used for a further quantification of coral mounds occurring in the Namibian CMP. Using ESRI ArcGIS v.10, a total number of 2027 coral mounds was (manually) detected. Single peaks with a minimum height of ~3m of merging and clustering mounds have been counted separately. The distribution of coral mounds on the Namibian shelf as well as detailed maps showing examples for the three sub-clusters of the Namibian CMP defined as Squid Mounds (n=959 mounds), Coral Belt Mounds (n=896 mounds) and Escarpment Mounds (n=138 mounds) are presented in Fig. 5.1S.

S.3. ROV video surveys

Video and photo footage was obtained during seven dives with the ROV MARUM SQUID (SAAB Seaeye, UK, adapted and operated by MARUM, Bremen, Germany) crossing various coral mounds of

the Namibian CMP. Technical specifications of ROV SQUID are described in Hebbeln et al. (2017). Some ROV images showing the typical faunal coverage of the Namibian mounds, which is dominated by fossil coral rubble and framework of the cold-water coral *Lophelia pertusa* and colonized by scarce living fauna, are presented in Fig. 5.2S.

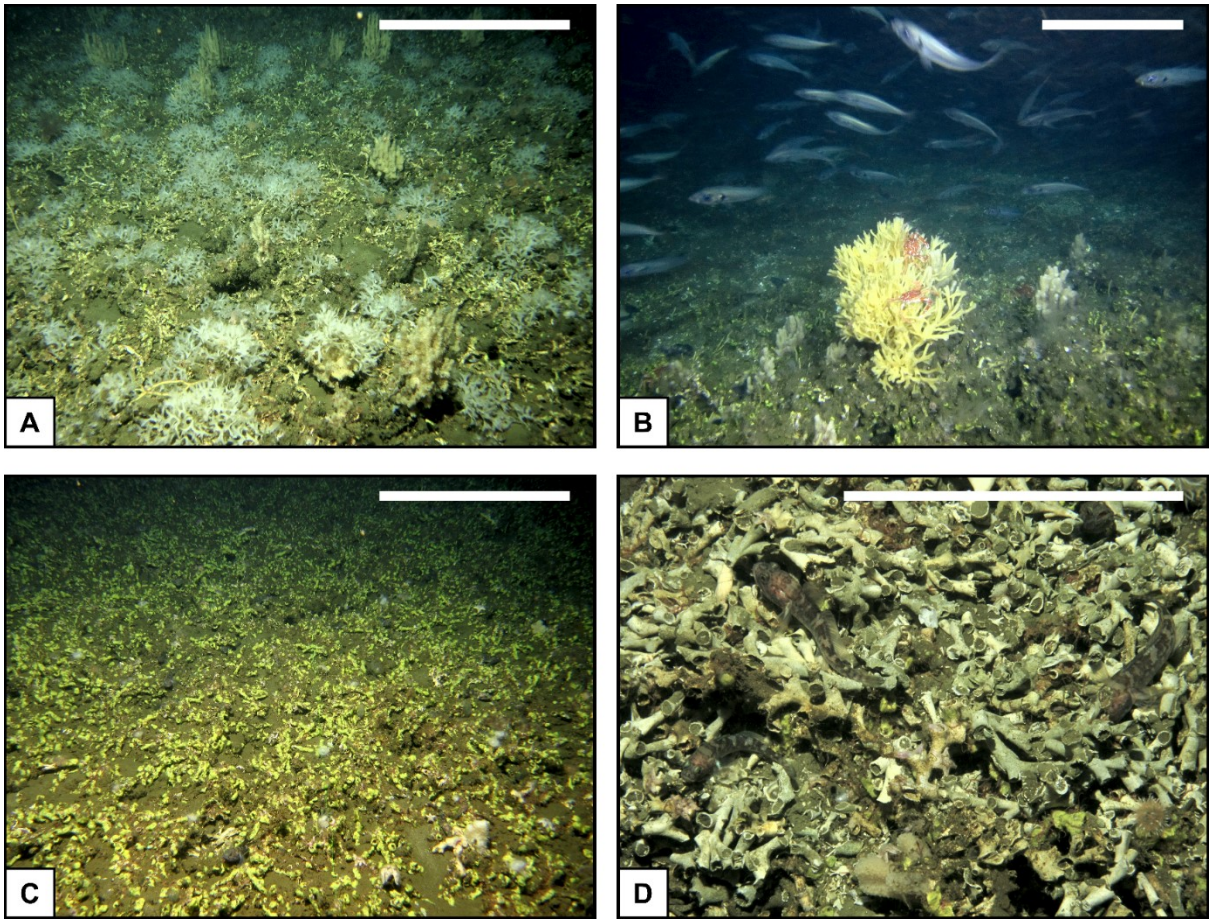

Figure 5.2S. ROV images collected during the M122 ANNA cruise. A) Coral mound surface densely covered by different sponges (cathedral-like and fingerstick-like sponges). B) A carangid swarm swimming over a mound surface with few sponge colonies. C) Mound surface with coral frameworks infested by the yellow bryozoan *Metroperiella* sp. D) Dense dead framework of *L. pertusa* with several gobiid fish. Scale bar: ~30cm.

S.4. CTD measurements

To determine the physical parameters of the water masses, 12 CTD casts were performed in the area of the Namibian CMP, arranged parallel and perpendicular to the shelf (water depth range: 150-250 m), while four casts were performed in deeper areas (water depth range: 286-391 m) west of the Namibian CMP (Fig. 5.1S). The CTD measurements were conducted using a SEABIRD "SBE 9 plus" underwater unit and a SEABIRD "SBE 11 plus V2" deck unit. Vertical profiles over the water column provided standard data for conductivity, potential temperature, pressure, and dissolved oxygen concentrations. All data presented here refer to the down casts of the individual CTD deployments and are presented in Fig. 5.3S. Metadata of the CTD casts are provided in Table 5.1S. Raw CTD data will be available in PANGAEA (www.pangaea.de).

Table 5.1S. Metadata of the CTD casts deployments

GeoB ID	Latitude (S)	Longitude (E)	Depth (m)	Day and time of deployment (dd.mm.yyyy / UTC)
20504-1	20° 44.067´	12° 49.330´	220	01.01.2016 07:58
20525-1	20° 43.990	12° 48.830	247	03.01.2016 17:31
20536-1	20° 46.470´	12° 49.450´	250	04.01.2016 15:32
20543-1	20° 30.180´	12° 40.060´	224	05.01.2016 12:03
20555-1	20° 43.118´	12° 50.985´	163	06.01.2016 23:10
20556-1	20° 42.802´	12° 52.079´	178	06.01.2016 23:55
20557-1	20° 41.979´	12° 52.079´	150	07.01.2016 00:51
20560-1	20° 54.341'	12° 55.303´	217	07.01.2016 15:12
20565-1	20° 58.913'	12° 53.818´	233	08.01.2016 11:05
20572-1	20° 35.249'	12° 55.002´	233	09.01.2016 09:04
20577-1	20° 30.049'	12° 43.970´	221	10.01.2016 14:21
20583-1	21° 5.565'	12° 39.948´	212	11.01.2016 14:08
CTD casts conducted on the slope, west of the Namibian coral mounds				
20551-1	20° 50.000´	12° 25.000´	391	06.01.2016 17:51
20552-1	20° 47.792´	12° 33.110´	333	06.01.2016 19:25
20553-1	20° 45.588´	12° 41.383´	310	06.01.2016 20:55
20554-1	20° 43.681´	12° 43.639´	286	06.01.2016 21:55

S.5. World Ocean Atlas data

All the CTD data collected during austral summer (M122 ANNA cruise, January 2016). In order to understand the oceanographic setting throughout the year, we compare the CTD data with the information derived from the World Ocean Atlas (WOA; Boyer et al., 2013). The ranges of the dissolved oxygen concentrations (DO) and temperatures from the WOA refer to the monthly means obtained from the closest reference point to the surveyed area (position displayed in Fig. 3.1S: 20°30'S, 12°30′E), 17 km W from the Namibian CMP). The WOA statistical mean is the average of all unflagged interpolated values at each standard depth level for each variable in each 1° square, which contains at least one measurement for the given oceanographic variable. Generally, the WOA data (Fig. 5.3S) reveal a similar depth-depended trend compared to the shipboard CTD data obtained during M122 during

austral summer, but show slightly higher DO and lower temperatures. This is likely due to the origin of the data (statistical mean based on interpolation of previously-collected oceanographic data) and the position of the reference point (Fig. 5.3S), 17 km west from the Namibian CMP. Indeed, the WOA data show higher closeness with data collected from the deeper CTD stations on the slope west of the Namibian CMP (Fig. 5.3S). Both datasets highlight how the Benguela OMZ dissolves westward as result of the gradual deviation from the high-productive surface waters on the Namibian shelf and mixing of the SACW (oxygen-depleted water mass carried along the shelf break by the PUC) with the oxygen-rich ESACW waters (further details are provided in the main text).

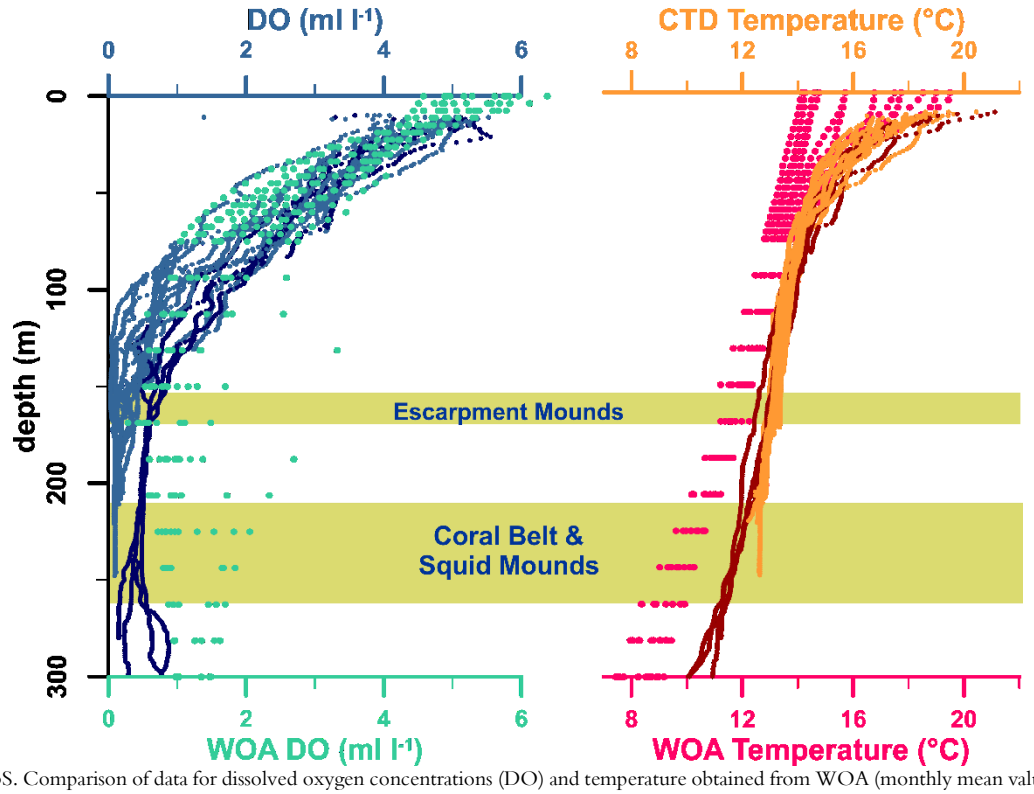

Figure 5.3S. Comparison of data for dissolved oxygen concentrations (DO) and temperature obtained from WOA (monthly mean values; Boyer et al., 2013) and from CTD deployments conducted during R/V *Meteor* cruise M122 in January 2016. DO values: WOA - green; CTD data from the Namibian CMP - light blue; CTD data from the deeper stations west of the Namibian CMP - dark blue. Temperatures: WOA - pink; CTD data from the Namibian CMP - orange; CTD data from the deeper stations west of the Namibian CMP – red.

S.6. Surface sediment and core sampling

Surface sediments were collected by grab sampler (GS, n=9) and the giant box corer (GBC, n=7) from the top of various coral mounds of the Namibian CMP (Hebbeln et al., 2017). Additionally, a gravity core (GeoB 20531-1) was collected from one of the Coral Belt Mounds, even penetrating the base of this mound (Fig. 5.4S). Fragments of *Lophelia pertusa* were selected from each surface sample from various core depths and used for uranium-series dating.

S.7. Age determination on coral fragments

In total, a set of 36 fragments of *L. pertusa* have been selected for uranium-series absolute age dating: 19 coral samples from the material collected with GS and GBC and 17 coral samples collected along a mound-penetrating gravity core. Prior to the analyses, all coral fragments were cleaned mechanically to

remove contaminants from the external surface of the fossil skeletons (e.g., borings by organisms, iron–manganese crusts, coatings) and prepared chemically using weak acid leaching and water rinsing procedures as described by Frank *et al.* (2004). The dating analyses were carried out with a multi-collector inductively coupled plasma mass spectrometer (Institute of Environmental Physics, University of Heidelberg, Germany; Wefing et al., 2017). The reproducibility of mass spectrometric measurements was assessed using the international Uranium standard material HU1 (Cheng *et al.*, 2000; Frank *et al.*, 2004; Wefing *et al.*, 2017). Metadata and ages are reported in Tables 5.5S and 5.6S. Ages are given in kilo years before present (ka BP; BP defined as 1950). All CWC fragments indicated minor physico-chemical alteration or dissolution, which may disturb Uranium-series ages. Measured ^{232}Th concentrations are small with <2.5 ppb for 94% of all samples (Tables 5S, 6S). Initial $\delta^{234}U_i$ values are variable and range between 146.6 ± 0.7‰ and 150.7 ± 0.6‰ (Tables 5S, 6S). All samples rely on $\delta^{234}U_i$ values within the narrow band of ±10‰ compared to the value of modern seawater (146.8‰; Andersen et al., 2010) and can therefore be treated as being reliable.

Coral ages obtained from the core record range from 9.5 to 5 ka BP. Coral mound aggradation rates (ARs) were calculated from age to age, following a continuous chronological order (Table 5.6S). The oldest and youngest coral ages in relation to the maximum and minimum core depths of the respective core interval were used for the calculation of the average AR (Fig. 5.5S).

Table 5.4s. Metadata of the sediment material used for the collection of fossil *L. pertusa* fragments used for uranium-series dating

Area	GeoB ID	Gear	Latitude (S)	Longitude (E)	Depth (m)	Sampling depth
NW Squid Mounds	20544-2	GS	20° 22.265´	12° 38.468´	160	0-10 cm
Squid Mounds	20545-1	GBC	20° 30.184´	12° 40.067´	224	0-32 cm
Squid Mounds	20571-1	GBC	20° 30.194´	12° 40.122´	225	0-30 cm
SE Squid Mounds	20572-4‘	GBC	20° 35.249´	12° 43.968´	221	0-20 cm (layer 1)
SE Squid Mounds	20572-4“	GBC	20° 35.249´	12° 43.968´	221	20-30 cm (layer 2)
Squid Mounds	20579-1’	GS	20° 30.128´	12° 39.901´	223	0-10 cm
Squid Mounds	20579-1“	GS	20° 30.128´	12° 39.901´	223	0-10 cm
Escarpment Mounds	20539-1	GBC	20° 45.018´	12° 51.733´	166	Bulk
Escarpment Mounds	20548-1	GS	20° 45.025´	12° 51.715´	162	0-10 cm
Escarpment Mounds	20549-1	GS	20° 45.014´	12° 51.778´	175	0-10 cm
N Coral Belt Mounds	20510-1	GBC	20° 43.962´	12° 49.119´	230	0-15 cm
N Coral Belt Mounds	20516-2	GBC	20° 45.834´	12° 49.887´	223	0-40 cm
N Coral Belt Mounds	20516-3	GC	20° 45.834´	12° 49.887´	225	(?) core top
N Coral Belt Mounds	20520-1	GS	20° 30.128´	12° 49.866´	234	0-10 cm
S Coral Belt Mounds	20563-1	GS	20° 59.040´	12° 55.096´	232	0-10 cm
S Coral Belt Mounds	20564-1	GS	20° 59.006´	12° 55.045´	234	0-10 cm
S Coral Belt Mounds	20565-2	GS	20° 58.918´	12° 55.003´	232	0-10 cm
S Coral Belt Mounds	20566-1	GBC	20° 54.346´	12° 53.829´	223	0-12 cm
S Coral Belt Mounds	20569-1	GS	20° 58.892´	12° 54.586´	243	0-10 cm

GBC: giant box core, GS: grab sample, GC: gravity core
For GeoB20572-4 and 20579-1, two *L. pertusa* fragments were collected for dating: ’ sample 1; “ sample 2

Table 5.5S. U-series age, isotope concentrations and ratios from *L. pertusa* fragments from surface sediment samples

GeoB ID	Lab-ID	^{232}Th (ppb)	± (abs.)	$\delta^{234}U_m$* (‰)	± (abs.)	$\delta^{234}U_i$* (‰)	± (abs.)	Age (ka BP)	± (abs.)	Age^{cor} (ka BP)	± (abs.)
20544-2	IUP-7667	0.2693	0.0007	145.6	0.9	147.7	0.9	5.032	0.021	5.015	0.022
20545-1	IUP-9818	0.1785	0.0004	145.5	0.4	147.7	0.4	5.169	0.015	5.155	0.015
20571-1	IUP-7836	n.d.		146.8	2.2	149.2	2.2	5.653	0.040	5.653	0.040
20572-4'	IUP-7838	n.d.		147.1	2.4	149.2	2.4	4.854	0.028	4.854	0.028
20572-4''	IUP-7669	0.6731	0.0012	144.5	0.7	146.6	0.7	5.032	0.019	4.986	0.030
20579-1'	IUP-7837	n.d.		146.4	0.9	148.4	0.9	4.796	0.026	4.796	0.026
20579-1''	IUP-9816	0.2641	0.0004	146.2	0.5	148.2	0.5	4.826	0.019	4.804	0.020
20539-1	IUP-7842	0.5767	0.0026	145.6	0.8	148.6	0.8	7.047	0.036	7.019	0.039
20548-1	IUP-9814	0.2646	0.0006	148.6	0.6	150.7	0.6	5.004	0.025	4.983	0.024
20549-1	IUP-7843	0.1755	0.0007	144.9	1.2	147.5	1.2	6.046	0.034	6.033	0.035
20510-1	IUP-7666	7.3430	0.0220	147.1	1.2	149.2	1.3	5.508	0.033	4.963	0.280
20516-2	IUP-7840	0.0038	0.0000	146.3	0.9	148.6	0.9	5.396	0.029	5.396	0.029
20516-3	IUP-7841	n.d.		145.3	0.6	147.5	0.6	5.291	0.029	5.291	0.029
20520-1	IUP-9817	2.1160	0.0031	146.5	0.6	148.3	0.6	4.518	0.018	4.353	0.09
20563-1	IUP-7845	0.6158	0.0026	144.5	1.1	146.9	1.1	5.794	0.029	5.76	0.033
20564-1	IUP-9815	0.1012	0.0002	145.8	0.5	148.0	0.5	5.387	0.016	5.38	0.015
20565-2	IUP-7846	0.0357	0.0005	143.7	1.1	145.9	1.1	5.245	0.030	5.242	0.030
20566-1	IUP-7844	n.d.		145.7	1.0	147.6	1.0	4.515	0.026	4.515	0.026
20569-1	IUP-7668	0.0759	0.0002	145.3	0.8	147.5	0.9	5.133	0.023	5.126	0.024

* Measured $^{234}U/^{238}U$ activity ratios ($\delta^{234}U_m$) are presented as deviation permil (‰) from the equilibrium value. Decay corrected $^{234}U/^{238}U$ activity ratios ($\delta^{234}Ui$) are calculated from the given ages and with $\lambda^{234}U$: 2.8263 x 10^{-6} yr^{-1}.

Age^{cor} Corrected ages, according to Frank et al. (2004) and Wefing et al., (2017).

n.d.: not determinable because lower than the analytical blank (<0.003 ng/g).

For GeoB20572-4 and 20579-1, two *L. pertusa* fragments were collected from the bulk sample for dating: ' sample 1; '' sample 2

Table 5.6S. U-series ages, isotope concentrations and ratios from *L. pertusa* fragments from gravity core Geob20531-1

Core depth (cm)	Lab ID	^{232}Th (ppb)	± (abs.)	$\delta^{234}U_m$* (‰)	± (abs.)	$\delta\ ^{234}U_i$* (‰)	± (abs.)	Age (ka BP)	± (abs.)	Age^{cor} (ka BP)	± (abs.)	AR** (cm kyr^{-1})
6	IUP-8168	0.2959	0.0006	145.4	0.5	147.5	0.5	5.046	0.019	5.024	0.022	
20	IUP-8169	0.1036	0.0004	146.9	0.5	149.2	0.5	5.586	0.020	5.579	0.020	25
75	IUP-8170	1.4375	0.0027	148.1	0.9	150.7	0.9	6.110	0.022	6.015	0.053	
98	IUP-8171	0.6229	0.0009	145.9	0.5	148.4	0.5	6.012	0.017	5.970	0.028	199
139.5	IUP-8172	0.2344	0.0009	145.5	0.8	148.3	0.8	6.690	0.078	6.671	0.079	59
201	IUP-8173	0.0828	0.0003	142.7	0.5	145.5	0.5	6.776	0.023	6.770	0.024	621
250	IUP-8174	0.4998	0.0015	142.4	0.7	145.3	0.7	7.055	0.032	7.023	0.036	194
311	IUP-8175	0.5084	0.0013	143.6	1.1	146.6	1.1	7.352	0.025	7.310	0.033	213
371.5	IUP-8176	0.8498	0.0022	144.0	0.6	147.1	0.6	7.496	0.028	7.433	0.043	492
435	IUP-8177	0.0566	0.0004	144.5	1.2	147.8	1.2	7.928	0.034	7.924	0.033	129
501	IUP-8178	0.3578	0.0007	143.7	0.5	147.2	0.5	8.593	0.024	8.571	0.028	102
545	IUP-8179	0.1294	0.0004	143.3	0.5	146.9	0.5	8.652	0.028	8.645	0.030	595
589	IUP-8180	2.5156	0.0080	143.9	0.6	147.5	0.6	9.006	0.034	8.833	0.094	234
635	IUP-8181	0.4137	0.0011	143.2	0.5	147.1	0.5	9.356	0.033	9.328	0.035	93
674.5	IUP-8182	0.3358	0.0007	142.6	0.5	146.5	0.6	9.480	0.025	9.459	0.029	302
684.5	IUP-8183	0.1929	0.0005	142.7	0.6	146.5	0.6	9.440	0.026	9.425	0.027	
687.5	IUP-8184	0.6496	0.0013	143.7	0.7	147.5	0.7	9.405	0.034	9.350	0.044	

* Measured $^{234}U/^{238}U$ activity ratios ($\delta^{234}U_m$) are presented as deviation permil (‰) from the equilibrium value. Decay corrected $^{234}U/^{238}U$ activity ratios ($\delta^{234}U^i$) are calculated from the given ages and with $\lambda^{234}U$: 2.8263 x 10^{-6} yr-1.

** AR: Aggradation rate. AR is negligible within the uncertainties for all data except for the values at 75 cm and 589 cm core depth. See age-depth plot (Fig. 5.4S).

Age^{cor} Corrected ages, according to Frank et al. (2004) and Wefing et al., (2017). Ka BP refers to 1950.

n.d.: not determinable because lower than the analytical blank (<0.003 ng/g).

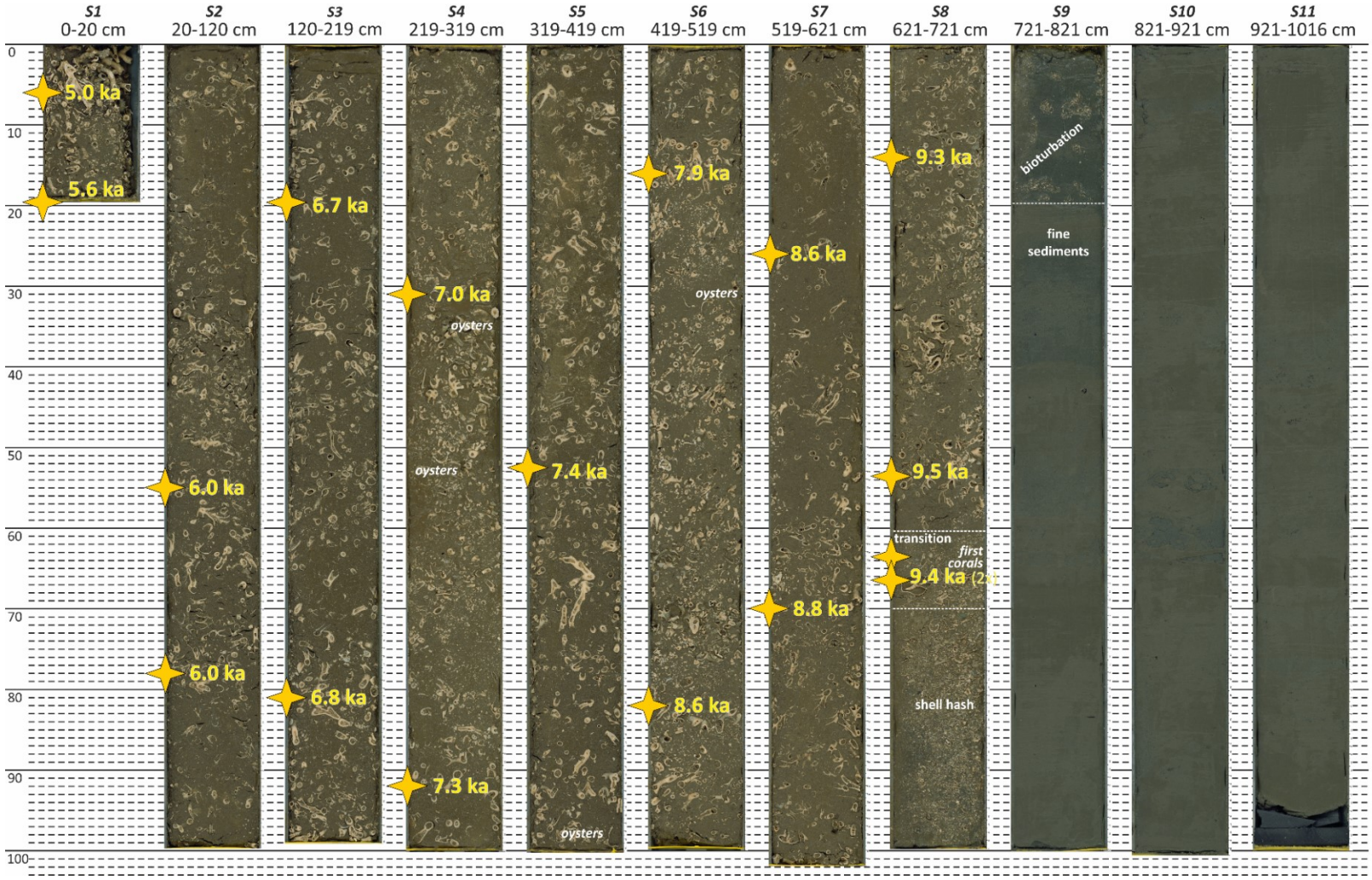

Figure 5.4S. Line scan of gravity core GeoB 20531-1 collected from one of the small Coral Belt Mounds of the Namibian CMP (total recovery: 1021 cm; water depth: 231 m). From the core base to 741 cm core depth, the core is composed of fine hemipelagic sediments. From 741-670 cm core depth, the core is composed of bioturbated sediments (741-721 cm core depth) and shell hash within fine sediments (721-661); note: first coral fragments appear already in the upper part of the shell hash layer (671-661 cm core depth). From 661 cm to the core top, the core is entirely composed of *Lophelia* fragments embedded in fine sediments, with an occasional occurrence of oyster shells and other bioclasts. U-series datings obtained from coral fragments collected throughout the core are displayed (yellow stars).

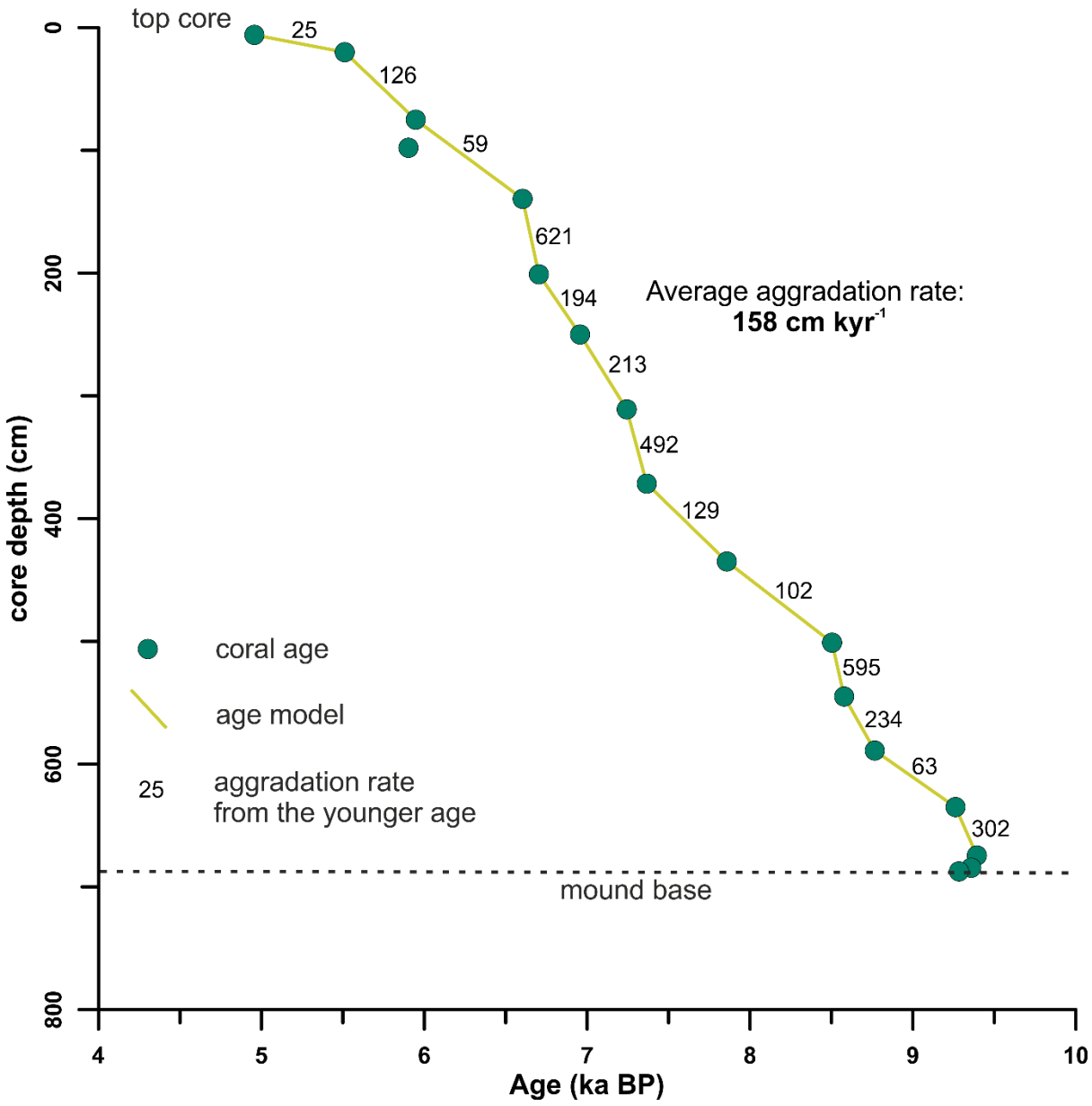

Figure 5.5S. Coral ages vs. core depth. Coral ages were obtained from fragments of the cold-water coral *Lophelia pertusa* collected at various core depths from core GeoB 20531-1 (see Table 6S). The core was collected from one of the small Coral Belt Mounds (Fig. 3.1S) and penetrated the mound base at ~6.51 m (see core image in Fig. 5.4S). Coral mound aggradation rates (given in cm kyr^{-1}) were calculated from age to age and are given next to the green line. The average aggradation rate is 158 cm kyr^{-1}.

6. Conclusion

6.1 Thesis objectives

The work presented here provides an overall perspective on the spatial and temporal variability of the Namibian coral mounds and the environmental conditions on the northern Namibian shelf that controlled their development. To this end, a combination of different datasets, methodologies and approaches were used to test and collected results according to the hypotheses formulated (chapter 1. Introduction):

> *Hypothesis I. Coral mounds can be found under unfavourable conditions for CWC if the main supportive control (food supply) is guaranteed.*

The results in Manuscript I show the different environmental conditions (temperature, DO, food supply, current speed and direction) affecting the CMPs in the SE Atlantic: Namibia and Angola (Cuanza CMP). Focusing on the Namibian coral mounds, bottom-water temperature and DO range between 11.8 – 13.2°C and 0-0.15 mL L^{-1}, respectively. Such oxygen-depleted conditions, combined with relatively high temperatures for CWC, likely explain the lack of living CWC nowadays. However, benthic landers also provided evidence of CWC-supporting parameters: high quantity/quality of SPOM is periodically (tidally) delivered to the coral mounds, at the same time as DO.

> *Hypothesis II. The spatial distribution and morphology of the coral mounds is indicative of the processes influencing their formation. Therefore, quantitative measurements of spatial-morphometric variables can be linked to the measurements of CWC-supporting environmental conditions.*

The environmental conditions supporting CWC off Namibia can be "recorded" by the spatial distribution and morphometric parameters of the coral mounds. The spatial distribution of the Namibian coral mounds follows three patterns at different scales: *first*- (CMP-scale), *second*- (sub-province clusters), and *third*- (mound scale) order patterns. These spatial patterns are variably matching the results from geomorphometric analysis (slope, aspect) of the underlying topography as well as the water column parameters. Consequently, the spatial distribution of the Namibian mounds seems to be controlled by the interplay of underlying topography and hydrodynamic regime, as it has been partially observed for other CMPs. The results from quantitative morphometric analyses on the Namibian coral mounds provided useful insights into their formation. Size-related parameters (footprint area, volume, height and PAX length) offered a perspective on the overall variability between the sub-provinces identified, Squid and Coral Belt Mounds. With these mounds having no buried portions, volume estimation provides a relevant measurement for the carbonate budget stored within these coral mounds. Cross-correlations with other parameters (PAR, PAX angle, average slope), highlight key steps in the development of early-stage coral mounds, like elongation, merging, and limited gain in height compared to lateral extension.

These results also show the transition from "inherited" (controlled by the underlying topography) to "developed" (controlled by the hydrodynamic regime) morphology, as observed by Wheeler *et al.* (2007).

Hypothesis III. In many CMPs, coral mound development is negatively affected by a drop in surface productivity and limited food supply. However, the consumption of DO by extremely high primary and export productivity can be also lethal for CWC, interrupting coral mound formation.

The uranium-series dating from a mound base presented in Manuscript III shows that off Namibia the CWC started to grow at 9.6 ka. The spatial analysis (Manuscript II) highlighted a relatively shallow occurrence of coral mounds on the Namibian shelf. This suggests that the initiation and formation of these coral mounds mostly benefited from the post-glacial sea-level rise drowning the continental shelves. The ages obtained from surface samples mark the extinction of the Namibian CWC in the Mid-Holocene (~5ka) and document a short and intense aggradational history. The present-day conditions (Manuscript I) points to the extremely low DO conditions off Namibia as the potential cause of the demise of the CWC. Different paleoceanographic records in this area indicate a strengthening of the BUS during the Mid-Holocene, related to insolation-induced changes in wind stress. The increased upwelling has been intensifying the local oxygen minimum zone, causing the demise of CWC off Namibia from the Mid-Holocene until today. Finally, the temporal development of the Namibian coral mounds represents a case study which allows to detect the impact of the glacial-deglacial cycle as well as orbital-induced climate changes on the initiation and cessation of coral mound development.

The three manuscripts combined are forming the core of this thesis and provide first and comprehensive overview on the spatial and temporal development of the Namibian coral mounds. From the settlement of the first CWC planulae to the demise of the CWC, we can outline in which way environmental conditions, measured nowadays and reconstructed for the past using paleoceanographic proxies, played their role on the 4D evolution of the Namibian coral mounds. Indeed, the modern environmental conditions (presented in Manuscript I) represent a key aspect for the investigations of the spatial and temporal development of the coral mounds seeing the importance of these data also for the discussion of the long-term development of the Namibian mounds presented in the Manuscripts II and III.
These studies show that the spatial and temporal development of the Namibian mounds are strongly connected to each other. The temporal development of the Namibian mounds is marked by one short-single-rapid aggradation event, which enabled a straightforward discussion of morphometric data of early stage mounds, depicting the transition from inherited towards developed mound morphologies. The distribution in rather shallow waters might explain the occurrence/preservation of only a single aggradation phase, as well as the relative small size and large number of the Namibian mounds. Information on lateral aggradation and merging of coral mounds within a relatively short period in high-

density CMP has improved the understanding on the spatio-temporal evolution of the Namibian mounds, as well as of other CMPs.

By investigating the three main themes of CWC/coral mound research (environmental conditions, spatial and temporal development), this thesis highlights how small changes on the controlling factors might have a significant impact on CWC proliferation and coral mound formation. Under rapid anthropogenic climate/ocean changes, it is important to understand these processes in order to design policies limiting the human impact on CWC-based deep-sea ecosystems.

6.2. Future research directions

Besides the results of this thesis, there are further investigations, which should be considered for understanding the spatio-temporal development of the Namibian coral mounds.

At first sight, one key process in mound formation has not been fully addressed in this thesis: sedimentary context and sediment supply off Namibia. PARASOUND and seismic profiles, combined with failed gravity cores during M122 cruise (Hebbeln *et al.*, 2017), indicated absent or only thin off-mound sediment deposits. This did not allow a direct paleoceanographic reconstruction of the Namibian coral mounds, as done in many other CMPs (e.g., Fentimen *et al.*, 2020; Fink *et al.*, 2013; Matos *et al.*, 2017). The Namibian coral mounds have no buried portion and sit directly on top of an erosive surface characterized by extremely variable features (Manuscript II). This discontinuity cut the shelf edge* clinoforms observable on the PARASOUND profile cross-cutting the Escarpment-Western Flank (Fig. 4.3). These clinoforms are likely indicative of the latest siliciclastic deposition from the extensive fluvial system carving the Etendeka Plateau-Skeleton Coast (east of the Namibian CMP), which likely took place from Late Cretaceous progradational phase of the shelf (sagging of the passive SW African margin) until the late Miocene (Light *et al.*, 1993). From the late Miocene, the initiation of the BUS and the atmospheric processes behind it (Berger and Wefer, 2002; Diester-Haass *et al.*, 2002; Hoetzel *et al.*, 2017; Rommerskirchen *et al.*, 2011; Siesser, 1980) caused the aridification/desertification along the Namibian coast (Bakker, 1975; Kaseke *et al.*, 2016; M Van Zinderen Bakker and Mercer, 1986; Rogers and Bremner, 1991). Under these climatic conditions, the rivers on the Skeleton Coast turned out to have only ephemeral activity (Krapf *et al.*, 2005). Therefore, the primary source of sediments on the Namibian shelf is provided by the ultra-long littoral transport by the Benguela current of the sediments from the Orange river (Garzanti *et al.*, 2014). This transport is also responsible for most of the sand accumulation forming the coastal dunes of the Namib Desert and Skeleton Coast, which might in turn be a potential secondary sediment source by the action of trade winds and/or bergwinds (Krapf *et al.*, 2005; Shannon and Nelson, 1996b). However, the sediment supplied by the Benguela current and the winds on the northern Namibian shelf, represents a small portion (lithogenic fraction) of the suspended sediment that can be collected by modern sediment traps (Vorrath *et al.*, 2018). This likely suggests that the Namibian mounds "absorbed" most of the suspended sediments supplied by the hydrodynamic regime, a pattern that also has been described for the early phase of the giant Irish coral mounds (Titschack et al., 2009).

*considering the top of the Escarpment as the inner shelf break of the Namibian shelf

The reconstruction of the sediment source on the Namibian mounds might highlight a further control of the BUS on their formation. Additionally, understanding the morphosedimentary history of the northern Namibian shelf might indicate how the BUS controlled depositional-erosional processes as well as benthic communities over geological timescales and/or glacial-interglacial cycles.

The material from on-mound sediment cores might also offer further information on the specific environmental conditions during the development of the Namibian coral mounds. The BUS-supported eutrophic conditions, as well as the related OMZ, might have severely affected the metabolism of the CWC, and therefore the shape and composition of their corallites. In this case, undergoing studies on the morphological plasticity of CWC and DO-related geochemical proxies likely will enable a better understanding on how the Namibian CWC cope with the conditions dictated by the BUS. Morphological plasticity and reconstruction of DO might be discussed with similar information from other CMPs, highlighting a potential survival adaptability of *Lophelia pertusa*.

Besides the results obtained from the Namibian CMP, this thesis highlights the potential of quantitative morphometric analyses as tool to investigate the spatial development of coral mounds. In the literature, morphology and dimensions of coral mounds have been treated mostly as descriptive features, mentioning ranges of sizes and or indication of the shape of the mound base (round, elongated, V-shaped, etc.). Some morphometric parameters such as mound height and length are commonly described for coral mounds (e.g., Angeletti *et al.*, 2020; Carranza *et al.*, 2012; Colman *et al.*, 2005; De Mol *et al.*, 2002; Hebbeln *et al.*, 2014). However, only few studies used such analytical information to classify coral mounds (e.g., Lim *et al.*, 2018; Lo Iacono *et al.*, 2014; Mortensen *et al.*, 2001; Vandorpe *et al.*, 2017). Two studies (Correa *et al.*, 2012b; Hebbeln *et al.*, 2019) tried to correlate morphometric data with environmental conditions. The morphometric dataset of Correa et al. (2012) does not show any correlation between bottom current and mound morphometrics, likely because these "coral mounds" are composed by CWC colonies growing on top of mass wasting boulders and blocks (see also Hebbeln *et al.*, 2012). The results from Hebbeln *et al.* (2019) highlight how environmental conditions played a key role in the distribution of the coral mounds, using few shape indicators compared to the method of Correa *et al.* (2012b). Knowing that the entire structure of the Namibian coral mounds is composed by CWC frameworks and baffled sediments (GeoB 20531-1, Appendix Manuscript III) led us to apply the methodology of Correa et al. (2012) to provide a morphometric dataset to be discussed with the environmental conditions measured during M122. As highlighted in Manuscript II, the positive correlation of these two datasets, combined with other geomorphometric and spatial information (slope, aspect, heatmaps), revealed that a quantitative morphometric analysis is a powerful tool for the investigation of the development of coral mounds. The application of this methodology to other CMPs would provide a tool to standardize spatial-morphometric investigations on coral mounds. This will likely allow the comparison among coral mounds, which are morphologically, dimensionally and spatially different, as well as enable the evaluation of the controls on their morphology and their formation, as done with the Namibian sub-provinces.

Most of the knowledge on CWC and coral mounds came from the results on the CMPs in the NE Atlantic. This makes the results obtained on the Namibian coral mounds extremely valuable to understand how the CWC ecosystems flourish, develop and demise under conditions not encountered elsewhere, although other relevant CMPs developed under similar high export productivity and low DO conditions (e.g., Mauritania, Angola; Colman *et al.*, 2005; Hanz *et al.*, 2019; Hebbeln *et al.*, 2020; Wienberg *et al.*, 2018). With this perspective, exploratory data (no data were acquired on the Namibian CMP before the M122 cruise, except the MBES) acquired in a relatively short period and in a remote region were processed with the aim to obtain the best overall knowledge on the Namibian mounds. Moreover, the results obtained after analysing the such datasets will provide promising perspective on already existing similar datasets. Many MBES data from other CMPs, already acquired and processed, might turn into material for cost-efficient analyses (e.g., spatial-morphometric analyses) and provide results relevant for the CWC research, as achieved in Manuscript II.

Considering the results obtained from a fossil CMP, such a "one-stop-shop" approach might be useful to extend on coral mounds to be discovered in the future, as well as to continue investigation off Namibia. Indeed, further coral mounds NE of SQM on the way to the Angola-Cuanza CMP were detected during M122 (Hebbeln *et al.*, 2017). The discovery of the coral mounds at the mouth of Kunene river (Rush *et al.*, 2019) and the living CWC colonies on top/flanks on the Angolan mounds (Hanz *et al.*, 2019; Le Guilloux *et al.*, 2009) suggest that further exploration would expand the spatial range of the Namibian CMP, likely showing a latitudinal gradient in "vitality" of CWC colonies along the SW African margin. This might also reveal a discontinuous system of CMPs like it has been observed along the Moroccan, Irish and Norwegian margins. Consequently, the potential of the SE Atlantic for new discoveries appears to be large, suggesting that this thesis at some time in the future will be considered as the "first-stop-shop".

Aknowledgements

First and foremost I would like to thank my supervisor, Dierk Hebbeln, initially for granting me this position, but also for his challenging supervision and advices, as well as his endless support in every stage of my PhD. Scientific freedom, which Dierk endorsed, helped me growing as a researcher, culminating with my participation with different activities during my PhD project. I could not undertaken this amazing journey without his rare example of scientific critcicism, experience and wisdom. My external supervisor, is also gratefully acknowledged for reviewing this thesis.

I am immensely grateful to Claudia Wienberg for her guidance, discussion, inspiration, confrontation, music before the 90's and tips for traveling in France. This thesis would have not become what it is without her unconditioned support. Jürgen Titschack is also deeply aknowledged for being always available (although his full agenda and especially when I did not expect) with exhaustive answers of my basic questions and for his (well-recognised) criticism, which helped me to build new perspectives to see my scientific work (and not only).

I have been glad to be part of the big AG Hebbeln family, where everybody has been able to teach or explain me something through talks, zoom meetings, paper-cakes and questionable-quality espresso. In this "deep-sea ecosystem", I want to thank Dharma and Haozhuang for being great officemates and making together such "biodiverse hotspot" that was our office. I am sure I will miss it a lot. I thank also my latest officemate, Cova, who got me involved in her projects and shared with me her ecology experience. I am very grateful to Chelsea for the last-minute proofreading of this thesis.

I thank also Furu Mienis and Ulrike Hanz for the acquisition, processing and sharing lander data, which became fundamental for the work of this thesis. Thanks should also go to Wolf-Christian Dullo for the CTD measurements.

The *Maestro* Paul Wintersteller is also thanked for introducing me to the hydroacoustic world in his *bottega*, beside the technical advices and assistance. Stefanie Gaide, Christian dos Santos, Debora Duarte are thanked also for helping me to solve hydroacoustic problems.

Furthermore, I would like to thank all the people of the Comparative Sedimentology Lab of the University of Miami, especially Prof. Gregor Eberli who hosted me and gave me the possibility to live a scientific and personal experience in Miami that I'll never forget. I will thank also Prof. Sam Purkis who has been very kind with his expertise to support my research. A special thank goes to the Kim Galvez and Sarah Bashah: without your company, my research stay would have been so great.

As a seafarer, I have to thank the work of several crews who supported this thesis (or actually saw me working on it while I was onboard). However, firstly, I own a deep gratitude to all of M122 ANNA cruise participants, whose work was the fundamental for this PhD thesis. I wish your effort has been well highlighted through the pages of this thesis. I had to work on the reviews of Manuscript III when I was

on *RV Meteor M151*, with Norbert Frank and Andrea Schröder-Ritzau, who gave relevant support to complete that article. Manuscript II was partially prepared after shifts on the *MV Roman Rebel*. *Go raibh maith agat* to the lads and colleagues from Green Rebel! Some parts of this thesis were written where I dreamed to be starting this PhD project (and actually also being relatively close to the Namibian mounds): in the core lab of the *DV JOIDES Resolution* in the middle of South Atlantic. I am deeply grateful to all the people who supported me to make possible my participation on IODP Exp. 390, as well as, its scientific and technical crew for the great experience together!

This thesis is dedicated to my parents Maria and Giuseppe, and my grandmother Anna Maria, who guided me through the maze of life and supported me to achieve my goals and my dreams, besides being my "hydrodynamic regime". A special thanks goes also to my siblings Anna, Vito and Valentina who gave always the motivation to be their inspiring big brother, although I apparently failed since you became all engineers.

I guess my Noistadt crew deserves also particular thanks here: Federica, Mattia and Francesco (il Pennuto). You have no idea how great was your company to me and how I am happy to have had such friends in Bremen and in my life. Any crew has a capitain, but this one has a "chief scientist". To me, you are the best friend, soul mate, barista that I could ever have in this adventure and I have no words to thank you my dear Walter, vecchia roccia.

MARUM has been longly my port where I had the chance to cross lives of many other seafarers, who shared with me a piece of their trip (and vice versa). I am grateful for what you gave me during the last years, ahoy mates!

References

Addamo, A.M., Vertino, A., Stolarski, J., García-Jiménez, R., Taviani, M. and Machordom, A. (2016) Merging scleractinian genera: the overwhelming genetic similarity between solitary *Desmophyllum* and colonial *Lophelia*. *BMC Evolutionary Biology*, **16,** 108.

Adkins, J.F., Cheng, H., Boyle, E.A., Druffel, E.R.M. and Edwards, R.L. (1998) Deep-sea coral evidence for rapid change in ventilation of the deep North Atlantic 15,400 years ago. *Science*, **280,** 725-728.

Aloisi, G., Pierre, C., Rouchy, J.-M., Foucher, J.-P. and Woodside, J. (2000) Methane-related authigenic carbonates of eastern Mediterranean Sea mud volcanoes and their possible relation to gas hydrate destabilisation. *Earth and Planetary Science Letters*, **184,** 321-338.

Anagnostou, E., Sherrell, R.M., Gagnon, A., LaVigne, M., Field, M.P. and McDonough, W.F. (2011) Seawater nutrient and carbonate ion concentrations recorded as P/Ca, Ba/Ca, and U/Ca in the deep-sea coral Desmophyllum dianthus. *Geochimica et Cosmochimica Acta*, **75,** 2529-2543.

Andrews, A.H., Cailliet, G.M., Kerr, L.A., Coale, K.H., Lundstrom, C. and DeVogelaere, A.P. (2005) Investigations of age and growth for three deep-sea corals from the Davidson Seamount off central California. In: *Cold-Water Corals and Ecosystems* (Eds A. Freiwald and J.M. Roberts), pp. 1021-1038. Springer Berlin Heidelberg, Berlin, Heidelberg.

Angeletti, L., Bettuzzi, M. and Morigi, M.P. (2019) 12 Tomography of Cold-Water Corals-Bearing Cores. In: *Mediterranean Cold-Water Corals: Past, Present and Future: Understanding the Deep-Sea Realms of Coral* (Eds C. Orejas and C. Jiménez), pp. 109-113. Springer International Publishing, Cham.

Angeletti, L., Castellan, G., Montagna, P., Remia, A. and Taviani, M. (2020) The "Corsica Channel Cold-Water Coral Province" (Mediterranean Sea). *Frontiers in Marine Science*, **7**.

Anselmetti, F.S., Eberli, G.P. and Ding, Z.-D. (2000) From the Great Bahama Bank into the Straits of Florida: A margin architecture controlled by sea-level fluctuations and ocean currents. *GSA Bulletin*, **112,** 829-844.

Arnold, J.R. and Libby, W.F. (1949) Age determinations by radiocarbon content: checks with samples of known age. *Science*, **110,** 678-680.

Baco, A.R., Morgan, N., Roark, E.B., Silva, M., Shamberger, K.E.F. and Miller, K. (2017) Defying dissolution: Discovery of deep-sea scleractinian coral reefs in the North Pacific. *Scientific Reports*, **7,** 5436.

Bahr, A., Doubrawa, M., Titschack, J., Austermann, G., Koutsodendris, A., Nürnberg, D., Albuquerque, A.L., Friedrich, O. and Raddatz, J. (2020) Monsoonal forcing of cold-water coral growth off southeastern Brazil during the past 160 kyr. *Biogeosciences*, **17,** 5883-5908.

Bahr, A., Spadano Albuquerque, A., Ardenghi, N., Batenburg, S., Bayer, M., Catunda, M., Conforti, A., Dias, B., Dias Ramos, R. and Egger, L. (2016) South American hydrological balance and paleoceanography during the Late Pleistocene and Holocene (SAMBA)–cruise no. M125, march 21–April 15, 2016-Rio de Janeiro (Brazil)–Fortaleza (Brazil).

Bakker, E.M.v.Z. (1975) The origin and palaeoenvironment of the Namib Desert biome. *Journal of Biogeography*, **2,** 65-73.

Bargain, A., Marchese, F., Savini, A., Taviani, M. and Fabri, M.-C. (2017) Santa Maria di Leuca Province (Mediterranean Sea): Identification of suitable mounds for cold-water coral settlement using geomorphometric proxies and Maxent methods. *Frontiers in Marine Science*, **4**.

Barnes, J.W., Lang, E.J. and Potratz, H.A. (1956) Ratio of ionium to uranium in coral limestone. *Science*, **124,** 175-176.

Barton, C. (2002) Marie Tharp, oceanographic cartographer, and her contributions to the revolution in the Earth sciences. *Geological Society, London, Special Publications*, **192,** 215-228.

Baussant, T., Nilsen, M., Ravagnan, E., Westerlund, S. and Ramanand, S. (2017) Physiological responses and lipid storage of the coral *Lophelia pertusa* at varying food density. *Journal of Toxicology and Environmental Health, Part A*, **80,** 266-284.

Berger, W.H. and Wefer, G. (2002) On the reconstruction of upwelling history: Namibia upwelling in context. *Marine Geology*, **180,** 3-28.

Bernecker, M. and Weidlich, O. (1990) The Danian (Paleocene) coral limestone of Fakse, Denmark: A model for ancient aphotic, azooxanthellate coral mounds. *Facies*, **22,** 103.

Bernecker, M. and Weidlich, O. (2005) Azooxanthellate corals in the Late Maastrichtian - Early Paleocene of the Danish basin: bryozoan and coral mounds in a boreal shelf setting. In: *Cold-Water Corals and Ecosystems* (Eds A. Freiwald and J.M. Roberts), pp. 3-25. Springer Berlin Heidelberg, Berlin, Heidelberg.

Beyer, A., Schenke, H.W., Klenke, M. and Niederjasper, F. (2003) High resolution bathymetry of the eastern slope of the Porcupine Seabight. *Marine Geology*, **198,** 27-54.

Bøe, R., Bellec, V.K., Dolan, M.F.J., Buhl-Mortensen, P., Rise, L. and Buhl-Mortensen, L. (2016) Cold-water coral reefs in the Hola glacial trough off Vesterålen, North Norway. *Geological Society, London, Memoirs*, **46,** 309-310.

Boetius, A., Ravenschlag, K., Schubert, C.J., Rickert, D., Widdel, F., Gieseke, A., Amann, R., Jørgensen, B.B., Witte, U. and Pfannkuche, O. (2000) A marine microbial consortium apparently mediating anaerobic oxidation of methane. *Nature*, **407,** 623-626.

Boolukos, C.M., Lim, A., O'Riordan, R.M. and Wheeler, A.J. (2019) Cold-water corals in decline – A temporal (4 year) species abundance and biodiversity appraisal of complete photomosaiced cold-water coral reef on the Irish Margin. *Deep Sea Research Part I: Oceanographic Research Papers*, **146,** 44-54.

Boutton, T.W. (1991) *Stable carbon isotope ratios of natural materials: 2 Atmospheric, terrestrial, marine, and freshwater environments*. Academic Press, Inc, United States.

Boyer, T.P., antonov, j.I., Baranova, O.K., coleman, C., Garcia, H.E., Grodsky, A., HJohnson, D.R., Locarnini, R.A., Mishonov, A.V., O'Brien, T.D., Paver, C.R., Reagan, J.R., Seidov, D., Smolyar, I.V. and Zweng, M.M. (2013) *World Ocean Database 2013.*, Silver Spring, MD, NOAA Printing Office.

Bradley, W.H., Cushman, J.A. and Henbest, L.G. (1940) *Geology and biology of North Atlantic deep-sea cores between Newfoundland and Ireland: Summary of the report. Foreword*. US Government Printing Office.

Breitburg, D., Levin, L.A., Oschlies, A., Grégoire, M., Chavez, F.P., Conley, D.J., Garçon, V., Gilbert, D., Gutiérrez, D., Isensee, K., Jacinto, G.S., Limburg, K.E., Montes, I., Naqvi, S.W.A., Pitcher, G.C., Rabalais, N.N., Roman, M.R., Rose, K.A., Seibel, B.A., Telszewski, M., Yasuhara, M. and Zhang, J. (2018) Declining oxygen in the global ocean and coastal waters. *Science*, **359,** eaam7240.

Broch, H. (1922) *Riffkorallen im Nordmeer einst und jetzt. Naturwissenschaften*, **10,** 804-806.

Broecker, W.S. and Thurber, D.L. (1965) Uranium-series dating of corals and oolites from Bahaman and Florida Key limestones. *Science*, **149,** 58-60.

Broecker, W.S., Thurber, D.L., Goddard, J., Ku, T.-L., Matthews, R. and Mesolella, K.J. (1968) Milankovitch hypothesis supported by precise dating of coral reefs and deep-sea sediments. *Science*, **159,** 297-300.

Brooke, S. and Ross, S.W. (2014) First observations of the cold-water coral *Lophelia pertusa* in mid-Atlantic canyons of the USA. *Deep Sea Research Part II*, **104,** 245-251.

Brooke, S. and Schroeder, W.W. (2007) State of deep coral ecosystems in the Gulf of Mexico region: Texas to the Florida Straits. *The state of deep coral ecosystems of the United States*, 271-306.

Brooke, S. and Young, C.M. (2009) In situ measurement of survival and growth of *Lophelia pertusa* in the northern Gulf of Mexico. *Marine Ecology Progress Series*, **397,** 153-161.

Brown, N.L. and Morrison, G.K. (1978) W.H.O.I./Brown conductivity, temperature, and depth microprofiler. Woods Hole Oceanographic Institution. .

Buhl-Mortensen, L., Serigstad, B., Buhl-Mortensen, P., Olsen, M.N., Ostrowski, M., Błażewicz-Paszkowycz, M. and Appoh, E. (2017a) First observations of the structure and megafaunal community of a large *Lophelia* reef on the Ghanaian shelf (the Gulf of Guinea). *Deep Sea Research Part II: Topical Studies in Oceanography*, **137,** 148-156.

Buhl-Mortensen, L., Vanreusel, A., Gooday, A.J., Levin, L.A., Priede, I.G., Buhl-Mortensen, P., Gheerardyn, H., King, N.J. and Raes, M. (2010) Biological structures as a source of habitat heterogeneity and biodiversity on the deep ocean margins. *Marine Ecology*, **31,** 21-50.

Buhl-Mortensen, P., Buhl-Mortensen, L. and Purser, A. (2017b) Trophic ecology and habitat provision in cold-water coral ecosystems. In: *Marine Animal Forests: The Ecology of Benthic Biodiversity Hotspots* (Eds S. Rossi, L. Bramanti, A. Gori and C. Orejas), pp. 919-944. Springer International Publishing, Cham.

Burke, A., Robinson, L.F., McNichol, A.P., Jenkins, W.J., Scanlon, K.M. and Gerlach, D.S. (2010) Reconnaissance dating: A new radiocarbon method applied to assessing the temporal distribution of Southern Ocean deep-sea corals. *Deep Sea Research Part I: Oceanographic Research Papers*, **57,** 1510-1520.

Burke, R.G. and Robson, J. (1975) An evaulation of the BO'SUN multi-beam sonar system. *International Hydrographic Review*, **52**.

Büscher, J.V., Form, A.U. and Riebesell, U. (2017) Interactive effects of ocean acidification and warming on growth, fitness and survival of the cold-water coral *Lophelia pertusa* under different food availabilities. *Frontiers in Marine Science*, **4**.

Cairns, S.D. (1979) The deep-water Scleractinia of the Caribbean Sea and adjacent waters. *Studies on the Fauna of Curaçao and other Caribbean Islands*.

Cairns, S.D. (1996) The marine fauna of New Zealand: Scleractinia (Cnidaria: Anthozoa). *Oceanographic Literature Review*, **3,** 293.

Cairns, S.D. (2001a) A brief history of taxonomic research on azooxanthellate Scleractinia (Cnidaria: Anthozoa). *Bulletin of the Biological Society of Washington*, **10,** 191-203.

Cairns, S.D. (2001b) A generic revision and phylogenetic analysis of the Dendrophylliidae (Cnidaria: Scleractinia). *Smithsonian Contributions to Zoology*.

Cairns, S.D. (2007) Deep-water corals: an overview with special reference to diversity and distribution of deep-water scleractinian corals. *Bulletin of Marine Science*, **81,** 311-322.

Caress, D.W. and Chayes, D. (1995) New software for processing sidescan data from sidescan-capable multibeam sonars. *Challenges for Our Global Environment: Conference Proceedings, Oceans '95 MTS/IEEE*, 997-10000.

Carpine-Lancre, J., Fisher, R., Harper, B., Hunter, P., Jones, M., Kerr, A., Laughton, A., Ritchie, S., Scott, D. and Whitmarsh, M. (2003) The history of GEBCO 1903-2003: the 100-year story of the General Bathymetric Chart of the Oceans.

Carr, M.-E. (2001) Estimation of potential productivity in Eastern Boundary Currents using remote sensing. *Deep Sea Research Part II: Topical Studies in Oceanography*, **49,** 59-80.

Carr, M.-E. and Kearns, E.J. (2003) Production regimes in four Eastern Boundary Current systems. *Deep Sea Research Part II: Topical Studies in Oceanography*, **50,** 3199-3221.

Carranza, A., Recio, A.M., Kitahara, M., Scarabino, F., Ortega, L., López, G., Franco-Fraguas, P., De Mello, C., Acosta, J. and Fontan, A. (2012) Deep-water coral reefs from the Uruguayan outer shelf and slope. *Marine Biodiversity*, **42,** 411-414.

Carreiro-Silva, M., Cerqueira, T., Godinho, A., Caetano, M., Santos, R.S. and Bettencourt, R. (2014) Molecular mechanisms underlying the physiological responses of the cold-water coral *Desmophyllum dianthus* to ocean acidification. *Coral Reefs*, **33,** 465-476.

Case, D.H., Robinson, L.F., Auro, M.E. and Gagnon, A.C. (2010) Environmental and biological controls on Mg and Li in deep-sea scleractinian corals. *Earth and Planetary Science Letters*, **300,** 215-225.

Cathalot, C., Van Oevelen, D., Cox, T.J.S., Kutti, T., Lavaleye, M., Duineveld, G. and Meysman, F.J.R. (2015) Cold-water coral reefs and adjacent sponge grounds: hotspots of benthic respiration and organic carbon cycling in the deep sea. *Frontiers in Marine Science*, **2**.

Chapman, P. and Shannon, L.V. (1987) Seasonality in the oxygen minimum layers at the extremities of the Benguela system. *South African Journal of Marine Science*, **5,** 85-94.

Chapron, L., Peru, E., Engler, A., Ghiglione, J.F., Meistertzheim, A.L., Pruski, A.M., Purser, A., Vétion, G., Galand, P.E. and Lartaud, F. (2018) Macro- and microplastics affect cold-water corals growth, feeding and behaviour. *Scientific Reports*, **8,** 15299.

Cheng, H., Adkins, J., Edwards, R.L. and Boyle, E.A. (2000) U-Th dating of deep-sea corals. *Geochimica et Cosmochimica Acta*, **64,** 2401-2416.

Coates, A.G. and Kauffman, E.G. (1973) Stratigraphy, paleontology and paleoenvironment of a Cretaceous coral thicket, Lamy, New Mexico. *Journal of Paleontology*, **47,** 953-968.

Cohen, A.L., Gaetani, G.A., Lundälv, T., Corliss, B.H. and George, R.Y. (2006) Compositional variability in a cold-water scleractinian, *Lophelia pertusa*: New insights into "vital effects". *Geochemistry, Geophysics, Geosystems*, **7**.

Collart, T., Verreydt, W., Hernández-Molina, F.J., Llave, E., León, R., Gómez-Ballesteros, M., Pons-Branchu, E., Stewart, H. and Van Rooij, D. (2018) Sedimentary processes and cold-water coral mini-mounds at the Ferrol canyon head, NW Iberian margin. *Progress in Oceanography*, **169,** 48-65.

Colman, J.G., Gordaon, D.M., Lane, A.P., Forde, M.J. and Fitzpatrick, J. (2005) Carbonate mounds off Mauretania, Northwest Africa: status of deep-water corals and implications for management of fishing and oil exploration activities. In: *Cold-water Corals and Ecosystems* (Eds A. Freiwald and J.M. Roberts), pp. 417-441. Springer, Berlin-Heidelberg.

Coma, R. (2002) Seasonality of in situ respiration rate in three temperate benthic suspension feeders. *Limnology and Oceanography*, **47,** 324-331.

Comas, M., Pinheiro, L., Ivanov, M. and TTR-17 Leg 1 Scientific Party (2009) Deep-water coral mounds in the Alboran Sea: the Melilla mound field revisited. In: *Geo-Marine Research on the Mediterranean and European-Atlantic Margins. International Conference and TTR-17 Post-Cruise Meeting of the Training-through-Research Programme. Granada, Spain, 2–5 February 2009. IOC Workshop Report No. 220 (English)*, pp. 8-9. UNESCO.

Copard, K., Colin, C., Henderson, G.M., Scholten, J., Douville, E., Sicre, M.A. and Frank, N. (2012) Late Holocene intermediate water variability in the northeastern Atlantic as recorded by deep-sea corals. *Earth and Planetary Science Letters*, **313-314,** 34-44.

Corbera, G., Lo Iacono, C., Gràcia, E., Grinyó, J., Pierdomenico, M., Huvenne, V.A.I., Aguilar, R. and Gili, J.M. (2019) Ecological characterisation of a Mediterranean cold-water coral reef: Cabliers Coral Mound Province (Alboran Sea, western Mediterranean). *Progress in Oceanography*, **175,** 245-262.

Corbera, G., Lo Iacono, C., Standish, C.D., Anagnostou, E., Titschack, J., Katsamenis, O., Cacho, I., Van Rooij, D., Huvenne, V.A.I. and Foster, G.L. (2021) Glacio-eustatic variations and sapropel events as main controls on the Middle Pleistocene-Holocene evolution of the Cabliers Coral Mound Province (W Mediterranean). *Quaternary Science Reviews*, **253,** 106783.

Cordes, E.E., McGinley, M.P., Podowski, E.L., Becker, E.L., Lessard-Pilon, S., Viada, S.T. and Fisher, C.R. (2008) Coral communities of the deep Gulf of Mexico. *Deep Sea Research Part I: Oceanographic Research Papers*, **55,** 777-787.

Correa, T.B.S., Eberli, G.P., Grasmueck, M., Reed, J.K. and Correa, A.M.S. (2012a) Genesis and morphology of cold-water coral ridges in a unidirectional current regime. *Marine Geology*, **326–328,** 14-27.

Correa, T.B.S., Grasmueck, M., Eberli, G.P., Reed, J.K., Verwer, K. and Purkis, S.A.M. (2012b) Variability of cold-water coral mounds in a high sediment input and tidal current regime, Straits of Florida. *Sedimentology*, **59,** 1278-1304.

Costello, M.J., McCrea, M., Freiwald, A., Lundälv, T., Jonsson, L., Bett, B.J., van Weering, T.C.E., de Haas, H., Roberts, J.M. and Allen, D. (2005) Role of cold-water *Lophelia pertusa* coral reefs as fish habitat in the NE Atlantic. In: *Cold-Water Corals and Ecosystems* (Eds A. Freiwald and J.M. Roberts), pp. 771-805. Springer, Berlin-Heidelberg.

Cyr, F., van Haren, H., Mienis, F., Duineveld, G. and Bourgault, D. (2016) On the influence of cold-water coral mound size on flow hydrodynamics, and vice versa. *Geophysical Research Letters*, **43,** 775-783.

Davies, A.J., Duineveld, G., Lavaleye, M., Bergman, M.J., van Haren, H. and Roberts, J.M. (2009) Downwelling and deep-water bottom currents as food supply mechanisms to the cold-water coral *Lophelia pertusa* (Scleractinia) at the Mingulay Reef Complex. *Limnology & Oceanography*, **54,** 620-629.

Davies, A.J., Duineveld, G.C., van Weering, T.C., Mienis, F., Quattrini, A.M., Seim, H.E., Bane, J.M. and Ross, S.W. (2010) Short-term environmental variability in cold-water coral habitat at Viosca Knoll, Gulf of Mexico. *Deep Sea Research Part I: Oceanographic Research Papers*, **57,** 199-212.

Davies, A.J. and Guinotte, J.M. (2011) Global habitat suitability for framework-forming cold-water corals. *Plos One*, **6,** e18483.

Davies, A.J., Wisshak, M., Orr, J.C. and Roberts, J.M. (2008) Predicting suitable habitat for the cold-water coral *Lophelia pertusa* (Scleractinia). *Deep-Sea Research I*, **55,** 1048-1062.

Davy, S.K., Allemand, D. and Weis, V.M. (2012) Cell biology of cnidarian-dinoflagellate symbiosis. *Microbiology and Molecular Biology Reviews*, **76,** 229-261.

De Clippele, L.H., Gafeira, J., Robert, K., Hennige, S., Lavaleye, M.S., Duineveld, G.C.A., Huvenne, V.A.I. and Roberts, J.M. (2017a) Using novel acoustic and visual mapping tools to predict the small-scale spatial distribution of live biogenic reef framework in cold-water coral habitats. *Coral Reefs*, **36,** 255-268.

De Clippele, L.H., Huvenne, V.A.I., Orejas, C., Lundälv, T., Fox, A., Hennige, S.J. and Roberts, J.M. (2017b) The effect of local hydrodynamics on the spatial extent and morphology of cold-water coral habitats at Tisler Reef, Norway. *Coral Reefs*, **37,** 253-266.

De Clippele, L.H., Rovelli, L., Ramiro-Sánchez, B., Kazanidis, G., Vad, J., Turner, S., Glud, R.N. and Roberts, J.M. (2021a) Mapping cold-water coral biomass: an approach to derive ecosystem functions. *Coral Reefs*, **40,** 215-231.

De Clippele, L.H., van der Kaaden, A.-S., Maier, S., de Froe, E. and Roberts, J.M. (2021b) Biomass mapping for an improved understanding of the contribution of cold-water coral carbonate mounds to C and N cycling. *Frontiers in Marine Science*, 1608.

De Haas, H., Huvenne, V., Wheeler, A., Unnithan, V. and crew, S.s. (2002) Cruise report (RV Pelagia Cruise 64PE197): A TOBI side scan sonar survey of coldwater coral carbonate mounds in the Rockall Trough and Porcupine Sea Bight-Texel-Southampton-Galway, 21 June–14 July 2002. *R Netherl Sea Res (NIOZ), Texel, The Netherlands*.

De Haas, H., Mienis, F., Frank, N., Richter, T.O., Steinbacher, R., de Stigter, H., van der Land, C. and van Weering, T.C.E. (2009) Morphology and sedimentology of (clustered) cold-water coral mounds at the south Rockall Trough margins, NE Atlantic Ocean. *Facies*, **55,** 1-26.

De Mol, B., Henriet, J.-P. and Canals, M. (2005) Development of coral banks in the Porcupine Seabight: do they have Mediterranean ancestors? In: *Cold-Water Corals and Ecosystems* (Eds A. Freiwald and J.M. Roberts), pp. 515-533. Springer, Berlin-Heidelberg.

De Mol, B., Van Rensbergen, P., Pillen, S., Van Herreweghe, K., Van Rooij, D., McDonnell, A., Huvenne, V., Ivanov, M., Swennen, R. and Henriet, J.-P. (2002) Large deep-water coral banks in the Porcupine Basin, southwest of Ireland. *Marine Geology*, **188,** 193-231.

De Mol, L., Van Rooij, D., Pirlet, H., Greinert, J., Frank, N., Quemmerais, F. and Henriet, J.-P. (2011) Cold-water coral habitats in the Penmarc'h and Guilvinec Canyons (Bay of Biscay): Deep-water versus shallow-water settings. *Marine Geology*, **282,** 40-52.

de Pourtalès, L.F. (1871) *Deep-sea corals*. University Press: Welch, Bigelow, & Company.

Delibrias, G. and Taviani, M. (1984) Dating the death of Mediterranean deep-sea scleractinian corals. *Marine Geology*, **62,** 175-180.

Diaz, R.J. and Rosenberg, R. (1995) Marine benthic hypoxia: a review of its ecological effects and the behavioural responses of benthic macrofauna. *Oceanogr. Marine Biol. Annu. Rev*, **33,** 245-303.

Dickson, R.R. and McCave, I.N. (1986) Nepheloid layers on the continental slope west of Porcupine Bank. *Deep Sea Research Part A. Oceanographic Research Papers*, **33,** 791-818.

Diesing, M. and Thorsnes, T. (2018) Mapping of cold-water coral carbonate mounds based on geomorphometric features: an object-based approach. *Geosciences*, **8,** 34.

Diester-Haass, L., Meyers, P.A. and Vidal, L. (2002) The late Miocene onset of high productivity in the Benguela Current upwelling system as part of a global pattern. *Marine Geology*, **180,** 87-103.

Dodds, L.A., Black, K.D., Orr, H. and Roberts, J.M. (2009) Lipid biomarkers reveal geographical differences in food supply to the cold-water coral *Lophelia pertusa* (Scleractinia). *Marine Ecology Progress Series*, **397,** 113-124.

Dodds, L.A., Roberts, J.M., Taylor, A.C. and Marubini, F. (2007) Metabolic tolerance of the cold-water coral *Lophelia pertusa* (Scleractinia) to temperature and dissolved oxygen change. *Journal of Experimental Marine Biology and Ecology*, **349,** 205-214.

Dolan, M.F.J., Grehan, A.J., Guinan, J.C. and Brown, C. (2008) Modelling the local distribution of cold-water corals in relation to bathymetric variables: Adding spatial context to deep-sea video data. *Deep Sea Research Part I: Oceanographic Research Papers*, **55,** 1564-1579.

Dons, C. (1944) *Norges korallrev. Det kongelige norske videnskabers selskabs forhandlinger*, **16,** 37-82.

Dorey, N., Gjelsvik, Ø., Kutti, T. and Büscher, J.V. (2020) Broad Thermal Tolerance in the Cold-Water Coral Lophelia pertusa From Arctic and Boreal Reefs. *Frontiers in Physiology*, **10**.

Dorschel, B., Hebbeln, D., Foubert, A., White, M. and Wheeler, A.J. (2007a) Hydrodynamics and cold-water coral facies distribution related to recent sedimentary processes at Galway Mound west of Ireland. *Marine Geology*, **244,** 184-195.

Dorschel, B., Hebbeln, D., Rüggeberg, A. and Dullo, C. (2007b) Carbonate budget of a cold-water coral carbonate mound: Propeller Mound, Porcupine Seabight. *International Journal of Earth Sciences*, **96,** 73-83.

Dorschel, B., Hebbeln, D., Rüggeberg, A. and Dullo, W.-C. (2005) Growth and erosion of a cold-water coral covered carbonate mound in the Northeast Atlantic during the Late Pleistocene and Holocene. *Earth and Planetary Science Letters*, **233,** 33-44.

Douarin, M., Elliot, M., Noble, S.R., Sinclair, D., Henry, L.-A., Long, D., Moreton, S.G. and Murray Roberts, J. (2013) Growth of north-east Atlantic cold-water coral reefs and mounds during the Holocene: A high resolution U-series and ^{14}C chronology. *Earth and Planetary Science Letters*, **375,** 176-187.

Druffel, E.R.M., King, L.L., Belastock, R.A. and Buesseler, K.O. (1990) Growth rate of a deep-sea coral using 210Pb and other isotopes. *Geochimica et Cosmochimica Acta*, **54,** 1493-1499.

Dubois-Dauphin, Q., Bonneau, L., Colin, C., Montero-Serrano, J.-C., Montagna, P., Blamart, D., Hebbeln, D., Van Rooij, D., Pons-Branchu, E., Hemsing, F., Wefing, A.-M. and Frank, N. (2016) South Atlantic intermediate water advances into the North-east Atlantic with reduced Atlantic meridional overturning circulation during the last glacial period. *Geochemistry, Geophysics, Geosystems*, **17,** 2336-2353.

Duineveld, G., Lavaleye, M., Berghuis, E. and de Wilde, P. (2001) Activity and composition of the benthic fauna in the Whittard Canyon and the adjacent continental slope (NE Atlantic). *Oceanologica Acta*, **24,** 69-83.

Duineveld, G., Lavaleye, M., Bergman, M., De Stigter, H. and Mienis, F. (2007) Trophic structure of a cold-water coral mound community (Rockall Bank, NE Atlantic) in relation to the near-bottom particle supply and current regime. *Bulletin of Marine Science*, **81,** 449-467.

Duineveld, G., Lavleye, M. and Berghuis, E. (2004) Particle flux and food supply to a seamount cold-water coral community (Galicia Bank, NW Spain). *Marine Ecology Progress Series*, **277,** 13-23.

Duineveld, G.C.A., Jeffreys, R.M., Lavaleye, M.S.S., Davies, A.J., Bergman, M.J.N., Watmough, T. and Witbaard, R. (2012) Spatial and tidal variation in food supply to shallow cold-water coral reefs of the Mingulay Reef complex (Outer Hebrides, Scotland). *Marine Ecology Progress Series*, **444,** 97-115.

Duineveld, G.C.A., Lavaleye, M.S.S., Berghuis, E.M., de Wilde, P.A.W.J., van der Weele, J., Kok, A., Batten, S.D. and de Leeuw, J.W. (1997) Patterns of benthic fauna and benthic respiration on the celtic continental margin in relation to the distribution of phytodetritus. *Internationale Revue der gesamten Hydrobiologie und Hydrographie*, **82,** 395-424.

Dullo, W.-C., Flögel, S. and Rüggeberg, A. (2008) Cold-water coral growth in relation to the hydrography of the Celtic and Nordic European continental margin. *Marine Ecology Progress Series*, **371,** 165-176.

Eisele, M., Frank, N., Wienberg, C., Hebbeln, D., López Correa, M., Douville, E. and Freiwald, A. (2011) Productivity controlled cold-water coral growth periods during the last glacial off Mauritania. *Marine Geology*, **280,** 143-149.

Eisele, M., Frank, N., Wienberg, C., Titschack, J., Mienis, F., Beuck, L., Tisnerat-Laborde, N. and Hebbeln, D. (2014) Sedimentation patterns on a cold-water coral mound off Mauritania. *Deep-Sea Research Part II*, **99,** 307-315.

Eisele, M., Hebbeln, D. and Wienberg, C. (2008) Growth history of a cold-water coral covered carbonate mound - Galway Mound, Porcupine Seabight, NE-Atlantic. *Marine Geology*, **253,** 160-169.

Emeis, K.-C., Struck, U., Leipe, T. and Ferdelman, T.G. (2009) Variability in upwelling intensity and nutrient regime in the coastal upwelling system offshore Namibia: results from sediment archives. *International Journal of Earth Sciences*, **98,** 309-326.

Emery, K.O. and Dietz, R.S. (1941) Gravity coring instrument and mechanics of sediment coring. *GSA Bulletin*, **52,** 1685-1714.

Emiliani, C. (1955) Pleistocene temperatures. *The Journal of geology*, **63,** 538-578.

Emiliani, C., Hudson, J.H., Shinn, E.A. and George, R.Y. (1978) Oxygen and carbon isotopic growth record in a reef coral from the Florida Keys and a deep-sea coral from Blake Plateau. *Science*, **202,** 627-629.

Epstein, S., Buchsbaum, R., Lowenstam, H.A. and Urey, H.C. (1953) Revised carbonate-water isotopic temperature scale. *Geological Society of America Bulletin*, **64,** 1315-1326.

Farfan, G.A., Cordes, E.E., Waller, R.G., DeCarlo, T.M. and Hansel, C.M. (2018) Mineralogy of deep-sea coral aragonites as a function of aragonite saturation state. *Frontiers in Marine Science*, **5**.

Farmer, E.C., deMenocal, P.B. and Marchitto, T.M. (2005) Holocene and deglacial ocean temperature variability in the Benguela upwelling region: Implications for low-latitude atmospheric circulation. *Paleoceanography*, **20**.

Farr, H.K. (1980) Multibeam bathymetric sonar: Sea beam and hydro chart. *Marine Geodesy*, **4,** 77-93.

Feenstra, E.J., Birgel, D., Heindel, K., Wehrmann, L.M., Jaramillo-Vogel, D., Grobéty, B., Frank, N., Hancock, L.G., Van Rooij, D., Peckmann, J. and Foubert, A. (2020) Constraining the formation of authigenic carbonates in a seepage-affected cold-water coral mound by lipid biomarkers. *Geobiology*, **18,** 185-206.

Fentimen, R., Feenstra, E., Rüggeberg, A., Hall, E., Rime, V., Vennemann, T., Hajdas, I., Rosso, A., Van Rooij, D., Adatte, T., Vogel, H., Frank, N., Krengel, T. and Foubert, A. (2020) The influence of Atlantic climate variability on the long-term development of Mediterranean cold-water coral mounds (Alboran Sea, Melilla Mound Field). *Clim. Past Discuss.*, **2020,** 1-49.

Ferdelman, T.G., Kano, A., Williams, T., Henriet, J.P. and Scientists, I.E. (2006) Proceedings of the IODP Expedition 307. Modern carbonate mounds: Porcupine drilling. *IODP Management International, Washington DC, doi:10.2204/iodp.proc.307.2006*.

Findlay, H.S., Artioli, Y., Moreno Navas, J., Hennige, S.J., Wicks, L.C., Huvenne, V.A.I., Woodward, E.M.S. and Roberts, J.M. (2013) Tidal downwelling and implications for the carbon biogeochemistry of cold-water corals in relation to future ocean acidification and warming. *Global Change Biology*, **19,** 2708-2719.

Fink, H.G., Wienberg, C., De Pol-Holz, R. and Hebbeln, D. (2015) Spatio-temporal distribution patterns of Mediterranean cold-water corals (*Lophelia pertusa* and *Madrepora oculata*) during the past 14,000 years. *Deep-Sea Research Part I*, **103,** 37-48.

Fink, H.G., Wienberg, C., De Pol-Holz, R., Wintersteller, P. and Hebbeln, D. (2013) Cold-water coral growth in the Alboran Sea related to high productivity during the Late Pleistocene and Holocene. *Marine Geology*, **339,** 71-82.

Fink, H.G., Wienberg, C., Hebbeln, D., McGregor, H.V., Schmiedl, G., Taviani, M. and Freiwald, A. (2012) Oxygen control on Holocene cold-water coral development in the eastern Mediterranean Sea. *Deep-Sea Research Part I*, **62,** 89-96.

Flögel, S., Dullo, W.C., Pfannkuche, O., Kiriakoulakis, K. and Rüggeberg, A. (2014) Geochemical and physical constraints for the occurrence of living cold-water corals. *Deep Sea Research Part II: Topical Studies in Oceanography*, **99,** 19-26.

Flot, J.-F., Dahl, M. and André, C. (2013) *Lophelia pertusa* corals from the Ionian and Barents seas share identical nuclear ITS2 and near-identical mitochondrial genome sequences. *BMC Research Notes*, **6,** 144.

Foresman, T. (1997) The history of GIS (Geographic Information Systems). Prentice Hall Series in Geographic Information Science.

Fosså, J.H., Lindberg, B., Christensen, O., Lundälv, T., Svellingen, I., Mortensen, P.B. and Alsvag, J. (2005) Mapping of *Lophelia* reefs in Norway: experiences and survey methods. In: *Cold-water Corals and Ecosystems* (Eds A. Freiwald and J.M. Roberts), pp. 359-391. Springer, Berlin-Heidelberg.

Fosså, J.H., Mortensen, P.B. and Furevik, D.M. (2002) The deep-water coral *Lophelia pertusa* in Norwegian waters: distribution and fishery impacts. *Hydrobiologia*, **471,** 1-12.

Foubert, A., Beck, T., Wheeler, A.J., Opderbecke, J., Grehan, A., Klages, M., Thiede, J., Henriet, J.-P. and the Polarstern ARK-XIX/3a Shipboard Party (2005) New View of the Belgica Mounds, Porcupine, NE Atlantic: preliminary results from the Polarstern ARK-XIX/3a ROV cruise. In: *Cold-water Corals and Ecosystems* (Eds A. Freiwald and J.M. Roberts), pp. 403-415. Springer, Berli-Heidelberg.

Foubert, A., Depreiter, D., Beck, T., Maignien, L., Pannemans, B., Frank, N., Blamart, D. and Henriet, J.-P. (2008) Carbonate mounds in a mud volcano province off north-west Morocco: Key to processes and controls. *Marine Geology*, **248,** 74-96.

Foubert, A., Huvenne, V.A.I., Wheeler, A., Kozachenko, M., Opderbecke, J. and Henriet, J.P. (2011) The Moira Mounds, small cold-water coral mounds in the Porcupine Seabight, NE Atlantic: Part B—Evaluating the impact of sediment dynamics through high-resolution ROV-borne bathymetric mapping. *Marine Geology*, **282,** 65-78.

Foubert, A., Van Rooij, D., Blamart, D. and Henriet, J.P. (2007) X-ray imagery and physical core logging as a proxy of the content of sediment cores in cold-water coral mound provinces: a case study from Porcupine Seabight, SW of Ireland. *International Journal of Earth Sciences*, **96,** 141-158.

Frank, N., Freiwald, A., López Correa, M., Wienberg, C., Eisele, M., Hebbeln, D., Van Rooij, D., Henriet, J.P., Colin, C., van Weering, T., de Haas, H., Buhl-Mortensen, P., Roberts, J.M., De Mol, B., Douville, E., Blamart, D. and Hatte, C. (2011) Northeastern Atlantic cold-water coral reefs and climate. *Geology*, **39,** 743-746.

Frank, N., Lutringer, A., Paterne, M., Blamart, D., Henriet, J.-P., van Rooij, D. and van Weering, T.C.E. (2005) Deep-water corals of the northeastern Atlantic margin: carbonate mound evolution and upper intermediate

water ventilation during the Holocene. In: *Cold-Water Corals and Ecosystems* (Eds A. Freiwald and J.M. Roberts), pp. 113-133. Springer, Berlin-Heidelberg.

Frank, N., Paterne, M., Ayliffe, L., van Weering, T.C.E., Henriet, J.-P. and Blamart, D. (2004) Eastern North Atlantic deep-sea corals: tracing upper intermediate water $D^{14}C$ during the Holocene. *Earth and Planetary Science Letters*, **219,** 297-309.

Frank, N., Ricard, E., Lutringer-Paquet, A., van der Land, C., Colin, C., Blamart, D., Foubert, A., Van Rooij, D., Henriet, J.-P., de Haas, H. and van Weering, T. (2009) The Holocene occurrence of cold water corals in the NE Atlantic: Implications for coral carbonate mound evolution. *Marine Geology*, **266,** 129-142.

Frankowiak, K., Wang, X.T., Sigman, D.M., Gothmann, A.M., Kitahara, M.V., Mazur, M., Meibom, A. and Stolarski, J. (2016) Photosymbiosis and the expansion of shallow-water corals. *Science Advances*, **2,** e1601122.

Frederiksen, R., Jensen, A. and Westerberg, H. (1992) The distribution of the scleractinian coral *Lophelia pertusa* around the Faroe islands and the relation to internal tidal mixing. *Sarsia*, **77,** 157-171.

Freiwald, A. (1998) *Geobiology of Lophelia pertusa (Scleractinia) reefs in the North Atlantic*, Universität Bremen.

Freiwald, A. (2002) Reef-forming cold-water corals. In: *Ocean Margin Systems* (Eds G. Wefer, D. Billett, D. Hebbeln, B.B. Jorgensen, M. Schlüter and T.C.E. van Weering), pp. 365-385. Springer, Berlin, Heidelberg.

Freiwald, A., Beuck, L., Rüggeberg, A., Taviani, M., Hebbeln, D. and R/V Meteor Cruise M70-1 participants (2009) The white coral community in the central Mediterranean Sea revealed by ROV surveys. *Oceanography*, **22,** 58-74.

Freiwald, A. and Dullo, W.-C. (2000) Cruise Report RV Poseidon Cruise 265 [POS265], Thòrshavn–Galway–Kiel, 13th September—1st October 2000.

Freiwald, A., Fosså, J.H., Grehan, A., Koslow, T. and Roberts, J.M. (2004) *Cold-water coral reefs: out of sight-no longer out of mind*. UNEP-WCMC, Cambridge, UK, Biodiversity Series 22, 84 pp.

Freiwald, A., Henrich, R. and Pätzold, J. (1997) Anatomy of a deep-water coral reef mound from Stjernsund, West-Finnmark, northern Norway. *SEPM*, 141-161.

Freiwald, A., Hühnerbach, V., Lindberg, B., Wilson, J.B. and Campbell, J. (2002) The Sula Reef Complex, Norwegian shelf. *Facies*, **47,** 179-200.

Freiwald, A., Rogers, A., Hall-Spencer, J., Guinotte, J.M., Davies, A.J., Yesson, C., Martin, C.S. and Weatherdon, L.V. 2017. Global distribution of cold-water corals (version 5.0). Fifth update to the dataset in Freiwald et al. (2004) by UNEP-WCMC, in collaboration with Andre Freiwald and John Guinotte. Cambridge (UK). UN Environment World Conservation Monitoring Centre. URL: https://archive.org/details/coldwatercoralre04frei.

Freiwald, A., Rogers, A., Hall-Spencer, J., Guinotte, J.M., Davies, A.J., Yesson, C., Martin, C.S. and Weatherdon, L.V. (2021) Global distribution od cold-water corals (version 5.1). Fifth update to the dataset in Freiwald et al. (2004) by UNEP-WCMC, in collaboration with Andre Freiwald and John Guinotte. Cambridge (UK): UN Environment Programme World Conservation Monitoring Centre.

Freiwald, A. and Wilson, J.B. (1998) Taphonomy of modern deep, cold-temperate water coral reefs. *Historical Biology*, **13,** 37-52.

Gagnon, A.C., Adkins, J.F., Fernandez, D.P. and Robinson, L.F. (2007) Sr/Ca and Mg/Ca vital effects correlated with skeletal architecture in a scleractinian deep-sea coral and the role of Rayleigh fractionation. *Earth & Planetary Science Letters*, **261,** 280-295.

Galvez, K.C. (2020) *The distribution and growth patterns of cold-water corals in the Straits of Florida*, University of Miami.

Garzanti, E., Vermeesch, P., Andò, S., Lustrino, M., Padoan, M. and Vezzoli, G. (2014) Ultra-long distance littoral transport of Orange sand and provenance of the Skeleton Coast Erg (Namibia). *Marine Geology*, **357,** 25-36.

Gay, A., Lopez, M., Berndt, C. and Séranne, M. (2007) Geological controls on focused fluid flow associated with seafloor seeps in the Lower Congo Basin. *Marine Geology*, **244,** 68-92.

Geissler, W.H., Schwenk, T. and Wintersteller, P. 2013. Walvis Ridge Passive-Source Seismic Experiment (WALPASS) – Cruise No. MSM20/1 – January 06 – January 15, 2012 - Cape Town (South Africa) – Walvis Bay (Namibia). MARIA S. MERIAN-Berichte, MSM20/1, 54 pp., DFG-Senatskommission für Ozeanographie.

Genin, A., Dayton, P.K., Lonsdale, P.F. and Spiess, F.N. (1986) Corals on seamount peaks provide evidence of current acceleration over deep-sea topography. *Nature*, **322,** 59-61.

GENUS (2017) GENUS (Geochemistry and Ecology of the Namibian Upwelling System) Project, 2017 How does the benguela Upwelling System work? Podcast video https://www.youtube.com/watch?v=8C9p6_qxgEI&t=1s.

Georgian, S.E., DeLeo, D., Durkin, A., Gomez, C.E., Kurman, M., Lunden, J.J. and Cordes, E.E. (2016) Oceanographic patterns and carbonate chemistry in the vicinity of cold-water coral reefs in the Gulf of Mexico: Implications for resilience in a changing ocean. *Limnology and Oceanography*, **61,** 648-665.

Georgian, S.E., Shedd, W. and Cordes, E.E. (2014) High-resolution ecological niche modelling of the cold-water coral *Lophelia pertusa* in the Gulf of Mexico. *Marine Ecology Progress Series*, **506,** 145-161.

Gibson, R. and Atkinson, R. (2003) Oxygen minimum zone benthos: adaptation and community response to hypoxia. *Oceanogr. Marine Biol. Annu. Rev*, **41,** 1-45.

Giraudeau, J., Bailey, G.W. and Pujol, C. (2000) A high-resolution time-series analyses of particle fluxes in the Northern Benguela coastal upwelling system: carbonate record of changes in biogenic production and particle transfer processes. *Deep Sea Research Part II: Topical Studies in Oceanography*, **47,** 1999-2028.

Glogowski, S., Dullo, W.C., Feldens, P., Liebetrau, V., von Reumont, J., Hühnerbach, V., Krastel, S., Wynn, R.B. and Flögel, S. (2015) The Eugen Seibold coral mounds offshore western Morocco: oceanographic and bathymetric boundary conditions of a newly discovered cold-water coral province. *Geo-Marine Letters*, **35,** 257–269.

Gómez, C.E., Wickes, L., Deegan, D., Etnoyer, P.J. and Cordes, E.E. (2018) Growth and feeding of deep-sea coral *Lophelia pertusa* from the California margin under simulated ocean acidification conditions. *PeerJ*, **6,** e5671-e5671.

Gori, A., Grover, R., Orejas, C., Sikorski, S. and Ferrier-Pagès, C. (2014) Uptake of dissolved free amino acids by four cold-water coral species from the Mediterranean Sea. *Deep Sea Research Part II: Topical Studies in Oceanography*, **99,** 42-50.

Gori, A., Reynaud, S., Orejas, C. and Ferrier-Pagès, C. (2015) The influence of flow velocity and temperature on zooplankton capture rates by the cold-water coral *Dendrophyllia cornigera*. *Journal of Experimental Marine Biology and Ecology*, **466,** 92-97.

Grasmueck, M., Eberli, G.P., Viggiano, D.A., Correa, T., Rathwell, G. and Luo, J. (2006) Autonomous underwater vehicle (AUV) mapping reveals coral mound distribution, morphology, and oceanography in deep water of the Straits of Florida. *Geophysical Research Letters*, **33, L23616, doi,** 10.1029/2006GL027734.

Guinan, J., Brown, C., Dolan, M.F.J. and Grehan, A.J. (2009) Ecological niche modelling of the distribution of cold-water coral habitat using underwater remote sensing data. *Ecological Informatics*, **4,** 83-92.

Gunnerus, J.E. (1768) Om nogle norske coraller. *Det Kongelige Norske Videnskabers Selskabs Skrifter*.

Hamilton, E.L. (1976) Variations of density and porosity with depth in deep-sea sediments. *Journal of Sedimentary Research*, **46,** 280-300.

Hanz, U., Wienberg, C., Hebbeln, D., Duineveld, G., Lavaleye, M., Juva, K., Dullo, W.C., Freiwald, A., Tamborrino, L., Reichart, G.J., Flögel, S. and Mienis, F. (2019) Environmental factors influencing benthic communities in the oxygen minimum zones on the Angolan and Namibian margins. *Biogeosciences*, **16,** 4337-4356.

Harris, P., Purkis, S. and Reyes, B. (2018) Statistical pattern analysis of surficial karst in the Pleistocene Miami oolite of South Florida. *Sedimentary Geology*, **367,** 84-95.

Harris, P.M., Purkis, S.J. and Ellis, J. (2011) Analyzing spatial patterns in modern carbonate sand bodies from Great Bahama Bank. *Journal of Sedimentary Research*, **81,** 185-206.

Hebbeln, D., Bender, M., Gaide, S., Titschack, J., Vandorpe, T., Van Rooij, D., Wintersteller, P. and Wienberg, C. (2019) Thousands of cold-water coral mounds along the Moroccan Atlantic continental margin: Distribution and morphometry. *Marine Geology*, **411,** 51-61.

Hebbeln, D., Pfannkuche, O., Reston, T. and Ratmeyer, V. 2006. Northeast Atlantic 2004, Cruise No. 61, April 19-June 6 2004, University of Hamburg, Germany.

Hebbeln, D., Van Rooij, D. and Wienberg, C. (2016) Good neighbours shaped by vigorous currents: Cold-water coral mounds and contourites in the North Atlantic. *Marine Geology*, **378,** 171-185.

Hebbeln, D., Wienberg, C. and and cruise participants 2012. Report and preliminary results of R/V MARIA S. MERIAN cruise MSM20-4. WACOM. Bridgetown-Freeport, 14.03.-07.04.2012.

Hebbeln, D., Wienberg, C., Bender, M., Bergmann, F., Dehning, K., Dullo, W.-C., Eichstädter, R., Flöter, S., Freiwald, A., Gori, A., Haberkern, J., Hoffmann, L., Mendes João, F., Lavaleye, M., Leymann, T., Matsuyama, K., Meyer-Schack, B., Mienis, F., Bernardo Moçambique, I., Nowald, N., Orejas Saco del Valle, C., Cordova, C.R., Saturov, D., Seiter, C., Titschack, J., Vittori, V., Wefing, A.-M., Wilsenack, M. and Wintersteller, P. 2017. ANNA - Cold-water coral ecosystems off Angola and Namibia. Cruise M122 – December 30, 2015 – January 31, 2016 – Walvis Bay (Namibia) – Walvis Bay (Namibia). METEOR-Berichte/Reports, M122, 66 pp, DFG-Senatskommission für Ozeanographie.

Hebbeln, D., Wienberg, C. and cruise participants 2015. Report and Preliminary Results of R/V MARIA S. MERIAN Cruise MSM36. MoccoMeBo. Malaga-Las Palmas, February 18–March 17 2014.

Hebbeln, D., Wienberg, C., Dullo, W.-C., Freiwald, A., Mienis, F., Orejas, C. and Titschack, J. (2020) Cold-water coral reefs thriving under hypoxia. *Coral Reefs*, **39,** 853-859.

Hebbeln, D., Wienberg, C., Wintersteller, P., Freiwald, A., Becker, M., Beuck, L., Dullo, C., Eberli, G.P., Glogowski, S., Matos, L., Forster, N., Reyes-Bonilla, H. and Taviani, M. (2014) Environmental forcing of the Campeche cold-water coral province, southern Gulf of Mexico. *Biogeosciences*, **11,** 1799-1815.

Hedges, J.I. and Oades, J.M. (1997) Comparative organic geochemistries of soils and marine sediments. *Organic Geochemistry*, **27,** 319-361.

Heezen, B.C., Tharp, M. and Ewing, M. (1959) *The Floors of the Oceans: I. The North Atlantic*. Geological Society of America, 0 pp.

Heindel, K., Titschack, J., Dorschel, B., Huvenne, V.A.I. and Freiwald, A. (2010) The sediment composition and predictive mapping of facies on the Propeller Mound--A cold-water coral mound (Porcupine Seabight, NE Atlantic). *Continental Shelf Research*, **30,** 1814-1829.

Hemsing, F. (2017) *Cold-water corals as archives for ocean dynamics, environmental conditions and glacial reef accumulation* Universität Heidelberg.

Hemsing, F., Hsieh, Y.-T., Bridgestock, L., Spooner, P.T., Robinson, L.F., Frank, N. and Henderson, G.M. (2018) Barium isotopes in cold-water corals. *Earth and Planetary Science Letters*, **491,** 183-192.

Hennige, S.J., Wicks, L.C., Kamenos, N.A., Bakker, D.C.E., Findlay, H.S., Dumousseaud, C. and Roberts, J.M. (2014) Short-term metabolic and growth responses of the cold-water coral Lophelia pertusa to ocean acidification. *Deep Sea Research Part II: Topical Studies in Oceanography*, **99,** 27-35.

Hennige, S.J., Wicks, L.C., Kamenos, N.A., Perna, G., Findlay, H.S. and Roberts, J.M. (2015) Hidden impacts of ocean acidification to live and dead coral framework. *Proc Biol Sci*, **282,** 20150990.

Henriet, J.-P., De Mol, B., Pillen, S., Vanneste, M., Van Rooij, D., Versteeg, W., Croker, P.F., Shannon, P.M., Unnithan, V., Bouriak, S. and Chachkine, P. (1998) Gas hydrate crystals may help build reefs. *Nature*, **391,** 647-649.

Henriet, J., Guidard, S. and Team, O.P. (2002) Carbonate mounds as a possible example for microbial activity in geological processes. In: *Ocean Margin Systems*, pp. 439-455. Springer.

Henry, L.-A. and Roberts, J.M. (2007) Biodiversity and ecological composition of macrobenthos on cold-water coral mounds and adjacent off-mound habitat in the bathyal Porcupine Seabight, NE Atlantic. *Deep Sea Research I*, **54,** 654-672.

Henry, L.-A. and Roberts, J.M. (2017) Global biodiversity in cold-water coral reef ecosystems. In: *Marine Animal Forests: The Ecology of Benthic Biodiversity Hotspots* (Eds S. Rossi, L. Bramanti, A. Gori and C. Orejas Saco del Valle), pp. 235-256. Springer International Publishing, Cham.

Hill, T., Spero, H., Guilderson, T., LaVigne, M., Clague, D., Macalello, S. and Jang, N. (2011) Temperature and vital effect controls on bamboo coral (*Isididae*) isotope geochemistry: A test of the "lines method". *Geochemistry, Geophysics, Geosystems*, **12.**

Hoetzel, S., Dupont, L.M., Marret, F., Jung, G. and Wefer, G. (2017) Steps in the intensification of Benguela upwelling over the Walvis Ridge during Miocene and Pliocene. *International Journal of Earth Sciences*, **106,** 171-183.

Holmes, M.E., Schneider, R.R., Müller, P.J., Segl, M. and Wefer, G. (1997) Reconstruction of past nutrient utilization in the Eastern Angola Basin based on sedimentary $^{15}N/^{14}N$ ratios. *Paleoceanography*, **12,** 604-614.

Horn, B.K. (1981) Hill shading and the reflectance map. *Proceedings of the IEEE*, **69,** 14-47.

Hovland, M. (1990) Do carbonate reefs form due to fluid seepage? *Terra Nova*, **2,** 8-18.

Hovland, M., Croker, P.F. and Martin, M. (1994a) Fault-associated seabed mounds (carbonate knolls?) off western Ireland and north-west Australia. *Marine and Petroleum Geology*, **11,** 232-246.

Hovland, M., Farestveit, R. and Mortensen, P.B. (1994b) Large cold-water coral reefs off mid-Norway - a problem for pipe-laying? In: *Oceanology International*, Brighton, UK.

Hovland, M. and Mortensen, P.B. (1999) *Norske Korallrev Og Prosessor i Havbunnen.(Deep-water Coral-reefs and Processes on the Sea Floor)*. John Grieg Forlag.

Hovland, M. and Thomsen, E. (1997) Cold-water corals—are they hydrocarbon seep related? *Marine Geology*, **137,** 159-164.

Hübscher, C., Dullo, C., Flögel, S., Titschack, J. and Schönfeld, J. (2010) Contourite drift evolution and related coral growth in the eastern Gulf of Mexico and its gateways. *International Journal of Earth Sciences*, **99,** 191-206.

Hutchings, L., van der Lingen, C.D., Shannon, L.J., Crawford, R.J.M., Verheye, H.M.S., Bartholomae, C.H., van der Plas, A.K., Louw, D., Kreiner, A., Ostrowski, M., Fidel, Q., Barlow, R.G., Lamont, T., Coetzee, J., Shillington, F., Veitch, J., Currie, J.C. and Monteiro, P.M.S. (2009) The Benguela Current: An ecosystem of four components. *Progress in Oceanography*, **83,** 15-32.

Huvenne, V., Beyer, A., de Haas, H., Dekindt, K., Henriet, J.-P., Kozachenko, M., Olu-Le Roy, K., Wheeler, A.J. and the TOBI/Pelagia 197 and CARACOLE cruise participants (2005) The seabed appearance of different coral bank provinces in the Porcupine Seabight, NE Atlantic: results from sidescan sonar and ROV seabed mapping. In: *Cold-water Corals and Ecosystems* (Eds A. Freiwald and J.M. Roberts), pp. 535-569. Springer, Heidelberg.

Huvenne, V.A.I., Blondel, P. and Henriet, J.-P. (2002) Textural analyses of sidescan sonar imagery from two mound provinces in the Porcupine Seabight. *Marine Geology*, **189,** 323-341.

Huvenne, V.A.I., De Mol, B. and Henriet, J.-P. (2003) A 3D seismic study of the morphology and spatial distribution of buried coral banks in the Porcupine Basin, SW of Ireland. *Marine Geology*, **198,** 5-25.

Huvenne, V.A.I., Masson, D.G. and Wheeler, A.J. (2009a) Sediment dynamics of a sandy contourite: the sedimentary context of the Darwin cold-water coral mounds, Northern Rockall Trough. *International Journal of Earth Sciences*, **98,** 865-884.

Huvenne, V.A.I., Tyler, P.A., Masson, D.G., Fisher, E.H., Hauton, C., Hühnerbach, V., Le Bas, T.P. and Wolff, G.A. (2011) A picture on the wall: Innovative mapping reveals cold-water coral refuge in submarine canyon. *Plos One*, **6(12),** e28755.

Huvenne, V.A.I., Van Rooij, D., De Mol, B., Thierens, M., O'Donnell, R. and Foubert, A. (2009b) Sediment dynamics and palaeo-environmental context at key stages in the Challenger cold-water coral mound formation: Clues from sediment deposits at the mound base. *Deep-Sea Research Part I*, **56,** 2263-2280.

Inthorn, M., Mohrholz, V. and Zabel, M. (2006a) Nepheloid layer distribution in the Benguela upwelling area offshore Namibia. *Deep Sea Research Part I: Oceanographic Research Papers*, **53,** 1423-1438.

Inthorn, M., Wagner, T., Scheeder, G. and Zabel, M. (2006b) Lateral transport controls distribution, quality, and burial of organic matter along continental slopes in high-productivity areas. *Geology*, **34,** 205-208.

Joubin, M.L. (1922) *Les coraux de mer profonde nuisibles aux chalutiers. Office Scientifique et Technique des Peches Maritimes*, **Notes et Memoires,** 5-16.

Junker, T., Mohrholz, V., Siegfried, L. and van der Plas, A. (2017) Seasonal to interannual variability of water mass characteristics and currents on the Namibian shelf. *Journal of Marine Systems*, **165,** 36-46.

Kano, A., Ferdelman, T.G. and Williams, T. (2010) The Pleistocene cooling built Challenger Mound, a deep-water coral mound in the NE Atlantic: Synthesis from IODP Expedition 307. *The Sedimentary Record*, **8,** 4-9.

Kano, A., Ferdelman, T.G., Williams, T., Henriet, J.-P., Ishikawa, T., Kawagoe, N., Takashima, C., Kakizaki, Y., Abe, K., Sakai, S., Browning, E.L., Li, X. and Integrated Ocean Drilling Program Expedition 307 Scientists (2007) Age constraints on the origin and growth history of a deep-water coral mound in the northeast Atlantic drilled during Integrated Ocean Drilling Program Expedition 307. *Geology*, **35,** 1051-1054.

Karstensen, J., Stramma, L. and Visbeck, M. (2008) Oxygen minimum zones in the eastern tropical Atlantic and Pacific oceans. *Progress in Oceanography*, **77,** 331-350.

Kaseke, K.F., Wang, L., Wanke, H., Turewicz, V. and Koeniger, P. (2016) An analysis of precipitation isotope distributions across Namibia using historical data. *PLOS ONE*, **11,** e0154598.

Kazanidis, G., Henry, L.-A., Vad, J., Johnson, C., De Clippele, L.H. and Roberts, J.M. (2021) Sensitivity of a cold-water coral reef to interannual variability in regional oceanography. *Diversity and Distributions*, **27,** 1719-1731.

Keeling, R.F., Körtzinger, A. and Gruber, N. (2010) Ocean deoxygenation in a warming world. *Annual Review of Marine Science*, **2,** 199-229.

Kenyon, N., Ivanov, M. and Akhmetzhanov, A. (1998) Cold water carbonate mounds and sediment transport on the Northeast Atlantic margin - Preliminary results of geological and geophysical investigations during the TTR-7 cruise of R/V Professor Logachev.

Kenyon, N.H., Akhmetzhanov, A.M., Wheeler, A.J., van Weering, T.C.E., de Haas, H. and Ivanov, M.K. (2003) Giant carbonate mud mounds in the southern Rockall Trough. *Marine Geology*, **195,** 5-30.

Kenyon, N.H., Stride, A.H. and Belderson, R.H. (1975) Plan views of active faults and other features on the lower Nile cone. *GSA Bulletin*, **86,** 1733-1739.

Keppner, G. (1991) Ludger Mintrop. *The Leading Edge*, **10,** 21-28.

Kim, J.-H., Schneider, R.R., Müller, P.J. and Wefer, G. (2002) Interhemispheric comparison of deglacial sea-surface temperature patterns in Atlantic eastern boundary currents. *Earth and Planetary Science Letters*, **194,** 383-393.

King, T.M., Rosenheim, B.E., Post, A.L., Gabris, T., Burt, T. and Domack, E.W. (2018) Large-scale intrusion of circumpolar deep water on antarctic margin recorded by stylasterid corals. *Paleoceanography and Paleoclimatology*, **33,** 1306-1321.

Kiriakoulakis, K., Freiwald, A., Fisher, E. and Wolff, G.A. (2007) Organic matter quality and supply to deep-water coral/mound systems of the NW European Continental Margin. *International Journal of Earth Sciences*, **96,** 159-170.

Kiriakoulakis, K., Harper, E. and Wolff, G.A. (2005) Lipids and nitrogeen isotopes of two deep-water corals from the North-East Atlantic: initial results and implications for their nutrition. In: *Cold-Water Corals and Ecosystems* (Eds A. Freiwald and J.M. Roberts), pp. 715-729. Springer, Berlin-Heidelberg.

Kirst, G.J., Schneider, R.R., Müller, P.J., von Storch, I. and Wefer, G. (1999) Late Quaternary Temperature Variability in the Benguela Current System Derived from Alkenones. *Quaternary Research*, **52,** 92-103.

Koopers, A.A.P. and Coggon, R. (2020) Exploring Earth by scientific ocean drilling: 2050 Science Framework, pp. 124.

Kopte, R., Brandt, P., Dengler, M., Tchipalanga, P.C.M., Macuéria, M. and Ostrowski, M. (2017) The Angola Current: Flow and hydrographic characteristics as observed at 11°S. *Journal of Geophysical Research: Oceans*, **122,** 1177-1189.

Koseki, S., Giordani, H. and Goubanova, K. (2019) Frontogenesis of the Angola–Benguela Frontal Zone. *Ocean Sci.*, **15,** 83-96.

Kostianoy, A.G. and Lutjeharms, J.R.E. (1999) Atmospheric effects in the Angola-Benguela frontal zone. *Journal of Geophysical Research: Oceans*, **104,** 20963-20970.

Kostylev, E.V., Brian, J.T., J. Brian, Fader, B.J.G., Courtney, R.C., Cameron, D.M.G. and Pickrill, A.R. (2001) Benthic habitat mapping on the Scotian Shelf based on multibeam bathymetry, surficial geology and sea floor photographs. *Marine Ecology Progress Series*, **219,** 121-137.

Kraay, G.W., Zapata, M. and Veldhuis, M.J.W. (1992) Separation of chlorophylls c_1c_2, and c_3 of marine phytoplankton by reversed-phase-C_{18}-high-performance liquid chromatography. *Journal of Phycology*, **28,** 708-712.

Krapf, C.B.E., Stanistreet, I.G. and Stollhofen, H. (2005) Morphology and fluvio-aeolian Interaction of the tropical latitude, ephemeral braided-river dominated Koigab Fan, North-West Namibia. In: *Fluvial Sedimentology VII*, pp. 99-120.

Krengel, T. (2020) *550,000 years of marine climate variability in the western Mediterranean Sea revealed by cold-water corals*, Universität Heidelberg.

Lamy, F., Hebbeln, D., Röhl, U. and Wefer, G. (2001) Holocene rainfall variability in southern Chile: a marine record of latitudinal shifts of the Southern Westerlies. *Earth and Planetary Science Letters*, **185,** 369-382.

Larsson, A.I., Lundälv, T. and van Oevelen, D. (2013) Skeletal growth, respiration rate and fatty acid composition in the cold-water coral *Lophelia pertusa* under varying food conditions. *Marine Ecology Progress Series*, **483,** 169-184.

Laughton, A.S., Whitmarsh, R.B., Rusby, J.S.M., Somers, M.L., Revie, J., McCartney, B.S. and Nafe, J.E. (1972) A continuous east-west fault on the Azores-Gibraltar ridge. *Nature*, **237,** 217-220.

Lavaleye, M., Duineveld, G., Lundälv, T., White, M., Guihen, D., Kiriakoulakis, K. and Wolff, G.A. (2009) Cold-water corals on the Tisler reef: Preliminary observations on the dynamic reef environment. *Oceanography*, **22,** 76-84.

Le Danois, E. (1948) *Les profondeurs de la mer*. Payot, Paris.

Le Guilloux, E., Olu, K., Bourillet, J.F., Savoye, B., Iglésias, S.P. and Sibuet, M. (2009) First observations of deep-sea coral reefs along the Angola margin. *Deep Sea Research Part II: Topical Studies in Oceanography*, **56,** 2394-2403.

Levin, L.A., Huggett, C.L. and Wishner, K.F. (1991) Control of deepsea benthic community structure by oxygen and organic-matter gradients in the eastern Pacific Ocean. *Journal of Marine Research*, **49,** 763-800.

Light, M.P.R., Maslanyj, M.P., Greenwood, R.J. and Banks, N.L. (1993) Seismic sequence stratigraphy and tectonics offshore Namibia. *Geological Society, London, Special Publications*, **71,** 163.

Lim, A., Huvenne, V.A.I., Vertino, A., Spezzaferri, S. and Wheeler, A.J. (2018) New insights on coral mound development from groundtruthed high-resolution ROV-mounted multibeam imaging. *Marine Geology*, **403,** 225-237.

Lim, A., Wheeler, A.J. and Arnaubec, A. (2017) High-resolution facies zonation within a cold-water coral mound: The case of the Piddington Mound, Porcupine Seabight, NE Atlantic. *Marine Geology*, **390,** 120-130.

Lim, A., Wheeler, A.J. and Conti, L. (2021) Cold-water coral habitat mapping: trends and developments in acquisition and processing methods. *Geosciences*, **11,** 9.

Lim, A., Wheeler, A.J., Price, D.M., O'Reilly, L., Harris, K. and Conti, L. (2020) Influence of benthic currents on cold-water coral habitats: a combined benthic monitoring and 3D photogrammetric investigation. *Scientific Reports*, **10,** 19433.

Lindberg, B. (2004) Cold-water coral reefs on the Norwegian shelf-acoustic signature, geological, geomorphological and environmental setting. *Doctor Scientiarum Thesis, Department of Geology, University of Tromsø, Norway*.

Lindberg, B., Berndt, C. and Mienert, J. (2007) The Fugløy Reef at 70°N; acoustic signature, geologic, geomorphologic and oceanographic setting. *International Journal of Earth Sciences*, **96,** 201-213.

Lindberg, B. and Mienert, J. (2005) Postglacial carbonate production by cold-water corals on the Norwegian Shelf and their role in the global carbonate budget. *Geology*, **33,** 537-540.

Linné, C. (1758) *Systema Naturae per regna tria naturae, secundum classes, ordines, genera, species, cum characteribus, differentiis, synonymis, locis. Editio decima, reformata*, vol. 1: 824 pp. *Laurentius Salvius: Holmiae*.

Little, S.H., Wilson, D.J., Rehkämper, M., Adkins, J.F., Robinson, L.F. and van de Flierdt, T. (2021) Cold-water corals as archives of seawater Zn and Cu isotopes. *Chemical Geology*, **578,** 120304.

Lo Iacono, C., Gràcia, E., Ranero, C.R., Emelianov, M., Huvenne, V.A.I., Bartolomé, R., Booth-Rea, G. and Prades, J. (2014) The West Melilla cold water coral mounds, Eastern Alboran Sea: Morphological characterization and environmental context. *Deep-Sea Research Part II: Topical Studies in Oceanography*, **99,** 316-326.

Lo Iacono, C., Savini, A., Huvenne, V.A.I. and Gràcia, E. (2019) 15 Habitat Mapping of Cold-Water Corals in the Mediterranean Sea. In: *Mediterranean Cold-Water Corals: Past, Present and Future: Understanding the Deep-Sea Realms of Coral* (Eds C. Orejas and C. Jiménez), pp. 157-171. Springer International Publishing, Cham.

Lopes, D.A. and Hajdu, E. (2014) Carnivorous sponges from deep-sea coral mounds in the Campos Basin (SW Atlantic), with the description of six new species (Cladorhizidae, Poecilosclerida, Demospongiae). *Marine Biology Research*, **10,** 329-356.

López Correa, M., Montagna, P., Joseph, N., Rüggeberg, A., Fietzke, J., Flögel, S., Dorschel, B., Goldstein, S.L., Wheeler, A. and Freiwald, A. (2012) Preboreal onset of cold-water coral growth beyond the Arctic Circle revealed by coupled radiocarbon and U-series dating and neodymium isotopes. *Quaternary Science Reviews*, **34,** 24-43.

Lundalv, T. and Jonsson, L. (2003) Cold-water corals in the Skagerrak - more significant than expected but in deep peril. In: *Second International Symposium on Deep-sea Corals, Erlangen, Germany*.

Lunden, J.J., McNicholl, C.G., Sears, C.R., Morrison, C.L. and Cordes, E.E. (2014) Acute survivorship of the deep-sea coral *Lophelia pertusa* from the Gulf of Mexico under acidification, warming, and deoxygenation. *Frontiers in Marine Science*, **1**.

Lutjeharms, J.R.E. and Stockton, P.L. (1987) Kinematics of the upwelling front off southern Africa. *South African Journal of Marine Science*, **5,** 35-49.

M Van Zinderen Bakker, E. and Mercer, J.H. (1986) Major late Cainozoic climatic events and palaeoenvironmental changes in Africa viewed in a world wide context. *Palaeogeography Palaeoclimatology Palaeoecology*, **56,** 217-235.

Mackay, K.A., Rowden, A.A., Bostock, H.C. and Tracey, D.M. (2014) Revisiting Squires' coral coppice, Campbell Plateau, New Zealand. *New Zealand Journal of Marine and Freshwater Research*, **48,** 507-523.

Maier, C., Hegeman, J., Weinbauer, M.G. and Gattuso, J.P. (2009) Calcification of the cold-water coral *Lophelia pertusa,* under ambient and reduced pH. *Biogeosciences*, **6,** 1671-1680.

Mandt, M., Gade, K. and Jalving, B. (2001) Integrating DGPS-USBL position measurements with inertial navigation in the HUGIN 3000 AUV. In: *Proceedings of the 8th Saint Petersburg International Conference on Integrated Navigation Systems, Saint Petersburg, Russia*, pp. 28-30.

Mangini, A., Godoy, J.M., Godoy, M.L., Kowsmann, R., Santos, G.M., Ruckelshausen, M., Schroeder-Ritzrau, A. and Wacker, L. (2010) Deep sea corals off Brazil verify a poorly ventilated Southern Pacific Ocean during H2, H1 and the Younger Dryas. *Earth and Planetary Science Letters*, **293,** 269-276.

Mangini, A., Lomitschka, M., Eichstädter, R., Frank, N., Vogler, S., Bonani, G., Hajdas, I. and Patzold, J. (1998) Coral provides way to age deep water. *Nature*, **392,** 347-348.

MAREANO (2020) Coral reefs off Norway, http://mareano.no/kart/mareano_en.html#maps/4738.

Marenzeller, E.v. (1904) Steinkorallen. *Wissenschaflichte Ergebnisse der deutschen Tiefsee-Expedition auf dem Dampfer*.

Mariotti, A., Gadel, F., Giresse, P. and Kinga, M. (1991) Carbon isotope composition and geochemistry of particulate organic matter in the Congo River (Central Africa): Application to the study of Quaternary sediments off the mouth of the river. *Chemical Geology: Isotope Geoscience section*, **86,** 345-357.

Martorelli, E., Petroni, G., Chiocci, F.L. and the Pantelleria Scientific Party (2011) Contourites offshore Pantelleria Island (Sicily Channel, Mediterranean Sea): depositional, erosional and biogenic elements. *Geo-Marine Letters*, **31,** 481-493.

Masson, D.G., Bett, B.J., Billett, D.S.M., Jacobs, C.L., Wheeler, A.J. and Wynn, R.B. (2003) The origin of deep-water, coral-topped mounds in the northern Rockall Trough, Northeast Atlantic. *Marine Geology*, **194,** 159-180.

Matos, L., Mienis, F., Wienberg, C., Frank, N., Kwiatkowski, C., Groeneveld, J., Thil, F., Abrantes, F., Cunha, M.R. and Hebbeln, D. (2015) Interglacial occurrence of cold-water corals off Cape Lookout (NW Atlantic): First evidence of the Gulf Stream influence. *Deep-Sea Research Part I*, **105,** 158-170.

Matos, L., Wienberg, C., Titschack, J., Schmiedl, G., Frank, N., Abrantes, F., Cunha, M.R. and Hebbeln, D. (2017) Coral mound development at the Campeche cold-water coral province, southern Gulf of Mexico: Implications of Antarctic Intermediate Water increased influence during interglacials. *Marine Geology*, **392,** 53-65.

Mazzini, A., Akhmetzhanov, A., Monteys, X. and Ivanov, M. (2012) The Porcupine Bank Canyon coral mounds: oceanographic and topographic steering of deep-water carbonate mound development and associated phosphatic deposition. *Geo-Marine Letters*, **32,** 205-225.

McCrea, J.M. (1950) On the isotopic chemistry of carbonates and a paleotemperature scale. *The Journal of Chemical Physics*, **18,** 849-857.

McCulloch, M., Trotter, J., Montagna, P., Falter, J., Dunbar, R., Freiwald, A., Försterra, G., López Correa, M., Maier, C., Rüggeberg, A. and Taviani, M. (2012) Resilience of cold-water scleractinian corals to ocean acidification: Boron isotopic systematics of pH and saturation state up-regulation. *Geochimica et Cosmochimica Acta*, **87,** 21-34.

Menapace, W., Chahid, D., Duarte, D., Fleischmann, T., Heitmann-Bacza, C., Kramer, L., Krupiński, S., Leymann, T., Mai, H.A., Morales, N., Otte, F., Schmidt, C., Tamborrino, L., Vittori, V., Xu, S. and Zehnle, H. (2021) Long-term monitoring of fluid and solid emissions at the African-Eurasian tectonic boundary in the

ALBOran Sea and the Gulf of CAdiz, Cruise No. M167, 11.10. 2020-05.11. 2020, Emden (Germany)-Emden (Germany), ALBOCA II.

Mesolella, K.J., Matthews, R., Broecker, W.S. and Thurber, D.L. (1969) The astronomical theory of climatic change: Barbados data. *The Journal of Geology*, **77,** 250-274.

Messing, C.G., Neumann, A.C. and Lang, J.C. (1990) Biozonation of deep-water lithoherms and associated hardgrounds in the northeastern Straits of Florida. *Palaios*, **5,** 15-33.

Micallef, A., Krastel, S. and Savini, A. (2018) Introduction. In: *Submarine Geomorphology* (Eds A. Micallef, S. Krastel and A. Savini), pp. 1-9. Springer International Publishing, Cham.

Mienis, F. and de Haas, H. (2004) Report of the cruise R/V PELAGIA cruise 64PE229, Cadiz-Galway, 15.08.–09.09. 2004. *Royal Netherlands Institute for Sea Research (NIOZ), Texel, the Netherlands.*

Mienis, F., De Stigter, H.C., De Haas, H., Van der Land, C. and Van Weering, T.C.E. (2012a) Hydrodynamic conditions in a cold-water coral mound area on the Renard Ridge, southern Gulf of Cadiz. *Journal of Marine Systems*, **96-97,** 61-71.

Mienis, F., de Stigter, H.C., de Haas, H. and van Weering, T.C.E. (2009) Near-bed particle deposition and resuspension in a cold-water coral mound area at the Southwest Rockall Trough margin, NE Atlantic. *Deep Sea Research I*, **56,** 1026-1038.

Mienis, F., de Stigter, H.C., White, M., Duineveld, G., de Haas, H. and van Weering, T.C.E. (2007) Hydrodynamic controls on cold-water coral growth and carbonate-mound development at the SW and SE Rockall Trough Margin, NE Atlantic Ocean. *Deep Sea Research I*, **54,** 1655-1674.

Mienis, F., Duineveld, G.C.A., Davies, A.J., Lavaleye, M.M.S., Ross, S.W., Seim, H., Bane, J., van Haren, H., Bergman, M.J.N., de Haas, H., Brooke, S. and van Weering, T.C.E. (2014) Cold-water coral growth under extreme environmental conditions, the Cape Lookout area, NW Atlantic. *Biogeosciences*, **11,** 2543-2560.

Mienis, F., Duineveld, G.C.A., Davies, A.J., Ross, S.W., Seim, H., Bane, J. and van Weering, T.C.E. (2012b) The influence of near-bed hydrodynamic conditions on cold-water corals in the Viosca Knoll area, Gulf of Mexico. *Deep Sea Research Part I: Oceanographic Research Papers*, **60,** 32-45.

Mienis, F., van Weering, T., de Haas, H., de Stigter, H., Huvenne, V. and Wheeler, A. (2006) Carbonate mound development at the SW Rockall Trough margin based on high resolution TOBI and seismic recording. *Mar Geol*, **233,** 1-19.

Mikkelsen, N., Erlenkeuser, H., Killingley, J.S. and Berger, W.H. (1982) Norwegian corals: radiocarbon and stable isotopes in *Lophelia pertusa*. *Boreas*, **11,** 163-171.

Miller, R.J., Hocevar, J., Stone, R.P. and Fedorov, D.V. (2012) Structure-forming corals and sponges and their use as fish habitat in Bering Sea submarine canyons. *PLOS ONE*, **7,** e33885.

Milliman, J.D. (1993) Production and accumulation of calcium carbonate in the ocean: Budget of a nonsteady state. *Global Biogeochemical Cycles*, **7,** 927-957.

Milliman, J.D., Manheim, F.T., Pratt, R.M. and Zarudski, E.F.K. 1967. Alvin dives on the continental margin off the southeastern United States, July 2-13 1967, Woods Hole Oceanographic Institution, Woods Hole, Mass.

Mills, D.B., Francis, W.R., Vargas, S., Larsen, M., Elemans, C.P.H., Canfield, D.E. and Wörheide, G. (2018) The last common ancestor of animals lacked the HIF pathway and respired in low-oxygen environments. *eLife*, **7,** e31176.

Mohn, C., Rengstorf, A., White, M., Duineveld, G., Mienis, F., Soetaert, K. and Grehan, A. (2014) Linking benthic hydrodynamics and cold-water coral occurrences: A high-resolution model study at three cold-water coral provinces in the NE Atlantic. *Progress in Oceanography*, **122,** 92-104.

Mohrholz, V., Bartholomae, C.H., Van der Plas, A.K. and Lass, H.U. (2008) The seasonal variability of the northern Benguela undercurrent and its relation to the oxygen budget on the shelf. *Continental Shelf Research*, **28,** 424-441.

Mohrholz, V., Eggert, A., Junker, T., Nausch, G., Ohde, T. and Schmidt, M. (2014) Cross shelf hydrographic and hydrochemical conditions and their short term variability at the northern Benguela during a normal upwelling season. *Journal of Marine Systems*, **140,** 92-110.

Montagna, P., McCulloch, M., Douville, E., López Correa, M., Trotter, J., Rodolfo-Metalpa, R., Dissard, D., Ferrier-Pagès, C., Frank, N., Freiwald, A., Goldstein, S., Mazzoli, C., Reynaud, S., Rüggeberg, A., Russo, S. and Taviani, M. (2014) Li/Mg systematics in scleractinian corals: Calibration of the thermometer. *Geochimica et Cosmochimica Acta*, **132,** 288-310.

Montagna, P., McCulloch, M., Taviani, M., Mazzoli, C. and Vendrell, B. (2006) Phosphorus in cold-water corals as a proxy for seawater nutrient chemistry. *Science*, **312,** 1788-1791.

Montero-Serrano, J.-C., Frank, N., Tisnérat-Laborde, N., Colin, C., Wu, C.-C., Lin, K., Shen, C.-C., Copard, K., Orejas, C., Gori, A., De Mol, L., Van Rooij, D., Reverdin, G. and Douville, E. (2013) Decadal changes in the mid-depth water mass dynamic of the Northeastern Atlantic margin (Bay of Biscay). *Earth and Planetary Science Letters*, **364,** 134-144.

Montoya, J.P. (2007) Natural Abundance of ^{15}N in marine planktonic ecosystems. In: *Stable isotopes in ecology and environmental science* 2nd Edn. edn, pp. 176-202. Blackwell, Malden, MA.

Moore, D.R. and Bullis Jr, H.R. (1960) A deep-water coral reef in the Gulf of Mexico. *Bulletin of Marine Science*, **10,** 125-128.

Mortensen, P.B., Buhl-Mortensen, L., Gebruk, A.V. and Krylova, E.M. (2008) Occurrence of deep-water corals on the Mid-Atlantic Ridge based on MAR-ECO data. *Deep Sea Research Part II: Topical Studies in Oceanography*, **55,** 142-152.

Mortensen, P.B., Hovland, M., Brattegard, T. and Farestveit, R. (1995) Deep water bioherms of the scleractinian coral *Lophelia pertusa* (L.) at 64° n on the Norwegian shelf: Structure and associated megafauna. *Sarsia*, **80,** 145-158.

Mortensen, P.B., Hovland, M., Fosså, J.H. and Furevik, D.M. (2001) Distribution, abundance and size of *Lophelia pertusa* coral reefs in mid-Norway in relation to seabed characteristics. *Journal of Marine Biological Association of the United Kingdom*, **51,** 999-1013.

Mosch, T., Sommer, S., Dengler, M., Noffke, A., Bohlen, L., Pfannkuche, O., Liebetrau, V. and Wallmann, K. (2012) Factors influencing the distribution of epibenthic megafauna across the Peruvian oxygen minimum zone. *Deep Sea Research Part I: Oceanographic Research Papers*, **68,** 123-135.

Mouchi, V., Crowley, Q.G., Jackson, A.L., Mcdermott, F., Monteys, X., Rafélis, M.D., Rueda, J.L. and Lartaud, F. (2014) Potential seasonal calibration for palaeoenvironmental reconstruction using skeletal microstructures and strontium measurements from the cold-water coral *Lophelia pertusa*. *Journal of Quaternary Science*, **29,** 803-814.

Mueller, C.E., Larsson, A.I., Veuger, B., Middelburg, J.J. and van Oevelen, D. (2014) Opportunistic feeding on various organic food sources by the cold-water coral *Lophelia pertusa*. *Biogeosciences*, **11,** 123-133.

Mullins, H.T., Newton, C.R., Heath, K. and Van Buren, H.M. (1981) Modern deep-water coral mounds north of Little Bahama Bank; criteria for recognition of deep-water coral bioherms in the rock record. *Journal of Sedimentary Research*, **51,** 999-1013.

Mullins, H.T., Thompson, J.B., McDougall, K. and Vercoutere, T.L. (1985) Oxygen-minimum zone edge effects: Evidence from the central California coastal upwelling system. *Geology*, **13,** 491-494.

Muñoz, A., Cristobo, J., Rios, P., Druet, M., Polonio, V., Uchupi, E. and Acosta, J. (2012) Sediment drifts and cold-water coral reefs in the Patagonian upper and middle continental slope. *Marine and Petroleum Geology*, **36,** 70-82.

Murray, F., De Clippele, L.H., Hiley, A., Wicks, L., Roberts, J.M. and Hennige, S. (2019) Multiple feeding strategies observed in the cold-water coral *Lophelia pertusa*. *Journal of the Marine Biological Association of the United Kingdom*, **99,** 1281-1283.

Murray, J., Sir and Hjort, J. (1912) *The depths of the ocean*. Macmillan.

Naumann, M.S., Orejas, C. and Ferrier-Pagès, C. (2014) Species-specific physiological response by the cold-water corals *Lophelia pertusa* and *Madrepora oculata* to variations within their natural temperature range. *Deep Sea Research Part II: Topical Studies in Oceanography*, **99,** 36-41.

Neumann, A.C., Kofoed, J.W. and Keller, G.H. (1977) Lithoherms in the Straits of Florida. *Geology*, **5,** 4-10.

Nordgaard, O. (1912) Et gammelt Lophoheliarev i Trondhjemsfjorden. *Det Kongelige Norske videnskabers selskabs skrifter*.

O'Reilly, B.M., Readman, P.W., Shannon, P.M. and Jacob, A.W.B. (2003) A model for the development of a carbonate mound population in the Rockall Trough based on deep-towed sidescan sonar data. *Marine Geology*, **198,** 55-66.

Odum, H.T. (1971) *Environment, power and society*. Wiley-Interscience, New York, USA.

Opderbecke, J. (1997) At-sea calibration of a USBL underwater vehicle positioning system. In: *Oceans' 97. MTS/IEEE Conference Proceedings*, **1**, pp. 721-726. IEEE.

Orejas, C., Gori, A., Rad-Menéndez, C., Last, K.S., Davies, A.J., Beveridge, C.M., Sadd, D., Kiriakoulakis, K., Witte, U. and Roberts, J.M. (2016) The effect of flow speed and food size on the capture efficiency and feeding behaviour of the cold-water coral Lophelia pertusa. *Journal of Experimental Marine Biology and Ecology*, **481,** 34-40.

Orejas, C., Wienberg, C., Titschack, J., Tamborrino, L., Freiwald, A. and Hebbeln, D. (2021) *Madrepora oculata* forms large frameworks in hypoxic waters off Angola (SE Atlantic). *Scientific Reports*, **11,** 15170.

Orphan, V.J., House, C.H., Hinrichs, K.-U., McKeegan, K.D. and DeLong, E.F. (2001) Methane-consuming archaea revealed by directly coupled isotopic and phylogenetic analysis. *science*, **293,** 484-487.

Paull, C.K., Neumann, A.C., am Ende, B.A., Ussler III, W. and Rodriguez, N.M. (2010) Lithoherms on the Florida–Hatteras slope. *Marine Geology*, **166,** 83–101.

Pawlowicz, R., Beardsley, B. and Lentz, S. (2002) Classical tidal harmonic analysis including error estimates in MATLAB using T_TIDE. *Computers & Geosciences*, **28,** 929-937.

Peckmann, J. and Thiel, V. (2004) Carbon cycling at ancient methane–seeps. *Chemical Geology*, **205,** 443-467.

Perdue, E.M. and Koprivnjak, J.-F. (2007) Using the C/N ratio to estimate terrigenous inputs of organic matter to aquatic environments. *Estuarine, Coastal and Shelf Science*, **73,** 65-72.

Pettersson, H. (1948) The Swedish Deep-Sea Expedition. *Nature*, **162,** 324-325.

Peura, M. and Iivarinen, J. (1997) Efficiency of simple shape descriptors. In: *Advances in visual form analysis* (Eds A. C., L.P. Cordella and G. Sanniti di Baja), pp. 443-451. World Scientific, Singapore.

Piggot, C.S. (1936) Apparatus to secure core samples from the ocean-bottom. *GSA Bulletin*, **47,** 675-664.

Pinheiro, L.M., Ivanov, M.K., Sautkin, A., Akhmanov, G., Magalhães, V.H., Volkonskaya, A., Monteiro, J.H., Somoza, L., Gardner, J., Hamouni, N. and Cunha, M.R. (2003) Mud volcanism in the Gulf of Cadiz: results from the TTR-10 cruise. *Marine Geology*, **195,** 131-151.

Pirlet, H., Wehrmann, L.M., Brunner, B., Frank, N., Dewanckele, J., Van Rooij, D., Foubert, A., Swennen, R., Naudts, L. and Boone, M. (2010) Diagenetic formation of gypsum and dolomite in a cold-water coral mound in the Porcupine Seabight, off Ireland. *Sedimentology*, **57,** 786-805.

Pirlet, H., Wehrmann, L.M., Foubert, A., Brunner, B., Blamart, D., De Mol, L., Van Rooij, D., Dewanckele, J., Cnudde, V. and Swennen, R. (2012) Unique authigenic mineral assemblages reveal different diagenetic histories in two neighbouring cold-water coral mounds on Pen Duick Escarpment, Gulf of Cadiz. *Sedimentology*, **59,** 578-604.

Pontoppidan, E. (1755) *The natural history of Norway*. A. Linde, London.

Poole, R. and Tomczak, M. (1999) Optimum multiparameter analysis of the water mass structure in the Atlantic Ocean thermocline. *Deep Sea Research Part I: Oceanographic Research Papers*, **46,** 1895-1921.

Portilho-Ramos, R.d.C., Titschack, J., Wienberg, C., Siccha Rojas, M.G., Yokoyama, Y. and Hebbeln, D. (2022) Major environmental drivers determining life and death of cold-water corals through time. *PLOS Biology*, **20,** e3001628.

Pratje, O. (1934) Sind die Bodenprofile aus den Röhrenloten ohne Unterbrechungen. *Versuche über die Arbeitsweise der Röhrenlote. Annin Hydrogr. mar. Met*, **62,** 137-144.

Pratt, N., Chen, T., Li, T., Wilson, D.J., van de Flierdt, T., Little, S.H., Taylor, M.L., Robinson, L.F., Rogers, A.D. and Santodomingo, N. (2019) Temporal distribution and diversity of cold-water corals in the southwest Indian Ocean over the past 25,000 years. *Deep Sea Research Part I: Oceanographic Research Papers*, **149,** 103049.

Pratt, R.M., Squires, D.F. and Stetson, T.R. (1962) *Coral banks occurring in deep water on the Blake Plateau. American Museum novitates, n. 2114.*

Purkis, S.J. and Harris, P. (2017) Quantitative interrogation of a fossilized carbonate sand body – The Pleistocene Miami oolite of South Florida. *Sedimentology*, **64,** 1439-1464.

Purkis, S.J., Koppel, J.V.D., Burgess, P.M., Budd, D.A., Hajek, E.A. and Purkis, S.J. (2016) Spatial self-organization in carbonate depositional environments. In: *Autogenic dynamics and self-organization in sedimentary systems* (Eds D.A. Budd, E.A. Hajek and S.J. Purkis), **106**, pp. 216. SEPM Society for Sedimentary Geology, Tulsa, Oklahoma.

Purkis, S.J., Rowlands, G.P., Riegl, B.M. and Renaud, P.G. (2010) The paradox of tropical karst morphology in the coral reefs of the arid Middle East. *Geology*, **38,** 227-230.

Purser, A., Bergmann, M., Lundälv, T., Ontrup, J. and Nattkemper, T.W. (2009) Use of machine-learning algorithms for the automated detection of cold-water coral habitats: a pilot study. *Marine Ecology Progress Series*, **397,** 241-251.

Purser, A., Larsson, A.I., Thomsen, L. and van Oevelen, D. (2010) The influence of flow velocity and food concentration on *Lophelia pertusa* (Scleractinia) zooplankton capture rates. *Journal of Experimental Marine Biology and Ecology*, **395,** 55-62.

Purser, A., Ontrup, J., Schoening, T., Thomsen, L., Tong, R., Unnithan, V. and Nattkemper, T.W. (2013) Microhabitat and shrimp abundance within a Norwegian cold-water coral ecosystem. *Biogeosciences*, **10,** 5779-5791.

R Core Team (2010) A language and environment for statistical computing, Vienna, Austria.

Raddatz, J., Liebetrau, V., Rüggeberg, A., Hathorne, E., Krabbenhöft, A., Eisenhauer, A., Böhm, F., Vollstaedt, H., Fietzke, J., López Correa, M., Freiwald, A. and Dullo, W.C. (2013) Stable Sr-isotope, Sr/Ca, Mg/Ca, Li/Ca and Mg/Li ratios in the scleractinian cold-water coral *Lophelia pertusa*. *Chemical Geology*, **352,** 143-152.

Raddatz, J., Liebetrau, V., Trotter, J., Rüggeberg, A., Flögel, S., Dullo, W.C., Eisenhauer, A., Voigt, S. and McCulloch, M. (2016) Environmental constraints on Holocene cold-water coral reef growth off Norway: Insights from a multiproxy approach. *Paleoceanography*, **31,** 1350-1367.

Raddatz, J. and Rüggeberg, A. (2021) Constraining past environmental changes of cold-water coral mounds with geochemical proxies in corals and foraminifera. *The Depositional Record*, **7,** 200-222.

Raddatz, J., Rüggeberg, A., Liebetrau, V., Foubert, A., Hathorne, E.C., Fietzke, J., Eisenhauer, A. and Dullo, W.-C. (2014) Environmental boundary conditions of cold-water coral mound growth over the last 3 million years in the Porcupine Seabight, Northeast Atlantic. *Deep Sea Research Part II: Topical Studies in Oceanography*, **99,** 227-236.

Raddatz, J., Titschack, J., Frank, N., Freiwald, A., Conforti, A., Osborne, A., Skornitzke, S., Stiller, W., Rüggeberg, A., Voigt, S., Albuquerque, A.L.S., Vertino, A., Schröder-Ritzrau, A. and Bahr, A. (2020) *Solenosmilia variabilis*-bearing cold-water coral mounds off Brazil. *Coral Reefs*, **39,** 69-83.

Rae, C.M.D. (2005) A demonstration of the hydrographic partition of the Benguela upwelling ecosystem at 26°40'S. *African Journal of Marine Science*, **27,** 617-628.

Ragnarsson, S.Á., Burgos, J.M., Kutti, T., van den Beld, I., Egilsdóttir, H., Arnaud-Haond, S. and Grehan, A. (2017) The impact of anthropogenic activity on cold-water corals. In: *Marine Animal Forests: The Ecology of Benthic Biodiversity Hotspots* (Eds S. Rossi, L. Bramanti, A. Gori and C. Orejas), pp. 989-1023. Springer International Publishing, Cham.

Ramos, A., Sanz, J.L., Ramil, F., Agudo, L.M. and Presas-Navarro, C. (2017) The giant cold-water coral mounds barrier off Mauritania. In: *Deep-Sea Ecosystems Off Mauritania: Research of Marine Biodiversity and Habitats in the Northwest African Margin* (Eds A. Ramos, F. Ramil and J.L. Sanz), pp. 481-525. Springer Netherlands, Dordrecht.

Reed, J.K. (2002) Deep-water *Oculina* coral reefs of Florida: biology, impacts, and management. *Hydrobiologia*, **471,** 43-55.

Reinking, J. (2010) Marine Geodesy. In: *Sciences of Geodesy - I: Advances and Future Directions* (Ed G. Xu), pp. 275-299. Springer Berlin Heidelberg, Berlin, Heidelberg.

Remia, A. and Taviani, M. (2005) Shallow-buried Pleistocene Madrepora-dominated coral mounds on a muddy continental slope, Tuscan Archipelago, NE Tyrrhenian Sea. *Facies*, **50,** 419-425.

Renard, V. and Allenou, J.-P. (1979) Sea Beam, Multi-Beam Echo-Sounding in "Jean Charcot" - Description, Evaluation and First Results. *The International Hydrographic Review*, **56**.

Rengstorf, A.M., Grehan, A., Yesson, C. and Brown, C. (2012) Towards high-resolution habitat suitability modeling of vulnerable marine ecosystems in the deep-sea: resolving terrain attribute dependencies. *Marine Geodesy*, **35,** 343-361.

Reolid, J., Reolid, M., Betzler, C., Lindhorst, S., Wiesner, M.G. and Lahajnar, N. (2017) Upper Pleistocene cold-water corals from the Inner Sea of the Maldives: taphonomy and environment. *Facies*, **63,** 8.

Rincón-Tomás, B., Duda, J.P., Somoza, L., González, F.J., Schneider, D., Medialdea, T., Santofimia, E., López-Pamo, E., Madureira, P., Hoppert, M. and Reitner, J. (2019) Cold-water corals and hydrocarbon-rich seepage in Pompeia Province (Gulf of Cádiz) – living on the edge. *Biogeosciences*, **16,** 1607-1627.

Roark, E.B., Guilderson, T.P., Flood-Page, S., Dunbar, R.B., Ingram, B.L., Fallon, S.J. and McCulloch, M. (2005) Radiocarbon-based ages and growth rates of bamboo corals from the Gulf of Alaska. *Geophysical Research Letters*, **32**.

Roberts, J.M., Brown, C.J., Long, D. and Bates, C.R. (2005a) Acoustic mapping using a multibeam echosounder reveals cold-water coral reefs and surrounding habitats. *Coral Reefs*, **24,** 654-669.

Roberts, J.M., Long, D., Wilson, J.B., Mortensen, P. and Gage, J.D. (2003) The cold-water coral *Lophelia pertusa* (Scleractinia) and enigmatic seabed mounds along the north-east Atlantic margin: are they related? *Marine pollution bulletin*, **46,** 7-20.

Roberts, J.M., Peppe, O.C., Dodds, L., Mercer, D.J., Thomson, W.T., Gage, J.D. and Meldrum, D.T. (2005b) Monitoring environmental variability around cold-water coral reefs: the use of a benthic photolander and the potential of seafloor observatories. In: *Cold-water Corals and Ecosystems* (Eds A. Freiwald and J.M. Roberts), pp. 483-502. Springer, Berlin-Heidelberg.

Roberts, J.M., Wheeler, A.J. and Freiwald, A. (2006) Reefs of the deep: The biology and geology of cold-water coral ecosystems. *Science*, **312,** 543-547.

Roberts, J.M., Wheeler, A.J., Freiwald, A. and Cairns, S.D. (2009) *Cold-water corals. The biology and geology of deep-sea coral habitats*. Cambridge University Press, 336 pp.

Robinson, L.F., Adkins, J.F., Fernandez, D.P., Burnett, D.S., Wang, S.-L., Gagnon, A.C. and Krakauer, N. (2006) Primary U distribution in scleractinian corals and its implications for U series dating. *Geochemistry, Geophysics, Geosystems*, **7**.

Robinson, L.F., Adkins, J.F., Frank, N., Gagnon, A.C., Prouty, N.G., Brendan Roark, E. and de Flierdt, T.v. (2014) The geochemistry of deep-sea coral skeletons: A review of vital effects and applications for palaeoceanography. *Deep-Sea Research Part II*, **99,** 184-198.

Robinson, L.F., Adkins, J.F., Scheirer, D.S., Fernandez, D.P., Gagnon, A. and Waller, R.G. (2007) Deep-sea scleractinian coral age and depth distribution in the Northwest Atlantic for the last 225,000 years. *Bulletin of Marine Science*, **81,** 371-391.

Rogers, A.D. (1999) The biology of *Lophelia pertusa* (Linnaeus 1758) and other deep-water reef-forming corals and impacts from human activities. *International Review of Hydrobiology*, **84,** 315-406.

Rogers, J. and Bremner, J.M. (1991) The Benguela Ecosystem. Part VII: Marine-geological aspects. In: *Oceanography and Marine Biology - An Annual Review* (Eds H. Barnes and M. Barnes), **29**, pp. 1-85.

Rommerskirchen, F., Condon, T., Mollenhauer, G., Dupont, L. and Schefuß, E. (2011) Miocene to Pliocene development of surface and sub-surface temperatures in the Benguela Current System. *Paleoceanography*, **26,** PA3216.

Rüggeberg, A., Dorschel, B., Dullo, W.-C. and Hebbeln, D. (2005) Sedimentary patterns in the vicinity of a carbonate mound in the Hovland Mound Province, northern Porcupine Seabight. In: *Cold-Water Corals and Ecosystems* (Eds A. Freiwald and J.M. Roberts), pp. 87-112. Springer Berlin Heidelberg, Berlin, Heidelberg.

Rüggeberg, A., Dullo, C., Dorschel, B. and Hebbeln, D. (2007) Environmental changes and growth history of a cold-water carbonate mound (Propeller Mound, Porcupine Seabight). *International Journal of Earth Sciences*, **96,** 57-72.

Rüggeberg, A., Flögel, S., Dullo, W.-C., Hissmann, K. and Freiwald, A. (2011) Water mass characteristics and sill dynamics in a subpolar cold-water coral reef setting at Stjernsund, northern Norway. *Marine Geology*, **282,** 5-12.

Rüggeberg, A., Flögel, S., Dullo, W.-C., Raddatz, J. and Liebetrau, V. (2016) Paleoseawater density reconstruction and its implication for cold-water coral carbonate mounds in the northeast Atlantic through time. *Paleoceanography*, **31,** 365-379.

Ruhl, H.A. (2008) Community change in the variable resource habitat of the abyssal northeast Pacific. *Ecology*, **89,** 991-1000.

Rush, D., Lavaleye, M. and participants, c. 2019. RV Pelagia cruise report 64PE449 KUNOXI - Kunene coral mound provinces and Namibian oxygen depleted biogeochemistry - February 15th-March 10th, 2019, Texel, The Netherlands.

Sahling, H., Rickert, D., Lee, R.W., Linke, P. and Suess, E. (2002) Macrofaunal community structure and sulfide flux at gas hydrate deposits from the Cascadia convergent margin, NE Pacific. *Marine Ecology Progress Series*, **231,** 121-138.

Samperiz, A., Robinson, L.F., Stewart, J.A., Strawson, I., Leng, M.J., Rosenheim, B.E., Ciscato, E.R., Hendry, K.R. and Santodomingo, N. (2020) Stylasterid corals: A new paleotemperature archive. *Earth and Planetary Science Letters*, **545,** 116407.

Sanders, H. (1969) Benthic marine diversity and the stability-time hypothesis. *Brookhaven Sym. Biol.*, 71-81.

Sars, M. (1865) *Om de i Norge forekommende fossile dyrelevinger fra Quartaerpedrioden*. Unversitetsprogram for forste halvaar, Christiania, 164 pp.

Savini, A. and Corselli, C. (2010) High-resolution bathymetry and acoustic geophysical data from Santa Maria di Leuca Cold Water Coral province (Northern Ionian Sea—Apulian continental slope). *Deep Sea Research Part II: Topical Studies in Oceanography*, **57,** 326-344.

Schlager, W. and Purkis, S.J. (2013) Bucket structure in carbonate accumulations of the Maldive, Chagos and Laccadive archipelagos. *International Journal of Earth Sciences*, **102,** 2225-2238.

Schlitzer, R. (2011) Ocean Data View, available at: http://odw.awi.de (last access: 12 February 2016).

Schmidt, M. and Eggert, A. (2016) Oxygen cycling in the northern Benguela Upwelling System: Modellingoxygen sources and sink. *Progress in Oceanography*, **149,** 145-173.

Schröder-Ritzrau, A., Freiwald, A. and Mangini, A. (2005) U/Th-dating of deep-water corals from the eastern North Atlantic and the western Mediterranean Sea. In: *Cold-Water Corals and Ecosystems* (Eds A. Freiwald and J.M. Roberts), pp. 691-700. Springer, Heidelberg.

Schroeder, W.W. (2002) Observations of *Lophelia pertusa* and the surficial geology at a deep-water site in the northeastern Gulf of Mexico. *Hydrobiology*, **471,** 29-33.

Searle, R.C. (1983) Submarine central volcanoes on the Nazca Plate — High-resolution sonar observations. *Marine Geology*, **53,** 77-102.

Shannon, L. (2001) Benguela Curent, Ocean Currents: A Derivative of Encyclopedia of Ocean Sciences,. 23-24.

Shannon, L., Boyd, A., Brundit, G. and taunton-Clark, J. (1986) On the existence of an El Niño-type phenomenon in the Benguela system. *Journal of Marine Research*, **44,** 495-520.

Shannon, L.V., Agenbag, J.J. and Buys, M.E.L. (1987) Large- and mesoscale features of the Angola-Benguela front. *South African Journal of Marine Science*, **5,** 11-34.

Shannon, L.V. and Nelson, G. (1996a) The Benguela: Large Scale Features and Processes and System Variability. In: *The South Atlantic: Present and Past Circulation*, pp. 163-210. Springer, Berlin-Heidelberg.

Shannon, L.V. and Nelson, G. (1996b) The Benguela: large scale features and processes and system variability. In: *The South Atlantic: Present and Past Circulation* (Eds G. Wefer, W.H. Berger, G. Siedler and D. Webb), pp. 163- 210. Springer, Berlin.

Sherwood, O.A. and Risk, M.J. (2007) Deep-Sea Corals: New Insights to Paleoceanography. In: *Developments in Marine Geology* (Eds C. Hillaire–Marcel and A. De Vernal), **1**, pp. 491-522. Elsevier.

Shi, N., Dupont, L.M., Beug, H.-J. and Schneider, R. (2000) Correlation between vegetation in Southwestern Africa and oceanic upwelling in the past 21,000 Years. *Quaternary Research*, **54,** 72-80.

Sibuet, M. and Olu, K. (1998) Biogeography, biodiversity and fluid dependence of deep-sea cold-seep communities at active and passive margins. *Deep Sea Research Part II: Topical Studies in Oceanography*, **45,** 517-567.

Siesser, W.G. (1980) Late Miocene Origin of the Benguela Upswelling System off Northern Namibia. *Science*, **208,** 283-285.

Sigman, D.M., DiFiore, P.J., Hain, M.P., Deutsch, C. and Karl, D.M. (2009) Sinking organic matter spreads the nitrogen isotope signal of pelagic denitrification in the North Pacific. *Geophysical Research Letters*, **36**.

Smith, F.G.W. (1954) Gulf of Mexico Madreporaria. *Gulf of Mexico - its origins, waters, and marine life. Fish Bull, US Fish Wildlife Serv*, **55,** 291-296.

Smith, J.E., Risk, M.J., Schwarcz, H.P. and McConnaughey, T.A. (1997) Rapid climate change in the North Atlantic during the Younger Dryas recorded by deep-sea corals. *Nature*, **386,** 818-820.

Smith, J.E., Schwarcz, H.P., Risk, M.J., McConnaughey, T.A. and Keller, N. (2000) Paleotemperatures from deep-sea corals: overcoming 'vital effects'. *Palaios*, **15,** 25-32.

Sokolova, I.M., Frederich, M., Bagwe, R., Lannig, G. and Sukhotin, A.A. (2012) Energy homeostasis as an integrative tool for assessing limits of environmental stress tolerance in aquatic invertebrates. *Marine Environmental Research*, **79,** 1-15.

Somoza, L., Dı, x, az del, R., x, o, V., León, R., Ivanov, M., Fernández-Puga, M.C., Gardner, J.M., Hernández-Molina, F.J., Pinheiro, L.M., Rodero, J., Lobato, A., Maestro, A., Vázquez, J.T., Medialdea, T. and Fernández-Salas, L.M. (2003) Seabed morphology and hydrocarbon seepage in the Gulf of Cádiz mud volcano area: Acoustic imagery, multibeam and ultra-high resolution seismic data. *Marine Geology*, **195,** 153-176.

Somoza, L., Ercilla, G., Urgorri, V., León, R., Medialdea, T., Paredes, M., Gonzalez, F.J. and Nombela, M.A. (2014) Detection and mapping of cold-water coral mounds and living *Lophelia* reefs in the Galicia Bank, Atlantic NW Iberia margin. *Marine Geology*, **349,** 73-90.

Spiess, F. (1985) *The Meteor Expedition: scientific results of the German Atlantic Expedition, 1925-1927*. Amerind Pub. Co., New Delhi ; New York, xvi, 429 p., 127, [3] p. of plates (some folded) pp.

Spiro, B., Roberts, M., Gage, J. and Chenery, S. (2000) $^{18}O/^{16}O$ and $^{13}C/^{12}C$ in an ahermatypic deep-water coral *Lophelia pertusa* from the North Atlantic: a case of disequilibrium isotope fractionation. *Rapid Communications in Mass Spectrometry*, **14,** 1332-1336.

Squires, D.F. (1964) Fossil coral thickets in Wairarapa, New Zealand. *Journal of Paleontology*, **38,** 904-915.

Squires, D.F. (1965) Deep-water coral structure on the Campbell Plateau, New Zealand. *Deep Sea Research and Oceanographic Abstracts*, **12,** 785-788.

Stalder, C., Spezzaferri, S., Rüggeberg, A., Pirkenseer, C. and Gennari, G. (2014) Late Weichselian deglaciation and early Holocene development of a cold-water coral reef along the Lopphavet shelf (Northern Norway) recorded by benthic foraminifera and ostracoda. *Deep Sea Research Part II: Topical Studies in Oceanography*, **99,** 249-269.

Stalder, C., Vertino, A., Rosso, A., Rüggeberg, A., Pirkenseer, C., Spangenberg, J.E., Spezzaferri, S., Camozzi, O., Rappo, S. and Hajdas, I. (2015) Microfossils, a key to unravel cold-water carbonate mound evolution through time: Evidence from the eastern Alboran Sea. *PLOS ONE*, **10,** e0140223.

Stanley, G.D. and Fautin, D.G. (2001) The origins of modern corals. *Science*, **291,** 1913-1914.

Stanley, G.D. and Swart, P.K. (1995) Evolution of the coral-zooxanthellae symbiosis during the Triassic: a geochemical approach. *Paleobiology*, **21,** 179-199.

Steinmann, L., Baques, M., Wenau, S., Schwenk, T., Spiess, V., Piola, A.R., Bozzano, G., Violante, R. and Kasten, S. (2020) Discovery of a giant cold-water coral mound province along the northern Argentine margin and its link to the regional Contourite Depositional System and oceanographic setting. *Marine Geology*, **427,** 106223.

Sternlicht, D.D. (2017) Historical development of side scan sonar. *The Journal of the Acoustical Society of America*, **141,** 4041-4041.

Stewart, H.A., Davies, J.S., Guinan, J. and Howell, K.L. (2014) The Dangeard and Explorer canyons, South Western Approaches UK: Geology, sedimentology and newly discovered cold-water coral mini-mounds. *Deep Sea Research Part II: Topical Studies in Oceanography*, **104,** 230-244.

Stolarski, J., Kitahara, M.V., Miller, D.J., Cairns, S.D., Mazur, M. and Meibom, A. (2011) The ancient evolutionary origins of Scleractinia revealed by azooxanthellate corals. *BMC Evolutionary Biology*, **11,** 316.

Stramma, L., Johnson, G.C., Sprintall, J. and Mohrholz, V. (2008) Expanding oxygen-minimum zones in the tropical oceans. *Science*, **320,** 655.

Strömgren, T. (1971) *Vertical and Horizontal Distribution of Lophelia Pertusa (Linné) in Trondheimsfjorden on the West Coast of Norway*. Universitetsforlaget.

Studer, A.S., Sigman, D.M., Martínez-García, A., Thöle, L.M., Michel, E., Jaccard, S.L., Lippold, J.A., Mazaud, A., Wang, X.T., Robinson, L.F., Adkins, J.F. and Haug, G.H. (2018) Increased nutrient supply to the Southern Ocean during the Holocene and its implications for the pre-industrial atmospheric CO2 rise. *Nature Geoscience*, **11,** 756-760.

Sundahl, H., Buhl-Mortensen, P. and Buhl-Mortensen, L. (2020) Distribution and suitable habitat of the cold-water corals *Lophelia pertusa*, *Paragorgia arborea*, and *Primnoa resedaeformis* on the Norwegian continental shelf. *Frontiers in Marine Science*, **7**.

Swart, P.K. (1983) Carbon and oxygen isotope fractionation in scleractinian corals: a review. *Earth-Science Reviews*, **19,** 51-80.

Sweetman, A.K., Thurber, A.R., Smith, C.R., Levin, L.A., Mora, C., Wei, C.-L., Gooday, A.J., Jones, D.O.B., Rex, M., Yasuhara, M., Ingels, J., Ruhl, H.A., Frieder, C.A., Danovaro, R., Würzberg, L., Baco, A., Grupe, B.M., Pasulka, A., Meyer, K.S., Dunlop, K.M., Henry, L.A. and Roberts, J.M. (2017) Major impacts of climate change on deep-sea benthic ecosystems. *Elementa Science of Anthropocene* **5,** 4.

Tahey, T.M., Duineveld, G.C.A., Berghuis, E.M. and Helder, W. (1994) Relation between sediment-water fluxes of oxygen and silicate and faunal abundance at continental shelf, slope and deep-water stations in the northwest Mediterranean. *Marine Ecology Progress Series*, **104,** 119-130.

Tamborrino, L., Titschack, J., Wienberg, C., Purkis, S., Eberli, G.P. and Hebbeln, D. (submitted) Spatial distribution and morphometry of the Namibian coral mounds controlled by the hydrodynamic regime and outer-shelf topography. *Submitted in Frontiers in Marine Sciences*.

Tamborrino, L., Wienberg, C., Titschack, J., Wintersteller, P., Mienis, F., Schröder-Ritzrau, A., Freiwald, A., Orejas, C., Dullo, W.-C., Haberkern, J. and Hebbeln, D. (2019) Mid-Holocene extinction of cold-water corals on the Namibian shelf steered by the Benguela oxygen minimum zone. *Geology*, **47,** 1185-1188.

Tambs-Lyche, H. (1958) *Zoogeographical and faunistic studies on west Norwegian marine animals*. John Griegs Boktrykkeri.

Tambutté, S., Holcomb, M., Ferrier-Pagès, C., Reynaud, S., Tambutté, É., Zoccola, D. and Allemand, D. (2011) Coral biomineralization: From the gene to the environment. *Journal of Experimental Marine Biology and Ecology*, **408,** 58-78.

Taviani, M., Angeletti, L., Beuck, L., Campiani, E., Canese, S., Foglini, F., Freiwald, A., Montagna, P. and Trincardi, F. (2016) Reprint of 'On and off the beaten track: Megafaunal sessile life and Adriatic cascading processes'. *Marine Geology*, **375,** 146-160.

Taviani, M., Remia, A., Corselli, C., Freiwald, A., Malinverno, E., Mastrototaro, F., Savini, A. and Tursi, A. (2005) First geo-marine survey of living cold-water *Lophelia* reefs in the Ionian Sea (Mediterranean basin). *Facies*, **50,** 409-417.

Teichert, C. (1958) Cold and deep water coral banks. *AAPG Bulletin*, **42,** 1064-1082.

Telford, W.M., Telford, W., Geldart, L., Sheriff, R.E. and Sheriff, R.E. (1990) *Applied geophysics*. Cambridge university press.

Theberge, A.E. and Cherkis, N.Z. (2013) A note on fifty years of multi-beam. In: *Hydro International*.

Thiem, Ø., Ravagnan, E., Fosså, J.H. and Berntsen, J. (2006) Food supply mechanisms for cold-water corals along a continental shelf edge. *Journal of Marine Systems*, **60,** 207-219.

Thomas, H.D. (1947) Some English Cretaceous and Eocene Hexacorals. *Quarterly Journal of the Geological Society*, **103,** 163-170.

Thresher, R.E., Tilbrook, B., Fallon, S., Wilson, N.C. and Adkins, J. (2011) Effects of chronic low carbonate saturation levels on the distribution, growth and skeletal chemistry of deep-sea corals and other seamount megabenthos. *Marine Ecology Progress Series*, **442,** 87-99.

Thurber, D.L., Broecker, W.S., Blanchard, R.L. and Potratz, H.A. (1965) Uranium-series ages of Pacific Atoll Coral. *Science*, **149,** 55-58.

Titschack, J., Baum, D., De Pol-Holz, R., López Correa, M., Forster, N., Flögel, S., Hebbeln, D. and Freiwald, A. (2015) Aggradation and carbonate accumulation of Holocene Norwegian cold-water coral reefs. *Sedimentology*, **62,** 1873-1898.

Titschack, J., Fink, H.G., Baum, D., Wienberg, C., Hebbeln, D. and Freiwald, A. (2016) Mediterranean cold-water corals – an important regional carbonate factory? *The Depositional Record*, **2,** 74-96.

Titschack, J., Thierens, M., Dorschel, B., Schulbert, C., Freiwald, A., Kano, A., Takashima, C., Kawagoe, N. and Li, X. (2009) Carbonate budget of a cold-water coral mound (Challenger Mound, IODP Exp. 307). *Marine Geology*, **259,** 36-46.

Tittensor, D.P., Baco, A.R., Brewin, P.E., Clark, M.R., Consalvey, M., Hall-Spencer, J., Rowden, A.A., Schlacher, T., Stocks, K.I. and Rogers, A.D. (2009) Predicting global habitat suitability for stony corals on seamounts. *Journal of Biogeography*, **36,** 1111-1128.

Todd, B.J., Fader, G.B.J., Courtney, R.C. and Pickrill, R.A. (1999) Quaternary geology and surficial sediment processes, Browns Bank, Scotian Shelf, based on multibeam bathymetry. *Marine Geology*, **162,** 165-214.

Turley, C.M., Roberts, J.M. and Guinotte, J.M. (2007) Corals in deep-water: will the unseen hand of ocean acidification destroy cold-water ecosystems? *Coral Reefs*, **26,** 445-448.

Tyrrell, T. and Lucas, M.I. (2002) Geochemical evidence of denitrification in the Benguela upwelling system. *Continental Shelf Research*, **22,** 2497-2511.

Urey, H.C. (1947) The thermodynamic properties of isotopic substances. *Journal of the Chemical Society (Resumed)*, 562-581.

Urey, H.C., Lowenstam, H., Buchsbaum, R. and Epstein, S. (1951) Carbonate-water isotopic temperature scale. *Geological Society of America Bulletin*, **62,** 417-426.

van de Flierdt, T., Robinson, L.F. and Adkins, J.F. (2010) Deep-sea coral aragonite as a recorder for the neodymium isotopic composition of seawater. *Geochimica et Cosmochimica Acta*, **74,** 6014-6023.

van der Kaaden, A.-S., van Oevelen, D., Rietkerk, M., Soetaert, K. and van de Koppel, J. (2020) Spatial self-organization as a new perspective on cold-water coral mound development. *Frontiers in Marine Science*, **7**.

van der Land, C., Eisele, M., Mienis, F., de Haas, H., Hebbeln, D., Reijmer, J.J.G. and van Weering, T.C.E. (2014) Carbonate mound development in contrasting settings on the Irish margin. *Deep Sea Research Part II*, **99,** 297–306.

van der Land, C., Mienis, F., de Haas, H., de Stigter, H.C., Swennen, R., Reijmer, J.J. and van Weering, T.C. (2011) Paleo-redox fronts and their formation in carbonate mound sediments from the Rockall Trough. *Marine Geology*, **284,** 86-95.

Van der Land, C., Mienis, F., De Haas, H., Frank, N., Swennen, R. and Van Weering, T.C. (2010) Diagenetic processes in carbonate mound sediments at the south-west Rockall Trough margin. *Sedimentology*, **57,** 912-931.

van Haren, H., Mienis, F., Duineveld, G.C.A. and Lavaleye, M.S.S. (2014) High-resolution temperature observations of a trapped nonlinear diurnal tide influencing cold-water corals on the Logachev mounds. *Progress in Oceanography*, **125,** 16-25.

van Oevelen, D., Duineveld, G., Lavaleye, M., Mienis, F., Soetaert, K. and Heip, C.H.R. (2009) The cold-water coral community as a hot spot for carbon cycling on continental margins: A food-web analysis from Rockall Bank (northeast Atlantic). *Limnology & Oceanography*, **54,** 1829-1844.

Van Rooij, D., Blamart, D., De Mol, L., Mienis, F., Pirlet, H., Wehrmann, L.M., Barbieri, R., Maignien, L., Templer, S.P., de Haas, H., Hebbeln, D., Frank, N., Larmagnat, S., Stadnitskaia, A., Stivaletta, N., van Weering, T., Zhang, Y., Hamoumi, N., Cnudde, V., Duyck, P. and Henriet, J.P. (2011) Cold-water coral mounds on the Pen Duick Escarpment, Gulf of Cadiz: The MiCROSYSTEMS project approach. *Marine Geology*, **282,** 102-117.

Van Rooij, D., De Mol, B., Huvenne, V., Ivanov, M. and Henriet, J.P. (2003) Seismic evidence of current-controlled sedimentation in the Belgica mound province, upper Porcupine slope, southwest of Ireland. *Marine Geology*, **195,** 31-53.

Van Rooij, D., Huvenne, V., Blamart, D., Henriet, J.-P., Wheeler, A. and De Haas, H. (2009) The Enya mounds: a lost mound-drift competition. *International Journal of Earth Sciences*, **98,** 849.

van Soest, R.W.M., Cleary, D.F.R., de Kluijver, M.J., Lavaleye, M.S.S., Maier, C. and van Duyl, F.C. (2007) Sponge diversity and community composition in Irish bathyal coral reefs. *Contributions to Zoology*, **76,** 121-142.

van Weering, T., Koster, B., Van Heerwaarden, J., Thomsen, L. and Viergutz, T. (2000) New technique for long-term deep seabed studies. *Sea Technology*, **41,** 17-+.

Vandorpe, T., Wienberg, C., Hebbeln, D., Van den Berghe, M., Gaide, S., Wintersteller, P. and Van Rooij, D. (2017) Multiple generations of buried cold-water coral mounds since the Early-Middle Pleistocene Transition in the Atlantic Moroccan Coral Province, southern Gulf of Cádiz. *Palaeogeography, Palaeoclimatology, Palaeoccology*, **485,** 293-304.

Veitch, J.A., Florenchie, P. and Shillington, F.A. (2006) Seasonal and interannual fluctuations of the Angola–Benguela Frontal Zone (ABFZ) using 4.5 km resolution satellite imagery from 1982 to 1999. *International Journal of Remote Sensing*, **27,** 987-998.

Vertino, A., Savini, A., Rosso, A., Di Geronimo, I., Mastrototaro, F., Sanfilippo, R., Gay, G. and Etiope, G. (2010) Benthic habitat characterization and distribution from two representative sites of the deep-water SML Coral Province (Mediterranean). *Deep Sea Research Part II: Topical Studies in Oceanography*, **57,** 380-396.

Viana, A.R., Faugeres, J.C., Kowsmann, R.O., Lima, J.A.M., Caddah, L.F.G. and Rizzo, J.G. (1998) Hydrology, morphology and sedimentology of the Campos continental margin, offshore Brazil. *Sedimentary Geology*, **115,** 133-157.

Vickery, K. (1998) Acoustic positioning systems. A practical overview of current systems. In: *Proceedings of the 1998 Workshop on Autonomous Underwater Vehicles (Cat. No. 98CH36290)*, pp. 5-17. IEEE.

Victorero, L., Blamart, D., Pons-Branchu, E., Mavrogordato, M.N. and Huvenne, V.A.I. (2016) Reconstrcution of the formation history of the Darwin Mounds, N Rockall Trough: How the dynamics of a sandy contourite affected cold-water coral growth. *Marine Geology*, **378,** 186-195.

von Bodungen, B., John, E.-C., Lutjeharms, J.R.E., Mohrholz, V. and Veitch, J. (2008) Hydrographic and biological patterns across the Angola–Benguela Frontal Zone under undisturbed conditions. *Journal of Marine Systems*, **74,** 189-215.

Vorrath, M.-E., Lahajnar, N., Fischer, G., Libuku, V.M., Schmidt, M. and Emeis, K.-C. (2018) Spatiotemporal variation of vertical particle fluxes and modelled chlorophyll a standing stocks in the Benguela Upwelling System. *Journal of Marine Systems*, **180,** 59-75.

Wang, H., Lo Iacono, C., Wienberg, C., Titschack, J. and Hebbeln, D. (2019) Cold-water coral mounds in the southern Alboran Sea (western Mediterranean Sea): Internal waves as an important driver for mound formation since the last deglaciation. *Marine Geology*, **412,** 1-18.

Wang, H., Titschack, J., Wienberg, C., Korpanty, C. and Hebbeln, D. (2021) The Importance of ecological accommodation space and sediment supply for cold-water coral mound formation, a case study from the Western Mediterranean Sea. *Frontiers in Marine Science*, **8**.

Wang, X.T., Sigman, D.M., Prokopenko, M.G., Adkins, J.F., Robinson, L.F., Hines, S.K., Chai, J., Studer, A.S., Martínez-García, A., Chen, T. and Haug, G.H. (2017) Deep-sea coral evidence for lower Southern Ocean surface nitrate concentrations during the last ice age. *Proceedings of the National Academy of Sciences*, **114,** 3352-3357.

Weber, J.N. (1973) Deep-sea ahermatypic scleractinian corals: isotopic composition of the skeleton. *Deep Sea Research and Oceanographic Abstracts*, **20,** 901-909.

Wefing, A.-M., Arps, J., Blaser, P., Wienberg, C., Hebbeln, D. and Frank, N. (2017) High precision U-series dating of scleractinian cold-water corals using an automated chromatographic U and Th extraction. *Chemical Geology*, **475,** 140-148.

Weinnig, A.M., Gómez, C.E., Hallaj, A. and Cordes, E.E. (2020) Cold-water coral (*Lophelia pertusa*) response to multiple stressors: High temperature affects recovery from short-term pollution exposure. *Scientific Reports*, **10,** 1-13.

Welschmeyer, N.A. and Lorenzen, C.J. (1985) Chlorophyll budgets: Zooplankton grazing and phytoplankton growth in a temperate fjord and the Central Pacific Gyres1. *Limnology and Oceanography*, **30,** 1-21.

Westphal, H., Beuck, L., Braun, S., Freiwald, A., Hanebuth, T., Hetzinger, S., Klicpera, A., Kudrass, H., Lantzsch, H., Lundälv, T., Mateu Vicens, G., Preto, N., von Reumont, J., Schilling, S., Taviani, M. and Wienberg, C. 2012. Phaeton. Cruise Report of Cruise No. MSM16/3, 13.10.-20.11 2010, Bremerhaven-Mindelo, Institut für Meereskunde, Univ Hamburg.

Wheeler, A., Bett, B., Billett, D. and Masson, D. (2000) High resolution side-scan sonar mapping of deep-water coral mounds: Surface morphology and processes affecting growth. *Eos Trans. Am. Geophys. Union*, **81,** F638.

Wheeler, A.J., Beyer, A., Freiwald, A., de Haas, H., Huvenne, V.A.I., Kozachenko, M., Olu-Le Roy, K. and Opderbecke, J. (2007) Morphology and environment of cold-water coral carbonate mounds on the NW European margin. *International Journal of Earth Sciences*, **96,** 37-56.

Wheeler, A.J., Kozachenko, M., Beyer, A., Foubert, A., Huvenne, V.A.I., Klages, M., Masson, D.G., Olu-Le Roy, K. and Thiede, J. (2005) Sedimentary processes and carbonate mounds in the Belgica Mound province, Porcupine Seabight, NE Atlantic. In: *Cold-water Corals and Ecosystems* (Eds A. Freiwald and J.M. Roberts), pp. 571-603. Springer, Berlin-Heidelberg.

Wheeler, A.J., Kozachenko, M., Henry, L.A., Foubert, A., de Haas, H., Huvenne, V.A.I., Masson, D.G. and Olu, K. (2011) The Moira Mounds, small cold-water coral banks in the Porcupine Seabight, NE Atlantic: Part A—an early stage growth phase for future coral carbonate mounds? *Marine Geology*, **282,** 53-64.

Wheeler, A.J., Kozachenko, M., Masson, D.G. and Huvenne, V. (2008) Influence of benthic sediment transport on cold-water coral bank morphology and growth: the example of the Darwin Mounds, north-east Atlantic. *Sedimentology*, **55,** 1875-1887.

Wheeler, A.J., Lim, A., Butschek, F., O'Reilly, L., Harris, K. and O'Driscoll, P. (2021) The "Little MonSta" deep-sea benthic, precision deployable, multi-sensor and sampling lander array. *Sensors*, **21,** 3355.

White, M. (2003) Comparison of near seabed currents at two locations in the Porcupine Sea Bight—implications for benthic fauna. *Journal of the Marine Biological Association of the United Kingdom*, **83,** 683-686.

White, M. (2007) Benthic dynamics at the carbonate mound regions of the Porcupine Sea Bight continental margin. *International Journal of Earth Sciences*, **96,** 1-9.

White, M. and Dorschel, B. (2010) The importance of the permanent thermocline to the cold water coral carbonate mound distribution in the NE Atlantic. *Earth and Planetary Science Letters*, **296,** 395-402.

White, M., Mohn, C., de Stigter, H. and Mottram, G. (2005) Deep-water coral development as a function of hydrodynamics and surface productivity around the submarine banks of the Rockall Trough, NE Atlantic. In: *Cold-Water Corals and Ecosystems* (Eds A. Freiwald and J.M. Roberts), pp. 503-514. Springer, Berlin-Heidelberg.

White, M., Roberts, J.M. and Van Weering, T.C.E. (2007) Do bottom-intensified diurnal tidal currents shape the alignement of carbonate mounds in the NE Atlantic? *Geo-Marine Letters*, **27,** 391-397.

White, M., Wolff, G.A., Lundälv, T., Guihen, D., Kiriakoulakis, K., Lavaleye, M. and Duineveld, G. (2012) Cold-water coral ecosystem (Tisler Reef, Norwegian Shelf) may be a hotspot for carbon cycling. *Marine Ecology Progress Series*, **465,** 11-23.

Whiticar, M.J. (1999) Carbon and hydrogen isotope systematics of bacterial formation and oxidation of methane. *Chemical Geology*, **161,** 291-314.

Wienberg, C., Beuck, L., Heidkamp, S., Hebbeln, D., Freiwald, A., Pfannkuche, O. and Monteys, X. (2008) Franken Mound: facies and biocoenoses on a newly-discovered "carbonate mound" on the western Rockall Bank, NE Atlantic. *Facies*, **54,** 1-24.

Wienberg, C., Frank, N., Mertens, K.N., Stuut, J.-B., Marchant, M., Fietzke, J., Mienis, F. and Hebbeln, D. (2010) Glacial cold-water coral growth in the Gulf of Cadiz: Implications of increased palaeo-productivity. *Earth and Planetary Science Letters*, **298,** 405-416.

Wienberg, C., Hebbeln, D., Fink, H.G., Mienis, F., Dorschel, B., Vertino, A., Lopez Correa, M. and Freiwald, A. (2009) Scleractinian cold-water corals in the Gulf of Cadiz-First clues about their spatial and temporal distribution. *Deep-Sea Research Part I-Oceanographic Research Papers*, **56,** 1873-1893.

Wienberg, C. and Titschack, J. (2017) Framework-forming scleractinian cold-water corals through space and time: A late Quaternary North Atlantic perspective. In: *Marine Animal Forests: The Ecology of Benthic Biodiversity Hotspots* (Eds S. Rossi, L. Bramanti, A. Gori and C. Orejas Saco del Valle), pp. 699-732. Springer, Cham.

Wienberg, C., Titschack, J., Frank, N., De Pol-Holz, R., Fietzke, J., Eisele, M., Kremer, A. and Hebbeln, D. (2020) Deglacial upslope shift of NE Atlantic intermediate waters controlled slope erosion and cold-water coral mound formation (Porcupine Seabight, Irish margin). *Quaternary Science Reviews*, **237,** 106310.

Wienberg, C., Titschack, J., Freiwald, A., Frank, N., Lundälv, T., Taviani, M., Beuck, L., Schröder-Ritzrau, A., Krengel, T. and Hebbeln, D. (2018) The giant Mauritanian cold-water coral mound province: oxygen control on coral mound formation. *Quaternary Science Reviews*, **185,** 135-152.

Wienberg, C., Wintersteller, P., Beuck, L. and Hebbeln, D. (2013) Coral Patch seamount (NE Atlantic) - a sedimentological and megafaunal reconnaissance based on video and hydroacoustic surveys. *Biogeosciences*, **10,** 3421-3443.

Wille, P. (2005) *Sound images of the ocean: in research and monitoring*. Springer Science & Business Media.

William, T., Kano, A., Ferdelman, T., Henriet, J.-P., Abe, K., Andres, M.S., Bjerager, M., Browning, E.L., Cragg, B.A., De Mol, B., Dorschel, B., Foubert, A., Frank, T.D., Fuwa, Y., Gaillot, P., Gharib, J.J., Gregg, J.M., Huvenne, V.A.I., Léonide, P., Li, X., Mangelsdorf, K., Tanaka, A., Monteys, X., Novosel, I., Sakai, S., Samarkin, V.A., Sasaki, K., Spivack, A.J., Takashima, C. and Titschak, J. (2006) Cold-water coral mounds revealed. *Eos, Transactions American Geophysical Union*, **87,** 525-526.

Wilson, D.J., Crocket, K.C., van de Flierdt, T., Robinson, L.F. and Adkins, J.F. (2014) Dynamic intermediate ocean circulation in the North Atlantic during Heinrich Stadial 1: A radiocarbon and neodymium isotope perspective. *Paleoceanography*, **29,** 1072-1093.

Wilson, J.B. (1979) "Patch" development of the deep-water coral *Lophelia pertusa* (L.) on the Rockall bank. *Journal of the Marine Biological Association of the United Kingdom*, **59,** 165-177.

Wilson, M.F.J., O'Connell, B., Brown, C., Guinan, J.C. and Grehan, A.J. (2007) Multiscale terrain analysis of multibeam bathymetry data for habitat mapping on the continental slope. *Marine Geodesy*, **30,** 3-35.

Zabel, M., Boetius, A., Emeis, K.-C., Ferdelman, T.G. and Spieß, V. 2012. PROSA. METEOR-Berichte Cruise No. 76, April 12-August 24 2008, Univ of Hamburg.

Zabel, M., Mohrholz, V., Schulz-Vogt, H., Sommer, S. and Zettler, M. 2019. The Benguela System under climate change Effects of variability in physical forcing on carbon and oxygen budgets. Cruise M157, 04.08.2019 - 16.09.2019, Mindelo (Cape Verde) - Walvis Bay (Namibia). METEOR-Berichte/Reports, M157, 58 pp, DFG-Senatskommission für Ozeanographie.

Zhu, X. (2016) *GIS for environmental applications: a practical approach*. Routledge.

Zibrowius, H. (1980) *Les Scléractiniaires de la Méditerranée et de l'Atlantique nord-oriental*. Mémoires de l'Institut Océanographique, Monaco, 11, 284 pp.

Zibrowius, H. and Gili, J.M. (1990) Deep-water Scleractinia (Cnidaria: Anthozoa) from Namibia, South Africa, and Walvis Ridge, southeast Atlantic. *Scientia Marina*, **54,** 19-46.

Appendices

A.1 Additional scientific contributions

A.1.1. Authored and co-authored papers not included in the PhD thesis

In the following, title and abstracts of two manuscripts are presented, which do not count to the cumulative thesis presented above, but to which I contributed during the period of my PhD project.

The first manuscript is published as Tamborrino et al. (2019) in the journal *Marine and Petroleum Geology.*

Formation of tubular carbonate conduits at Athina mud volcano, eastern Mediterannean sea

Leonardo Tamborrino[a, b], Tobias Himmler[b], Marcus Elvert[b], Stefano Conti[a], Alessandro F. Gualtieri[a], Daniela Fontana[a], Gerhard Bohrmann[b]

Tubular carbonate conduits (TCC) represent the termination of fluid plumbing systems in environments of hydrocarbon seepage and play a relevant role in the discharge of methane from sub-seafloor sediments to the water column. However, the biogeochemical reactions and biological activities involved in their formation are not fully understood. To address this, TCC samples were collected with a remotely operated vehicle from 19 the seabed on the SW flank of the Athina mud volcano in the eastern Mediterranean Sea. Petrographic, mineralogical, stable carbon and oxygen isotope and lipid biomarker analyses were performed to elucidate the formation processes of the tubular carbonates. Clotted and fibrous aragonite form the internal lining of the cavities, while the outer portion of the tubes is formed by micritic Mg-calcite cementing hemipelagic sediment ^{13}C-depleted Mg-calcite and aragonite (as low as −14.4 ‰ V-PDB) and lipid biomarkers (archaeol, −89.8 ‰ 24 V-PDB) indicate that carbonate precipitation was influenced by sulfate-dependent anaerobic oxidation of methane (AOM). AOM locally enhances aragonite precipitation, thereby facilitating early lithification of the conduits within the mud volcano sediments. The size and morphology of the TCC comparable with the buried portion of tubeworm colonies found in the proximity of the sampling site. However, our results suggest that TCC likely formed by the action of burrowing organism rather than being mineralizations of the tubeworm colonies. This study provides new insights into the interpretation and understanding of TCC, highlighting the role of macrofaunal activity in the formation of migration pathways for hydrocarbon-rich fluids on the flank of a mud volcano.

[a] Dipartimento di Scienze Chimiche e Geologiche, Università di Modena e Reggio, Modena, Italy. [b] MARUM- Center for Marine Environmental Sciences and Department of Geosciences, University of Bremen, Bremen, Germany.

The second manuscript is published as Orejas et al. (2021) in the journal *Scientific reports:*

***Madrepora oculata* forms large frameworks in hypoxic waters off Angola (SE Atlantic)**

Covadonga Orejas[1,2], Claudia Wienberg[2], Jürgen Titschack[2,3], Leonardo Tamborrino[2], André Freiwald[2,3], Dierk Hebbeln[2]

[1]Instituto Español de Oceanografía, Centro Oceanográfico de Gijón (IEO, CSIC), Gijón, Spain. [2]MARUM–Center for Marine Environmental Sciences, University of Bremen, Bremen, Germany. [3]Department for Marine Research, Senckenberg Institute, Wilhelmshaven, Germany.

This study aims to map the occurrence and distribution of *Madrepora oculata* and to quantify density and colony sizes across recently discovered coral mounds off Angola. Despite the fact that the Angolan populations of *M. oculata* thrive under extreme hypoxic conditions within the local oxygen minimum zone, they reveal colonies with remarkable heights of up to 1250 mm—which are the tallest colonies ever recorded for this species—and average densities of 0.53 ± 0.37 (SD) colonies m^{-2}. This is particularly noteworthy as these values are comparable to those documented in areas without any oxygen constraints. The results of this study show that the distribution pattern documented for *M. oculata* appear to be linked to the specific regional environmental conditions off Angola, which have been recorded in the direct vicinity of the thriving coral community. Additionally, an estimated average colony age of 95 ± 76 (SD) years (total estimated age range: 16–369 years) indicates relatively old *M. oculata* populations colonizing the Angolan coral mounds. Finally, the characteristics of the Angolan populations are benchmarked and discussed in the light of the existing knowledge on *M. oculata* gained from the North Atlantic and Mediterranean Sea.

A.1.2. Conference contributions

Poster contribution to the Geobremen 2017 conference (organized by the Geological Society and Mineralogical Society of Germany).

Early Holocene cold-water coral mounds on the Namibian margin

Leonardo Tamborrino[a], Paul Wintersteller[a,b], Claudia Wienberg[a], Jürgen Titschack[a,c], Dierk Hebbeln[a]

A new large province of mounds build up by cold-water corals (CWC) has been discovered by a hydroacoustic survey on the northern Namibian margin. During RV Meteor cruise M122 in 2016, first video observations with the ROV SQUID and geological sampling clearly proofed these seafloor structures to be coral mounds formed by the ubiquitous species Lophelia pertusa. The newly discovered Namibian CWC mounds are spatially limited to an area geomorphologically characterized by a long NW-SE-trending straight escarpment (63 km long, 45 m high). In general, the coral mounds exhibit a rather circular shape and their heights increase from the south to the north on the western slope of the escarpment area (< 4 m in the south, up to 10-17 m in the northern area), while on the top of the central portion of the escarpment, the height ranges between 4-6 m. No living CWC were observed and, thus, the mounds experience today no active aggradation. First U/Th dating on fossil coral skeletons revealed that the CWC have thrived on the mounds until the Mid-Holocene. Water column information provided a potential explanation for the extinction of the Namibian CWC: at the water depth of the

coral mounds (160 – 240 m), dissolved oxygen concentrations of mostly below 0.5 ml/l are likely too low with respect to the oxygen thresholds (ca. 3-7.2 ml/l) described for *L. pertusa*. These low dissolved oxygen concentrations relate to the well-developed Oxygen Minimum Zone (OMZ) off Namibia that in turn is related to the highly productive Benguela upwelling system. This study provides a picture of the present-day setting of the Namibian CWC mounds, based on hydroacoustic surveys, ROV observations and hydrographic data (CTD). However, as the mounds are today solely covered by fossil corals, this indicates that the present-day setting is not suitable for the proliferation of CWC, while before the Mid-Holocene more suitable conditions for CWC must have prevailed allowing to thrive off Namibia. With dissolved oxygen being the most likely limiting factor for the CWC nowadays, it is hypothesised that better ventilated conditions in the past, possibly triggered by spatio-temporal variation of the Benguela Upwelling System causing a less developed OMZ, allowed the proliferation of the CWC in the Early Holocene.

[a]MARUM – Center for Marine Environmental Sciences, University of Bremen, Bremen, Germany. [b]Dept. of Geosciences, University of Bremen, Bremen, Germany. [c]Seckenberg am Meer, Wilhelmsahfen, Germany

Poster contribution to the *AGU Fall Meeting 2019*, 10-14 December 2018, Washington, DC, US. The MARUM Graduate School GLOMAR is thanked for funding to attend this conference.

Cold-water coral mounds on the Namibian shelf: high-resolution recorders of palaeoceanographic changes

Leonardo Tamborrino[a], Claudia Wienberg[a], Jürgen Titschack[a,b], Paul Wintersteller[a,c], Dierk Hebbeln[a]

Cold-water coral (CWC) ecosystems have been widely documented along the continental slopes around the Atlantic Ocean, but still new areas are awaiting their discovery. Frameworks built by colonial scleractinian CWC, like *Lophelia pertusa*, have the capacity to baffle bypassing sediments supporting the development of impressive three-dimensional seabed structures known as "coral mounds", which form over geological time scales. Under optimal environmental conditions, thriving CWC ecosystems can trigger coral mound aggradation rates of several meters per kiloyear making these mounds to potential high-resolution palaeoceanographic archives. Only few coral mound provinces (CMP) have been reported from shallow shelf settings, though the largest CMP discovered so far exists on the Norwegian shelf. Here, we present the discovery of a new large CMP, extending over a remarkable distance of (at least) 100 km along the northern Namibian shelf (~20-21°S). More than 2,000 coral mounds varying in height between a few metres up to 20 m were detected in 160-270 m water depth. Nowadays, the Namibian coral mounds (NCM) are characterised by exposed fossil *Lophelia pertusa*-remains. First uranium-series datings obtained from various surface coral samples revealed that *L. pertusa* became regionally extinct at ~5 ka, suggesting a simultaneous cessation in mound development within the entire NCM province. Based on an age for mound initiation of 9.5 ka, the average aggradation rates for the larger mounds can be estimated to ~4 m/kyr with most likely time windows having experienced

considerably higher aggradation rates. The present-day extremely low dissolved oxygen concentrations within the Benguela oxygen minimum zone (OMZ) provide a possible cause for the absence of living CWC. Their Mid-Holocene demise is coincident with intensification of the upwelling and the northward migration of the Angola-Benguela front, processes influencing the OMZ in the NCM area. The fate of the NCM provides a new example of how environmental changes steering the vitality of large benthic ecosystems can affect the morphological evolution of continental shelves.,

[a]MARUM – Center for Marine Environmental Sciences, University of Bremen, Bremen, Germany. [b]Senckenberg am Meer, Wilhelmshaven, Germany. [c]Faculty of Geosciences, University of Bremen, Bremen, Germany

Oral contribution to the GeoHab 2019 conference, 12-17 May 2019, Saint Petersburg, Russia. The participation for this conference was funded by Ron Mcdowell Award.

Spatial distribution and morphology of cold-water coral mounds on the Namibian shelf

Leonardo Tamborrino[a], Claudia Wienberg[a], Gregor Eberli[b], Jürgen Titschack[a, c], Paul Wintersteller[a, d], Tim Daskevic[d], Tilmann Schwenk[a,d], Dierk Hebbeln[a]

More than 2000 fossil cold-water coral mounds have been detected by high-resolution hydroacoustic surveys on the northern Namibian shelf. The Namibian coral mounds (NCM) occur between 160–230 m water depth, on a shelf-edge clinoform system characterized by a prominent NNW-SSE-oriented escarpment and other topographic features derived from erosional processes, originated before mound initiation. Coral mound distribution, development and morphology is primarily controlled by different environmental parameters (current regime, sediment input, etc.). However, morphometric analyses and facies mapping of the NCM reveal that their distribution and morphological variability reflect the different underlying topographic features, composed by erosional furrows. The latter resulted from the action of cascading density currents that carved the isobaths at the clinoform foresets sub-perpendicularly. In addition, the erosion of the shelf-edge clinoform system is likely affected by the action of the Poleward Undercurrent (PUC), a strong contour current flowing southward along the shelf break. Mounds in the northern area (Squid Mounds) are widespread over an almost plain topography, rooted on top of very smooth furrows. These mounds are greater in size (up to 20 m high, with diameters >500 m) and exhibit a more complex morphology (merged mounds) compared to the Coral Belt Mounds further south. These are relatively small (up to 12 m high, with diameters of ca. 200 m) and conical mounds occurring in a narrow belt of furrows. Multichannel seismic profiles show a reduced thickness, a low-angle clinoforms and slope for the uppermost unit of the clinoform system in the area of the northern Squid Mounds On the rather flat, low-angle slope, the furrows might have provided a better exposure of the corals to the PUC, justifying their relatively large size, high complexity and wide E-W-oriented cluster distribution. In the Coral Belt, the uppermost unit of the shelf-edge clinoform has been largely preserved as erosion by the PUC was hampered due to the occurrence of a "protecting" lobe composed of older clinothems north of the Coral Belt. Therefore, the coral mounds of the Coral Belt occur within well-

preserved furrows with a narrow distribution. A reduced sediment input in the Coral Belt, due to the lower exposure towards the prevailing current regime, might have led to the development of smaller mounds compared to the Squid Mounds. The spatial and morphological investigation of coral mounds, combined with multichannel seismic surveys, suggested that the geological configuration of the shelf-break in concert with hydrodynamic processes before mound initiation shaped the Namibian shelf-break as a geomorphological setting with topographic features that likely controlled mound distribution and potentially influenced mound development.

[a]MARUM – Center for Marine Environmental Sciences, University of Bremen, Bremen, Germany, [b]Rosenstiel School of Marine and Atmospheric Science, University of Miami, Miami, FL, USA. [c]Senckenberg am Meer, Wilhelmshaven, Germany. [d]Dept. of Geosciences–University of Bremen, Bremen, Germany.

A.2. *Curriculum vitae* and list of publication

Higher Education

Since 10/2016	**PhD Student** Marine Sedimentology, MARUM – University of Bremen, Germany *Project title:* Spatio-temporal distribution of cold-water coral and coral mounds in SE Atlantic.
11/2011 – 02/2014	**Master of Science** Geological Sciences and Technologies, University of Modena and Reggio Emilia, Italy *M.Sc. dissertation*: Authigenic seep-carbonates from Athina Mud Volcano (Anaximander Seamounts, eastern Mediterranean Sea): a mineralogical, geochemical and lipid biomarker study.
04/2013 – 07/2013	**Erasmus Placement project** *(MSc. Internship)* Lipid biomarker analyses associated to authigenic seep-carbonates from Athina Mud volcano (Anaximander Seamounts, NE Mediterranean Sea). MARUM, University of Bremen, Germany
09/2008 – 09/2011	**Bachelor of Science** Geological sciences, University of Modena and Reggio Emilia, Italy *B.Sc. Dissertation:* Compositional and sedimentological study of methane-derived carbonates associated to gas hydrates dissociation in the Northern Apennines.
02/2010 – 06/2010	***Erasmus project*** *(BSc. Internship)* Geological survey and rock sampling along the NW coast of Malta Island and geo-mechanical and physics test on the samples collected, University of Malta, Malta

Professional Experience

Work experience

03/2021 – present	Offshore geophysicist, Green Rebel, Cork, Ireland Acquisition and processing of bathymetric and subseafloor datasets.
09/2015 - 07/2016	Predoctoral researcher, CSIC - IACT, University of Granada, Spain. Mineral pattern formation in Archean rocks and self-assembly materials in alkaline silica-rich environments
04/2014	Grant holder, Dept. of Geosciences – CIRCe, University of Padua, Italy Chemical-physical modelling of Portland cements kinetics through advanced mineralogical techniques based on Rietveld method.

Research expeditions

04-05/2022 **DV JOIDES RESOLUTION IODP Exp. 390**

The South Atlantic Transect: a multidisciplinary IODP investigation along a crustal flow line across the western flank of the southern Mid-Atlantic Ridge, Cape Town (S. Africa) – Cape Town (S. Africa), 07th April – 07th June 2022.

11/2020 ***R V Meteor*** **M167 ALBOCA II**

Menapace and cruise participants. *Long-term monitoring fluid and solid emissions at the African-Eurasian tectonic boundary in the ALBOran Sea and the Gulf of Cadiz*, Emden (Germany) - Emden (Germany), 11th October – 05th November 2020.

10/2018 ***R V Meteor*** **M151 ATHENA**

Frank N. and cruise participants. *Atlantic Thermocline Ocean and Ecosystems Dynamic during Natural Climate Change.* P. Delgada-Funchal (Portugal), 06th-31st October 2018.

04/2017 ***R V Polarstern*** **PS105**

Echosounding Training Cruise on R V POLARSTERN, Gran Canaria (Spain) – Bremerhaven (Germany).

11-12/2014 ***R V Meteor*** **M112/2**

Bohrmann, G., and cruise participants. *Dynamic of Mud Volcanoes and Seeps in the Calabrian Accretionary Prism, Ionian Sea.* Catania (Italy)-Catania (Italy), 06th November -15th December, 2014.

Field campaigns

03/2016 **Alkaline lakes in the Kenyan Rift Valley**, CSIC-IACT, University of Granada,

Geological mapping and sampling of magmatic, metamorphic and sedimentary rocks at the hot springs in the alkaline lakes in the Kenyan Rift Valley

01/2016 "**Dallol, Aux frontiers de la vie"** fieldtrip CSIC-IACT, University of Granada

Geological-mineralogical surveys and portable Raman measurements on the products of the hyper-acidic and hyper-saline hot springs in Dallol, Danakil, Ethiopia.

List of publication

Tamborrino L., Titschack J., Wienberg C., Purkis S., Eberli G., Hebbeln D., Spatial distribution and morphometry of the Namibian coral mounds controlled by the hydrodynamic regime and outer-shelf topography. Submitted in Frontiers in Marine Sciences.

Orejas C., Wienberg, C., Titschack, J., **Tamborrino, L.**, Freiwald A., Hebbeln, D. *Madrepora oculata* forms large frameworks in hypoxic waters off Angola (SE Atlantic), Scientific Reports, 11(1), 1-13.

Tamborrino L., Wienberg C., Titschack J., Wintersteller P., Mienis F., Freiwald A., Orejas C., Dullo W.C., Haberkern J. Hebbeln D., 2019. Mid-Holocene extinction of cold-water corals on the Namibian shelf steered by the Benguela oxygen minimum zone. Geology, 47(12), 1185-1188.

Hanz U., Wienberg C., Hebbeln D., Duineveld G., Lavaleye M., Juva K., Dullo W.-C., Freiwald A., **Tamborrino L.**, Reichart G.-J., Flögel S., Mienis F., 2019. Environmental factors influencing cold-water coral ecosystems in the oxygen minimum zones on the Angolan and Namibian margins. Biogeoscience.

Tamborrino L., Himmler T., Elvert M., Gualtieri A.F., Fontana D., Conti S., Bohrmann G., 2019. Formation of tubular carbonate concretions at Athina mud volcano, eastern Mediterranean Sea. Marine and Petroleum Geology, 107, 20-31, doi.org/10.1016/j.marpetgeo.2019.05.003.

García-Ruiz, J. M., Nakouzi, E., Kotopoulou, E., **Tamborrino, L.**, Steinbock, O., Biomimetic mineral self-organization from silica-rich spring waters. Science Advances 3, e1602285 (2017).

Ferrari G., Russo V., Dragoni M., Artioli G., Dalconi M.C., Secco M., **Tamborrino L.**, Valentini L., 2015. The influence of C_3A on the dissolution kinetics of alite/gypsum mixtures in the presence of PCEs. Special Proceedings -11th Int. Conf. on "Superplasticizers and Other Chemical Admixtures in Concrete", Ottawa, 2015.

Posters & Oral Presentations

Tamborrino L., C. Wienberg., J. Titschack, P. Wintersteller, T. Daskevic, T. Schwenk, G. Eberli, D. Hebbeln. Spatial distribution and morphology of cold-water coral mounds on the Namibian shelf. GeoHab 2019, S. Petersburg (Russia). *Oral.*

Tamborrino L., Wienberg C., Titschack J., Wintersteller P., Hebbeln D. Cold-water coral mounds on the Namibian shelf: high-resolution recorders of palaeoceanographic changes. AGU Fall Meeting 2018, Washington DC (US). *Poster.*

Tamborrino L., Wintersteller P., Wienberg C., Titschack J., Hebbeln D. Early Holocene cold-water coral mounds on the Namibian margin, GeoBremen 2017, Bremen (Germany). *Poster.*

Tamborrino L., Garcia-Ruiz J.M., Otalora F., Mazurier A., Kotopoulou E., El Albani A. Crystallographical study of pseudomorph patterns of Dresser Formation (Pilbara Craton, Australia), 5th International School of Crystallization, Granada (Spain), 2016. *Poster.*

Workshops & Summer Schools

ECORD Petrophysics Summer School, University of Leicester, UK, 29thJune-5th July 2019.

ECORD-PROCEED "Expanding frontiers of scientific ocean drilling", Austrian Academy of Sciences, Vienna, Austria, 6th-7th April 2019.

ECORD-Magellan "Navigating the IODP proposal system", NOC- University of Southampton, UK, 24th-26th September 2018.

ECORD Summer School 2017 "Current-Controlled Sea Floor Archives: Coral Mounds and Contourites", MARUM, Bremen, Germany, August 2017.

COSPAR Capacity Building Workshop "Crystallography for Space Sciences" INOE/BUAP, Puebla, Mexico, April 2016.

ECORD Summer School 2014 "Sub-seafloor Biosphere: Current Advances and Future Challenges", MARUM, Bremen, Germany, September 2014.

Awards & Scholarship

ECORD Scholarship for participation to an ECORD Summer School (Petrophysics Summer School 2019).

Ron MacDowell Award for student support for GeoHab 2019 conference.

University of Modena and Reggio Emilia M.Sc. and B.Sc. Prizes ("Premio di Laurea") for final marks and outstanding student resume.

ER.GO Emilia Romagna Agency for High Education Rights Scholarship (academic years 2008/2013)

Other activities

07/2017-04/2019	Ph.D. representative, GLOMAR-MARUM, University of Bremen, Germany
10/2016-10/2017	"Once upon a time… a scientific fairy tale" Science communication project, MARUM, University of Bremen, Germany.
04/2012-02/2014	Student Delegate, Dept. of Chemical and Geological Sciences, University of Modena and Reggio Emilia, Italy

Versicherung an Eides Statt / *Affirmation in lieu of an oath*

gem. § 5 Abs. 5 der Promotionsordnung vom 18.06.2018 /
according to § 5 (5) of the Doctoral Degree Rules and Regulations of 18 June, 2018

Ich / I, Leonardo Tamborrino, Markgrafenstr. 45, 78467 Konstanz, 3106557

(Vorname / First *Name*, Name / *Name*, Anschrift / *Address*, ggf. Matr.-Nr. / *student ID no., if applicable)*

versichere an Eides Statt durch meine Unterschrift, dass ich die vorliegende Dissertation selbständig und ohne fremde Hilfe angefertigt und alle Stellen, die ich wörtlich dem Sinne nach aus Veröffentlichungen entnommen habe, als solche kenntlich gemacht habe, mich auch keiner anderen als der angegebenen Literatur oder sonstiger Hilfsmittel bedient habe und die zu Prüfungszwecken beigelegte elektronische Version (PDF) der Dissertation mit der abgegebenen gedruckten Version identisch ist. / *With my signature I affirm in lieu of an oath that I prepared the submitted dissertation independently and without illicit assistance from third parties, that I appropriately referenced any text or content from other sources, that I used only literature and resources listed in the dissertation, and that the electronic (PDF) and printed versions of the dissertation are identical.*

Ich versichere an Eides Statt, dass ich die vorgenannten Angaben nach bestem Wissen und Gewissen gemacht habe und dass die Angaben der Wahrheit entsprechen und ich nichts verschwiegen habe. / *I affirm in lieu of an oath that the information provided herein to the best of my knowledge is true and complete.*

Die Strafbarkeit einer falschen eidesstattlichen Versicherung ist mir bekannt, namentlich die Strafandrohung gemäß § 156 StGB bis zu drei Jahren Freiheitsstrafe oder Geldstrafe bei vorsätzlicher Begehung der Tat bzw. gemäß § 161 Abs. 1 StGB bis zu einem Jahr Freiheitsstrafe oder Geldstrafe bei fahrlässiger Begehung. / *I am aware that a false affidavit is a criminal offence which is punishable by law in accordance with § 156 of the German Criminal Code (StGB) with up to three years imprisonment or a fine in case of intention, or in accordance with § 161 (1) of the German Criminal Code with up to one year imprisonment or a fine in case of negligence.*

Konstanz, 11.07.2022

Ort / *Place*, Datum / *Date*

Leonardo Tamborrino

Unterschrift / *Signature*